



PRODUCTION OF CARBON PRODUCTS USING A COAL EXTRACTION PROCESS

DE-FC26-02NT41596

FINAL REPORT

Period of Performance:
September 11, 2002 to August 31, 2004

Principal Investigator:
Dady Dadyburjor

Additional Authors:
Philip R. Biedler, Chong Chen, L. Mitchell Clendenin, Manoj Katakdaunde,
Elliot B. Kennel, Nathan D. King, Liviu Magean, Peter G. Stansberry,
Alfred H. Stiller, John W. Zondlo

West Virginia University
Department of Chemical Engineering
College of Engineering and Mineral Resources
PO Box 6102
Morgantown WV 26506-6102

Sponsored by:

U.S. Department of Energy
National Energy Technology Laboratory
626 Cochran Mills Road
PO Box 10940
Pittsburgh PA 15236-0940
Project Monitor: John Stipanovich

ABSTRACT

Project Title: Production of Foams, Fibers and Pitches using a Coal Extraction Process

NETL Contract Number: DE-FC26-02NT41596

Principal Investigator: Dady Dadyburjor

NETL Project Manager: John Stipanovich

This Department of Energy National Energy Technology Laboratory sponsored project developed carbon products, using mildly hydrogenated solvents to extract the organic portion of coal to create synthetic pitches, cokes, carbon foam and carbon fibers. The focus of this effort was on development of lower cost solvents, milder hydrogenation conditions and improved yield in order to enable practical production of these products.

This technology is needed because of the long-term decline in production of domestic feedstocks such as petroleum pitch and coal tar pitch. Currently, carbon products represents a market of roughly 5 million tons domestically, and 19 million tons worldwide. Carbon products are mainly derived from feedstocks such as petroleum pitch and coal tar pitch. The domestic supply of petroleum pitch is declining because of the rising price of liquid fuels, which has caused US refineries to maximize liquid fuel production. As a consequence, the long term trend has a decline in production of petroleum pitch over the past 20 years.

The production of coal tar pitch, as in the case of petroleum pitch, has likewise declined significantly over the past two decades. Coal tar pitch is a byproduct of metallurgical grade coke (met coke) production. In this industry, modern met coke facilities are recycling coal tar as fuel in order to enhance energy efficiency and minimize environmental emissions. Met coke production itself is dependent upon the production requirements for domestic steel. Hence, several met coke ovens have been decommissioned over the past two decades and have not been replaced. As a consequence sources of coal tar are being taken off line and are not being replaced. The long-term trend is a reduction in coal tar pitch production.

Thus import of feedstocks, mainly from Eastern Europe and China, is on the rise despite the relatively large transportation cost. To reverse this trend, a new process for producing carbon products is needed. The process must be economically competitive with current processes, and yet be environmentally friendly as well.

The solvent extraction process developed uses mild hydrogenation of low cost oils to create powerful solvents that can dissolve the organic portion of coal. The insoluble portion, consisting mainly of mineral matter and fixed carbon, is removed via centrifugation or filtration, leaving a liquid solution of coal chemicals and solvent. This solution can be further refined via distillation to meet specifications for products such as synthetic pitches, cokes, carbon foam and fibers. The most economical process recycles 85% of the solvent, which itself is obtained as a low-cost byproduct from industrial processes such as coal tar or petroleum refining. Alternatively, processes have been developed that can recycle 100% of the solvent, avoiding any need for products derived from petroleum or coal tar.

DISCLAIMER

This report was prepared as an account of work sponsored by an agency of the United States Government. Neither the United States Government nor any agency thereof, nor any of their employees, makes any warranty, express or implied, or assumes any legal liability or responsibility for the accuracy, completeness, or usefulness of any information, apparatus, product, or process disclosed, or represents that its use would not infringe privately owned rights. Reference herein to any specific commercial product, process, or service by trade name, trademark, manufacturer, or otherwise does not necessarily constitute or imply its endorsement, recommendation, or favoring by the United States Government or any agency thereof. The views and opinions of authors expressed herein do not necessarily state or reflect those of the United States Government or any agency thereof.

TABLE OF CONTENTS

TABLE OF CONTENTS	4
LIST OF FIGURES	7
LIST OF TABLES	12
1.0. EXECUTIVE SUMMARY	14
1.1 Background	14
1.2 Summary of Key Accomplishments	15
2.0 INTRODUCTION	16
2.1 Carbon Product Markets	16
2.1.1 Pitches	17
2.1.2 Cokes	17
2.1.3 Aluminum Industry	19
2.1.4 Graphite Electrodes for Arc Furnaces for Metals Smelting	21
2.2 Declining Supplies of US Feedstocks for Carbon Products	21
2.3 Coal as a Material Feedstock	24
2.4 Methods for Converting Coal to Material Feedstocks	27
2.4.1. Pyrolysis	27
2.4.2 Liquefaction	27
2.4.3 Indirect Liquefaction	28
2.4.4 Direct Liquefaction	28
2.4.5 Reaction Pathways of Coal Liquefaction	29
2.5 Commercial Coal Liquefaction Processes	31
2.5.1 H-Coal Process	31
2.5.2 Solvent Refined Coal (SRC) Process	31
2.5.3 Exxon Donor Solvent (EDS) Process	32
2.6 Liquefaction Solvents	33
2.7 Catalytic Effects of Mineral Matter in Coal	34
2.8 Effect of Hydrogen Pressure on Coal Solubility	35
2.9 Temperature Effects upon Coal Liquefaction Reactions	36
2.10 Air Blowing of Coke Precursors	37
2.10.1 Effect of Air Blowing on Coke Yield	41
2.10.2 Effects of Air Blowing on Viscosity	42

2.10.3 Williams, Landel, and Ferry Viscosity Model.....	43
2.10.4 Van Krevelen Analysis	45
3.0 EXPERIMENTAL.....	48
3.1 Hydrogenation Reactions	48
3.1.1 Materials	48
3.1.2 Catalyst Treatment	50
3.1.3 Solvent Hydrogenation	52
3.2 Coal Digestion/Dissolution.....	53
3.2.1 Parametric Studies in Mini-Reactors	53
3.2.2 Reaction Procedure	56
3.2.3 Reactor Scale Up Studies	58
3.2.4 Hydrotreatment Facility.....	62
3.3 Distillation and Air Blowing.....	66
3.3.1 Feed Pitch Preparation.....	68
3.3.2 Air-blowing Procedure.....	71
3.4 Characterization.....	72
3.4.1 Softening Point.....	73
3.4.2 Density	73
3.4.3 Ash Content	73
3.4.4 Optical Microscopy.....	74
3.4.5 Elemental Analysis	74
3.4.6 Coking Value	74
3.4.7 Viscosity.....	75
3.4.8 Pyridine Insoluble Content	76
3.4.9 Toluene Solubility.....	78
3.4.10 Fourier-Transform Infrared Spectroscopy (FTIR).....	78
3.4.11 Pyridine Insoluble Content	79
3.4.12 Fourier Transform Infrared (FTIR)	81
3.4.13 Thermogravimetric Analysis	83
3.4.14 Simulated Distillation	83
3.5 Mesophase Pitch	84
4.0 RESULTS AND ANALYSIS	86
4.1 Coal Conversion using Different Solvents	86
4.1.1 Solvent Hydrogenation	87
4.1.2 Coal Conversion in HCO, CBB and RCO	99
4.1.3 Recovered Solvent Evaluation.....	100
4.1.4 Mass Balances with Fresh Solvents	101
4.1.5 Mass Balances with Recovered Solvents.....	103
4.1.6 Ash Balance	103

4.1.7 Hydrogenation Products.....	107
4.1.8 Parametric Studies in Mini Reactors.....	108
4.2 Scale-Up Studies.....	112
4.2.1 Variation of Hydrogenation Parameters	118
4.2.2 Successive Hydrogenation Runs	124
4.3 Pitch Processing	129
4.3.1 Ash Content.....	129
4.3.2 Coke Yield and Softening Point	131
4.3.3 Elemental Analysis	133
4.3.4 Optical Texture	136
4.3.5 Characterization of Feed Pitches Prior to Air Blowing	142
4.3.6 Air Blowing Effect on Softening Point.....	143
4.3.7 Conradson Carbon and Modified Carbon Determination.....	147
4.3.8 Effect of Air Blowing on Pitch Density.....	152
4.3.9 Effect of Air Blowing on Pitch Viscosity.....	155
4.3.10 Effect of Air Blowing on Pyridine Insoluble Content	168
4.3.11 Air Blowing Effects on Toluene Solubility	169
4.3.12 Kinetic Modeling of Chemical Changes due to Air Blowing.....	170
4.3.13 Thermogravimetric Studies on Feed and Air-Blown Pitches	174
4.3.14 Elemental Analysis and Van Krevelen Plots	184
4.3.15 Fourier Transform Infrared (FTIR) Analysis on Air-Blown Pitches	191
4.4 Characterization of Cokes from Synthetic Feedstocks	195
4.4.1 Atomic Analyses.....	197
4.4.2 Vacuum Distillation of Coke Precursors	202
4.5 Coal Derived Carbon Foam	207
4.6 Isotropic and Mesophase-Based Fibers and Composites	219
5.0 ECONOMIC CONSIDERATIONS.....	223
6.0 REFERENCES	227

LIST OF FIGURES

Figure 1. Metallurgical coke oven schematic showing coal tar pitch recovery.....	17
Figure 2. Marathon-Ashland Delayed Coker	19
Figure 3. Hall-Heroult Reduction Cell (prebake type).	20
Figure 4. Arc furnace with Graphite electrodes.	21
Figure 5. Close- up of arc furnace electrodes, operating at 3000 °C.	21
Figure 6. Koppers Industries estimates.	22
Figure 7. Vanadium levels in commercial US green anode coke have been rising.....	23
Figure 8. Sulfur levels are increasing in US green anode coke.	23
Figure 9. One Typical Molecular Unit in Coal.	25
Figure 10. Conceptual Reaction Sequences in Coal Liquefaction.	30
Figure 11. Schematic Sketch of the Typical SRC Process.	32
Figure 12. Wyodak Coal Conversion vs. Ash Content.....	35
Figure 13. Oxidation Schemes of Coal-tar and Petroleum Pitches.....	38
Figure 14. Dependency of TI Yields from Coal-tar Pitch on Gas Flow Rate.....	39
Figure 15. Relative Carbonization of Petroleum Feedstocks.....	40
Figure 16. First-order Plots for Pyridine Insolubles Formation from VR2	41
Figure 17. Arrhenius Plot for VR2 Pentane Insolubles	41
Figure 18. Shear Stress Response upon Start up of Shear Flow for the Parent Pitch.....	43
Figure 19. Plot of (T – T _r) vs. Log A _T for a Range of Mesophase-Containing Pitches...	45
Figure 20. H/C versus O/C Diagram.	45
Figure 21. H/C versus O/C for I) Wood, II) Cellulose, III) Lignin, IV) Peat,	46
Figure 22. Van Krevelen Diagrams Showing Oxidation Paths of.....	47
Figure 23. Catalyst Basket Design.	51
Figure 24. Completed and Loaded Catalyst Basket.	52
Figure 25. Diagram of the Tube Bomb Mini-Reactor.	54
Figure 26. Overview of Reactor System Showing Sand Bath and Shaker Mechanism. .	55
Figure 27. Product Removal Thimble / Flask Apparatus.	58
Figure 28. Experimental Flow Sheet for Production of Carbon Product Precursors.....	62
Figure 29. Process Diagram for Hydrogenated Synpitch Production.	63
Figure 30. Lower Level Reactor Used to Chemically Digest Coal.	64
Figure 31. Upper Level Reactor, Used to Combine Coal and Solvent.	64
Figure 32. Remote Control Panel.	65
Figure 33. Vacuum Distillation Setup to Recover Solvent from the Pitch Product.	66
Figure 34. Soxhlet Condenser Apparatus.	68
Figure 35. Diagram of the 1-liter Autoclave used in Air-blowing Experiments.	71
Figure 36. Diagram of Ring Stand Setup.	76
Figure 37. Soxhlet Apparatus Setup.	77
Figure 38. Diagram of Ring Stand Setup.	80
Figure 39. Soxhlet Apparatus Setup.	81
Figure 40. Spectra-tech Pellet Apparatus.....	82
Figure 41. Thermogravimetric (TGA) Data for Pyrolysis Products of A240	85
Figure 42. Temperature and Pressure for HCBB Level 1 Hydrogenation.	88
Figure 43. Temperature and Pressure for HCBB Level 2 Hydrogenation.	89

Figure 44. Temperature and Pressure for HCBB Level 3 Hydrogenation	89
Figure 45. Temperature and Pressure for HSO Level 3 Hydrogenation	90
Figure 46. Temperature and Pressure for HMO Level 3 Hydrogenation.	90
Figure 47. Boiling Point Curves of Raw Solvents.	92
Figure 48. Boiling Point Curves of CBB Solvents.	92
Figure 49. Boiling Point Curves of Slurry Oils.	93
Figure 50. Boiling Point Curves of Maraflex Oils.	93
Figure 51. First Derivative of Boiling Point Curve for CBB vs Temperature.	94
Figure 52. First Derivative of Boiling Point Curve for HCBB-L1 vs Temperature.	95
Figure 53. First Derivative of Boiling Point Curve for HCBB-L2 vs Temperature.	95
Figure 54. First Derivative of Boiling Point Curve for HCBB-L3 vs Temperature.	96
Figure 55. Derivative of Boiling Point Curve for HSO-L3 vs Temperature.	96
Figure 56. First Derivative of Boiling Point Curve for Maraflex Oil vs Temperature.	97
Figure 57. First Derivative of Boiling Point Curve for HMO-L3 vs Temperature.	97
Figure 58. Amount of Sulfur (left) and Nitrogen in Solvents.	99
Figure 59. Overall & Coal-alone Conversion Yields with Fresh HCO, CBB and RCO100	
Figure 60. Overall and Coal-alone Conversion Yields with Recovered.....	101
Figure 61. Pressure Profiles for Fresh Solvents CBB, HCO and RCO	106
Figure 62. Pressure Profiles for Recovered Solvents CBB, HCO and RCO	106
Figure 63. Hydrogenation Product Distribution for Fresh and Recovered Solvents	108
Figure 64. Conversion vs. Temperature at P = 0 psig N ₂	109
Figure 65. Conversion vs. Temperature at P = 500 psig N ₂	109
Figure 66. Coal Conversion for Raw Solvents (T = 400°C).....	110
Figure 67. Conversion vs. Hydrogenation Level (T = 400°C).	111
Figure 68. Coal Conversion vs. Solvent Choice (T = 400°C).	112
Figure 69. Scale-Up Reaction Conversion vs. Solvent Choice.	114
Figure 70. Solvent C/H Ratios vs. Digestion Conversions (daf).	116
Figure 71. Solvent H _{ar} / (H _{ar} + H _{al}) vs. Digestion Conversions (daf).	116
Figure 72. Solvent H _{ar} / H _{al} Ratios vs. Digestion Conversions (daf).	117
Figure 73. Solvent (C=C) _{ar} / (H _{ar} + H _{al}) Ratios vs. Digestion Conversions (daf).....	117
Figure 74. Solvent (C=C) _{ar} / H _{ar} Ratios vs. Digestion Conversions (daf).	118
Figure 75. Coal-alone Conversion at Different Temperature	120
Figure 76. Pressure Profiles at 450 °C and 350 °C for Fresh and Recovered CBB	121
Figure 77. Optical Micrographs of Coke Samples.....	122
Figure 78. (C) Pass 1 Coke at 450 °C. (D) Pass 2 Coke at 450 °C.	122
Figure 79. Coal-alone Conversion for Fresh and Recovered CBB.....	123
Figure 80. Pressure Profiles for Fresh and Recovered CBB r.	124
Figure 81. Optical Micrographs of Coke Samples.....	125
Figure 82. Left: Pass 1 Coke Under N ₂ . Right: Pass 2 Coke Under N ₂	126
Figure 83. Successive Recovered Solvent Conversion at 400 °C.....	127
Figure 84. Variation of Successive Recovered Conversion.....	128
Figure 85. Coal-alone Conversion Results for Fresh and Successively Recovered	129
Figure 86. Variation of Coal-alone Conversion for Fresh and Successively.....	129
Figure 87. Ash Content in Coal Digest Liquids and Air Blown Digests.	131
Figure 88. Softening Point (°C) for Air Blown Digests.....	132
Figure 89. Relation Between Coke Yield and Softening Point for Solvents.	133

Figure 90. Relation Between Coke Yield and Softening Point for Solvents.	133	
Figure 91. Optical Micrograph of Pitch Sample with Fresh CBB at 400 °C	136	
Figure 92. Optical Micrograph of Pitch Sample with Fresh HCO at 400 °C.....	137	
Figure 93. Optical Micrograph of Pitch Sample with Fresh RCO at 400 °C.....	137	
Figure 94. Optical Micrograph of Pitch Sample with Recovered CBB at 400 °C.....	137	
Figure 95. Optical Micrograph of Pitch Sample with Recovered HCO at 400 °C	138	
Figure 96. Optical Micrograph of Pitch Sample with Recovered RCO at 400 °C.....	138	
Figure 97. Optical Micrograph of Pitch Sample with Fresh CBB at 350 °C	138	
Figure 98. Optical Micrograph of Pitch Sample with Recovered CBB at 350 °C.....	139	
Figure 99. Optical Micrograph of Pitch Sample with Fresh CBB at 450 °C	139	
Figure 100. Optical Micrograph of Pitch Sample with Recovered CBB at 450 °C.....	139	
Figure 101. Optical Micrograph of Pitch Sample with Fresh CBB at 400 °C	140	
Figure 102. Optical Micrograph of Pitch Sample with Recovered CBB at 400 °C.....	140	
Figure 103. Optical Micrographs of Pass 1 Coke with CBB.	141	
Figure 104. Optical Micrographs Pass 2 Coke with CBB.	141	
Figure 105. Optical Micrographs of Pass 1 Coke with HCO	141	
Figure 106. Optical Micrographs of Pass 2 Coke with HCO.	142	
Figure 107. Optical Micrographs of Single-Pass Coke with RCO.	142	
Figure 108. Optical Micrographs of Pass 2 Coke with RCO.	142	
Figure 109. Softening Point Effects of Nitrogen and Air-blowing at 300°C.....	144	
Figure 110. Softening Point Effects of Nitrogen and Air-blowing at	145	
Figure 111. Softening Point Temperatures of Petroleum Pitch.....	146	
Figure 112. Softening Point Temperatures of Coal-tar Pitch.....	146	
Figure 113. Softening Point Temperatures of Coal-extract Feed Pitch.....	147	
Figure 114. Softening Points of Air-blown Reaction at 300°C for all Three Pitches....	147	
Figure 115. Conradson Coke Yield of Petroleum Pitch	148	
Figure 116. Conradson Coke Yield of Coal-tar Pitch.....	148	
Figure 117. Conradson Coke Yield of Coal-extract Pitch.....	149	
Figure 118. Modified Protocol Coke Yield of A240 Petroleum Pitch	149	
Figure 119. Modified Protocol Coke Yield of Koppers Coal-tar Pitch.....	150	
Figure 120. Modified Protocol Coke Yield of Synthetic Coal-extract Pitch.	150	
Figure 121. Conradson Carbon Coke Yield of Coal Digests.	151	
Figure 122. Modified Protocol Coke Yield of Coal Digests.	152	
Figure 123. Density of Petroleum Pitches Air-blown at 250, 275, and 300°C.	153	
Figure 124. Density of Coal Tar Pitches Air-blown at 250, 275, and 300°C.	153	
Figure 125. Density of Coal-extract Pitches Air-blown at 250, 275, and 300°C.	154	
Figure 126. Air Blown Sample Densities.	155	
Figure 127. Temperature Dependence of Visc. for A240 Petroleum Pitch at 250°C....	156	
Figure 128. Temperature Dependence of Visc. for A240 Petroleum Pitch at 275°C....	157	
Figure 129. Temperature Dependence of Visc. for A240 Petroleum Pitch at 300°C....	157	
Figure 130. Temperature Dependence of Visc. for Koppers Coal-tar Pitch at 250°C...	158	
Figure 131. Temperature Dependence of Visc. for Koppers Coal-tar Pitch at 275°C...	158	
Figure 132. Temperature Dependence of Viscosity for Koppers Coal-tar Pitch at	159	
Figure 133. Temperature Dependence of Viscosity for Synthetic Coal-extract Pitch... <td> <td>159</td> </td>	<td>159</td>	159
Figure 134. Temperature Dependence of Viscosity for Synthetic Coal-extract Pitch... <td> <td>160</td> </td>	<td>160</td>	160
Figure 135. Temperature Dependence of Viscosity for Synthetic Coal-extract Pitch... <td> <td>160</td> </td>	<td>160</td>	160

Figure 136. WFL Model of A240 Petroleum Pitch at 250°C	161
Figure 137. WFL Model of A240 Petroleum Pitch at 275°C.	161
Figure 138. WFL Model of A240 Petroleum Pitch at 300°C.	162
Figure 139. WFL Model of Koppers Coal-tar Pitch (CTP) at 250°C.	162
Figure 140. WFL Model of Koppers Coal-tar Pitch (CTP) at 275°C.	163
Figure 141. WFL Model of Koppers Coal-tar Pitch (CTP) at 300°C.	163
Figure 142. WFL Model of Coal-extract Pitch (CTP) at 250°C.....	164
Figure 143. WFL Model of Coal-extract Pitch (CTP) at 275°C.....	164
Figure 144. WFL Model of Coal-extract Pitch (CTP) at 300°C.....	165
Figure 145. Viscosity Vs Temperature for Air-Blown Coal Digest A086.	165
Figure 146. Viscosity Vs Temperature for Air-Blown Coal Digest A090.	166
Figure 147. Viscosity Vs Temperature for Air-Blown Coal Digest A095.	166
Figure 148. Viscosity Vs Temperature for Air-Blown Coal Digest A098.	167
Figure 149. Viscosity Vs Temperature for Air-Blown Coal Digest A100.	167
Figure 150. Viscosity Vs Temperature for Air-Blown Coal Digest B003.	168
Figure 151. Pyridine Insoluble Content of A240 Petroleum Pitch.	168
Figure 152. Pyridine Insoluble Content of Koppers Coal-tar Pitch.	169
Figure 153. Pyridine Insoluble Content of Synthetic Coal-extract Pitch.	169
Figure 154. Toluene Insolubles of Coal Digests.....	170
Figure 155. Rate Constant Data for the Air-blowing Kinetics	172
Figure 156. Rate Constant Data for the Air-blowing Kinetics of Coal-tar Pitch.	172
Figure 157. Rate Constant dData for the Air-blowing Kinetics of Coal-extract Pitch. .	173
Figure 158. Activation Energies for the Air-blowing of Petroleum Pitch A240	174
Figure 159. Petroleum Pitch Weight Loss From Air Blowing at 250°C.	175
Figure 160. Petroleum Pitch Weight Loss From Air Blowing at 275°C.	175
Figure 161. Petroleum Pitch Weight Loss From Air Blowing at 300°C.	176
Figure 162. Coal Tar Pitch Weight Loss From Air Blowing at 250°C.....	176
Figure 163. Coal Tar Pitch Weight Loss From Air Blowing at 275°C.....	177
Figure 164. Coal Tar Pitch Weight Loss From Air Blowing at 300°C.....	177
Figure 165. Coal Extract Weight Loss from Air Blowing at 250°C.....	178
Figure 166. Coal Extract Weight Loss from Air Blowing at 275°C.....	178
Figure 167. Coal Extract Weight Loss From Air Blowing at 300°C.....	179
Figure 168. Volatile Fraction Remaining for AB A240 at 250°C.	180
Figure 169. Volatile Fraction Remaining for AB A240 at 275°C.	180
Figure 170. Volatile Fraction Remaining for AB A240 at 300°C.	181
Figure 171. Volatile Fraction Remaining for AB CTP at 250°C.....	181
Figure 172. Volatile Fraction Remaining for AB CTP at 275°C.....	182
Figure 173. Volatile Fraction Remaining for AB CTP at 300°C.....	182
Figure 174. Volatile Fraction for AB Coal Extract at 250°C.	183
Figure 175. Volatile Fraction for AB Coal Extract at 275°C.	183
Figure 176. Volatile Fraction for AB Coal Extract at 300°C.	184
Figure 177. C-H Atomic Ratio vs AB Time A240.	185
Figure 178. C-H Atomic Ratio vs. AB Time CTP.....	185
Figure 179. C-H Atomic Ratio Versus Air-blown Time for Coal-extract.	186
Figure 180. Oxygen Content for Air-blown Petroleum Pitch.	187
Figure 181. Oxygen Content for Air-blown Coal-tar Pitch.	187

Figure 182. Oxygen Content for Air-blown Coal-extract Pitch.	188
Figure 183. Van Krevelen Plot.	189
Figure 184. Van Krevelen Plot for A240 Petroleum Pitch.	190
Figure 185. Van Krevelen Plot for Coal-Tar Pitch.	190
Figure 186. Van Krevelen Plot for Coal Extract Pitch.	191
Figure 187. Air Blowing Effect on C/H Atomic Ratio at 250 °C.	192
Figure 188. Air Blowing Effect on Oxygen Content at 250 °C.	192
Figure 189. Air Blowing Effect on Aliphatic/Aromatic Ratio at 250 °C.	193
Figure 190. Air Blowing Effect on C/H Atomic Ratio at 275 °C.	193
Figure 191. Air Blowing Effect on Oxygen Content at 275 °C.	194
Figure 192. Air Blowing Effect on Aliphatic/Aromatic Ratio at 275 °C.	194
Figure 193. Air Blowing Effect on C/H Atomic Ratio at 300 °C.	194
Figure 194. Air Blowing Effect on Oxygen Content at 300 °C.	195
Figure 195. Air Blowing Effect on Aliphatic/Aromatic Ratio at 300 °C.	195
Figure 196. Photomicrographs (160X) of Green Cokes Made From A090.	196
Figure 197. Photomicrographs (160X) of Green Cokes Made From A095	196
Figure 198. Photomicrographs (160X) of Green Cokes Made From A098.	200
Figure 199. Photomicrographs (160X) of Green Cokes Made From A100.	197
Figure 200. Photomicrographs (160X) of Green Cokes Made From B003.	197
Figure 201. Sulfur Concentrations in Digest Processing.	198
Figure 202. Nitrogen Concentrations in Digest Processing.	198
Figure 203. Hydrogen Concentrations in Digest Processing.	199
Figure 204. Carbon Concentrations in Digest Processing.	199
Figure 205. Solvent Atomic C/H Ratio vs. Air-Blown Softening Point (°C).	200
Figure 206. Solvent Aromaticity vs. Softening Point (°C).	201
Figure 207. Coal Digest C/H Atomic Ratio vs. Air-Blown Softening Point (°C).	201
Figure 208. Coal Digest Aromaticity Factor vs. Air-Blown Softening Points (°C).	202
Figure 209. Softening Point (°C) for Air Blown and Distilled Samples.	203
Figure 210. Alternate Protocol Coke Yield (w/ Distilled Coal Liquids).	204
Figure 211. Photomicrographs (160X) of Green Cokes Made From A090	204
Figure 212. Photomicrographs (160X) of Green Cokes Made From A095	205
Figure 213. Photomicrographs (160X) of Green Cokes Made From A098	205
Figure 214. Photomicrographs (160X) of Green Cokes Made From A100.	205
Figure 215. Photomicrographs (160X) of Green Cokes Made From B003.	206
Figure 216. Giesler Fluidity Curve of a Typical Foaming Precursor(coal).	209
Figure 217. Dilatation Rate Curve of a Typical Foaming Precursor (Coal).	209
Figure 218. TGA Curve of a Typical Foaming Precursor (Coal).	210
Figure 219. Relation of Fluidity and Dilatation of Coal Foaming Precursors	211
Figure 220. Relation of Compressive Strength.	214
Figure 221. Optical Texture of Carbon Foam Derived from.	216
Figure 222. Isotherms and the Corresponding t-plots of the Carbon Foam.	218
Figure 223. SEM Photomicrograph of Synpitch-Derived Carbon Fibers.	221
Figure 224. Stress-Strain Plot for A-240/Bakerstown Synpitch Fiber.	222

INDEX OF TABLES

Table 1. Estimated Domestic and World Markets for Carbon Products.....	16
Table 2. The ASTM System for Classifying Coals by Rank.....	25
Table 3. Typical Compositions of Coals and Liquid Hydrocarbons.'.....	26
Table 4. Fundamental Properties Important in Coal Liquefaction.	31
Table 5. Effectiveness of Some Typical Solvents for Hydrogenation.	33
Table 6. Coke Yield (wt %) for Air-blown Pitch A and Pitch B.	42
Table 7. Characteristics of Kingwood Coal.	49
Table 8. Elemental Analysis Results for Coal and Four (4) Candidate Solvents.	49
Table 9. Catalyst Properties.	51
Table 10. Catalyst Basket Parameters.....	51
Table 11. Solvent Hydrogenation Reaction Conditions.	53
Table 12. Hydrogenation Reaction Conditions.....	61
Table 13. A240 Petroleum Pitch properties.	69
Table 14. Koppers Coal-tar Pitch Properties.	69
Table 15. Petrographic Analysis of Marfolk Eagle.	70
Table 16. Elemental Analysis (wt %).	70
Table 17. Proximate Analysis (dry basis, wt %).	70
Table 18. Air Oxidation Reaction Times of Three Pitches.....	72
Table 19. Solvent Hydrogenation Reaction Conditions.	87
Table 20. Solvent Hydrogenation Results.	91
Table 21. Elemental and FTIR Analysis Data for Solvents.....	98
Table 22. Mass Balances of Coal Digestion Reactions with Fresh Solvents.....	102
Table 23. Mass Balances of Coal Digestion Reactions with Recovered Solvents.	103
Table 24. Ash Balances of Coal Digestion Reactions with Fresh Solvents.....	104
Table 25. Ash Balances of the Coal Digestion Reactions with Recovered Solvents.	105
Table 26. Scale-Up Digestion Details.....	112
Table 27. Atomic C/H Ratios for Coal Liquid Digests and Feed Coal.	114
Table 28. Composition of Hydrogenation Reaction Products for CBB.	121
Table 29. PAH Species in Fresh and Recovered CBB	124
Table 30. Elemental Composition of Digestion Reaction Species for CBB.	125
Table 31. Properties of Hydrogenation Products using Fresh Solvent.	130
Table 32. Properties of Hydrogenation Products using Recovered Solvent.	130
Table 33. Elemental Composition of Solvents at Different Processing Points.....	135
Table 34. Carbon Balance of Select Hydrogenation Runs For all Three Solvents.	135
Table 35. Hydrogen Balance of Hydrogenation Runs for Three Solvents.	136
Table 36. Properties of the Feed Pitch.	143
Table 37. Sample Identification.	154
Table 38. Activation Energies for the Air-blowing of Three Types of Pitches.	171
Table 39. Details of Vacuum Distillation of Coal Digests.	203
Table 40. Effect of Devolatilization on Maximum Fluidity and Softening Point.	211
Table 41. Effect of Heat Treatment on Foam Precursor Properties.....	212
Table 42. General Properties of Carbon Foam Derived from Different Precursors.	213
Table 43. Compressive Strength of Carbon Foams	214
Table 44. Tensile Measurements of Synthetic Pitch Fiber.	220

Table 45. Tensile Measurements of Synthetic Pitch Fiber.	221
Table 46. Materials Cost Balance for Synthetic Binder Pitch.	223
Table 47. Materials Cost Balance for Synthetic Binder Pitch	225
Table 48. Mass and Cost Balance for Green Coke.	226

1.0. EXECUTIVE SUMMARY

1.1 Background

This DOE National Energy Technology Laboratory-sponsored effort has developed new technical approaches to produce carbon products from bituminous coal using mildly hydrogenated aromatic oils as part of a solvent extraction process. The focus of this effort was on development of lower cost solvents, milder hydrogenation conditions and improved yield. All three goals were achieved.

The solvent extraction process relies on the ability of certain solvents to dissolve the organic portion of coal. The insoluble portion, consisting mainly of mineral matter and fixed carbon, is removed via centrifugation or filtration, leaving a liquid solution of coal chemicals and solvent. This solution can be further refined via distillation in order to remove low-boiling-point, low-molecular-weight species, thus permitting the properties to be tailored to meet product specifications.

In this way, synthetic pitches can be created. Pitches, such as binder pitch or impregnation pitch, can be commercially viable products in their own right. Alternatively, pitches can be precursors for various types of solid carbon cokes (such as anode coke or needle cokes). Pitches can also be spun into carbon fibers. Structural carbons, such as carbon foams, can also be created by processing pitches.

This technology is needed because of the long-term decline in production of domestic feedstocks such as petroleum pitch and coal tar pitch. Petroleum pitch is usually obtained as the residue from distillation in refineries. However, the rising price of liquid fuels militates in favor of refinery processes that maximize liquid fuel production. As a consequence, the long term trend has been for American petroleum refineries to produce less petroleum pitch every year.

The production of coal tar pitch, as in the case of petroleum pitch, has likewise declined significantly over the past two decades. Coal tar pitch is a byproduct of the production process for metallurgical grade coke (met coke). Because met coke is a low margin business, it has been in a long term decline. Several met coke ovens have been decommissioned over the past two decades and have not been replaced. In addition, modern coke ovens recycle coal tar as fuel in order to enhance energy efficiency and minimize environmental emissions. As a consequence, then, old sources of coal tar are being taken off line and are not being replaced. The long-term trend is a reduction in coal tar plant.

Because carbon feedstocks are in decreasing domestic supply, the trend has been to import feedstocks, mainly from Eastern Europe and China, despite the relatively large transportation cost.

To reverse this trend, a new process for producing carbon products is needed. The process must be economically competitive with current processes, and yet be environmentally friendly as well.

Solvent extraction processes provide this opportunity. The use of low-cost materials such as coal-derived aromatic oils results in a materials cost of \$120 per ton of

pitch product. Given that the current market price for binder pitch is in the range of \$300 per ton, a profitable process is possible if production costs are sufficiently low.

1.2 Summary of Key Accomplishments

a. *Low cost solvents have been identified* with equivalent performance compared to specialty solvents such as tetralin (hydrogenated naphthalene). Although very effective, the relatively high cost of tetralin (~\$1000 per ton) makes it difficult to produce products such as binder pitch, with a market price of about \$280 per ton as of 2004. If the solvent cost is much higher than the market price of the intended product, it is necessary to recover and recycle nearly 100% of the solvent used in the process. This can be problematic in many processes. Accordingly, the efforts of the present study emphasized the use of commercial grade aromatic oils as solvents. The solvent cost is thus \$200 per ton or less. The effectiveness of the lower cost aromatic oils was found to be similar to the higher priced tetralin-based processes.

b. A mild hydrogenation technique was found to be effective in greatly increasing the solubility of coal in the low cost solvents described above. Hydrogen donor solvents were originally developed in support of synthetic fuels efforts, in which case as much as 10% by weight hydrogen must be added to the original coal to yield a satisfactory synthetic crude. In addition to the obvious expense of adding hydrogen (on-site production cost of at least \$1000 per ton versus \$50 per ton of raw coal), the addition of so much hydrogen typically requires a hydrogen overpressure of up to 3000 psi at temperatures in excess of 400 °C, resulting in the need for substantial capital investment in high pressure autoclaves.

The processes developed in this effort require substantially less hydrogen, typically in the range of half a percent hydrogen by weight. Thus only a few dollars worth of hydrogen is required to produce a ton of synthetic pitch. Similarly, pressure requirements are also significantly reduced as only a several hundred psi are required for these processes.

c. *Very high solubility was achieved using the mildly hydrogenated solvents* described above. Approximately 90% dissolution of bituminous coal on a dry, ash-free basis was achieved, which is comparable to the performance of tetralin. In addition, this is a significant improvement compared to previous processes that used n-methyl pyrrolidone as a solvent, which resulted in solubilities of up to about 70%. As a result, the processes used for synthetic pitch production are shown to have a lower materials cost, and yet result in higher performance compared to competing processes. It appears that it is possible for synthetic pitch to compete against conventional supplies of petroleum pitch and coal tar pitch.

d. Lower pressure processes for synthesizing carbon foam have been realized, by modifying the properties of precursor pitches. By reducing the pressure requirement from hundreds of psi to approximately ambient pressure, much simpler processing

conditions are required. This in turn can reduce capital investment requirements and increase the material throughput.

e. Parameters for production of spinnable coal-derived pitches have been derived, and the performance envelope for various pitch derived fibers has been established. Results obtained in this study are less optimistic than previous published results, however. Our results suggest that coal derived isotropic carbon fibers so far have been comparable to petroleum pitch fibers, rather than exceeding the state of the art as had been reported elsewhere.

2.0. Introduction

2.1 Carbon Product Markets

The Carbon Products industry is an essential part of the US and world economy. As shown in the below table over 19,000,000 tons of carbon products are produced worldwide, with approximately 3,500,000 tons produced in the United States. Yet, production of many of these products is on the decline in the US, mainly due to the long-term difficulty of supplying fossil fuel-based feedstocks.

Table 1. Estimated Domestic and World Markets for Carbon Products.¹

Product	Primary Feedstocks	Main Applications	Domestic Annual Sales, Tons	Worldwide Annual Sales, Tons
Binder Pitch ²	Coal Tar Pitch Petroleum Pitch	Anodes (Al smelting) Arc furnace electrodes (steelmaking)	800,000	1,500,000
Impregnation Pitch	Petroleum Pitch Coal Tar Pitch	Electrodes, Composites	180,000	380,000
Mesophase Pitch	Petroleum Pitch Coal Tar Pitch	High performance composites, fibers	800	3700
Anode Coke	Petroleum Pitch	Anodes (Al smelting)	1,800,000	8,000,000
Needle Coke	Petroleum Pitch (US) PP + CTP (Japan)	Arc furnace electrodes (Steelmaking)	400,000	1,300,000
Carbon Fiber (PAN) ³	Petrochemicals	Non-graphitic composites	10,000	24,000
Pitch Fibers ⁴	Coal tar pitch, Petroleum Pitch	Graphitic composites	200	3000
Carbon Black ⁵	Petroleum Pitch, Coal Tar Pitch	Rubber additives, various other	1,800,000	8,000,000
Carbon Foam ⁶	Petrochemicals, Coal, Coal Tar Pitch	Structures, electrochemical systems,	200	200
Carbon Nanofibers ⁷	Natural Gas, Gasified Coal	Polymer additives	50	150
Other Carbon Nanomaterials	Various	TBD	<1	<1

2.1.1 Pitches

As indicated in the previous table, pitches can be derived from either petroleum or coal. Pitches are hydrocarbon materials that exhibit softening characteristics above ambient temperature, prior to devolatilization. That is, pitch is solid at ambient temperature and undergoes a phase change as it is heated. Pitches typically do not have a true melting temperature, since they are often comprised of many chemical species. Thus, raw coal is not considered to be a pitch because coal usually devolatilizes before it softens. Although “tar” is sometimes used interchangeably with “pitch,” in general, “tar” refers to a hydrocarbon material prior to distillation, and the “pitch” is the remainder after lighter, lower-boiling-point chemicals have been distilled off.

Metallurgical coke ovens produce metallurgical grade coke by devolatilizing coal at high temperatures. The volatile chemicals are condensed as coal tar, which is collected and sent to a distillation plant. The lower boiling point liquids are distilled into different fractions, leaving behind a pitch. This pitch can be tailored into different grades such as binder pitch or impregnation pitch.

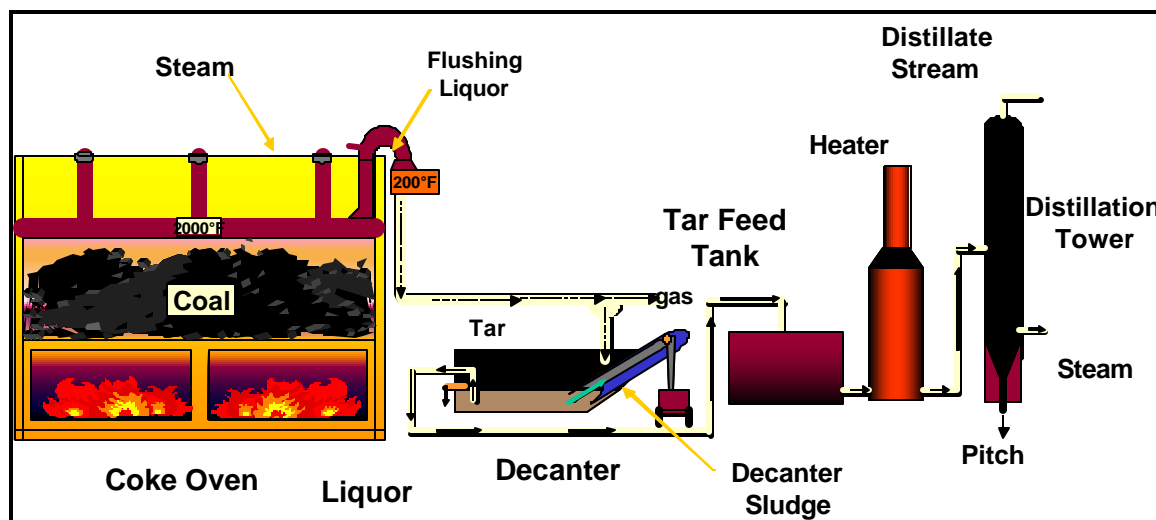


Figure 1. Metallurgical coke oven schematic showing coal tar pitch recovery. Courtesy of Koppers Industries.

Likewise, petroleum pitch is obtained as the bottoms from petroleum distillation. Petroleum pitch quality varies widely depending on the source of crude petroleum and the type of refining techniques used. Some petroleum pitches are of sufficiently high quality that they can be blended with coal tar pitch to be used as binder pitch or impregnation pitch. Other petroleum pitch can be used as a precursor for different types of coke.

2.1.2 Cokes

The basic constituent of most carbon and graphite products is coke. Coke is simply the carbon remainder from heating a hydrocarbon in a non-oxidizing environment. In the case of petroleum pitch, supplies depend upon delayed cokers. Delayed coking is

a thermal cracking process of crude petroleum derivatives. Initially, the feed material is heated and injected into a holding reservoir or coking drum, whereupon it devolatizes over a period of about a day, eventually liberating light hydrocarbons with the remainder forming petroleum coke (hence the term “delayed” coking, since the coke is formed some time after initial heating). To liberate the coke, the coking drum is opened and high pressure water jets are used to liberate the contents.

Depending on the type and quality of the feedstock and coking protocol, the resultant coke can be graded as (ranging from highest to lowest quality) needle coke, anode coke, sponge coke, or shot coke. Needle coke is formed from highly aromatic fractions from refinery cracking, which can form characteristic needle-like crystalline structures upon coking. These needle structures have a sufficiently long range order such that they can ultimately be annealed to the graphite crystal structure. Sponge coke, on the other hand, is formed from petroleum feedstocks having a large number of cross-linkages with less than 6 carbon atoms, which tend to produce isotropic or amorphous structures. This structure is unsuitable for graphitization. Shot coke results from coking feeds high in density and asphaltenes.

From the standpoint of carbon products, anode coke and needle coke grades are the most important, since they can result in carbon and graphite composites.

The coke that is produced in the delayed coker still contains several mass percent volatiles, and is referred to as a “green coke.” The green coke is typically sent to a calciner, or high-temperature heat treatment facility, which soaks the green coke at over 1300 °C, thus removing the residual hydrocarbons. The calcined coke can then be used as anode grade coke.

In the case of needle grades, conversion to graphite requires an additional heat treatment step. Full graphitization is normally accomplished at around 3100 °C in a high temperature resistively-heated Atcheson furnace.



Figure 2. Marathon-Ashland Delayed Coker. Photo courtesy Marathon Ashland and Jer-Co Industries Inc.

2.1.3 Aluminum Industry

The aluminum industry bears special mention because it represents one of the largest consumers of carbon products. Indeed, carbon is inherent to the current process of producing aluminum from aluminum oxide, Al_2O_3 (aluminum oxide is produced from natural ores via the Bayer Process). Then, the aluminum oxide is converted to aluminum metal through the Hall-Heroult process.

The Hall-Heroult process uses electrochemical means to reduce aluminum oxide to aluminum metal. Direct current flows from the anode through an electrolytic bath that contains the dissolved alumina. The aluminum is liberated from the oxygen in the aluminum oxide and deposited at the cathode. The oxygen combines with carbon from the anode to form carbon dioxide which is released as a gas. Thus, the anode is consumed during the process. A carbon lining is used as a containment vessel and to collect the current as it leaves the molten aluminum. The overall reaction for this process is highly endothermic:



Thus, the manufacture of one pound of aluminum requires the consumption of about 0.4 pounds of carbon. The carbon is supplied in two forms: anode grade coke, derived from petroleum pitch, and binder pitch, which is usually produced from coal tar pitch, although in recent years the decline in supply of coal tar has resulted in the use of blends of coal tar pitch with petroleum-derived additives. Briefly, anode grade coke and binder pitch are combined and baked. The binder pitch is initially a liquid and serves to bond the coke pieces together. Ultimately the binder rigidizes and a solid anode material is created. Although the electrical conductivity is not as high as that of graphite, anodes are conductive enough that they can be used in Hall-Heroult cells.

On an industrial level, the Hall-Heroult process is carried out in devices called reduction cells. A group of cells is connected in series to form a potline. Although there are two basic types of reduction cells, the Soderberg cell and the prebake cell, Soderberg cells (in which carbon anodes are baked in situ) are being phased out in some countries due to environmental reasons. Thus pre-bake cells are more representative of the preferred method for producing aluminum metal in the near term. A schematic of a pre-bake cell is shown below. It has a steel shell, lined with a refractory material and carbon. The refractory material serves to reduce energy losses from the cell, and the carbon serves as the cathode.

To summarize, the aluminum industry is the major consumer of carbon products because carbon must be consumed in order to produce aluminum metal from the oxide state found in nature. The consumable anodes used in modern aluminum smelting plants are created from a combination of calcined petroleum coke, and a binder pitch derived from coal as a byproduct of met coke production.

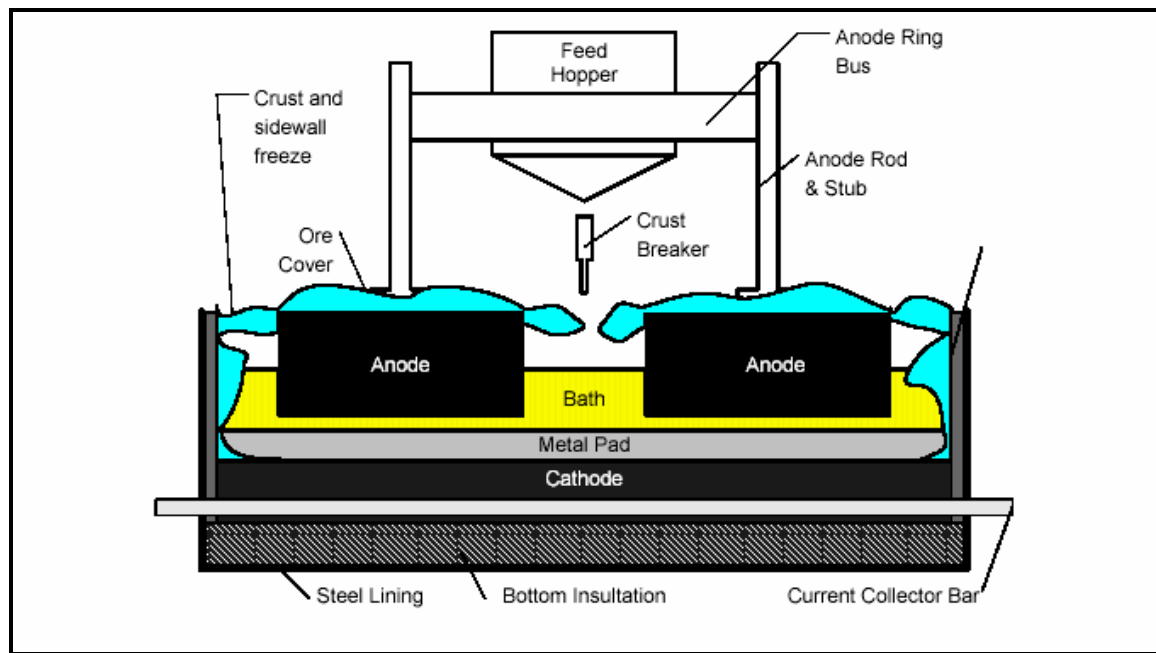


Figure 3. Hall-Heroult Reduction Cell (pre-bake type).

2.1.4 Graphite Electrodes for Arc Furnaces for Metals Smelting

In analogy with carbon required for anodes consumed in aluminum manufacture, arc furnaces represent a major application for graphite. Graphite is more highly ordered (anisotropic) than anode grade carbon. Hence, graphite is substantially more expensive than anode grade carbon, and is consumed in substantially lower quantities.



Figure 4. Arc furnace with Graphite electrodes. courtesy GrafTech International.



Figure 5. Close-up of arc furnace electrodes, operating at 3000 °C. Courtesy GrafTech International.

2.2 Declining Supplies of US Feedstocks for Carbon Products

As discussed in the preceding analysis, there are two main sources of feedstocks for carbon products used in metals smelting industries:

- a. *Coal tar pitch* is obtained as a condensable byproduct from metallurgical coke ovens. It is used as the primary source of binder pitch, although in recent years petroleum pitch is being used as an extender or blending agent.

b. *Petroleum pitch*, obtained at the bottoms from petroleum refining processes is used to produce virtually 100% of the anode coke and needle coke used in the metals smelting industries. The anode coke is used to produce Hall-Heroult anodes for the aluminum industry, and needle coke is used mainly for electrodes incorporated in arc furnaces. Petroleum pitch can also be used as an extender for binder pitch and impregnation pitch.

Both feedstocks are in short supply, and their future viability is in question. The supply of binder pitch in the US has been steadily decreasing over the past decades, as shown in the Figure below. One of the main reasons is it is a commodity business with small profit margins. In addition, there is an environmental burden created by coking coal to create met coke, which has decreased the attractiveness of producing met coke and consequently the coal tar byproduct. If new coke ovens are built in the US, they will likely combust nearly all of the volatiles to produce energy, with excess energy being used to produce electricity (referred to as a “non-recovery met coke oven”). Thus these newer ovens will not offset losses in coal tar production elsewhere.

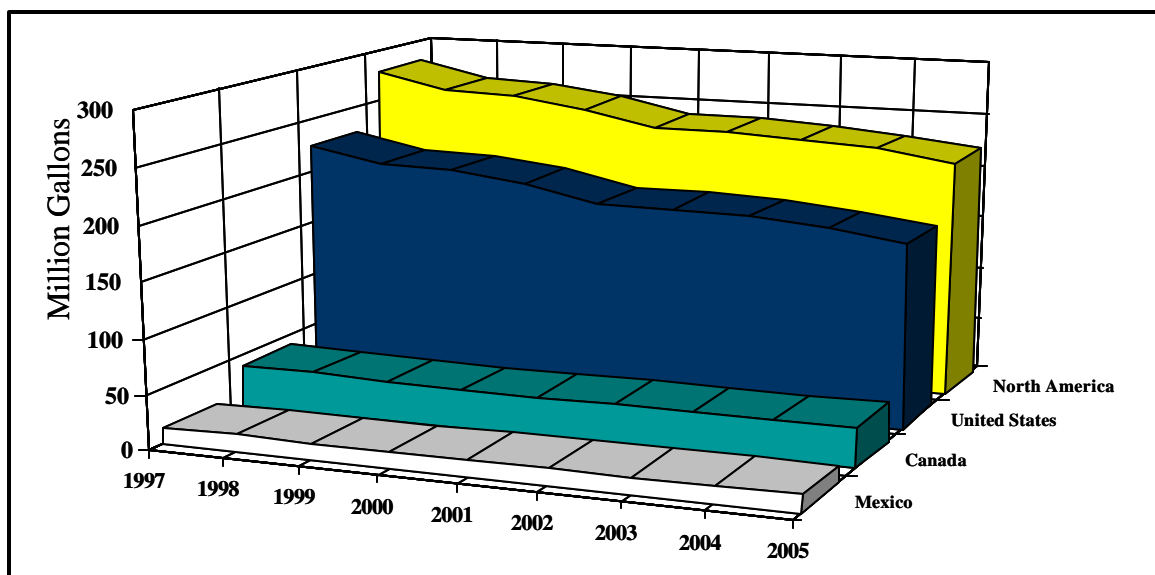


Figure 6. Koppers Industries estimates that coal tar pitch production will continue to decrease, despite increases in demand.

The supply of high quality anode coke has likewise been decreasing, with quality decreasing concomitantly. The figures below illustrate how vanadium and sulfur impurities, which need to be minimized in order to increase oxidation resistance, have been slowly increasing since the early 1980s. As a result, the overall quality of anodes is declining, resulting in lower production efficiency, and increased electric power consumption at the plant level.

The lower quality of anode coke can be attributed to the increased demand for liquid fuels from refineries. As a result, petroleum refineries seek to optimize production of liquid products and employ techniques such as catalytic cracking and hydrocracking

that minimize the generation of pitch precursor materials. In addition, as petroleum producers are challenged to produce more petroleum in response to increased worldwide demand, very little high purity sweet crude petroleum is being produced. The lower quality feedstocks result in higher impurity content. This trend is expected to continue as oil drilling accesses less desirable crude oil sources and refiners enhance refining processes to maximize liquid fuel yield.

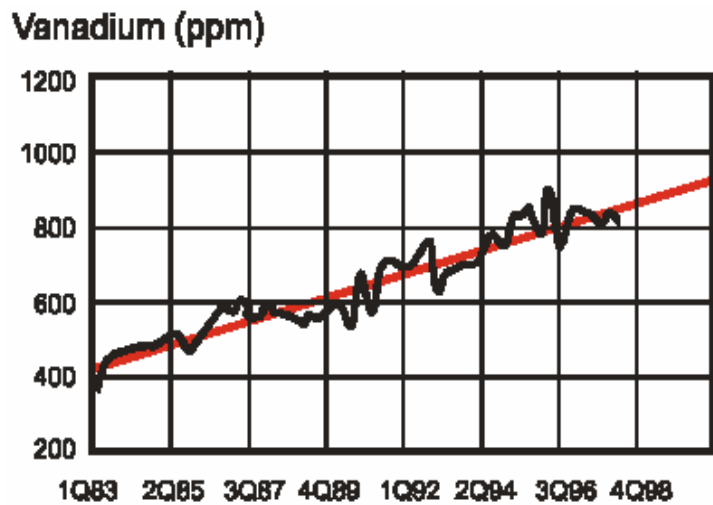


Figure 7. Vanadium levels in commercial US green anode coke have been rising for the past two decades.⁸

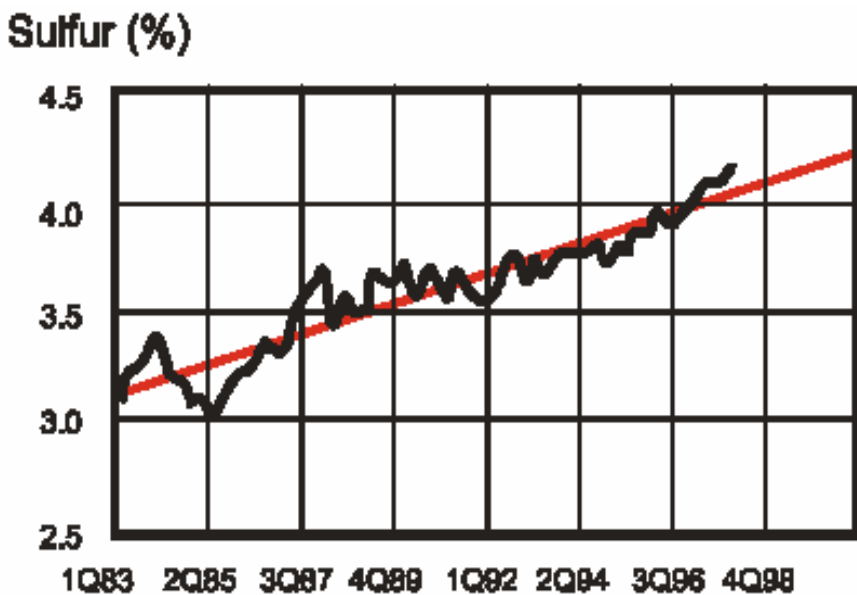


Figure 8. Sulfur levels are increasing in US green anode coke.

2.3 Coal as a Material Feedstock

The basic concept of the research described herein is that coal is not simply an energy source, but can also be thought of as an ore or chemical feedstock that can be processed to create value added products. The primary process investigated in this effort has been mild hydrogenation and solvent extraction to produce pitch and coke precursors. Accordingly, this methodology begins with a preliminary investigation of coal itself.

Coal formation involves two different stages: the biochemical stage and the geochemical stage. The biochemical stage begins with the formation of peat beds as plant material settles under water in low, swampy areas. At this stage, bacteria and fungi begin to decompose the plant material by removing oxygen and hydrogen and giving off water, carbon dioxide, and methane. The biochemical stage of coal formation ends as more and more sediment begins to cover the peat layer. As the peat is further submerged and the sediment layer gradually increases to approximately 40 centimeters, bacteria and fungi cease to exist, thus ending the biochemical stage.

The second stage of coalification is the geochemical stage. During this stage, the peat bed undergoes further decomposition due to the elevated temperature and pressure from further layers of sediment depositing on top of the peat bed. Oxygen and hydrogen are again eliminated as methane, carbon dioxide and water. As this proceeds, the carbon content is slowly increased. Depending on the time, temperature and pressure to which the coal is subjected, different degrees of coalification or ranks that vary from anthracite through bituminous and sub-bituminous coal to lignite are obtained.

Anthracite is the highest or most mature rank of coal, while lignite is the lowest. The American Society for Testing and Materials (ASTM) classifies coal by the amount of fixed carbon or volatile matter for medium-volatile bituminous coal through anthracite. The lower ranked coals, lignite through high-volatile A bituminous, are ranked by their heating value and agglomerating character. The ASTM classification is shown in the table below.

With the amount of carbon decreasing with decreasing rank, other elements like hydrogen and oxygen must increase in concentration, but the nitrogen and sulfur content vary little with rank. Instead, the content of the nitrogen and sulfur depends on the location where the coal was formed. It can be seen that as coal rank decreases, the hydrogen-to-carbon ratio increases. Also, the amount of oxygen decreases compared to carbon with increasing rank. All of these elements are bonded together to form various aromatic rings, aliphatic chains, and a wide range of functional groups.

Table 2. The ASTM System for Classifying Coals by Rank.⁹

Class	Group	Fixed	Volatile	Heating
Anthracite	Metaanthracite	>98	<2	
	Anthracite	92-98	2-8	
	Semianthracite	86-92	8-14	
Bituminous	Low-volatile	78-86	14-22	
	Medium-volatile	69-78	22-31	
	High-volatile A	<69	>31	>14,000
	High-volatile B			13,000-14,000
Sub bituminous	High-volatile C			10,500-13,000
	Sub bituminous A			10,500-11,500
	Sub bituminous B			9,500-10,500
Lignitic	Sub bituminous C			8,300-9,500
	Lignite A			6,300-8,300
	Lignite B			<6,300

Note: This classification system is based on ASTM standard D 388-66, which is published annually by ASTM in their compilation of standards. ^a The fixed carbon and volatile matter, reported as percentages, are determined on a dry, mineral-free basis. The mineral matter is calculated from the ash content by the Parr formula: mineral matter=1.08 [percent ash +0.55 (percent sulfur)] ^b The heating value, reported in British thermal units per pound, is expressed on a moist, mineral-free basis.

Most of the functional groups that are present in coal are those that include oxygen, like phenols, alcohols, ethers, carboxylic acids, and carbonyls. A complex model of a basic coal structure was proposed by Wiser based on the relative abundance of each atom and functional group. This model is shown in the figure below. Weak bonds in the coal structure are identified by the arrows. Coal liquefaction and dissolution requires breaking the molecular structure of coal into small soluble fragments at these weak bonds.

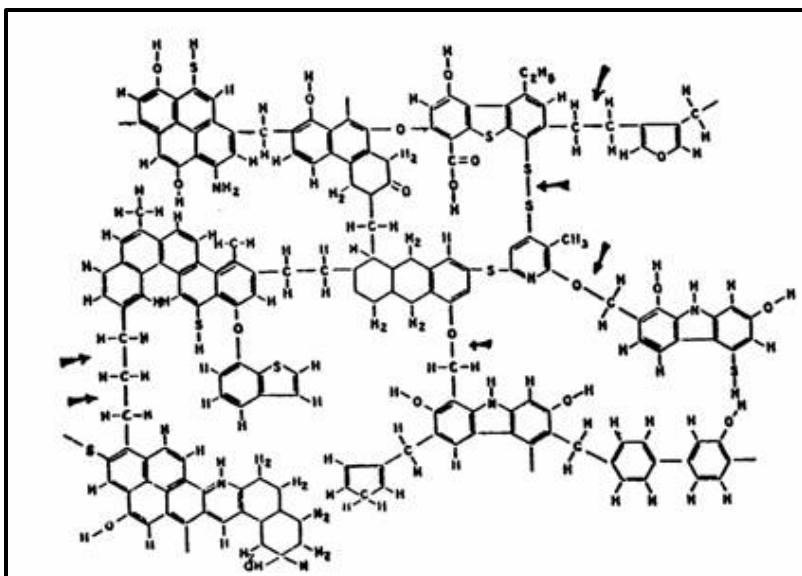


Figure 9. One Typical Molecular Unit in Coal.¹⁰

Petroleum and coal have been competitors in producing value-added carbon products. However, petroleum is usually preferred over coal, due to its liquid form and the nature of the properties of the products. In order for coal to be considered as a possible precursor to high-value carbon products, its products must have properties similar to that of petroleum. One of the major difference between coal and oil is that the molecular weight of crude oil has a range of 150 to 250, while the average molecular weight of coal usually exceeds 1000. Another major difference between coal and oil is that on average the atomic hydrogen-to-carbon ratio for coal is much lower than that of oil. The typical value for crude oil lies between 1.4 and 1.9, while the average value for coal is only about 0.8. For comparison, a list of typical hydrogen-to-carbon atomic ratios for several coals and hydrocarbons is shown below.

Table 3. Typical Compositions of Coals and Liquid Hydrocarbons.^{11,12}

Sample	Element, %wt (dry ash-free basis)				
	C	H	O	N	S
Meta-anthracite	97.9	0.21	1.7	0.2	-
Anthracite	95.9	0.89	1.8	0.3	1.8
Anthracite	92.8	2.7	2.9	1.0	0.6
Semianthracite	90.5	3.9	3.4	1.5	0.7
Low volatile bituminous	90.8	4.6	3.3	0.7	0.6
Medium volatile bituminous	89.1	5.0	3.6	1.7	0.6
High volatile A bituminous	84.9	5.6	6.9	1.6	1.0
High volatile B bituminous	81.9	5.1	10.5	1.9	0.6
High volatile C bituminous	77.3	4.9	14.3	1.2	2.3
Subbituminous A	78.5	5.3	13.9	1.5	0.8
Subbituminous B	72.3	4.7	21.0	1.7	0.3
Subbituminous C	70.6	4.8	23.3	0.7	0.6
Lignite	70.6	4.7	23.4	0.7	0.6
Asphaltine	87	6.5	3.5	2.2	0.37
Toluene	91.3	8.7	-	-	-
Petroleum Crude	83-87	11-14	-	0.2	1
Gasoline	86	14	-	-	-
Methane	75	25	-	-	-

The original hydrogen-to-carbon ratio must be increased in order for coal products to be comparable to those obtained from petroleum, in terms of liquid fuels. There are two different ways of performing this task: the addition of hydrogen or the rejection of carbon.

2.4 Methods for Converting Coal to Material Feedstocks

Several processes can be considered as means to convert coal into commercial feedstocks. Generally speaking, commercial processes are available that can handle organic forms of carbon and provide additional processing to convert organic carbon to value added carbon products. However, mineral matter, impurities and inorganic carbon are more difficult to effectively utilize. Thus the conversion of coal to a material feedstock can largely be reduced to a problem of selective purification and conversion.

2.4.1. Pyrolysis

Pyrolysis or carbonization is shown as the bottom process in the following figure. This technique employs the approach of rejecting carbon as its method of increasing the hydrogen-to-carbon ratio of raw coal. Pyrolysis takes place as coal is thermally treated in the absence of oxygen to form hydrogen rich liquids and gases and a carbon rich residue, termed either char or coke. This is done in the absence of oxygen, so that combustion reactions do not take place. This is the one method whereby a large number of carbon atoms are rejected as solids, with the liquid and gaseous products containing a much higher hydrogen/carbon ratio. Depending upon the temperature of operation, coal carbonization processes can be classified into two types: (1) Low temperature carbonization carried out at 500-700 °C and (2) High temperature carbonization carried out at temperatures in excess of 700 °C. The latter is employed for the manufacture of metallurgical coke as a main product while coal tar is also produced as a side product. The liquid products, or coal tar, formed from the condensed volatile matter, can be processed further by hydrogenation and desulfurization to create valuable products. These can be used as feedstocks for the production of dyes, plastics, synthetic fibers, pharmaceuticals, solvents and pitches. The quantities of gas, liquid, and char produced depend on the type of coal, the rate of heating, the nature of gas atmosphere surrounding the coal, and the ultimate temperature achieved.

2.4.2 Liquefaction

Liquefaction is the process of converting coals to liquids. Historically this has been accomplished primarily for the purpose of creating liquid fuels. The fundamental processes for producing coal derived liquid fuels were developed by German scientists prior to World War II. Although numerous variations of these processes exist, the basic processes can be grouped into two categories. Indirect liquefaction involves gasification and generation of diesel fuel or other liquids under the influence of catalysts.

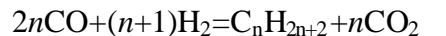
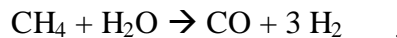
Direct liquefaction involves the use of hydrogen gas to cause chemical changes within the coal structure to produce a synthetic liquid crude, which is then refined via distillation into different fractions.

The processes developed in the present study are variants of direct liquefaction and may be referred to as partial direct liquefaction or mild direct liquefaction. In general, the production of synthetic crude requires the addition of several weight percent hydrogen. This in turn requires very high pressure and temperature. In addition, liquid fuels require largely aliphatic chemicals. By contrast, it can be appreciated that carbon

precursor feedstocks can be developed with an order of magnitude less hydrogen. Moreover, high value carbon products require an aromatic character rather than an aliphatic one. These factors militate strongly in favor of coal as a feedstock for carbon materials.

2.4.3 Indirect Liquefaction

Indirect liquefaction employs the approach of adding hydrogen as its method of increasing the hydrogen/carbon ratio. In this technique coal is converted to a gas by a combination of heat and catalysis through processes such as steam reforming and water gas shift. In the presence of a catalyst such as cobalt or iron, Fischer-Tropsch reactions can produce linear alkenes and alkanes as well as some oxygenates. The main reactions of interest are as follows:



Also, depending on the process conditions, the products can be highly selective to hydrocarbon liquids like gasoline, kerosene, diesel fuel, and fuel oil. Products such as methanol and acetone can also be produced depending on the specific type of catalyst. Several types of commonly used catalysts are Fe, Co, Ni, Ru and ZnO_2 . Also, the destruction of the original coal structure involves a large amount of energy and processing can be very expensive in terms of thermal efficiency.

2.4.4 Direct Liquefaction

Direct liquefaction has advantages over the other processes discussed here, in terms of both thermal efficiency and economics. Both of these advantages are derived from the fact that fewer chemical changes are required to convert solid coal into liquids than into gases, and the process conditions are milder. Like gasification, this scheme also involves addition of hydrogen as the method of increasing the hydrogen/carbon ratio. This scheme consists of two alternate processes: (1) hydrogen-donor solvent extraction or dissolution and (2) catalytic hydrogenation.

The first process is basically a reaction with a hydrogen donating solvent. The purpose of solvent extraction is to produce, with minimum treatment, a relatively clean burning fuel from coal. The fuel can be either in solid form, known as solvent refined coal (SRC), or in liquid form. Hydrogenation not only increases the hydrogen content in coal, but also reduces the undesirable heteroatoms, such as sulfur, nitrogen, and oxygen, by combining them with hydrogen. The degree of removal of these undesirable elements

depends on the degree of hydrogenation. In general, in solvent refined coal all the inorganic sulfur and part of the organic sulfur are removed, and the sulfur content is reduced to below 1 %. Two important factors in solvent extraction are the nature of the donor solvent and the presence of hydrogen pressure. To increase the hydrogen donor capability the solvent is frequently hydrogenated before use. In commercial practice the solvent is obtained by recycling part of the oil product stream. In the present research, this approach was followed to convert coal into a solid carbon product (pitch) instead of a liquid fuel.

When catalyst is added to the coal-solvent slurry, the process is known as direct catalytic hydrogenation, or hydroliquefaction. Catalysts such as cobalt molybdate, tungsten, molybdenum sulfide, and iron oxide have been successfully used. The operating conditions are approximately 450 °C and 2000-4000 psia hot hydrogen pressure. The degree of hydrogenation is much higher than that obtained with solvent extraction, and thus the problem of solid separation is much less severe due to enhanced conversion. Furthermore, most of the heteroatoms in coal are converted to H₂S, H₂O, and NH₃. These compounds leave with the gas stream, resulting in a much cleaner product than solvent-refined coal. The coal is converted to liquids ranging from heavy to light oils and gases.

Although historically direct liquefaction has been envisioned mainly as a means to produce fuels, it is also able to produce pitches and coke precursors. The production of fuel feedstocks is accomplished at a relatively high hydrogen concentration, say around 10 weight percent or higher. This requires very high pressure and temperature. On the other hand, conversion of coal and coal liquids to pitch can be accomplished with less than 1 weight percent hydrogen.

2.4.5 Reaction Pathways of Coal Liquefaction

It is proposed that the transfer of hydrogen to coal from a solvent follows a free radical mechanism, in which the coal molecules are thermally cleaved into free radicals, which seek stabilization.¹³ Wiser concluded that during each of these ruptures of the covalent bonds, two free radicals are formed, and that these free radicals are capped in one of three ways: (1) addition of atoms (such as hydrogen) or other radical groups to the free radicals, (2) rearrangement of atoms within the free radical, and (3) polymerization of the free radical.¹⁴

The first method of capping the free radical is the desired method when performing coal liquefaction with a hydrogen donor solvent. This allows the large coal molecules to be thermally degraded, capped with hydrogen, and stabilized as low molecular weight, hydrogen-rich species.¹⁵ The second and third methods take place when there is not a hydrogen donor solvent available or the hydrogen donor components in the solvent are limited. If the free radical species or the reacting solvent contains polycyclic aromatic units (H-shuttlers), the free radical species can cap themselves by shuttling hydrogen from the hydrogen rich part of the coal. Finally, if the free radical species is stable and in the presence of other free radical species, polymerization or retrograde reactions could take place. This is the basis for the formation of coke, char, and other large molecular weight, insoluble species. Therefore, for the formation of low molecular-weight carbon-product precursors, the first method is preferred.

The conversion of coal to liquid hydrocarbons can be visualized as a progressive hydrogenation through a series of intermediate products such as preasphaltenes, asphaltenes, carbenes and carboids. Berkowitz suggested a model for the general process occurring during donor-solvent liquefaction.¹⁶ The intermediate stabilized species are the preasphaltenes, which are further reduced in molecular weight to asphaltenes and then to distillable oils and hydrocarbon gases. The latter compounds are also generated at each step of the main reaction path as by-products. The first step in this reaction path is coal solubilization or autostabilization, which involves redistribution of hydrogen within the coal matrix, with the solvent acting as a net shuttler of hydrogen.¹⁷ The second step occurs when secondary hydrogenation takes place. Secondary hydrogenation depends on the specific reaction conditions and drives the products toward lower molecular weight species.

Tetralin can be used as a model hydrogen donor solvent for studying the chemistry and kinetics of coal liquefaction.¹⁸ A simple model is that tetralin donates hydrogen to form new chemical species in coal, i.e.,



Alternatively naphthalene can be formed via simple dehydrogenation of tetralin resulting in the formation of hydrogen gas.¹⁹

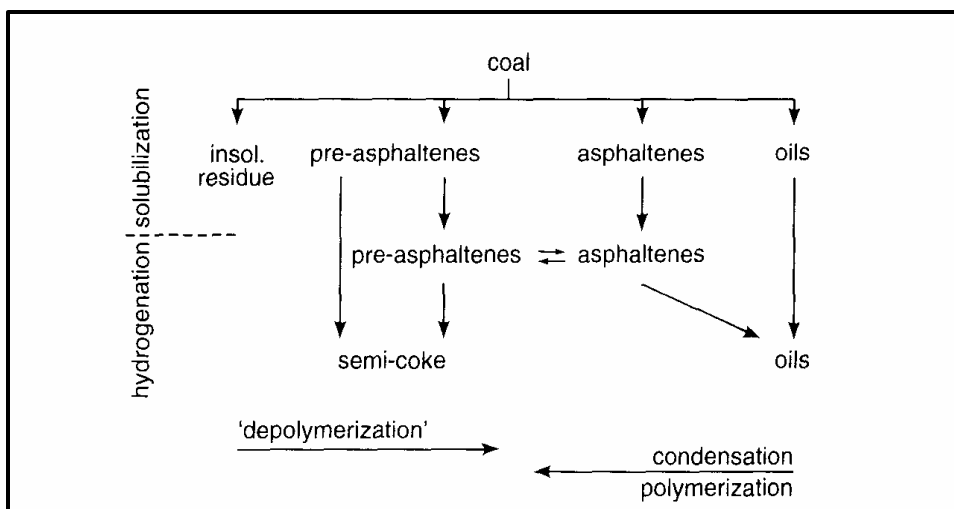


Figure 10. Conceptual Reaction Sequences in Coal Liquefaction.²⁰

Through laboratory studies and pilot plant operations, properties of coal that affect liquefaction results have been compiled and are summarized in the following table.

Table 4. Fundamental Properties Important in Coal Liquefaction.²¹

Property	Influence	Desired level
Rank	Liquids yield	Medium
Ash content	Operations and handling	Low
Moisture content	Thermal efficiency	Low
Hydrogen content	Liquids yield and hydrogen	High
Oxygen content	Gas and hydrogen yield	Low
Extractability	Liquids yield and quality	High
Aliphatic character	Liquids yield and quality	High
Reactive macerals ^a	Liquids yield	High
Particle size	Operations	Fine/very fine

^a Principally vitrinites and exinites

2.5 Commercial Coal Liquefaction Processes

Commercial liquefaction technologies involve hydrogenating coal in a solvent slurry under elevated temperatures and hydrogen pressures (370-480 °C and 1500-4000 psig). High temperatures are required to crack the coal thermally and produce reactive fragments while high hydrogen pressures are required to cap these sites with hydrogen. Depending on the reaction conditions lower molecular weight gases and liquids are formed and recovered from the remaining solid material. Three major commercial liquefaction technologies are discussed below.

2.5.1 H-Coal Process

The H-Coal process was developed by Hydrocarbon Research Inc. (now Hydrocarbon Technologies Inc, a subsidiary of Headwaters Inc) to convert high-sulfur coal into boiler fuels and synthetic crude oil. This process utilized a catalytic ebullated-bed reactor, in which the reaction mixture is recycled upward through the reactor to maintain the catalyst in a fluidized state. The process used crushed (60 mesh) coal slurried with recycled oil, pressurized to 3000 psig and mixed with compressed hydrogen. The mixture was then preheated and fed to the ebullated-bed catalytic reactor that operated between 340-370 °C. The gas product after separation into light hydrocarbons, ammonia and hydrogen sulfide, is mostly hydrogen, which is recompressed and combined with fresh coal-oil slurry. The liquid-solid mixture is separated in a flash separator to recover light and heavy hydrocarbons. The remaining solids and heavy oil are processed in a hydrocyclone and a vacuum distillation column. The process requires between 14000-20000 scf of hydrogen for every ton of coal, depending on the type of oil product desired. A portion of the hydrogen needed is produced in the process itself, while make-up hydrogen is required. The conversion of coal to liquid and gas products for this process is about 90 %.

2.5.2 Solvent Refined Coal (SRC) Process.

The SRC process is a non-catalytic process that converts high ash and high sulfur coal into gas, liquid, and/or solid fuels. The product from the process is a solid,

carbonaceous material that contains less than 1 % sulfur and 0.2 % ash. Pulverized coal mixed with process-derived solvent combines with gaseous hydrogen at 425-455 °C and 1030 psig. The product gases are processed to recover hydrogen which is recycled to the process. The slurry from the separator is processed in a filtration unit to recover a high molecular weight solvent which is then recycled and mixed with fresh raw coal. As mentioned earlier this principle of the SRC is used in the current research to study the process-derived solvent as a hydrogen donor. The final solid product contains very low amounts of sulfur and ash. The schematic of the process is shown in the figure below.

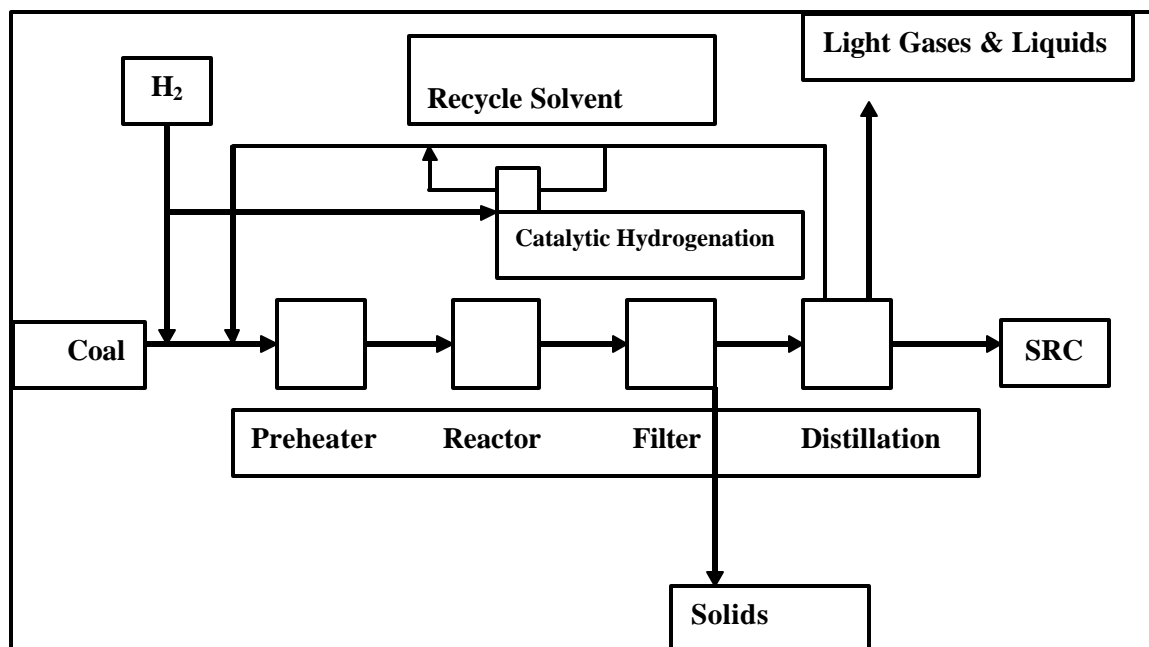


Figure 11. Schematic Sketch of the Typical SRC Process.²²

2.5.3 Exxon Donor Solvent (EDS) Process

The EDS process was developed by Exxon to produce liquid products from a wide range of coals. This is a non-catalytic process which recycles tetralin solvent, with a separate solvent rehydrogenation step. Crushed coal is slurried with recycled tetralin and mixed with recycled hydrogen at 425-465 °C and 1500-2000 psig. The products are separated into three fractions: light hydrocarbons, a naphtha fraction and heavy distillate. The heavy distillate is processed in a vacuum distillation column to yield jet fuel and heating oil. A portion of the heavy distillate between 205-455 °C boiling range is hydrotreated and recycled to form the slurry feed with fresh coal. The remaining bottoms product can be converted to heavy oil using a process called flexicoking. One of the unique features of the EDS process is the ability to adjust the recycled hydrogen donor solvent based on the characteristics of the raw coal feed. The quality of the solvent can be adjusted by controlling the reaction in the hydrotreatment step. By tailoring the donor solvent to match the feed coal, the liquid products can be optimized.

2.6 Liquefaction Solvents

Industrial processes involving coal-derived solvents as liquefaction solvents generally isolate process-derived recovered solvents, which can be recycled back to the process, thereby minimizing the addition of fresh solvent. The chemical composition of these recycle solvents controls the overall behavior of the coal liquefaction process.

Each class of chemical compounds found in industrial recycle solvents has been shown to have relative merits. The components to be considered include H-donors, H-shuttlers and H-abstractors. They have influence on the rate and extent of coal dissolution, coal conversion, hydrogen consumption, product distribution, and the ability to regenerate solvents. In the SRC process no commercial catalyst is employed and only the intrinsic mineral matter entering with the coal acts as a catalyst for coal liquid upgrading and/or maintenance of proper solvent quality. Thus, the SRC process is essentially similar to the work undertaken in this research, the only difference being it was continuous. An external catalyst is not necessary for dissolution, since the coal is often substantially dissolved through interaction with the solvent by the time the coal exits the reactor. The nature of the process and the selectivity to the various products are primarily governed by the composition of the recycle solvent.

Table 5. Effectiveness of Some Typical Solvents for Hydrogenation.²³

Solvent	Benzene Soluble(%, maf coal basis)
o-Cyclohexylphenol	81.6
1,2,3,4-Tetrahydro-5-hydroxynaphthalene	85.3
Tetralin	49.4
Cresol	32.1
Dicyclohexyl	27.2
Naphthalene	22.2
o-Phenylphenol	19.6

^a With 1 atm cold hydrogen pressure without catalyst. The reaction time is 0.5 hr at 400°C with a 4:1 solvent/coal ratio.

Coal conversion can be envisioned to occur in three stages: dissolution of the coal; defunctionalization of the coal and hydrogen-transfer; and rehydrogenation of the solvent. In each of these stages, the nature of the solvent can affect the rates of reaction and the distribution of the products. In the dissolution stage, because of high temperature, the highly crosslinked structure of coal fragments into radicals, which in the presence of H-donors are capped into stable species. In the absence of hydrogen-donor solvents, the original radicals or the smaller soluble species may recondense to form char or coke. The solvent governs product selectivity by controlling the path taken by the intermediate radicals. When a bond cleaves, at least three different pathways are available for product formation: H-abstraction, rearrangement and elimination, and addition to aromatics. The availability of H-donors will determine the preferred path. The specific chemical properties of interest in recycle solvents are:

- a. *Hydrogen-donor capacity of the solvent* – hydrogen donors are believed to be important in the defunctionalization of the dissolved coal and the prevention of char

formation. The principle sources of hydrogen appear to be partially hydrogenated aromatic hydrocarbons: tetralin and its homologs, partially hydrogenated pyrene, phenanthrene, and other polycyclic aromatic compounds.

b. *Physical solubilization of coal products* – effective solvents for coal solubilization must contain polar compounds. Assuming the concept of specific solubility parameters applies, the good solvents should contain such components as polyaromatics, phenols, pyridines, aromatic ethers, and quinolines and their derivatives.

c. *Hydrogen transfer capability (H-shuttling)* – hydrogen transfer is another mechanism for dissolving coal, whereby hydrogen may be supplied from the coal itself or from the SRC to cap off radicals and form smaller soluble species. Reports by Neavel indicate that naphthalene can dissolve 80 % of a vitrinite-rich bituminous coal at short contact times and at temperatures over 750 °F.²⁴ It was proposed that this dissolution was the result of the shuttling of hydrogen from one position in the coal to another. Naphthalene acts as an H-acceptor and the resultant free radical formed by the addition of an H-atom act as an H-donor. A reaction of this type is even more probable for phenanthrene or pyrene since they are better H-acceptors than naphthalene. The structures which can contribute to good shuttling properties within recycle solvents are: Naphthalene and its alkyl derivatives, phenanthrene and its alkyl derivatives, heterocyclic polyaromatics etc. This effect is explained in more detail in the later section.

d. *Chemical structures associated with char formation* – recycled solvents may contain compounds which are prone to or which can promote char formation. Heavy phenols and highly aromatic compounds are some of these compounds.²⁵

2.7 Catalytic Effects of Mineral Matter in Coal

Intrinsic mineral matter can be used to catalyze coal conversion reactions. For example, catalytic activity has been ascribed to the presence of pyrite (FeS_2) or the reduced form of pyrite, pyrrhotite.²⁶ Although potentially useful, catalysis is also potentially detrimental of polymerization is also catalyzed.

In a recent study on the hydrogenation of a high-vitrinite Indian coal (North Assam) in the absence of a solvent, the catalytic effect of mineral matter was studied by characterizing the coal ash and by adding specific minerals.²⁷ The best correlation to activity was found using (organic plus pyritic) sulfur. Other materials - iron, titanium and kaolinite (the prevalent clay) - also correlated with coal conversion to benzene- soluble products. Iron pyrite was suspected to be the active form of iron but conversion also increased with the addition of sulfur or titanium hydroxide.

In another study Whitehurst et al. proved that pyrite addition increased the pyridine solubility of four German coals.²⁸ Samples of a coal enriched in mineral matter were more extensively converted. These reactions were carried out in methyl naphthalene at 752 °F under 3000 psi of hydrogen for 2 hours. These studies indicate the effect of iron pyrite on the solvent-solvent interactions that occur during the liquefaction of coal. These results showed that the rate of solvent-solvent hydrogen transfer reactions occurred

at a higher rate in the presence of coal containing pyrite than in solvent-solvent reactions alone.

A different approach to study the effect of mineral matter in coal is to selectively remove the mineral matter content without altering the organic composition of the coal before reaction.²⁹ The mineral matter present in coal can be selectively removed depending on the type of pretreatment. After the pretreatment of these coals to remove the ash content, the coal conversion dropped with lower ash content (see the following figure) and the hydrogen consumption dropped with lower ash content signifying that some catalytic activity can be attributed to the presence of pyrite. The coal in this study was Wyodak-Anderson coal containing relatively little pyrite but catalysis of hydrogen gas reactions did respond to total ash content. Such behavior would indicate that even ion-exchangeable iron may have catalytic properties.

In summary there are clearly effects of coal mineral matter on the progress of liquefaction. Mineral matter catalyzed hydrogen gas consumption and other reactions of coal and its products. It also aids in solvent rehydrogenation but its activity is low. Acid demineralization, especially for subbituminous coal, increases coal reactivity but decreases conversions and SRC yields at long coal conversion times because of increases in both regressive and forward reactions.

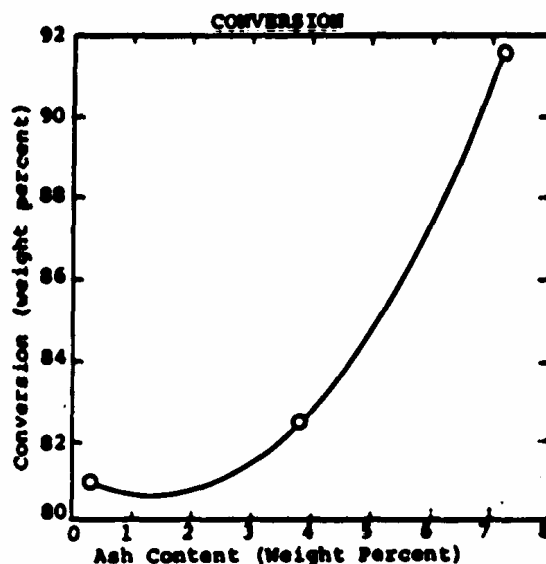


Figure 12. Wyodak Coal Conversion vs. Ash Content.³⁰

2.8 Effect of Hydrogen Pressure on Coal Solubility

The presence of a hydrogen atmosphere can greatly benefit the production of soluble coal increasing the product yield. Molecular hydrogen at high pressure could donate hydrogen and stabilize the coal free radicals in one of two ways: (1) directly donate hydrogen to the free radical or (2) transfer hydrogen to the donor solvent, which can then be transferred to the coal particle. Yen et al. showed that when tetralin is used as a donor solvent, the yield of benzene insolubles under a nitrogen atmosphere was 25.3%.³¹ When the atmosphere was changed to hydrogen, the yield of benzene

insolubles decreased to 13.8% indicating more conversion to benzene solubles. Tomic and Schobert also observed an increase in the amount of conversion when a hydrogen atmosphere is used instead of an inert atmosphere during liquefaction without solvents or catalysts.³² This increase in conversion is believed to occur as hydrogen reduced the amount of retrograde reactions at high temperature.

There also has been some work on the exact source of the hydrogen during the liquefaction reactions. This hydrogen can come from a variety of sources: the solvent, gaseous hydrogen, or from the coal itself. The most efficient source is the hydroaromatics in the solvent but if such materials are limited in concentration, hydrogen gas or coal become the dominant sources. Whitehurst et. al. have shown that even at short times hydrogen gas can be the dominant source of hydrogen for low rank coals where the demand for hydrogen is largest.³³

These liquefaction reactions are also sensitive to H-donors, hydrogen gas and H-shuttlers. The rate of coal dissolution is proportional to the concentration of hydroaromatics in synthetic recycle solvents. Whitehurst et al. found the conversion of Illinois #6 coal at 3 minutes in a series of solvents with varying tetralin concentrations increases with the tetralin content in the solvent.³⁴ This simple relationship is somewhat complicated by hydrogen donation from other sources such as hydrogen gas or the coal itself. It has been proved that low rank coals can give increased yields at short times by application of hydrogen pressure. For higher rank coals (bituminous) hydrogen donation from gas phase is small.³⁵ It is suggested that bituminous coals are efficient sources of hydrogen because a high proportion of the mass is plastic or mobile at liquefaction temperatures.

The donation of hydrogen from hydroaromatic structures in coal can be assisted by certain highly condensed aromatic molecules in the solvent. Such molecules are not net donors of hydrogen but can rapidly equilibrate with hydroaromatics in the coal and can thus "shuttle" hydrogen from one region of the coal to another. The following figure shows a group of solvents of limited H-donor capacity, containing naphthalene and phenanthrene homologs, where the amount of coal becoming soluble in 4 minutes is proportional to the concentration of polycondensed aromatic compounds in the solvent.³⁶ It is noteworthy that a good shuttling solvent can even induce higher solubility than a solvent containing 40 % tetralin (SS in the following figure). So, bituminous coals can give the highest yields and require little hydrogen, but the presence of either good hydrogen donors or hydrogen shuttlers is necessary for high conversion. Sub-bituminous or lower rank coals can give high yields of soluble material but at a slower rate.

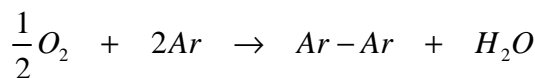
2.9 Temperature Effects upon Coal Liquefaction Reactions

Increasing the temperature of the reaction during coal liquefaction increases all reaction rates. This includes rates of coal dissolution, heteroatom rejection, hydrogen consumption, gas formation and charring.³⁷ The effects of increasing temperature on conversion for bituminous coals have been found to be small at short contact times. With subbituminous coals, for which the rates of dissolution are considerably slower than for bituminous coals, raising the temperature may be desirable for dissolving coal. With one subbituminous coal (Wyodak Anderson) increasing the temperature to 820, 840, 850, and 860 °F gave increasing conversion at short times. The net effect of increasing the

temperature of reaction in long contact time coal conversion is to decrease the SRC yield and increase the yield of light hydrocarbons. This is true either with or without hydrogen donors in the solvent. The products of high temperature conversion also contain lower concentrations of highly polar fractions and are therefore more soluble in hydrocarbons, which is why even though the SRC yield might decrease, the overall conversion is increased due to good solubility of the SRC and the increased light hydrocarbons content in the extracting hydrocarbons.

2.10 Air Blowing of Coke Precursors

It has been established that air-blowing modifies coal-tar and petroleum pitches. Both pitches follow the same overall trends in reference to softening point, coke yield, and solubility. Nevertheless, there are mechanistic differences that are a function of the precursor. For example, petroleum pitches are less aromatic than coal-tar pitches and this key chemical feature affects the way the two pitches react in air-blowing reactions. Several studies have been done to elucidate these reaction mechanisms. A general mechanism proposed by Barr et al. is shown by:



where Ar is a pitch molecule.³⁸ Note that this mechanism does not result in the addition of oxygen in the pitch product. Barr et al. suggested that the reaction consists of cross linked oligomers being formed, while Zeng et al. suggested that the reaction consisted of creating large planar macromolecules through extensive ring condensation. Zeng et al. emphasize the importance of chemical composition of the coal pitch and the selection of the processing temperature.³⁹ The results of Fernandez et al. and Zeng et al. are in agreement with the mechanism proposed by Barr et al.⁴⁰

Maeda et al. determined that the C/H atomic ratio increases as the temperature and time of air-blowing are increased.⁴¹ This suggested to them that a dehydrogenative condensation of pitch molecules was taking place.⁴² In this study, the air-processed coal-tar and hydrogenated coal-tar C/H atomic ratios increased significantly, but the increase in C/H atomic ratio for petroleum pitches was less. The mechanisms that Maeda et al. proposed can be seen below in the following figure.

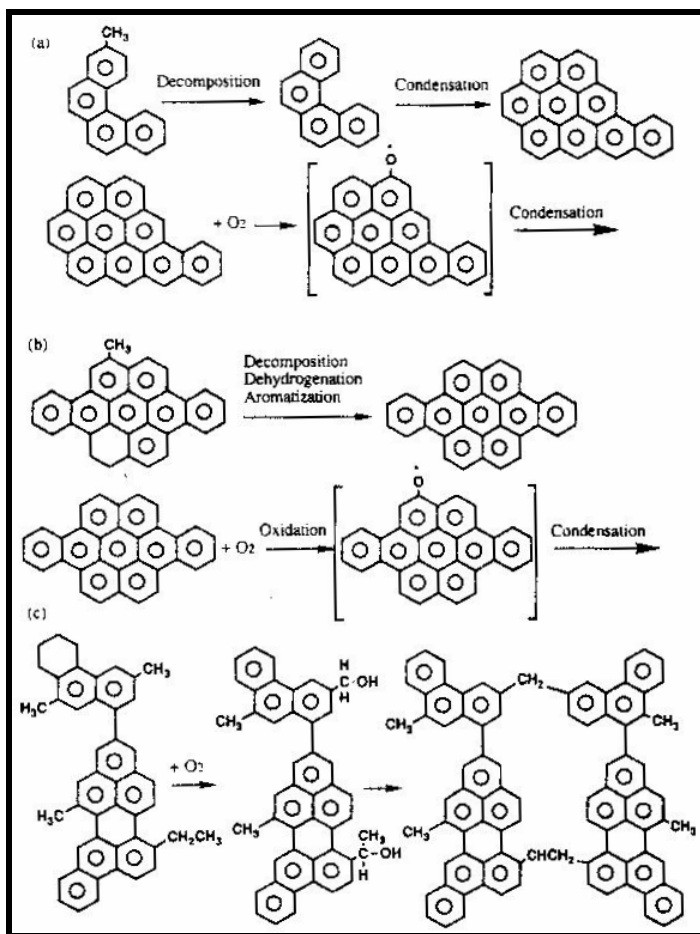


Figure 13. Oxidation Schemes of Coal-tar and Petroleum Pitches. (a) Coal-tar Pitch (b) Hydrogenated Coal-tar Pitch (c) Petroleum Pitch.⁴³

The coal-tar pitch represented in the following figure is subjected to a decomposition reaction where air-blowing first causes the side chains to be eliminated. At the same time, air-blowing also creates free radicals, promoting the condensation of constituents by dehydrogenation and aromatization.⁴⁴ Combination of these free radicals leads to more condensation reactions and significant increases in aromatic structures within the pitch. Air-blowing of the hydrogenated coal-tar pitch in the following figure starts out similarly by removing the side chains from the parent pitch. Additionally, the reaction proceeds through dehydrogenation and aromatization resulting in condensation and an increase in aromaticity. The petroleum pitch, however, goes through a different mechanism in which there is not an increase in polycondensed aromatic rings. Blanco et al. also observed a decrease in hydrogen content as air-blowing time of a coal-tar pitch was increased.⁴⁵ The parent pitch, with a softening point of 97°C, had an initial C/H atomic ratio of 1.64. The C/H atomic ratio increased to 1.87 while the softening point increased to 210°C after the parent pitch was air-blown for 30 hours. Similar trends in C/H atomic ratio were also reported in studies by Fernandez et al. and Menedez et al.⁴⁶

In an attempt to understand the chemistry further, Zeng et al. analyzed a petroleum pitch, coal-tar pitch, and hydrogenated coal-tar pitch by field-desorption mass

spectrometry (FD-MS). This technique determines the molecular weight of the constituent molecules in the pitches before and after air-blowing was conducted. It was found that air-blowing increased the average molecular weights of the petroleum pitch from approximately 670 to 700amu. The coal-tar pitch and hydrogenated coal-tar pitch increased from roughly 250 to 340amu and 415 to 515amu, respectively. Notice that the molecular weight of the petroleum pitch increased slightly while the coal-tar and hydrogenated coal-tar pitches had a dramatic increase of about 100amu. It was proposed that the coal-tar and hydrogenated coal-tar follow two similar mechanisms while the petroleum pitch mechanism differs slightly.

Yamaguchi of Osaka Gas Co. isolated specific aromatic hydrocarbons found in coal-tar pitches which were then air-blown at 330°C. By doing this a specific reaction mechanism could be proposed by knowing the starting product structure and determining the final product structure using FD-MS, gas chromatography-mass spectrometry (GC-MS), nuclear magnetic resonance (NMR), and Fourier-transform infrared spectroscopy (FT-IR). It was found that alkyl-substituted aromatic compounds polymerized through methylene, biphenyl, and ether-type bonding, leading some of the methylene functionality to change into carbonyl groups during the air-blowing reaction.⁴⁷

Choi et al. examined petroleum and coal-tar pitches that were thermally treated under both nitrogen and air.⁴⁸ They determined that the gas flow rate and pitch loads did not change the kinetics of the reactions significantly. This can be seen in the following figure where the toluene insoluble yield remains relatively constant over the changing pitch load and gas flow rates.

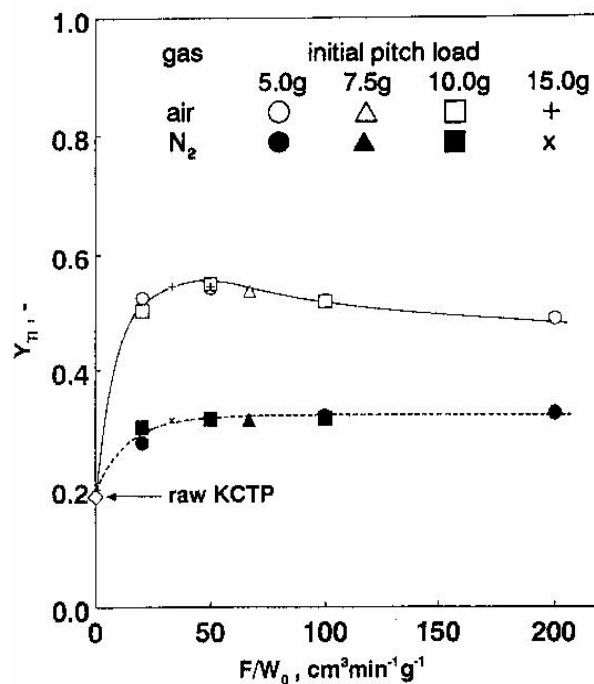


Figure 14. Dependency of TI Yields from Coal-tar Pitch on Gas Flow Rate in Air and Nitrogen with Different Initial Pitch Load.⁴⁹

Kinetic analyses are commonly accomplished by determining the solubility of pitch after processing as a function of time and temperature.⁵⁰ As an example of this approach to kinetic modeling, the work of Eser et al. is presented.⁵¹ Although Eser et al. were concerned with the kinetics of carbonization, and not air-blowing, the modeling methodology remains the same. These studies were undertaken to provide a better understanding of the mechanisms involved with the heating of petroleum feeds in coke formation. They determined the relative rates of carbonization by examining the amount of pyridine insolubles (PI) formed as a function of time and temperature as compared to A240 petroleum pitch, shown in the following figure.

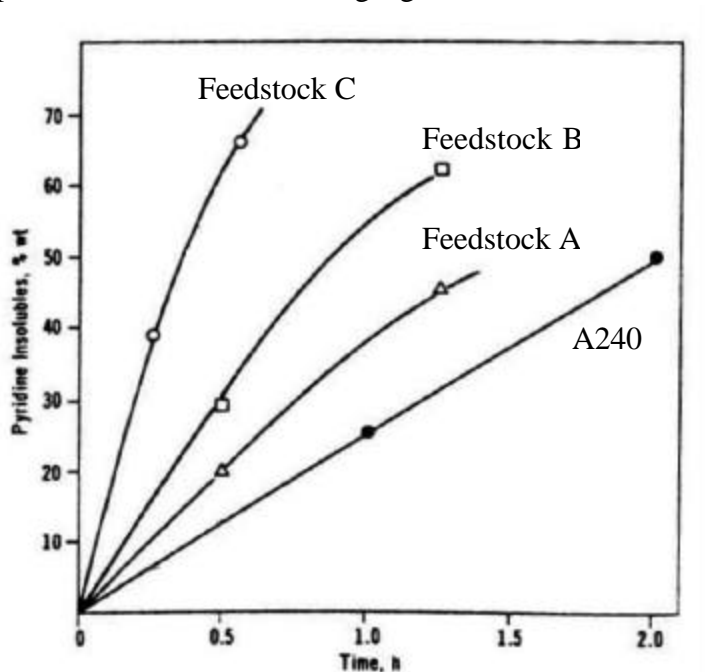


Figure 15. Relative Carbonization of Petroleum Feedstocks at a Heat Treatment Temperature of 723 K.

Esser et al. assumed that the carbonization followed first-order kinetics. The associated Arrhenius plots for the rates of PI formation are shown in figures below, for one of the petroleum materials. The slope and intercept of the line in the below figure is used to calculate activation energy and preexponential factor for carbonization, respectively. Based on the interpretation of the kinetic parameters, the authors were able to argue that petroleum fractions prone to high rates of carbonization produce isotropic cokes.

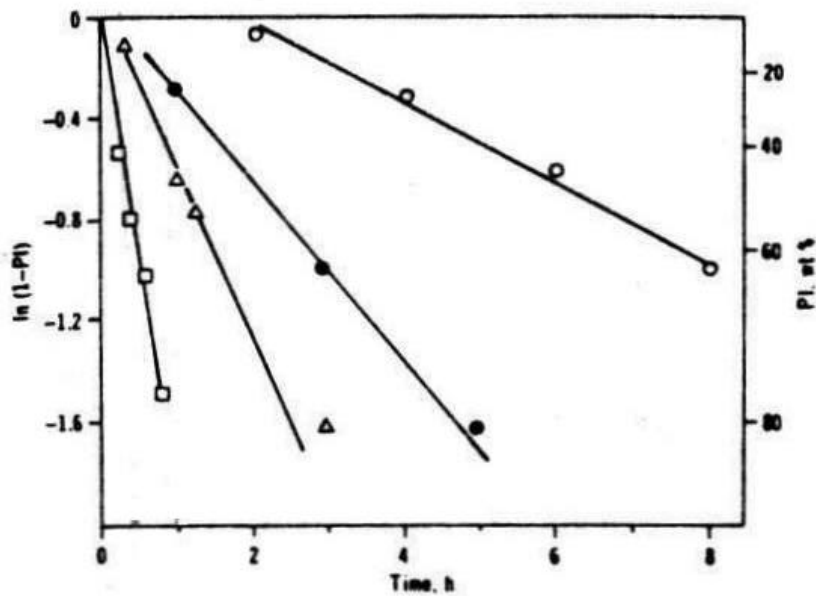


Figure 16. First-order Plots for Pyridine Insolubles Formation from VR2 Pentane Insolubles

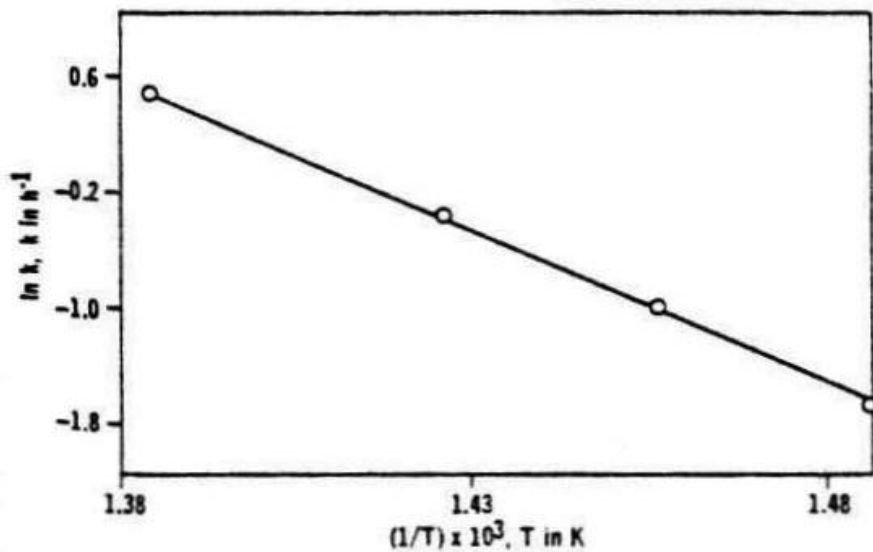


Figure 17. Arrhenius Plot for VR2 Pentane Insolubles

2.10.1 Effect of Air Blowing on Coke Yield

Yamaguchi et al. chose air-blowing as a method to modify pitch properties because they claim that the process more effectively increases coke yield than heat treatment, distillation, or any other methods.⁵²

Fernandez et al. studied the effects of air-blowing two types of coal-tar pitches (CTPA binder pitch and CTPB impregnating pitch) on coking properties for use as matrix materials in C/C composites.⁵³ They found that the coke yield dramatically increased as the extent of air-blowing progressed. This can be seen in the below table, where CTPA and CTPB are the parent pitches, and 0 through 3 designates air-blowing times in hours. They also showed that there is an increase in the density and strength, as well as a decrease in the porosity and reactivity, of the resultant cokes as air-blowing severity of the pitch increased.

Maeda et al. demonstrated similar results to those of Fernandez et al., and showed that as time increased during the air-blowing of coal-tar pitch at 360°C the coke yield could be increased.⁵⁴ In this instance, the coke yield increased from 67% for the parent pitch (softening point 82°C) to over 90% for the most severely modified pitch (softening 312.5°C).

Table 6. Coke Yield (wt %) for Air-blown Pitch A and Pitch B.

Sample	Coke Yield (wt%)
CTPA	48.4
CTPA0	54.3
CTPA1	70.8
CTPA2	72.1
CTPA3	79.4
CTPB	35.2
CTPB0	37.8
CTPB1	62.4
CTPB2	64.4
CTPB3	67.9

2.10.2 Effects of Air Blowing on Viscosity

A great deal of work has been published on various aspects of rheology related to isotropic and mesophase pitch, and during the transformation from isotropic to anisotropic pitch.^{55,56} Unfortunately, comparatively little work has been published on the effects of air-blowing pitches on rheology. However, Menendez et al. investigated the rheological behavior of a coal-tar impregnating pitch after it was air-blown for various times at 275°C using transient shear and controlled-strain oscillatory rheometry.⁵⁷ The rheological experiments were performed at a shear viscosity of approximately 50 Pa·sec⁻¹. The essential elements of this analytical technique are the ability to isolate two viscoelastic phenomena, i.e., one component associated with elastic behavior and the other component with viscous flow. As can be seen in the below figure, the parent pitch showed a purely viscous behavior, where there is no “overshoot” (the appearance of a spike in the figure) while the air-blown pitches showed increasing stress “overshoot” as time of air-blowing increased.

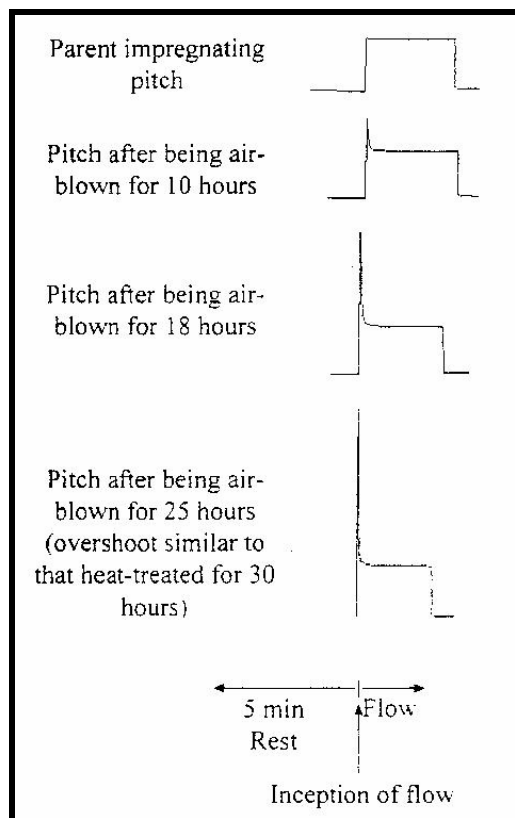


Figure 18. Shear Stress Response upon Start up of Shear Flow for the Parent Pitch and the Air-blown Pitches.⁵⁸

The air-blown pitch became a more elastic material as can be seen by the increased “overshoots”. The conclusion was made that the increased elasticity is attributed to the formation of large, cross linked aromatic molecules, as a result of air-blown.

2.10.3 Williams, Landel, and Ferry Viscosity Model

The Williams-Landel-Ferry (WLF) equation evolved from an empirical relationship describing viscosity dependence on temperature. The WLF expression can be related to fundamental principles. Beginning with Eyring's rate theories, Doolittle entailed thermodynamic principles to describe viscosity changes based on free volume concepts.⁵⁹ Cohen and Turnball further developed Doolittle's free volume model into a useable equation.⁶⁰ Later, Williams, Landel, and Ferry developed and incorporated the Doolittle equation into their own free volume expression, which became known as the WLF equation.⁶¹ This involved establishing a relationship with the activation energy of the material and the thermal energy introduced into the material. The activation energy can be related to the free volume in the sample and a reference temperature; i.e.,

$$\log \mathbf{m} = \log \mathbf{m}_r - \frac{C_{1,r}(T - T_r)}{C_{2,r} + T - T_r}$$

where \mathbf{m} is the viscosity at the reference temperature, T_r , and $C_{1,r}$ and $C_{2,r}$ are constants dependent upon the choice of reference temperature.

The WLF equation was employed by Nazem and Lewis for the rheological characterization of mesophase-containing pitches.⁶² Their method established a shift factor, A_T , which is the ratio of relaxation times for the pitch at a measured temperature and the reference temperature. Because of its thermodynamic significance, the glass transition temperature (T_g) is often used for the reference temperature in the WLF equation. This is because the free volume changes rapidly at the glass transition temperature in most pitch materials. When plotted against a temperature, the shift factor places the viscosities measured at different temperatures onto one line of a constant slope. They showed that the shift factor could be represented by the relationship:

$$\log A_T = \log \left(\frac{\mathbf{m} T_r}{\mathbf{m}_r T} \right).$$

The following equation is simply rearranged into a slope-intercept form. This was done by the logarithmic of the reference viscosity ($\log \mu_r$) being transferred to the left side of the below equation resulting in:

$$\log \frac{\mathbf{m}}{\mathbf{m}_r} = -k(T - T_r)$$

where

$$k = \frac{C_{1,r}}{C_{2,r} + T - T_r}.$$

The difference in the logarithmic of the temperature and reference temperature ($\log (T - T_r)$) was added to both sides of the below equation. After rearranging and collecting variables, the equation is now in slope-intercept form ($y = mx + b$) as shown in the following equation.

$$\log A_T = \log \left(\frac{\mathbf{m} T_r}{\mathbf{m}_r T} \right) = -k(T - T_r) + \log \frac{T_r}{T}$$

These equations are widely used to predict the viscosity behavior of both isotropic and mesophasic pitches. Remarkably, as shown in the previous figure, the WLF relationship holds for pitches that range from nearly isotropic to essentially crystalline in nature.

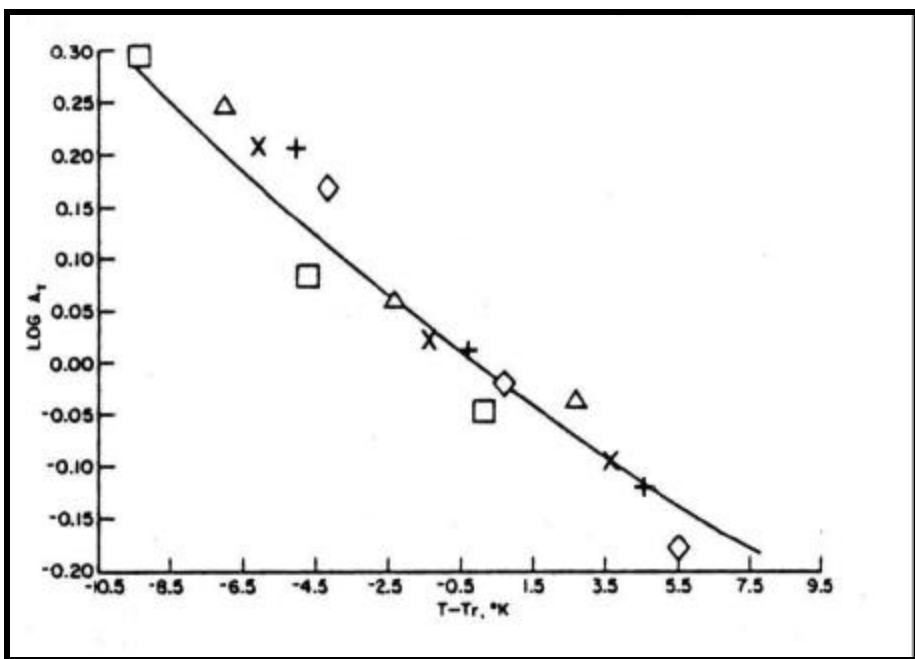


Figure 19. Plot of $(T - T_r)$ vs. Log A_T for a Range of Mesophase-Containing Pitches.⁶³

2.10.4 Van Krevelen Analysis

A graphical method for studying the chemical changes that occur during the coalification process was developed in 1950 by D.W. Van Krevelen.⁶⁴ This method consists of graphing the atomic hydrogen-to-carbon ratio versus the atomic oxygen-to-carbon ratio of organic materials. Depending on the slope and direction of these trends, the atomic ratios can indicate whether decarboxylation, dehydration, and dehydrogenation reactions are present.

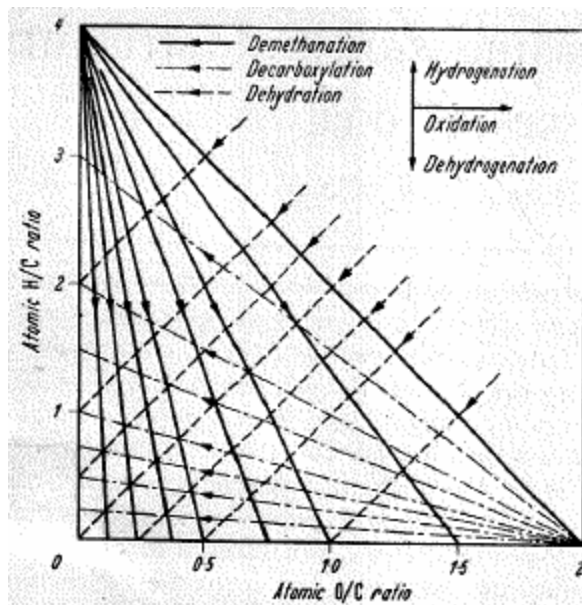


Figure 20. H/C versus O/C Diagram.⁶⁵

For example, Van Krevelen analyzed the elemental composition of a wide range of coals that varied in rank. He examined lignites, bituminous coals, and anthracites. He also included coal antecedents in his analysis: wood, cellulose, and lignin. Van Krevelen suggested that the process of coalification is associated first with little change in hydrogen content but with large decreases in oxygen content. Decreases in hydrogen content occur prevalently during the latter stages of coal maturation.

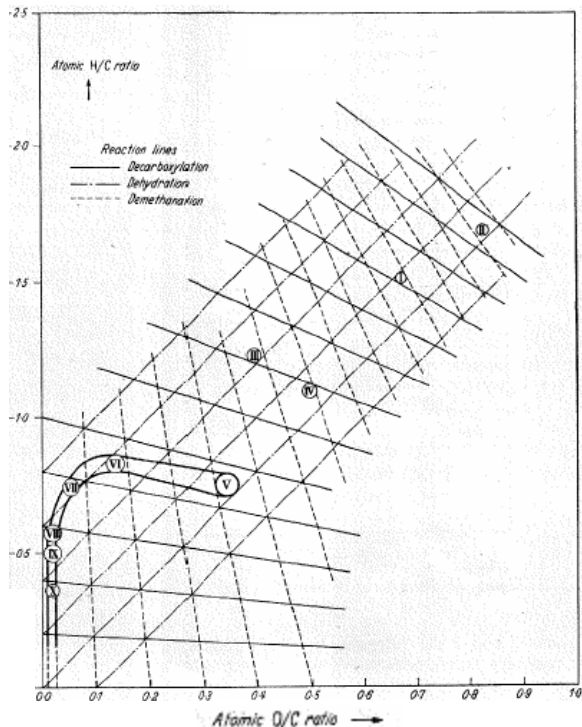


Figure 21. H/C versus O/C for I) Wood, II) Cellulose, III) Lignin, IV) Peat, V) Lignite, VI) Low Rank Bituminous Coal, VII) Medium Rank Bituminous Coal, VIII) High Rank Bituminous Coal, IX) Semi-anthracite, X) Anthracite.⁶⁶

To explain the chemical progression from low rank to high rank coal, Van Krevelen proposed that decarboxylation reactions take place upon going from lignite (V) to low rank bituminous coal (VI). Dehydration occurs predominantly proceeding from low rank bituminous (VI) to high rank bituminous coal (VIII). The final stage of coalification, the transformation of high rank bituminous coal (VIII) into anthracite (X), entails demethanation.

The use of the Van Krevelen plots can be extended to explain the mechanisms occurring during the thermal-chemical treatment of other bituminous materials. Joseph and Oberlin studied the effects of air oxidizing various carbonaceous materials at different temperatures and time.⁶⁷ They postulated that two parts are associated with oxidation. The first part involves a rapid release of hydrogen, after which oxygen content increases slowly, as shown in the figure below. Joseph and Oberlin also noted that the slopes of the oxidation paths were distinctly different and depend upon the elemental composition of the starting material. They pointed out as well that all of the materials studied tend to reach the same plateau at an O/C atomic ratio of about 0.5.

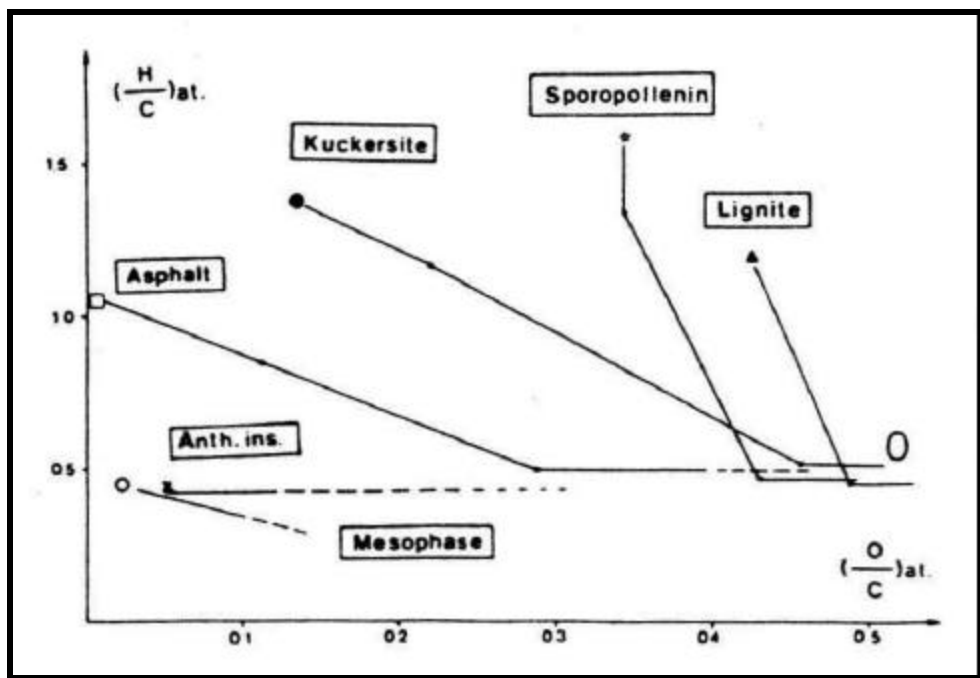


Figure 22. Van Krevelen Diagrams Showing Oxidation Paths of Various Organic Materials.

Generally, elemental analysis is performed to obtain the C, H, N, and S weight percentages, and oxygen is determined by difference. It is best to determine oxygen directly, as was done by Joseph and Oberlin, since there are errors associated with the determination of each element. This means that finding the percent oxygen by difference does not necessarily measure the content of oxygen accurately in many instances. A separate or direct measure of oxygen content is preferred to ensure that the C, H, S, N, and O contents are indeed accurate and that all five elements add up to 100 percent, in order to make the Van Krevelen plots reliable.

3.0 EXPERIMENTAL

3.1 Hydrogenation Reactions

3.1.1 Materials

a. *Kingwood Coal*. The coal was obtained and ground as received from Kingwood Mining Co. Several large pans of the coal were dried overnight in a vacuum oven then set to a temperature of 100°C with a slow nitrogen purge and 25-30 mm Hg vacuum. Once the coal had cooled, the vacuum was broken, and the coal was then placed into dark-glass containers and stored in a cold room to prevent oxidation. The properties of this coal are given in the following table.

b. *Carbon Black Base (CBB)* – Similar to Creosote Oil. CBB was received from Kopper's Industries in a 55-gallon barrel. The barrel was heated using electric heating bands. A motorized stirring mechanism was attached to the top of the barrel to mix the material so a uniform sample could be retrieved in two 5-gallon buckets. The oil became a paste at room temperature. Before a sample was taken from the 5-gallon containers, the CBB was warmed to about 100°C in an oven. The CBB was very fluid at this temperature, thus the taking of a representative sample after stirring was assured.

c. *RCC Slurry Oil (SO)* - This was obtained from Marathon-Ashland Petroleum, LLC, specifically from their Findlay, OH facility. Initially a small 1-gallon sample for testing was acquired. Later, more solvent was shipped from Marathon-Ashland Petroleum, LLC in two 5-gallon buckets.

d. *Heavy Oil (Anthracene Oil - AO)* - This solvent was received from Reilley Industries in a 5-gallon bucket. The sample obtained appeared to have some suspended solids material that did not melt even after heating to 100°C. A heated filtration was performed, and the solids content was determined to be 1.60%.

e. *Maraflex 1000 Oil (MO)* - Also received from Marathon-Ashland Petroleum, LLC in Findlay, OH. This oil is a lighter type of oil, which resembles clean engine oil. The elemental analyses of the four raw solvents and the coal sample are given in the table below.

f. *1,2,3,4 Tetrahydronaphthalene (Tetralin)* - Acquired from Aldrich Chemical Company. It was used as received with 97% purity. This solvent is the standard coal extraction / hydrogenation medium, used in this work as a control solvent.

g. *Tetrahydrofuran (THF)* - HPLC grade, acquired from Fisher Scientific. This solvent was used in all of the product extractions to determine the digestion efficiency.

h. *Di-methyl Sulfoxide (DMSO)* - Acquired from Fisher Scientific, certified ACS. This solvent was used as the sulfiding agent for the activation of the catalyst.

i. *Carbon Di-sulfide (CS₂)* - Acquired from Fisher Scientific. This solvent was used in the Simulated Distillation Chromatography analysis.

j. *Toluene* - Acquired from Fisher Scientific. This solvent was used in the determination of the solubilities of the digests and air-blown digests.

k. *Catalyst* - The catalyst chosen for these solvent hydrogenations was made available through a generous donation from the Criterion Catalyst and Technologies Corporation. Their 424 catalyst is a Ni/Mo catalyst on an alumina support and is used for heavy oil hydrotreaters at severe conditions (i.e. first stage hydrotreater, VGO hydrotreater, or lube oil hydrotreater). The catalyst is of proven high hydrogenation activity and was judged suitable for upgrading heavy, aromatic oils.

l. *Gases* - Hydrogen was used as the gaseous atmosphere in the solvent hydrogenations, and nitrogen was used as an inert gaseous blanket in the coal digestions. Compressed air was used in the coke precursor modification. All gases were obtained as laboratory standard grade from AirGas of West Virginia.

Table 7. Characteristics of Kingwood Coal.

Coal Bed	Kingwood
Seam	Kittanning
County	Preston
State	WV
ASTM Rank	High Volatile Bituminous
% Volatile Matter (dry)	33.17
% Ash (dry)	8.92
% Fixed Carbon (dry)	57.91
% Sulfur (dry)	1.84
NMP Extraction Yield, %	66.70
Mean-Max reflectance of vitrinite	1.08
Total Vitrinite	74.60
Total Liptinite	5.00
Total Inertinite	19.40

Table 8. Elemental Analysis Results for Coal and Four (4) Candidate Solvents.

	Kingwood Coal	Carbon Black Base (CBB)	RCC Slurry Oil (SO)	Maraflex 1000 Oil (MO)	Reilly Heavy Oil (AO)
C	77.44	91.58	87.38	92.22	92.41
H	4.95	5.71	9.56	7.77	6.21
N	1.18	1.09	0.44	0.37	0.94
S	1.58	0.48	2.62	0.96	0.27
O	5.93	1.15	-	-	0.17
C/H Ratio	1.52	1.34	0.76	0.99	1.24

3.1.2 Catalyst Treatment

The Ni/Mo and other catalysts are usually purchased in a metal oxide combination, although the most active form of these metals for hydrogenation is the sulfides. Therefore, a sulfiding step was performed according to the guidelines provided by Criterion Inc. First, the catalyst is weighed and loaded into the basket from the top. This requires respiratory protection and a chemical fume hood, to prevent inhalation of any catalyst dust. The top of the basket was sealed shut, and manually shaken to ensure that the screen would prevent fines from escaping. The basket was then lowered into the 5-gallon reactor and the reactor was sealed shut using an electric impact wrench. Then each of the reactor bolts was tightened using a large torque wrench incrementally to 200 lbs. The DMSO was then loaded into the reactor through the top port and then sealed. The reactor heater was set to approximately 210°C and the impeller was regulated at 1000 RPM. Once the reactor temperature reached the desired set point, the timer was started and the reactor was held at temperature for one hour. The final pressure of the reactor at the end of the hour was 240 psig. The reactor heater was turned off, and the stirrer left on until the reactor cooled down. The reactor was vented while still warm, to prevent any un-reacted DMSO from condensing in the reactor. The reactor, while still warm, was pressurized up to 500 psig with cold nitrogen gas, and then vented. This process was repeated twice.

The Ni/Mo catalyst is typically used in plug-flow reactors, but there were only stirred tank reactors available for this research, hence some support structure needed to be fashioned. The stirred tank reactor used in this study had a volume of five gallons, but it was decided that only half of the volume would be used, so as not to produce large quantities of potentially unusable solvents. Using this volume and the dimensions of the reactor, the estimated liquid level for the solvent hydrogenation runs was calculated to be approximately 9.1 inches. Then, using the bulk density of the catalyst particles (see the following table) and a reactant volume to catalyst volume ratio of 7 to 1, the size of an annular basket, was calculated. The 1/20" size catalyst was used.

The basket was constructed from 316 stainless steel materials purchased from McMaster-Carr. The basket was constructed in such a way to allow for solvent to flow through the screen, which held the catalyst particles securely. The solvent flows from inside to outside of the basket, with the reactor agitator set in the middle of the basket. The basket was propped up on legs to allow the solvent to flow under the basket, and the basket was short enough to allow for solvent to flow over the top of the basket when the agitator was on.

Table 9. Catalyst Properties.

Shape	Trilobe
Nominal Size, mm (in.)	1.3 (1/20)
Chemical Composition, wt% dry basis	
Nickel	3.0
Molybdenum	13.0
Surface Area, m^2/g	155
Pore Volume, $\text{cc/g (H}_2\text{O)}$	0.45
Flat Plate Crush Strength, N/cm (lb/mm)	245 (5.5)
Attrition Index ⁽¹⁾	99
Compacted Bulk Density, $\text{g/cc (lb/ft}^3\text{)}$ ⁽²⁾	0.81 (50)

Table 10. Catalyst Basket Parameters.

Reactor Volume (Gal)	5.0
Volume Used (Gal)	2.5
Estimated Liquid Level (in)	9.1
Reactor Length (in)	19.5
Reactor Inner Diameter (in)	9.0
Stir Rod Length (in)	17.75
Impeller Diameter (in)	4.0
Catalyst bulk density (lb/in^3)	0.029
Basket Length (in)	8.0
Basket Outer Diameter (in)	6.5
Basket Inner Diameter (in)	5.4
Basket Volume (in^3)	82.5
Amt of Catalyst (lb)	2.39
Basket Thickness (in)	0.6
Free Space from basket to reactor wall (in)	1.25

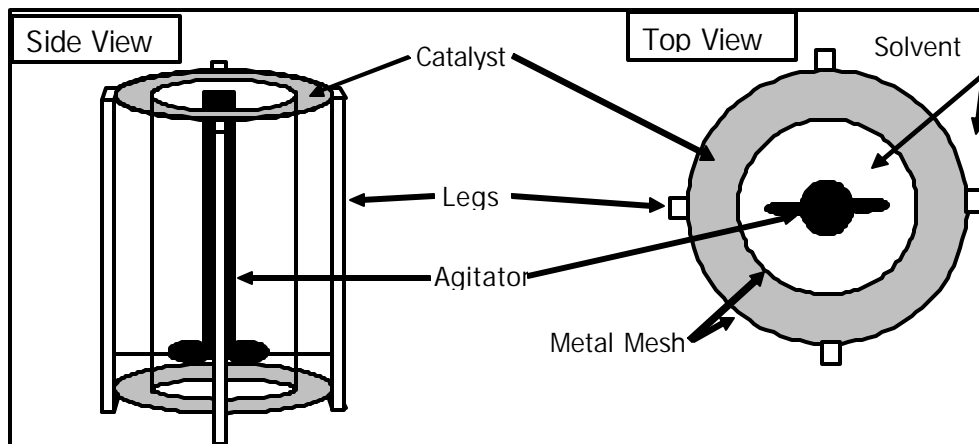


Figure 23. Catalyst Basket Design.

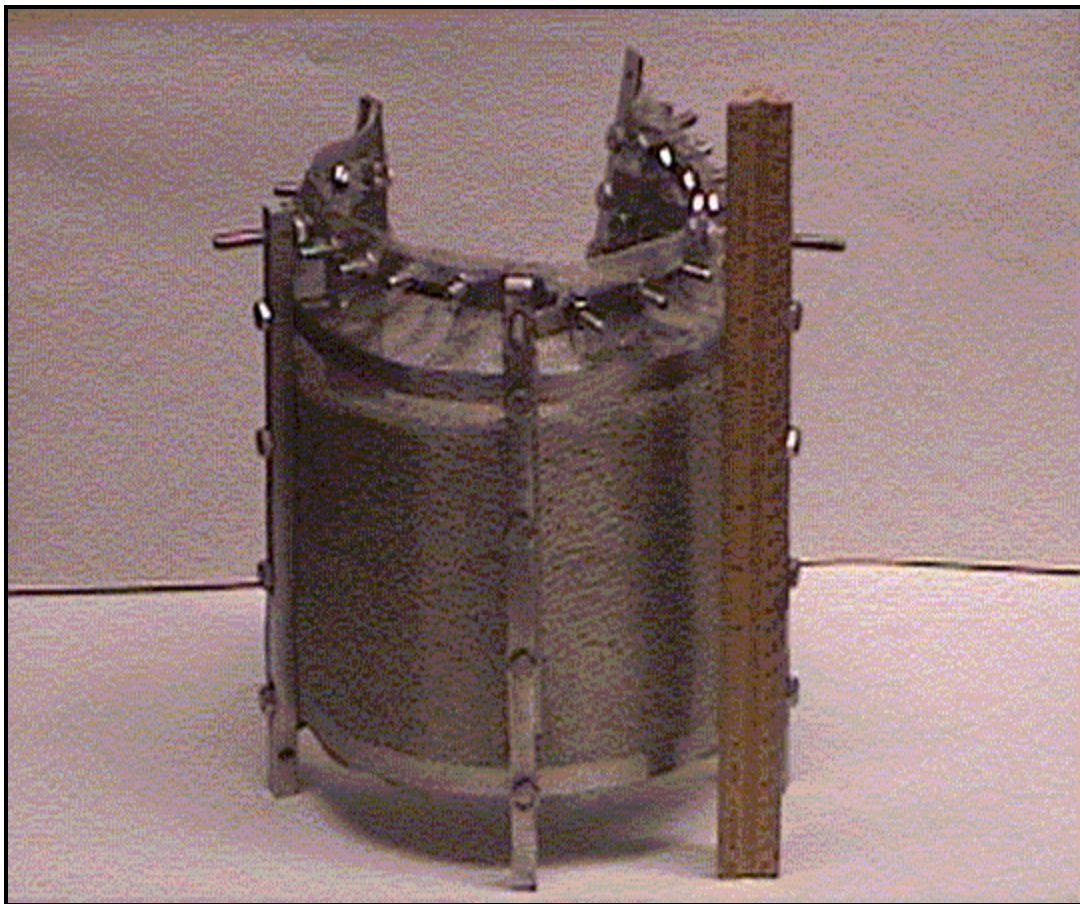


Figure 24. Completed and Loaded Catalyst Basket.

3.1.3 Solvent Hydrogenation

Four solvents were utilized in this study to determine the effectiveness of solvent hydrogenation on the coal digestion. The 5-gallon reactor was loaded with Kopper's Carbon Black Base (CBB) to flush out any residual DMSO, emptied, and then filled for the initial run with the CBB. The volume of solvent was 2.5 gallons, or approximately 588 in³. This volume would fill the reactor up to about 9.1 inches from the bottom of the reactor. Assuming the specific gravity of the warmed CBB was approximately 1.1, the mass of CBB to be charged to the reactor was 27.5lb or 12.49kg. The specific hydrogenation conditions for each solvent are given in a previous table. Once the reactor was loaded with the solvent, the reactor was purged twice and pressurized with hydrogen gas up to the desired level (in the first run, this was 500 psig H₂ cold). The reactor furnace was then heated to the reaction temperature while the impeller, controlled by the Reliance Electric SP500 VS Drive, rotated at 1000 rpm. The time, furnace temperature, reactor temperature, and reactor pressure were monitored during the entire process. Once the reactor reached the desired temperature the reaction was allowed to proceed for one hour. At this time the furnace was turned off and the reactor was allowed to cool slowly. This typically took an overnight period, and the reactor temperature was at about ambient conditions when noted the following morning. The change in the cold pressure from before the reaction to after the reactor had cooled completely was recorded, as this is

most likely the amount of hydrogen gas consumed. The reactor was then vented, and the furnace and impeller were then turned on again to warm the contents to allow for thorough draining. The contents were drained into 1-gallon tin cans and the mass of product was noted. For this work, there were three “levels” of hydrogenation used on the solvents. In the instances when a different solvent was to be hydrogenated, the new solvent would be added to the reactor, stirred around while warm, and then drained without any reaction. This flushing out process was done to attempt to remove any residual solvent from the previous runs. For all solvents used in this research simulated distillation and FTIR were performed on both the raw and hydrogenated solvents. This was done to analyze what differences existed between the raw and processed solvents.

Table 11. Solvent Hydrogenation Reaction Conditions.

Hydrogenation Level	Temperature (°C)	Pressure (psig cold)	Time (hr)
1	275	500	1
2	350	500	1
3	375	750	1

3.2 Coal Digestion/Dissolution

3.2.1 Parametric Studies in Mini-Reactors

Tubing bomb-type microreactors were used for laboratory scale experiments with hydrogenation and coal digestion, as shown in the accompanying diagram. These devices provide an inexpensive way to accumulate data. The microreactors are made of 316 stainless steel with a capacity of 50 cc. Usually two tubing bomb reactors are prepared for each hydrogenation run in order to provide data in tandem. The reactors are cleaned thoroughly before each use. The inside of the reactor is scoured using a cylindrical wire brush. The threads of the end caps are wiped clean using steel wool. Air is then blown into the reactor stem to remove any particulates from the stem. Once cleaned, one end of the reactor is sealed according to the following procedure. The TBMR was placed in a vise, and a small amount of copper anti-seize lubricant is applied to the threads. The lubricant helps to secure the Swagelok^(R) caps and prevents the caps from seizing to the reactor body under the high-temperature reaction conditions. The Swagelok(R) cap is placed on the reactor and tightened until hand tight. An extra turn is added using a wrench to seal the cap fully.

Reactants were weighed on an analytical balance to the nearest 0.1 mg and then added to the reactor. The coal-derived solvent was placed in the reactor first. Since the coal liquids are quite viscous, their mass was measured by difference (initial weight of the solvent container was determined and after solvent was added to the reactor, the final weight was determined, the difference between these two weights gave the weight of solvent added to the reactor). Once their mass was determined, the appropriate amount of coal was added to the reactor, based on the desired solvent-to-coal ratio. Finally, three stainless steel ball bearings were weighed and added to the reactor. These help to mix the

contents of the reactor during reaction. Once all the reactants were charged, the open end of the reactor was sealed according to the above procedure.

The hydrogenation reactions were run under either a nitrogen or hydrogen atmosphere. Air was removed from the reactors by using a pressure purge cycle. The reactors were pressurized to 1000 psig initially with hydrogen or nitrogen (depending on the specific hydrogenation run) and checked for leaks by immersion into water. The purge valve was then slowly opened to allow the reactor to reach atmospheric pressure. Opening the purge valve slowly was essential so that none of the reactor charge was lost during depressurization. This pressurization and release process was repeated two more times after which the oxygen concentration dropped down to less than 0.0005 %. Finally, the reactor was pressurized to the final desired cold reaction pressure. The gas inlet valve of the tubular reactor was then closed and capped with a Swagelok^(R) plug.

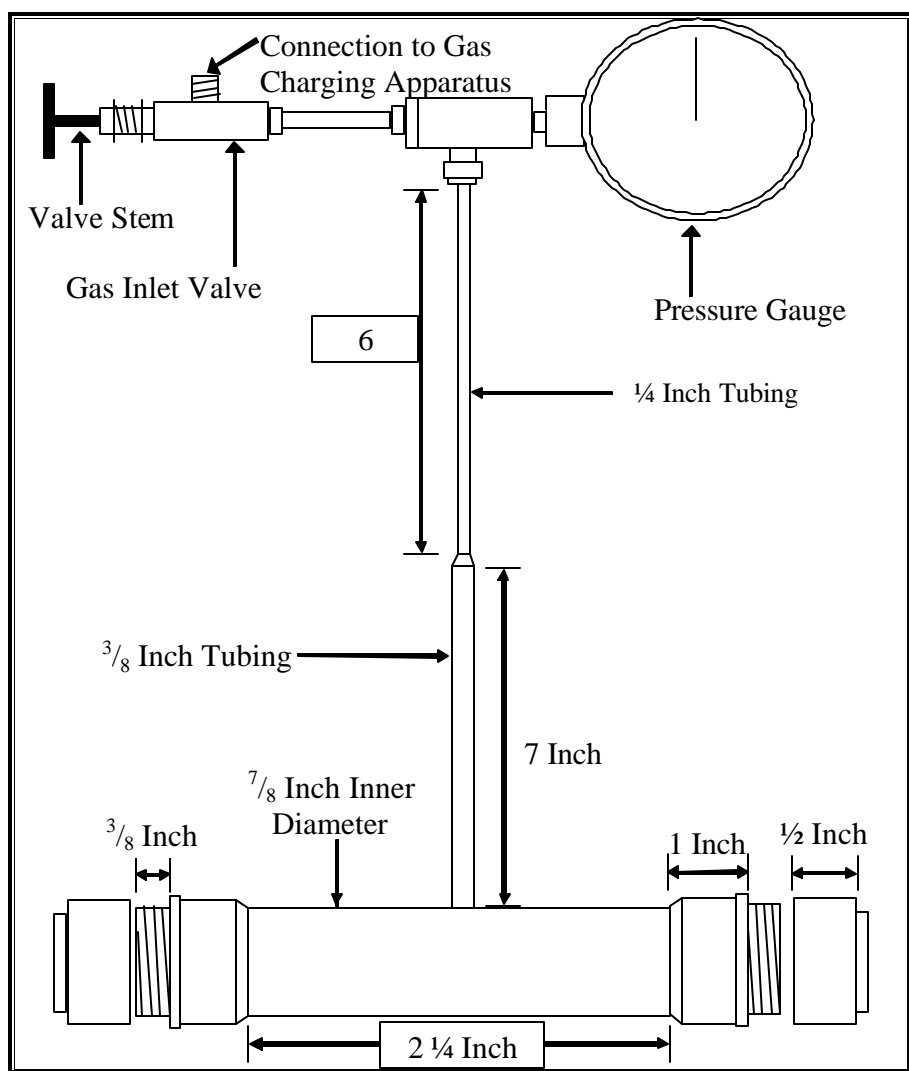


Figure 25. Diagram of the Tube Bomb Mini-Reactor.

A Techne SBL-2 fluidized sand bath is used to heat the reactors. A Techne TL-8D temperature controller regulated the sand bath temperature. The sand bath is filled with

three-quarters of a -100 mesh aluminum oxide powder, and is preheated to 20-25 °C, above the desired reaction temperature. This elevation in temperature is required due to its rapid decline which occurs when the cold reactors are immersed into the sand bath. The inlet airflow to the bath is adjusted so that light bubbling of the sand takes place and a uniform temperature is achieved in the bath.

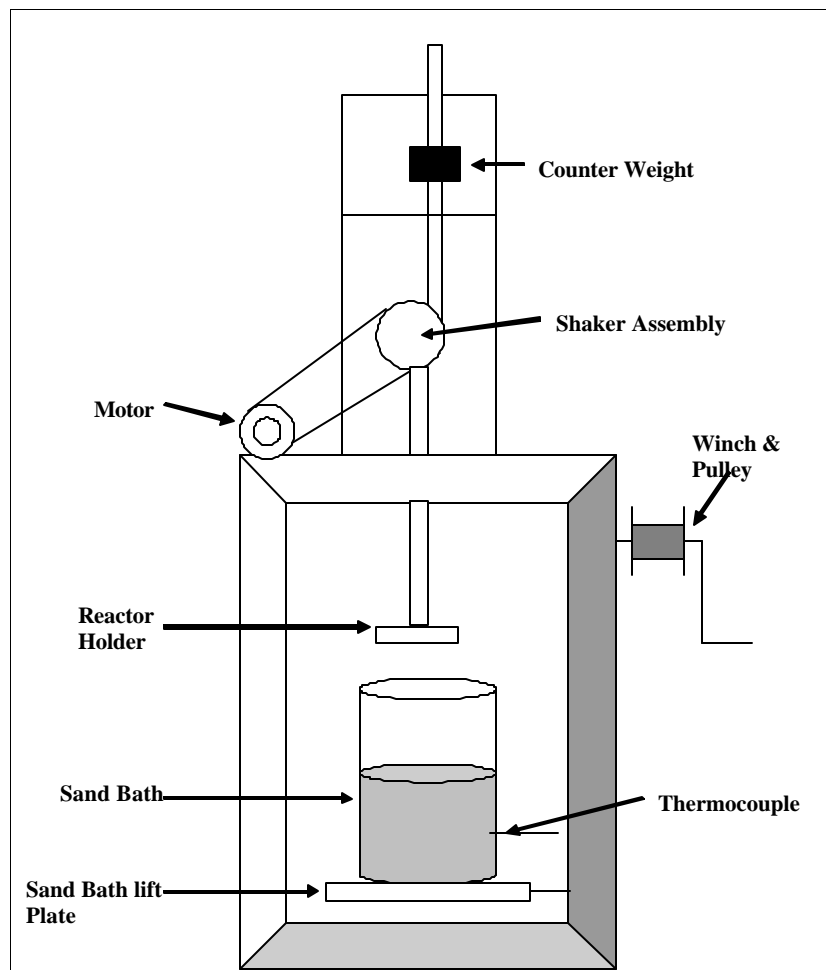


Figure 26. Overview of Reactor System Showing Sand Bath and Shaker Mechanism.

The digestion ability of different base solvents, including both petroleum-derived and coal-derived oils, and their hydrogenated variants was tested. Carbon Black Base (CBB), Slurry Oil (SO), Anthracene Oil (AO) and Maraflex Oil (MO) were among the solvents tested.

The coal digestions were performed in 30 cm³ tube bomb microreactors. Each tube bomb was fitted with a pressure gauge and valve to allow venting and pressurizing of the bomb. For all experiments, a solvent weight to coal weight ratio of 8:3 was chosen. The temperatures used in this study were 350°C, 400°C and 450°C. Half of the runs were purged with nitrogen and half of them were pressurized up to 500psig. The products of the reactions were then extracted using THF as the solvent in order to calculate the coal conversion for each run. Each run was done in duplicate, to help

validate the results. After the parametric experiments in the mini-reactors were complete, scale-up 1-gallon reactions were conducted using the best three solvents.

To heat the reactors for the hydrogenation runs, a Techne SBL-2 fluidized sand bath was used. The sand bath was filled to about 75% full with an aluminum oxide powder (app. 100 mesh). The temperature of this sand bath was maintained by the Techne TC-8D temperature controller, and the sand was fluidized by house air. The air flow was adjusted so there was a slight bubbling in the sand bath. This was low enough to prevent sand from escaping the overflow tray and high enough to ensure even heat distribution. To preheat the sand bath, the temperature was set above the desired reaction temperature (from 25° to 50° above reaction temperature, depending on the particular reaction temperature). The sand bath temperature was set to the desired temperature immediately prior to immersion of the reactors.

Each solvent was slightly different in texture and consistency. Carbon black base (CBB) was a paste at room temperature, while the other Anthracene Oil (AO), Slurry Oil (SO), Maraflex Oil (MO) were each thick, viscous liquids with varying amounts of solids. The CBB, AO and SO each required heating in an oven at about 100°C for about an hour with occasional stirring. Maraflex Oil viscosity was low enough to pour at ambient temperature.

Each tube bomb was weighed to determine the empty reactor weight. A sample of the solvent for this run was then placed into a small beaker. The beaker was then tared on a Denver Instruments Model A-200DS scale, so the amount of solvent could be determined by difference, since these solvents were all viscous fluids. The target weight for each run was 8g total solvent. After the solvent had been added to the reactor, the coal (app. 3g) was then weighed in a small plastic tray and added to the reactor. After the solvent and coal had been loaded into the tube bombs, six (6) 316 stainless steel ball bearings were weighed and loaded to serve as agitators. The filled weight of the tube bomb was also noted. The same procedure used to place the first end cap on the reactor was then repeated to cap the other end of the reactor.

Each tube bomb, once loaded and sealed, was pressurized with nitrogen gas, and tested for leaks. If there were any leaks, the caps were turned an additional quarter turn, or replaced if this did not work. If no leaks were detected, the tube bomb was then vented. This was done by opening the gas charging valve slowly, to prevent any fines from escaping the reactor or solvent from shooting up into the stem and causing a plug. The reactor was pressurized and purged two or three times with nitrogen. For each set of reaction conditions (solvent used, reaction temperature) there was a pressurized pair of reactors (nitrogen pressure of 500 psig) and an un-pressurized pair of reactors (purged with nitrogen but vented to atmosphere) to determine the effects of pressure on the coal digestion.

3.2.2 Reaction Procedure

After the reactors had been loaded, sealed and nitrogen purged/pressurized, they were mounted onto the shaking mechanism over the sand bath. The sand bath, which had been preheated, was set to the desired reaction temperature, and then raised up via a wench and pulley system to a level just below the reactors. The shaker was turned on at this point to a very low setting, and then the sand bath was raised the rest of the way,

until the reactor bodies were completely submerged into the sand. Two formed sheets of metal were then placed on top of the sand bath, with a gap left open for the reactor stems, to prevent the sand from escaping the bath. Next, the shaker controller, a Dayton Industries DC Speed Controller, was turned up to a level of approximately 40-45. This corresponded to a shaking speed of about 500 rpm, with a stroke length of about 2 inches.

At this point, the time was noted, and the reaction was allowed to proceed for a total time of one hour. The sand bath temperature and the reactor pressures were noted every 10-15 minutes. At about 58 minutes into the reaction the shaker mechanism was turned off, and the sand bath lowered. The excess sand was shaken off of the reactors, and then the reactors were removed from the shaker mechanism and immediately placed into a cold water bath to quench the reaction. This was done at 58 minutes into the reaction to allow for the time to lower the sand bath, loosen the bolt keeping the reactors mounted, and then remove the reactors and take them to the water bath.

To determine the effectiveness of a particular solvent/solvent combination in the conversion of coal, the products of the coal digestion were subsequently processed by THF Extraction. For each reactor, a marked 250-mL glass round flask was weighed and placed on a ring stand. Two Teflon boiling chips were also weighed and added to the flasks. A glass funnel was placed on the flask, and in the funnel was placed a weighed Whatman Glass MicroFibre Thimble (19mm ID, 90 mm length). Another glass funnel was placed on a ring clasp above the thimble, with the tip of the funnel just down into the thimble (see the following figure).

The reactor was then weighed, after air blowing all the water and sand off of the reactor body, to get an after-reaction weight for use in determining the mass of any gas produced in the reactor. Once this weight was obtained, the reactor was set into a fume hood and the gas charging valve was slowly opened to vent the reactor. Most of the unpressurized reactors had a negligible amount of gas produced during the reaction, and there was very little pressure to vent. Care was taken during venting to make certain that no liquid product was accidentally vented along with the gas. On certain samples where the product was likely to be a less viscous mixture the reactors were placed in a container full of dry ice and allowed to cool, and then vented. Once the reactors had been vented they were weighed again.

The reactor was next placed back in a vise, and the end cap on the valve stem side was loosened. The threads were wiped clean using tissue paper, to remove the copper lubricant. The reactor was then suspended over the funnel-thimble-funnel-flask setup. A heat gun was typically used to warm up the products enough to allow them to flow out of the reactor and down into the funnel. After the majority of the material had emptied out of the reactor, the reactor was then turned over and allowed to cool a bit, and then THF was poured into the reactor. A metal spatula was used to scrape the sides of the reactor, and then this was poured out into the funnel. This process was repeated, usually four or five more times, until the liquid poured out was close to being clear. Care had to be taken to keep the liquid level in the thimble from getting too high and causing the thimble to overflow. THF was also sprayed down the stem of the reactor from the gas charging valve to clear out any product that had moved up into the stem. In the event that there was a clog, the top part of the reactor apparatus (valve, pressure gauge, etc.) would be removed, and the clog would be removed by using a length of copper wire.

Any product in the end cap was scraped out with a metal spatula, and then the caps were washed with THF. Finally, the other end cap was removed from the reactor, the threads were wiped clean of copper lubricant, any product in this cap was scraped and then washed out, and then THF was sprayed into the reactor to clear out any remaining particulates. Once this was done, the funnel was washed with THF (and scraped if necessary), until all the product was in the thimble. During this process, it was occasionally noticed that a viscous material would collect around the base of the thimble in the funnel. Since it had made it through the thimble, it was decided to include this material in the soluble portion, and any of this present would be washed into the flask.

For any reactions that resulted in a more solid or chunky material in the product (mostly the slurry oil runs), the material would be chipped out of the reactor with metal spatulas, and then the washing process would be used to clean out the reactor. Great care had to be taken to keep any product from falling out of the reactor and not into the funnel. Once this had been done, all of the product would be in either the thimble or flowing through the thimble with the THF and into the flask.

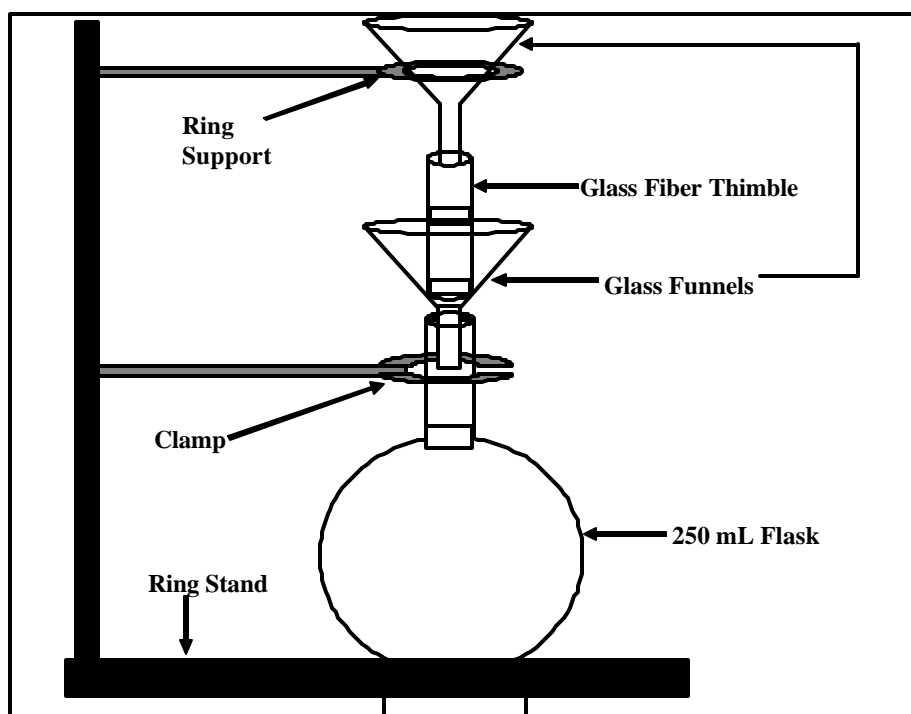


Figure 27. Product Removal Thimble / Flask Apparatus.

3.2.3 Reactor Scale Up Studies

The next step in this study was to produce a more sizeable quantity of pitch precursor using the best three solvents, based on the results of the tube bomb digestions. This pitch precursor was then be separated from the unconverted coal and thermally treated using an air blowing technique to produce a coke precursor. This demonstrates the ability to produce both pitch products as well as coke products.

The same coal and solvent combinations used in the tube bomb reactions were be used in this scale up. The ratio used in the tube bomb experiments was kept for this scale

up operation, along with the time, temperature, and the pressure. For this scale up, based on the results from the tube bomb reactions, the solvents used were Level 3 hydrogenated Carbon Black Base (HCBB-L3), Hydrogenated Maraflex Oil (HMO-L3) Hydrogenated Slurry Oil (HSO-L3), and a 50/50 mixture of HCBB-L3/HSO-L3.

A 1-gallon reactor, made by Autoclave Engineers, was first pressure tested to ensure it would hold the proper pressure. After several leaks were detected, the reactor was shipped back to the Autoclave Engineers to be retooled. After it was returned, pressure testing was again conducted, this time successfully. The reactor, having been retooled, was fairly clean and only required some wiping down with a solvent to remove any residual oil on the reactor. The lid was fitted with the required plugs, thermowell, and stirring mechanism.

Since the reactor was significantly larger, the amounts used would be increased to approximately 1.5L of solvent (measured in graduated beakers) and 600 g of the coal. The solvent and coal masses were recorded from the Mettler-Toledo PR 5002 scale. Again, the solvent was loaded into the reactor first, to prevent any sort of caking effect on the coal at the bottom of the reactor. After the reactor was fully loaded with solvent and coal, the reactor lid was placed onto the reactor, and the lid bolts were tightened with the electric impact wrench. Next, the bolts were each tightened with a large torque wrench to 50 lbs, 100 lbs, and finally 150 lbs. The reactor was purged with nitrogen gas, but left at 0 psig for the reaction.

The temperature of the reaction was maintained by using the Autoclave Engineers Modular Control Series Process Controller. The impeller was turned on to 1000 rpm and the reactor heater turned up to the desired reaction temperature. The first of the three reactions (HCBBL3) was run at the same conditions (400°C and 0 psig for one hour) as the tube bomb reactions. The subsequent reactions were run at a higher temperature of 425°C, for reasons to be explained in the results, Section 4. The reactor pressure and temperature were monitored during the hour. At the end of the reaction time, the heater was turned off and the impeller was left on while the reactor cooled down.

Once the reactor had cooled down to an acceptable temperature, the bolts were loosened on the lid, and then the lid was carefully taken off. This was all done while the reactor was still in the fume hood, since there would likely be noxious fumes, as the products were still at a slightly elevated temperature (usually at least 100°C). The products from these reactions were recovered using a vacuum line and an Erlenmeyer flask with a sidearm. Once the reactor had been emptied into the flask, the contents of the flask were reheated in an oven set to ~100°C, and then the product was transferred to plastic, pre-weighed, centrifuge bottles. The bottles were weighed on the Mettler scale and then placed into the Thermo Electron Corporation PR700M Centrifuge and ran for 30 minutes at 4000 rpm and 39°C, which was the maximum temperature allowable for operation of the centrifuge. After centrifugation, the liquid product was decanted out of the centrifuge bottles into a glass, pre-weighed bottle and then the product mass was determined. This was the effective converted portion of the coal, and the residue from the centrifugation was then put through a simple warm THF filtration, to remove any entrained product still left in the residue. This was done in an effort to close the mass balance and to determine coal conversion. The THF was stripped off of the soluble portion using the rotary evaporator, and then the product was vacuum dried overnight. The conversion was calculated according to the next equation. These products were

tested using proximate analysis (to determine ash and fixed carbon), simulated distillation, FTIR, and elemental analysis.

The conversion efficiency of coal to THF solubles using three coal-derived liquids as hydrogenation solvents in the direct hydrogenation of a high-volatile bituminous coal was investigated. The standard reaction temperature was 400 °C and the initial cold pressure was 500 psig of hydrogen in the cold reactor. The reaction time of one hour was used for initial experiments to study differences between solvents. These are the standard conditions for the study of reactions between coal and model hydrogen donor solvents. The solvent-to-coal ratio for the present work was 5 to 1. The reason for this high solvent-to-coal ratio is to maximize the quantity of the recovered process derived solvent available for recycle.

The products of the hydrogenation reactions were extracted using THF in order to determine the overall conversion as THF solubles. The quantity of the coal-derived solvent was included in the conversion calculation for the overall conversion whereas it is excluded for the coal-alone conversion. The extract (THF-soluble fraction) was vacuum distilled to recover a process-derived recycle solvent and a distillation residue. Vacuum distillation is performed to isolate the light fraction (termed “recycle solvent” hereafter). The light distillate is given the name “recycle solvent” because in many similar processes this fraction is recycled to the reactor for further hydrogenation reactions. Hence, testing the effectiveness of the isolated recycle solvents in subsequent hydrogenations was the main scope of this research. The results using fresh and recycle solvent were compared for their conversion yields. The other product, the heavy distillation residue, called pitch, was tested as a possible precursor for carbon-products. A process flow diagram for the overall experimental procedure is shown in the following figure. The following table gives an overview of the experiments performed in this series of experiments.

Table 12. Hydrogenation Reaction Conditions.

Run	Trial	Solvent	Temp. (°C)	Atmosphere	Pressure (psig Cold)	Solvent/ Coal mass ratio	Time (hr)
1	A-D	CBB	400	H ₂	500	5/1	1
2	A-D	HCO	400	H ₂	500	5/1	1
3	A-D	RCO	400	H ₂	500	5/1	1
4	A-D	Pass 1 Rec. CBB	400	H ₂	500	5/1	1
5	A-D	Pass 1 Rec. HCO	400	H ₂	500	5/1	1
6	A-D	Pass 1 Rec. RCO	400	H ₂	500	5/1	1
7	A-D	CBB	350	H ₂	500	5/1	1
8	A-D	CBB	450	H ₂	500	5/1	1
9	A-D	CBB	400	N ₂	500	5/1	1
10	A-D	Pass 1 Rec. CBB	350	H ₂	500	5/1	1
11	A-D	Pass 1 Rec. CBB	450	H ₂	500	5/1	1
12	A-D	Pass 1 Rec. CBB	400	N ₂	500	5/1	1

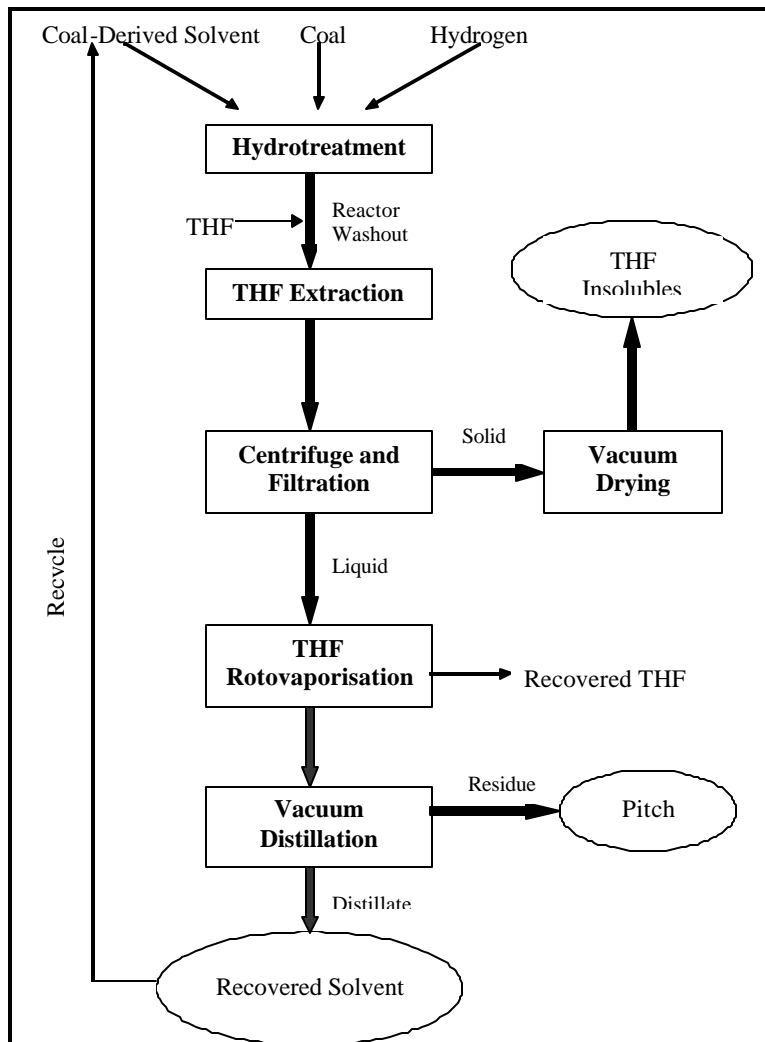


Figure 28. Experimental Flow Sheet for Production of Carbon Product Precursors.

3.2.4 Hydrotreatment Facility

A Hydrotreatment Facility was modified to permit large scale partial direct liquefaction (mild hydrogenation) reactions with hydrocarbon feedstocks such as pitches and different types of coal. The facility is equipped to handle hydrogenated liquids and coal.

The Hydrotreatment facility is laid out in two levels. A vertical design was chosen to facilitate flow of liquids via gravity. A schematic of the hydrotreating process is shown below, followed by a photograph of the lower level. At the upper level, a heated medium-pressure 10-gallon feed tank is used to form a slurry of hydrotreated solvent, untreated solvent, and coal. The slurry is preheated to 250°C to 350°C before its introduction to the feed pump.

The feed pump conveys the reactants continuously into a high-pressure 1-gallon autoclave which is used to partially liquefy the coal by transferring hydrogen from the solvent to the coal. Following hydrotreating of the coal, the Synpitch precursor in the 1-gallon autoclave is transferred to a let-down vessel for collection and cooling.

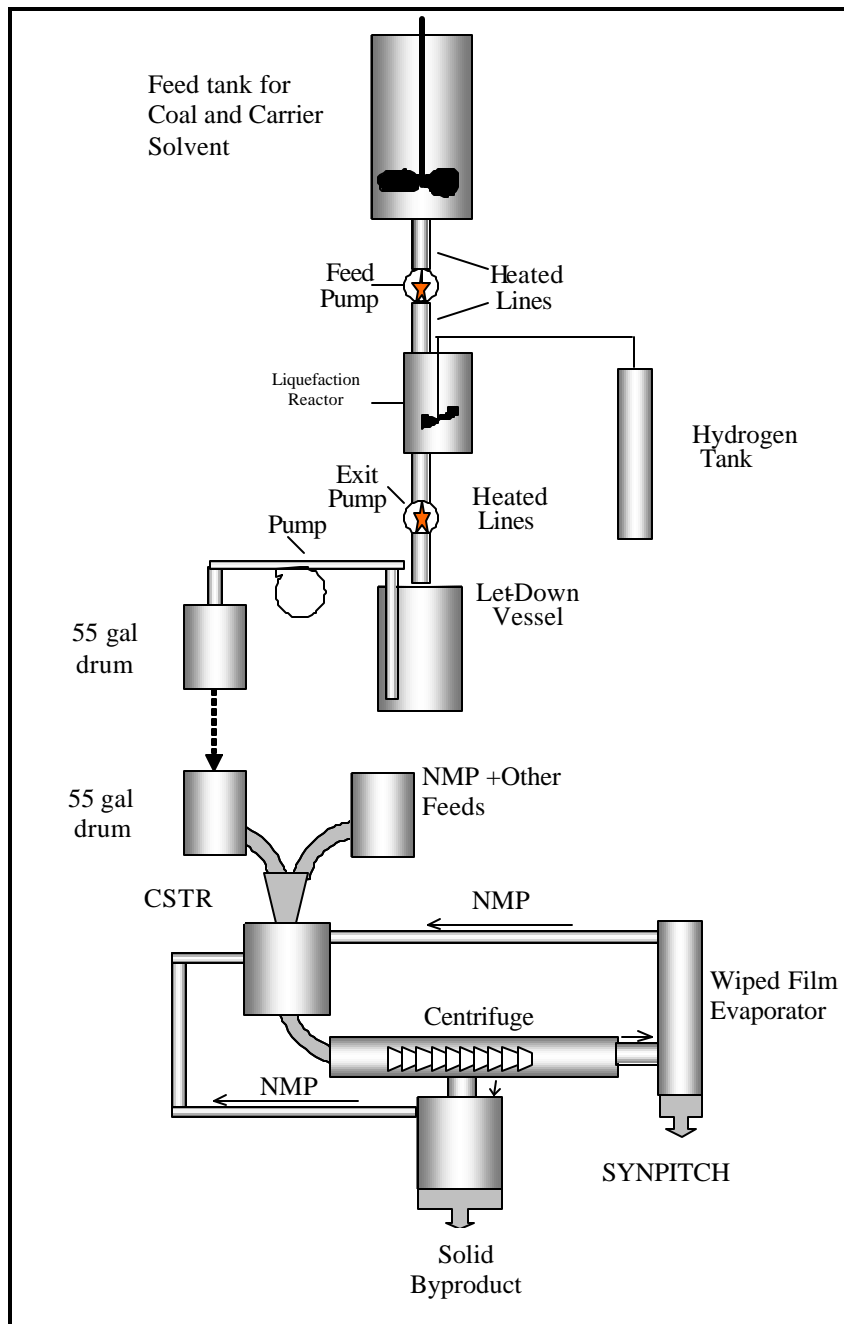


Figure 29. Process Diagram for Hydrogenated Synpitch Production.



Figure 30. Lower Level Reactor Used to Chemically Digest Coal.

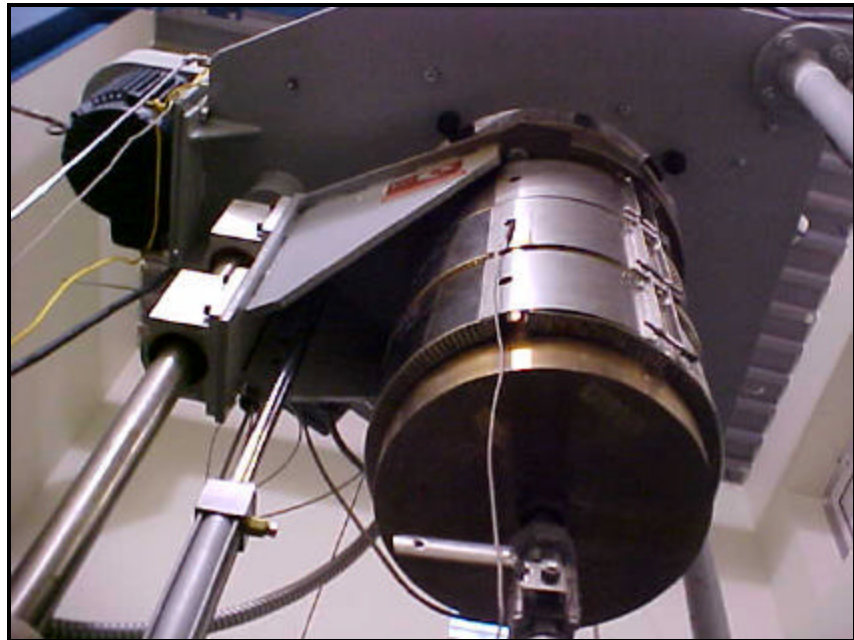


Figure 31. Upper Level Reactor, Used to Combine Coal and Solvent.



Figure 32. Remote Control Panel.

The Synpitch precursor is then transported to the Solvent Extraction Pilot Plant (SEPP) located in the High Bay of the National Research Center for Coal and Energy, approximately $\frac{1}{4}$ mile away. The material is loaded into a continuously-stirred tank reactor and reheated. It is then pumped to a centrifuge to remove suspended solids. The solids contain mineral matter (ash) and unconverted coal. The ash-free Synpitch is then fed to a wiped film evaporator (WFE) in order to remove light volatile molecules (primarily solvent components) from the pitch, thus increasing the average molecular weight of the pitch, and thus increasing the softening point. Manipulation of vacuum, temperature, and residence time during the operation of the wiped film evaporator can be optimized to produce Synpitch with specific properties depending on the intended application. The light volatiles can be recycled for use as a solvent in future batches.

Special consideration was given to safety because of the presence of hydrogen gas and flammable solvents. In retrospect, the presence of even a minor amount of hydrogen gas was a substantial facilities concern because of the need to operate within electrical safety codes. Non-sparking electrical motors, non-sparking wall outlets and special ground-fault isolations were among the constraints.⁶⁸ Water pipes in the facility had to be separately grounded so that they can not act as a spark source in case of an electrical ground fault. Originally consideration was given to collocating the Hydrotreating Facility in the High Bay with the Solvent Extraction Pilot Plant (SEPP). However, this plan was scrapped early on because it was realized that the wiring in the entire high-bay facility would have to be replaced in order to meet the requirements for a hydrogen-rated facility. Thus, the hydrotreating facility was created as a stand alone unit. The facility walls and doors were rated to withstand unintentional explosions. A control room is located outside the room containing the reactor, permitting operators to control the apparatus remotely. In addition, venting and blow-out panels were installed in the upper section.

3.3 Distillation and Air Blowing

Once the THF was removed from the extract, the THF-soluble hydrogenation products were separated using vacuum distillation. This was performed using the setup as shown in the below figure. The THF soluble product was gradually heated under vacuum until vapors of liquid products, which were fractions of the coal-derived solvent, start separating out. The flask containing the THF solubles and the part of the condensing tube attached above the flask were covered with glass wool insulation to avoid products condensing in the distillation flask. These separated products were condensed in another flask immersed in a dry ice bath. The dry ice bath helps the quenching process and prevents the lighter products from escaping to the vacuum pump cold trap. The typical distillation conditions were 270-280°C temperature and about 30 mm Hg vacuum. The residue from the vacuum distillation was considered to be the soluble coal product (pitch). The distillate was the recovered solvent which would be recycled back to the process. The vacuum distillation was carried out in such a way so as to isolate as much solvent as possible, so that a sufficient quantity was extracted from the process in order to maintain the same coal-to-solvent ratio in the subsequent hydrotreatment run using coal and the separated recovered solvent. However temperatures above 300 °C were not exceeded since too much viscous material was separated out and became stuck in the condensing tube. This material was very difficult to remove. The recovered solvent was isolated and set aside for further use as the hydrogenation solvent.

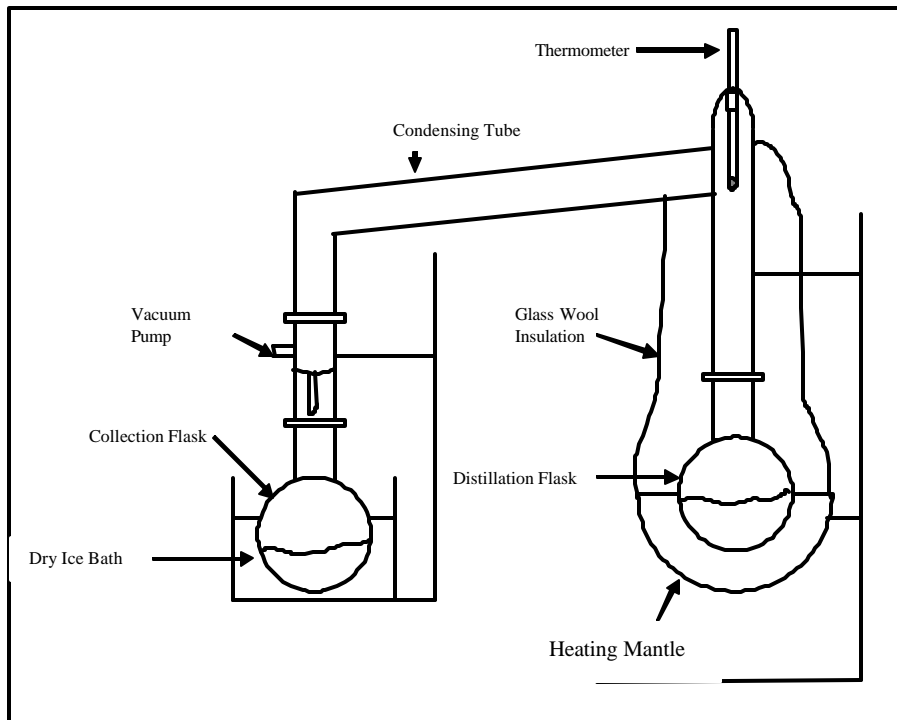


Figure 33. Vacuum Distillation Setup to Recover Solvent from the Pitch Product.

Once all of the products were removed from the reactors, and the level of liquid in the thimble had receded down below the bottom of the funnel, the top funnel was removed. The thimble was carefully lifted from the bottom funnel and placed down into

a glass Soxhlet extractor. The bottom funnel was then washed (and scraped if necessary), and the flask was filled with additional THF until it was about 2/3 to 3/4 full. The flask was then fitted to the bottom of the Soxhlet, and this was then placed onto a heating mantle. The top of the Soxhlet was fitted with a water cooled condenser. The cooling water was then turned on, and the heating mantle temperature was adjusted to get above the boiling point of THF (approximately 75°C). This was done using a variable autotransformer variac, set at about 60-62 on the dial. Once the contents of the flask began to boil, this was left to boil and reflux overnight, until the liquid in the Soxhlet had become mostly clear, signifying that all the soluble material in the thimble had been dissolved and moved into the flask.

The variac was then turned off, and the cooling water left on, to allow the mixture to cool to room temperature. The contents of the flask were centrifuged for 30 minutes at 2000 rpm in a glass centrifuge bottle to effect better separation. The liquid in the Soxhlet was emptied into the flask, and the thimble was allowed to drain into the soxhlet. Once the Soxhlet was mostly or all dried, the thimble was removed with tweezers and placed into a marked beaker to keep track of what run it was from. The Soxhlet was washed with THF and then emptied into the flask, and the flask was placed on a Buchler Instruments Rotary Evaporator using an oil bath set to 90°C to remove THF. After most of the THF had been removed from the flask, the temperature was increased to 110°C and left to run for a few minutes, and then a vacuum was applied. This was done until the boiling in the flask stopped. Care was taken to make certain that only the THF, not any product, was removed during the application of vacuum. After the flask had been allowed to cool, it was wiped clean of the oil and then taken to the Denver Instruments model A-200DS scale to be weighed. This mass was the THF soluble portion of the reaction products. The beaker containing the thimble was placed into a vacuum oven set to about 80-90°C and under a vacuum of 25-30 mm HG. A nitrogen purge was used to keep air out of the vacuum oven, and this was usually allowed to run overnight. The heat to the vacuum oven would be turned off, and it was allowed to cool, usually for a few hours. After the oven had cooled, the vacuum was broken, and the thimbles were weighed on the Denver Instruments model A-200DS scale. After subtracting the clean, dry thimble weight and the weight of the ball bearings, the weight remaining was comprised of the THF insoluble portion of the reaction products. For the purposes of calculating a conversion percentage, it was assumed that all of the THF insoluble portion would have come from the coal and not from the solvent. The coal conversion was calculated using the following equation.

$$\% \text{ Coal Conversion (daf)} = \frac{[(\text{Mass Dry Coal}) - (\text{Mass THF Insolubles})]}{\text{Mass Coal (daf)}} \times 100$$

THF was used in this process, rather than NMP (n-methyl pyrrolidone), which had previously been the solvent of choice at West Virginia University. NMP has a much higher boiling point (app. 202°C) which is in the range of many light hydrocarbon materials which would likely be present in the reaction products. During the rotary-evaporation step, this would likely lead to a loss of the soluble product while the NMP was removed. This was undesirable, and THF, having a much lower boiling point, was thought to be superior in determining coal conversion percentages.

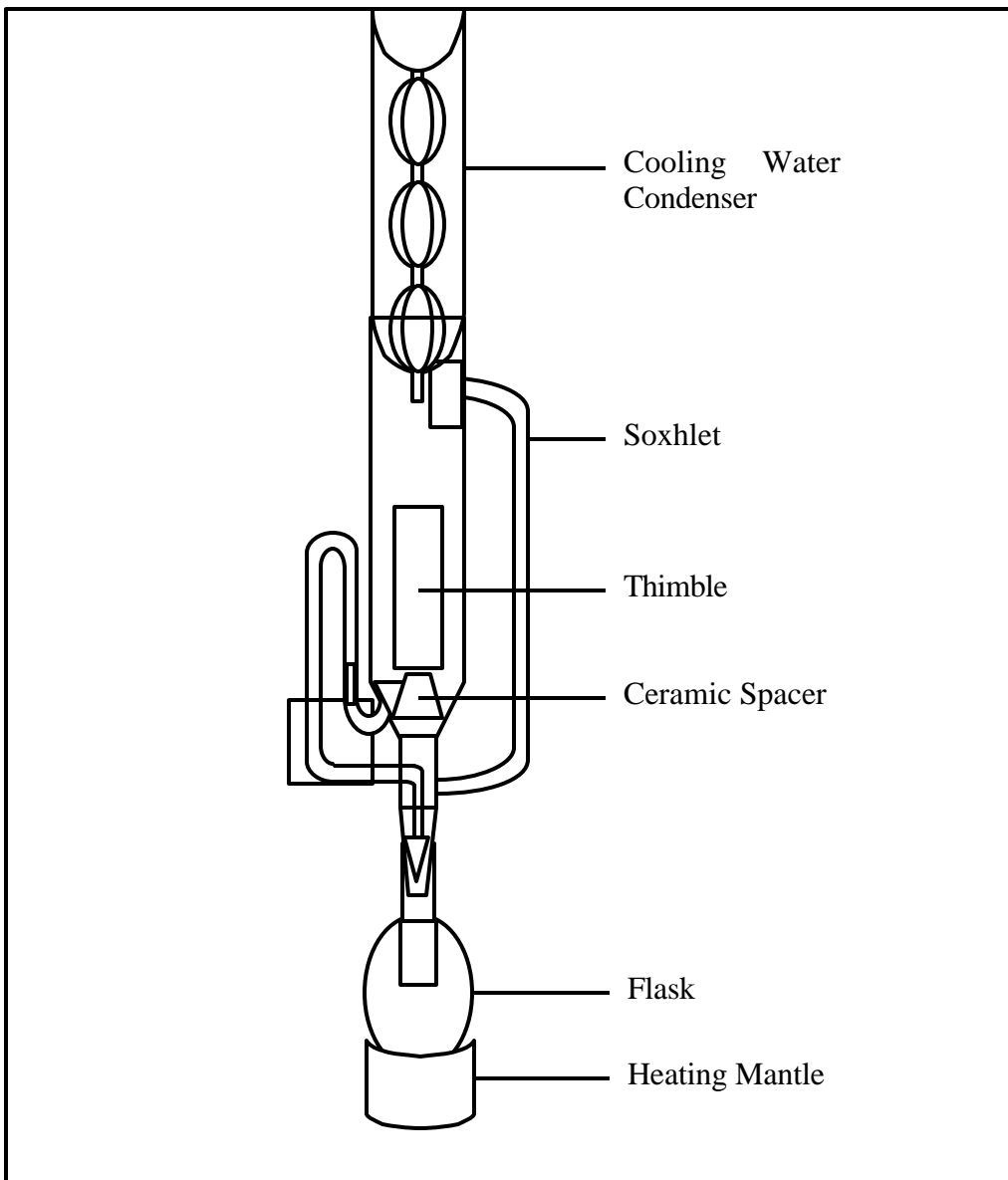


Figure 34. Soxhlet Condenser Apparatus.

3.3.1 Feed Pitch Preparation

The A240 petroleum pitch was used as received from the Marathon-Ashland Petroleum plant in Findlay, Ohio, without any modification prior to air-blowing. Coal tar pitch was received from Koppers Industries Inc. Since this pitch is laden with quinoline insolubles (QI), steps were undertaken for their removal. This was accomplished by placing approximately 1 kg of coal-tar pitch in a 10-L flask. Three to four liters of N-methyl pyrrolidone (NMP) were added to the pitch. The flask was then rotated in a hot oil bath at 100°C at atmospheric pressure for one hour using a Buchi R-152 rotary evaporator to dissolve the pitch.

Table 13. A240 Petroleum Pitch properties.

Ash (%)	0.035
Mettler Softening Pt. (°C)	116.9
Density (g/cc)	1.2365
WVU Coke Yield (%)	50.9
Conradson Coke Yield (%)	47.2
Toluene Insolubles (%)	5.735
Pyridine Insolubles (%)	0.84

After dissolution, the flask was removed from the rotary evaporator and the mixture apportioned into 750-mL centrifuge containers. Care was taken to ensure that the amount of solution was counterweighted evenly in the IEC PR-7000 centrifuge. Centrifugation was conducted at 4000 rpm (2000 times the force of gravity) for 1 hr to remove most of the un-dissolved solids, including ash. The supernatant liquid was decanted into a container, and then pressure filtered using a Millipore pressure filter apparatus at 15-20 psig using Fisher Brand G6 glass fiber filters (1.6 μ m retention). The filtrate was then returned to a clean 10-L flask to remove the NMP from the coal-tar pitch using the rotary evaporator under vacuum at about 80°C. After most of the NMP was removed, the oil-bath temperature was increased to approximately 110°C to remove the remaining NMP. The flask was removed from the rotary evaporator and the pitch was cooled in a refrigerated room. Dry ice was added to make the pitch brittle. The pitch was then chipped out very carefully, making sure not to break the flask, and placed into metal containers. The containers were then placed in a vacuum oven at approximately 170°C overnight using a nitrogen purge to remove any residual NMP solvent. The properties of the coal-tar pitch before and after the filtration can be seen in the following table.

Table 14. Koppers Coal-tar Pitch Properties.

	As Received	Post-filtration
Mettler Softening Pt. (°C)	109.9	108.1
Ash (%)	0.18	0.05
WVU Coke Yield (%)	-	53.95
Conradson Coke Yield (%)	-	48.0
Toluene Insolubles (%)	28.8	17
Quinoline/NMP Insolubles (%)	12.8	Nil

The coal-extract pitch used in the experiments was developed using West Virginia Marfolk Eagle Seam Coal. Characterization of this coal is shown in the next three tables.

Table 15. Petrographic Analysis of Marfolk Eagle.

County	Boone County
Mine	Massey's Marfork Operation
Vitrinite (% vol)	70.0
Liptinite (% vol)	7.6
Inertnites (% vol)	20.4
Mineral Matter (% vol)	2.0

Table 16. Elemental Analysis (wt %).

C	81.86
H	5.08
S	0.95
O	4.89
C/H atomic ratio	1.35

Table 17. Proximate Analysis (dry basis, wt %).

Fixed Carbon	62.0
Volatile Matter	32.0
Ash	6.0

The coal was set out in the laboratory overnight to remove surface moisture before grinding to approximately 20 Tyler mesh using a Holmes hammermill crusher. The coal was placed in metal pans and dried in vacuum ovens at a temperature of approximately 75°C under a nitrogen purge to remove any residual water.

Seven and a half liters of 1,2,3,4-tetrahydronaphthalene (tetralin) were added along with 3 kg of the 20-mesh coal (solvent to coal of 2.5 to 1, approximately) into a 5-gallon batch reactor. The reactor lid was then bolted to the body using a torque wrench to 150 lb-ft, according to specifications. The reactor was then purged of air with hydrogen for approximately 5 minutes and then pressurized to 500 psig hydrogen at room temperature. The reactor was then stirred while heating and brought to 450°C for 1.5 hr. About 3.5 hours were required to reach operating conditions. After reaction was complete, the reactor contents were cooled and about half of the mixture transferred to a 10-L flask. The flask was then placed on the rotary evaporator at 80°C to remove the tetralin and any other liquid reaction products. A heat gun was needed to assist in the removal of the solvent since tetralin was converted into naphthalene. The naphthalene condensed as a solid on the internal surfaces of the rotary evaporator causing plugging. To avoid blockage, heat was applied externally to the surface of the rotary evaporator

where any noticeable naphthalene accumulated. After most of the liquid was removed, the bath temperature was increased to 110°C to remove most of the remaining tetralin/naphthalene. This was followed by pouring 3-4 liters of NMP into the flask and dissolving the coal-extract pitch for 1 hour at 100°C. After dissolution, the flask was removed from the rotary evaporator and the mixture apportioned into 750-mL centrifuge containers. Centrifugation was conducted at 4000 rpm for 1 hr to remove most of the undissolved coal and ash. The supernatant liquid was then pressure filtered through G6 filters and the NMP was removed following the same method as for the coal-tar pitch mentioned above in the previous section. After cooling and removal, the pitch was then placed in a vacuum oven at approximately 170°C overnight using a nitrogen purge to remove any remaining solvent. This process was repeated for the remaining half of the reactor contents. After both batches of pitch were vacuum dried, they were ground and mixed together.

3.3.2 Air-blowing Procedure

Air-blowing of the pitches was conducted in a 1-L autoclave. The pitch was subjected to air-blowing at temperatures of 250°C, 275°C, and 300°C for various periods. A schematic of the reactor can be seen below in the following figure.

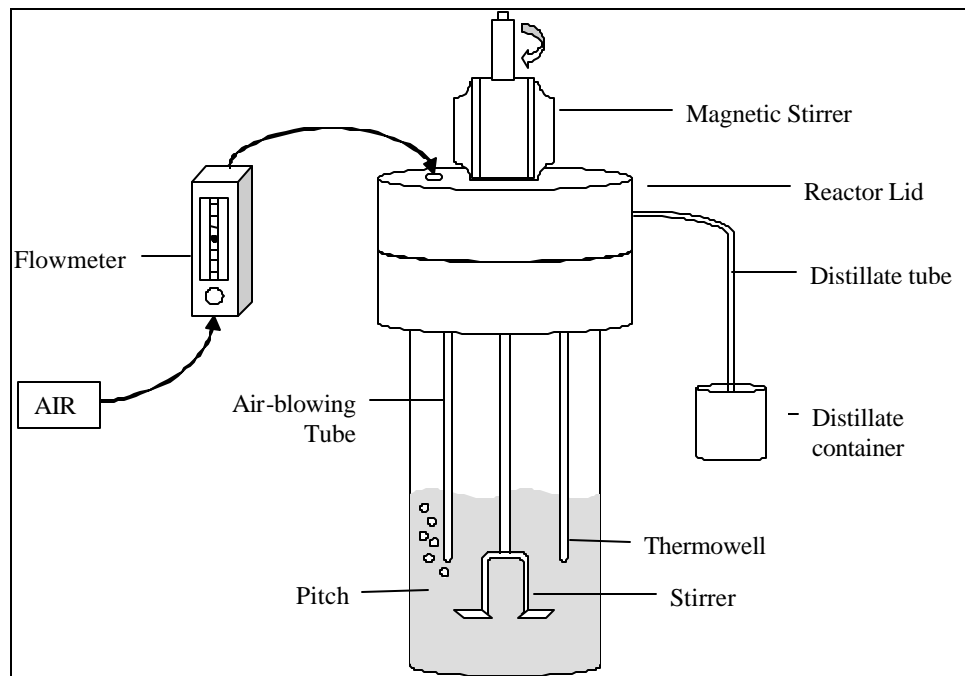


Figure 35. Diagram of the 1-liter Autoclave used in Air-blowing Experiments.

A Riteflow 150 mm flowmeter controlled the rate of airflow into the pitch. The air-blowing tube was placed into the pitch next to the stirrer to ensure good mixing of air. A thermocouple monitored the temperature of the pitch during air-blowing. The distillate tube allowed any light fractions of the pitch to escape into a collection container for weighing.

About 300 grams of pitch were weighed and placed into the 1-liter autoclave while the distillate container was placed at the end of the distillate tube. The reactor was then set to the desired temperature and allowed to heat up until the pitch became molten. While this was occurring, the airflow rate was set at approximately 1,182 ml/min (1.2 L/min) on the airflow meter to assure the airflow in the air tube was unobstructed. The flow rate could be held constant from batch to batch by using the manufacturers table of flow rate settings for air. Once the pitch was molten, the autoclave lid was attached and care was taken to make sure the thermocouple, magnetic stirrer, and distillate line were all performing properly. The reactor was then allowed to heat up further to the desired air-blowing temperature while being stirred. Upon reaching operating temperature, the stirrer was set to a speed of 750 rpm. During the reaction, the stirrer was stopped momentarily and turned by hand to ensure the material remained fluid and had not solidified.

Table 18. Air Oxidation Reaction Times of Three Pitches.

Temperature	Time (hr)		
	Ashland A240 Pitch	Koppers Coal-tar Pitch	Coal-extract pitch
250°C	9	8	3
	24	16	5
	30	24	-
	45	30	-
275°C	9	5	2
	17	10	5
	24	15	-
	28	21	-
300°C	6	3	1
	8	5	2
	14	8	3
	18	10	4

At the end of the reaction, the stirrer was stopped and the bolts on the reactor were loosened. The reactor lid was removed and set aside in a pan while the reactor was quenched to room temperature by immersion in cool water. After the reactor was cooled, the contents were chipped out and weighed along with any distillate that was recovered for mass balances. The reactor was cleaned out with a wire brush and solvent prior to each run to ensure no cross contamination occurred.

3.4 Characterization

The end use of the pitches is determined by their physical and chemical properties. Thus it is important to characterize the pitches based on their properties by some common techniques as mentioned below. This section also explains the standard procedure of doing these tests. The techniques used in this research to characterize the

pitch product were softening point, ash content, coking value, optical microscopy, and proton NMR.

3.4.1 Softening Point

For pitches, a distinct melting point cannot be determined because pitch is not a single, pure compound. The softening point is an ASTM test which reflects the ability of a sample to flow a prescribed distance. The measurement gives some insight into the molecular weight distribution of the species present in the pitch. In general, the higher the average molecular weight, the higher is the softening point. It can be beneficial in determining the end use of the pitch. For example a pitch having a low softening point (around 100 °C) can have applications such as binder or impregnation pitch. On the other hand, a pitch with high softening (around 200-250 °C) can be used for fiber spinning or coke making.

Softening point was determined using a Mettler FP80 HT, according to ASTM D3104-99. The pitch was passed through 80 and 20 mesh sieves. Then the pitch on top of the 20-mesh sieve was used to fill the sample cups on the hot plate. The pitch was then heated being very careful not to heat too much and cause it to smoke. After the pitch melted in the cup, more pitch was added until the sample cup was full. The samples were allowed to cool and a lead shot was placed on top of the cup. The sample cup was then placed in the Mettler apparatus and the softening point temperature determined.

3.4.2 Density

Density determinations were conducted using an AccuPyc 1330 pycnometer according to ASTM 2320-98. Five determinations were completed with the average value and standard deviation recorded later in the report. Since the reactor was quenched quickly after the reaction ended, the pitch solidified quickly and entrapped some of the air in the pitch. Air entrapment in the pitch resulted in spuriously low-density values. To resolve this problem 5-10 grams of the air-blown pitch were added to a ceramic crucible. The pitch was annealed at 100°C above the softening point for 20 minutes if the softening point was less than 200°C, or 30 minutes if the softening point was over 200°C. This allowed for the air in the pitch to escape so that an accurate density could be taken.

3.4.3 Ash Content

The amount of inorganic impurities present in the pitch sample was determined as the ash content. These impurities were derived from the inorganic material present in the original coal sample, which is basically the mineral matter in the coal. These inorganic materials were converted to inorganic oxides during the combustion process of the ash determination. Because this mineral matter is considered as an impurity in the final carbon artifacts, it is important for the ash content of the pitch to be low.

The ash content was determined using a Fisher Isotemp Programmable Furnace Model 497 in accordance with ASTM D3174 or ASTM D2415-98. Approximately 0.5 to 1 gram of sample was placed in a dry pre-weighed crucible and the crucible was partially

covered with a lid. The crucible was heated in air in the furnace at a rate 5 °C/min up to 500 °C and then at a rate of 3 °C/min up to 750 °C for 180 minutes and then cooled to ambient conditions at a rate of 10 °C/min. The weight of the sample remaining over the original sample weight gives the ash content.

3.4.4 Optical Microscopy

The optical texture of cokes can be determined by optical microscopy with a polarized-light microscope. The optical texture gives information regarding the surface and graphitization properties of the coke sample. The texture can range from an isotropic carbon (small, uniform domains) to anisotropic carbon (large, elongated domains). The commercial application of the coke sample depends on where it falls in the range of isotropic to anisotropic texture.

The optical structure was determined by means of a polarized-light optical microscope, Zeiss Axiostop, West Germany. The sample was dispersed in an epoxy resin mold, polished, and observed under polarized light. The domain size determines the optical texture. Isotropic coke has very small domains (< 0.5 micron) while an anisotropic coke has large elongated domains (> 100 micron).

3.4.5 Elemental Analysis

Elemental Analysis was completed on all of the pitch materials using a Thermoquest Flash EA 1112, using two separate methods. The first method measured the amount of C, H, S, and N (CHSN) while the second method determined the amount of oxygen directly. Measurements were conducted in triplicate to provide statistical results. The CHSN test was done by weighing approximately 2 to 3 milligrams of pitch into a tin sample cup. After this was done, about 2-3 milligrams of vanadium pentoxide, an oxidizer, were added to aid in the combustion. The instrument dropped the sample into a furnace in an oxygen environment to combust the sample completely. The combustion products passed through catalysts to convert the gases into other gases that are separable by gas chromatography and detected.

The second method measured the amount of oxygen that was contained in the sample. Approximately 3 milligrams of sample were weighed in a silver sample cup. Then approximately 2-3 mg of vanadium pentoxide was added on top of the sample to aid in the combustion. The sample undergoes nearly instant combustion while being transformed into the products N₂, CO, SO₂, and H₂O when dropped into the reactor at a temperature of 1060°C. The amount of oxygen was determined by measuring the amount of CO and SO₂ formed during the combustion of the material.

3.4.6 Coking Value

The coke yield determines the amount of carbon residue remaining after hydrogen and volatile matter were removed by thermal treatment, by heating the pitch in the absence of air. The heating process eliminates these volatiles and the pitch is transformed into coke when carbonization is complete. Most commercial applications require a coke yield of 50 to 60 percent by weight.

Industry-standard Conradson Carbon tests were carried out in accordance with ASTM D189 to determine the coke yield. First, ceramic crucibles were heated by flame to a red glow and immediately set in a desiccator. This process ensured that no moisture was present on the crucibles before weighing. The crucibles were then weighed and recorded. Between 0.4 – 0.6 grams of pitch were added to the crucible and recorded. The crucible was then placed in a small iron crucible and covered with a lid. The small iron crucible was then placed into a larger iron crucible with coke breeze lining the bottom half. The purpose of the coke breeze was to act as an oxygen scavenger to protect the pitch from combustion. A lid was then placed on the top of the large iron crucible and the crucible was set on top of a Meker-type burner. The crucible was heated on a medium flame for about 11.5 min and then held on a low flame for 13 min to complete the initial devolatilization. Finally, the flame was set to a high flame and held there for 7 min. on very high heat. After completion of the test, the flame was extinguished allowing the iron crucible to cool slightly. The ceramic crucible, still warm, was removed and set in a dessicator to completely cool to room temperature. The crucible was then weighed and a Conradson carbon yield was determined as a percentage of mass remaining based on the mass of initial pitch.

A modified in-house protocol is also used to determine the coke yield. The standard protocol is modified in that the coking of the pitch occurs more slowly, as opposed to the rather severe conditions encountered with the Conradson Carbon test. Slow heating is preferred in order to allow sufficient time for optical texture formation in the resultant cokes in order to determine coke structure. First, ceramic crucibles were heated by flame to a red glow and immediately set in a desiccator to ensure there was no moisture on the crucibles before weighing. The crucibles were weighed and recorded. Between 0.4 – 0.6 grams of pitch were added to the crucible and the weight recorded. Another larger crucible was filled halfway with coke breeze. A lid was put on the small crucible and set on top of the coke breeze followed by adding more coke breeze to the top of the small crucible until it was fully covered. As with the Conradson carbon test, the coke breeze acted as an oxygen barrier to prevent the pitch sample from burning. A lid was placed on the large crucible and set in a programmable furnace. The heating rate used was 5°C/min up to 600°C and held for 120 minutes. Then the sample was allowed to cool to room temperature and weighed. The modified protocol coke yield is calculated by using the following equation.

$$\%CY = \left(\frac{CWA - CWB}{PW} \right) * 100\%$$

Where CWA = weight of the crucible with the sample after coking, CWB = weight of the crucible, and PW = pitch weight.

Typically, the in-house modified protocol gives a slightly higher value of coke yield compared to the Conradson carbon method.

3.4.7 Viscosity

Viscosity was determined using a Brookfield DV-III Rheometer according to ASTM D5018-89. The instrument was checked for accuracy by determining the

viscosity of fluids of known rheology. Approximately 12 grams of pitch were placed into the sample chamber. The sample chamber was then heated up to approximately 15-20°C above the softening point of the pitch. A Brookfield SC4-34 spindle was used to deliver defined shear rates in order to determine shear stress. From this data, it is possible for the dedicated computer system to calculate the viscosity of the pitch at that temperature. After the viscosity of the pitch at the first temperature was determined, the temperature was raised 10°C and the method was repeated. The 10°C increments continued until the pitch viscosity was less than 1,000 cP.

3.4.8 Pyridine Insoluble Content

A pyridine extraction was done on the pitch to determine the amount of pyridine insoluble material present in the feed and air-blown pitches. One hundred milliliters of pyridine were added to a 500mL beaker while a magnetic stirrer was used to stir the solvent on a hot plate. A known amount of pitch, approximately 3 grams, was weighed and added to the pyridine. The mixture was then heated to the point where pyridine started to condense on the sides of the beaker at about 115°C and held for approximately ten minutes. A watch glass placed on top of the beaker helped in condensing the pyridine and prohibiting it from boiling off. After the solution was finished heating, the hot plate was turned off while allowing it to continue to stir. The weights of a 250mL round bottom flask, two boiling chips, and a thimble were recorded. The two boiling chips were added to the flask. The flask was clamped onto the bottom of a ring stand and a small funnel was placed into the top of the flask. The thimble was placed in this funnel and another funnel was placed on a ring support above the thimble. The bottom of the second funnel was barely inserted into the top of the thimble. This setup is shown below.

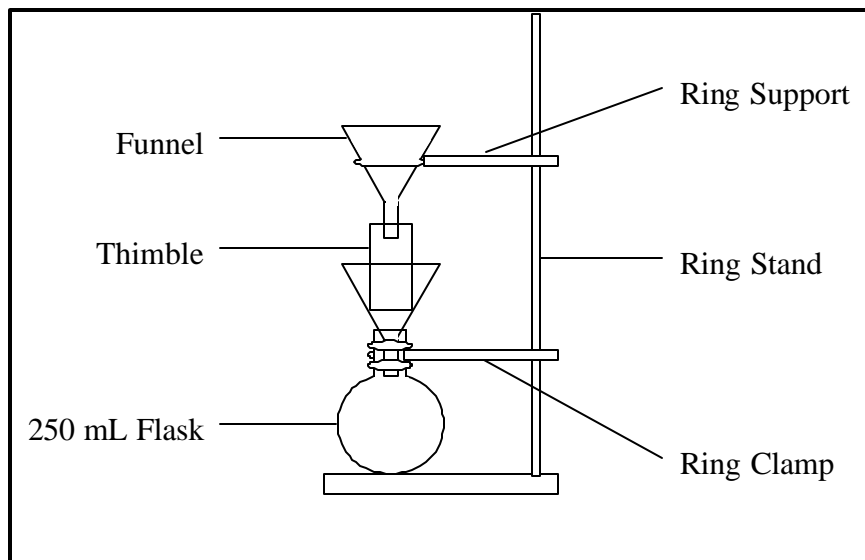


Figure 36. Diagram of Ring Stand Setup.

The mixture of pyridine was taken off the hotplate when cooled enough to the touch. A magnetic wand was used to remove the stirrer and residual material rinsed off

with pyridine into the funnel. The solution was poured into the top funnel making sure that the thimble below did not overflow. The thimble was drained into the flask and more solution was added to the thimble to keep it full until the beaker was empty. The beaker was rinsed out with pyridine into the thimble and the thimble was allowed to drain completely. The funnel was rinsed off and removed from the ring stand being careful not to knock over the thimble. A Soxhlet apparatus was obtained and a ceramic spacer was placed in the bottom of the Soxhlet. The spacer keeps the thimble above the level of the drain tube and prevents the thimble from overflowing during extraction. Using forceps, the thimble was placed on top of the crucible in the Soxhlet. The bottom funnel was rinsed with pyridine making certain there was no remaining solution left on it. The flask was removed from the ring stand and placed onto the bottom of the Soxhlet. The flask was set onto a heating mantle and the Soxhlet was attached to a condenser. A variac was used to heat the mantle up to the point that pyridine was condensing on the inside of the Soxhlet. The following figure shows the setup of the Soxhlet apparatus.

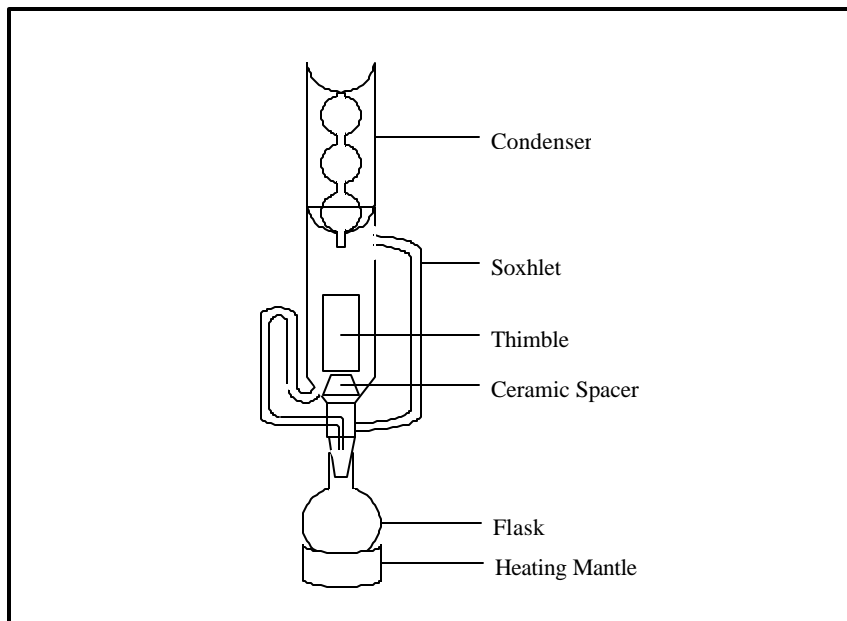


Figure 37. Soxhlet Apparatus Setup.

The Soxhlet extraction continued overnight or until the solution was clear, which generally required 24 hours. The heating mantle was then switched off and the flask and Soxhlet were left to cool. When cooled, the Soxhlet was tilted slightly until the solution was siphoned into the flask, making sure that solution from inside the thimble was not spilt out. When the thimble was completely drained, it was removed and placed in a beaker to dry. The solution was rinsed out of the Soxhlet into the flask and the solvent was removed using a rotary evaporator at 160°C. The flask and thimble were then dried in a vacuum oven at approximately 110°C overnight. Results are recorded in a later section.

The flask and thimble were weighed and the pyridine insoluble yield (% PI) was calculated using

$$\%PI = \left(\frac{ATW - TW}{PW} \right) * 100\%$$

Where ATW = weight of thimble and insolubles after dried in vacuum oven, TW = thimble weight, PW = pitch weight.

3.4.9 Toluene Solubility

This test determines the amount of insoluble material in the final digest and air-blown digest products. The test was done essentially the same as the THF extractions that were performed on the tube bomb reactor products; this time, however, the solvent was toluene. The same funnel-thimble-funnel-flask setup was used, and very similar procedures were followed. First, a beaker with about 125 mL of toluene was set on a stirring hot plate and a Teflon coated stirring rod was placed into the beaker. The stirrer was turned on, and the sample to be extracted was then weighed out. Approximately 3 grams of each sample was used, and once weighed out, it was added to the beaker of toluene, and the heat was turned on and adjusted so that the toluene would be heated to a point right around the boiling point, and a watch glass was placed on the top of the beaker to allow for refluxing of the toluene. The toluene refluxed for about 15 to 20 minutes, and then the beaker was removed from the hot plate. The stirring rod was removed from the beaker, and rinsed. Then the beaker was carefully emptied out of the beaker into the funnel-thimble-funnel-flask apparatus. After the beaker had been emptied and rinsed a couple of times, the thimble was placed into a Soxhlet refluxer and this was fitted onto the flask. This apparatus was then placed onto a heating mantle and fitted with a condenser. The toluene refluxed overnight, until no more pitch material leached out of the thimble. Once drained, the thimble was removed from the Soxhlet and dried in a vacuum oven, while the flask was heated in the rotary evaporator to remove the toluene, and then this too was dried overnight in a vacuum oven. The weights were recorded and the percent toluene insolubles and solubles were calculated.

3.4.10 Fourier-Transform Infrared Spectroscopy (FTIR)

Fourier-transform infrared spectroscopy (FTIR) was performed to look at the aromaticity and functional group changes that occurred with the solvents, coal digest liquids and air-blown digests during the various processing performed. The test was done using a Nicolet 510P FT-IR Spectrometer, and was done with a KBr Diffuse Reflection method for the coal digests and the air-blown products and with the ATR (Attenuated Total Reflectance) method for the solvents.

The ATR method was used for liquids that cannot easily be made into solid pellets. A sample of the solvent was poured onto the Zn-Se plate, which had been run clean as the background. This was then placed into the FTIR machine and the sample was taken.

To perform the FTIR on the digests, about 300 mg of potassium bromide (KBr) were weighed and added to a metal sample capsule. Next, coal digest (liquid) or air-blown pitch (solid) was added to the capsule. The capsule was then capped and a small piece of parafilm was wrapped around the cap to prevent any sample from escaping. The

capsule was then placed in a Wig-L-Bug shaker mechanism and shaken for 2 minutes at 3800 rpm. After this was done, the parafilm was removed and the capsule was tapped on the counter firmly to keep the sample from remaining in the cap when it was removed. The cap was then removed and the contents were carefully poured into the sample holder tray. A small spatula was used to smooth out the sample level in the holder tray, and the holder tray was then placed into the FTIR machine. The tray was placed into the instrument carefully to make certain that the laser would hit the center of the pellet. The instrument was purged with dry air for approximately 15 minutes and then the analysis was run.

Before any samples were analyzed in the FTIR, a background spectrum had to be run. This was a KBr-only sample, made in the same manner as the pitch and coal digest samples. This must be done every day, as KBr will readily absorb any atmospheric moisture, to ensure that the correct background signal can be subtracted from the sample readings. Once the background was run, the samples could be run; as many as needed, provided the background is regularly redone.

3.4.11 Pyridine Insoluble Content

A pyridine extraction was done on the pitch to determine the amount of pyridine insoluble material present in the feed and air-blown pitches. One hundred milliliters of pyridine were added to a 500mL beaker while a magnetic stirrer was used to stir the solvent on a hot plate. A known amount of pitch, approximately 3 grams, was weighed and added to the pyridine. The mixture was then heated to the point where pyridine started to condense on the sides of the beaker at about 115°C and held for approximately ten minutes. A watch glass placed on top of the beaker helped in condensing the pyridine and prohibiting it from boiling off. After the solution was finished heating, the hot plate was turned off while allowing it to continue to stir. The weights of a 250mL round bottom flask, two boiling chips, and a thimble were recorded. The two boiling chips were added to the flask. The flask was clamped onto the bottom of a ring stand and a small funnel was placed into the top of the flask. The thimble was placed in this funnel and another funnel was placed on a ring support above the thimble. The bottom of the second funnel was barely inserted into the top of the thimble. This setup can be seen below in the following figure.

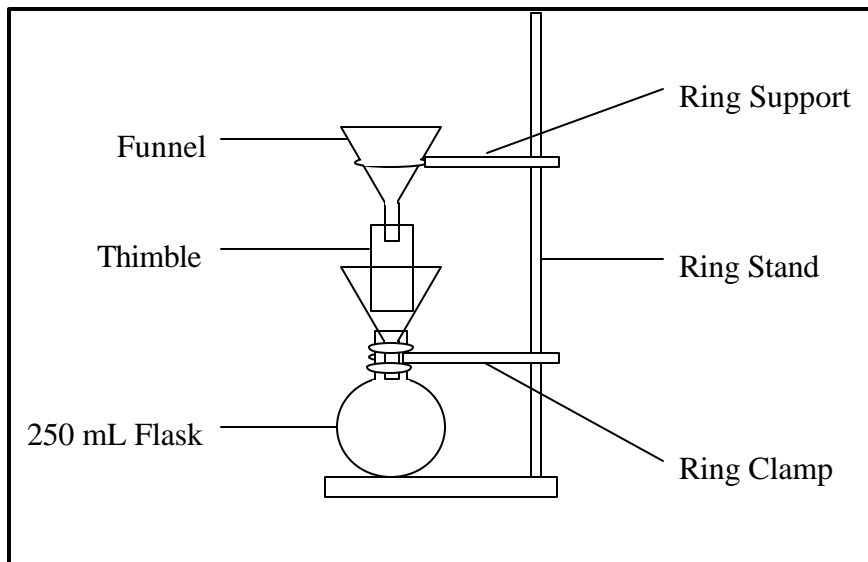


Figure 38. Diagram of Ring Stand Setup.

The mixture of pyridine was taken off the hotplate when cooled enough to the touch. A magnetic wand was used to remove the stirrer and residual material rinsed off with pyridine into the funnel. The solution was poured into the top funnel making sure that the thimble below did not overflow. The thimble was drained into the flask and more solution was added to the thimble to keep it full until the beaker was empty. The beaker was rinsed out with pyridine into the thimble and the thimble was allowed to drain completely. The funnel was rinsed off and removed from the ring stand being careful not to knock over the thimble. A Soxhlet apparatus was obtained and a ceramic spacer was placed in the bottom of the Soxhlet. The spacer keeps the thimble above the level of the drain tube and prevents the thimble from overflowing during extraction. Using forceps, the thimble was placed on top of the crucible in the Soxhlet. The bottom funnel was rinsed with pyridine making certain there was no remaining solution left on it. The flask was removed from the ring stand and placed onto the bottom of the Soxhlet. The flask was set onto a heating mantle and the Soxhlet was attached to a condenser. A variac was used to heat the mantle up to the point that pyridine was condensing on the inside of the Soxhlet. The following figure shows the setup of the Soxhlet apparatus.

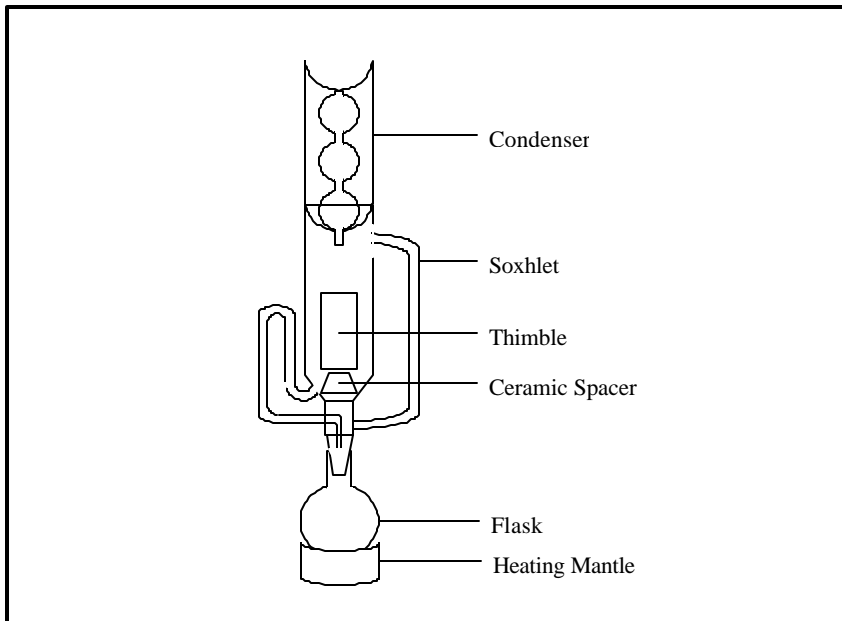


Figure 39. Soxhlet Apparatus Setup.

The Soxhlet extraction continued overnight or until the solution was clear, which generally required 24 hours. The heating mantle was then switched off and the flask and Soxhlet were left to cool. When cooled, the Soxhlet was tilted slightly until the solution was siphoned into the flask, making sure that solution from inside the thimble was not spilt out. When the thimble was completely drained, it was removed and placed in a beaker to dry. The solution was rinsed out of the Soxhlet into the flask and the solvent was removed using a rotary evaporator at 160°C. The flask and thimble were then dried in a vacuum oven at approximately 110°C overnight.

The flask and thimble were weighed and the pyridine insoluble yield (% PI) was calculated using

$$\% PI = \left(\frac{ATW - TW}{PW} \right) * 100\%$$

where ATW is the weight of thimble and insolubles after dried in vacuum oven, TW is the weight of the thimble and PW is the pitch weight.

3.4.12 Fourier Transform Infrared (FTIR)

Fourier-transform infrared spectroscopy (FTIR) was done to examine the aromaticity and functional group changes associated with air-blowing pitches. A Nicolet 510P FT-IR Spectrometer was used and the KBr-pellet method, as described by J. Yang, was followed.⁶⁹ First, about 300 mg of potassium bromide (KBr) were weighed and added to a sample capsule. Next, approximately 3 mg of pitch sample were added to the sample capsule with the KBr. The capsule was then capped and a thin piece of parafilm was wrapped around the cap to ensure no sample escapes. The capsule was then placed in a Wig-L-Bug and shaken for 2 minutes at 3800 rpm. After this was done, the parafilm

was removed and the capsule tapped on the counter firmly to make sure the sample did not remain in the cap when removed. The cap was then removed and the sample carefully poured into the pellet-press chamber manufactured by Spectra-Tech. The chamber was then tapped a few times to make certain the level of the sample was even. Next, the stainless steel rod was placed into the chamber on top of the sample. The assembled pellet press was held loosely in a hydraulic press for about 2 minutes while vacuum was applied. The vacuum assists in removing trapped air, which could interfere with making transparent KBr disks. The setup can be seen in the following figure.

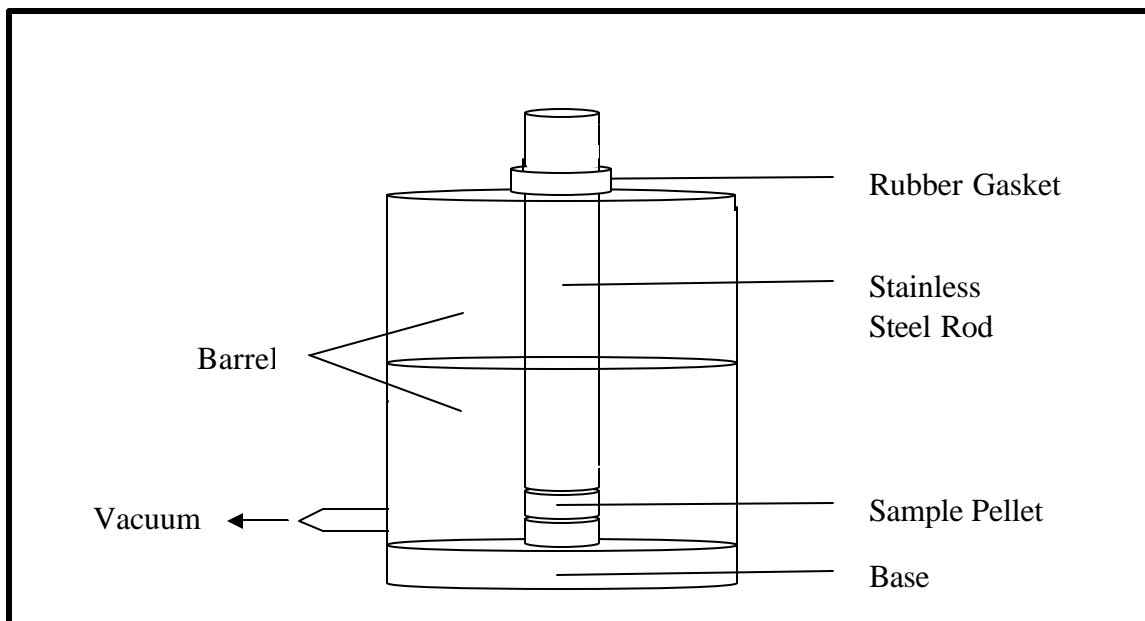


Figure 40. Spectra-tech Pellet Apparatus.

The pressure on the hydraulic press was then increased to approximately 2,000 psi for two minutes with the chamber still under vacuum. After this was done, the vacuum was released and the pressure on the hydraulic press was released. The sample chamber and rod were then placed upside down with a spacer on the top of the press to allow the pellet to be pushed out. A razor blade was sometimes required to pry the sample pellet from the stainless steel rod. This was done very carefully to ensure that the pellet was not broken or had any defects since it is very delicate. The pellet was then weighed and then placed into the FTIR sample holder. The sample holder was placed into the instrument carefully, ensuring that the laser was hitting the center of the pellet. The instrument was purged with dry air for approximately 15 minutes before the analysis was initiated. The analysis was carried out using an absorbance spectral resolution of 2 wavenumbers with 254 spectral scans.

A background spectrum is needed to analyze sample pellets in the FTIR. This is obtained by carrying out the same procedure above with no sample added to the capsule. Since KBr readily absorbs atmospheric water, a background spectrum needs to be run every few hours. This ensures that the correct background was subtracted on each of the samples. The potassium bromide should be stored at approximately 90°C under vacuum when not in use to remove the moisture. This procedure was used for each of the feed pitches and the air-blown pitches.

3.4.13 Thermogravimetric Analysis

Thermogravimetric data were obtained on all of the air-blown pitches and their feed materials using a TG-151 Thermo Gravimetric Analyzer (TGA) by Kahn Instruments. The TGA heated the sample up while measuring the change of weight over a specified time period and temperature rate. The quartz sample container was removed from the TGA and zeroed on a Mettler-Toledo MX/UMX balance. Approximately 100 mg of material were then added to the container. The quartz sample container was then carefully placed back onto the TGA. The body of the TGA was then raised carefully ensuring the container was not touching the walls. The body was then hand tightened onto the lid. The pitch was then heated at a rate of 3°C/min until it reached 900°C. The tests were all done in the presence of nitrogen at atmospheric pressure. The devolatilization of each sample could then be compared to illustrate the effects of air-blowing on pitches.

3.4.14 Simulated Distillation

Simulated distillations were carried out using a Varian CP-3800 Gas Chromatograph, fitted with a special auto-sampler (model # 8410) for liquid samples and special software, Star SD version 6.2, for simulated distillation. The samples were prepared in small 2 mL vials, and the solvent used was carbon disulfide (CS₂). A blank was prepared using CS₂ only, and then a small amount of the sample to be tested (app. 2-3 mg) was placed into the vial, which was then filled with CS₂ and shaken to mix thoroughly. This dilution is typically a fraction of about 1/100. Weights were not required, as the process is done on a volume basis. Samples were placed into the auto-sampler tray, along with a wash container of CS₂, and the Sim-Dist software was started. The software requires a method, a sample list, and prior preparation of the GC itself. For these runs, the Column and Injector temperatures ranged from 35°C to 425°C (this is the recommended maximum column temperature for the particular column used). Only one flame ionization detector (FID) was utilized, and the temperature was set to 380°C. This required both compressed air and hydrogen gas (at rates of 300 ml/min and 30 ml/min, respectively). To prepare the method, a standard method's parameters were compiled, and the temperatures and other settings were modified as described above to fit the desired analysis. This method was saved and then activated, which started the heating/cooling of the oven, detector, and injector. To prepare a sample table, a new sample table was opened, and the samples labeled according to their position in the sampler tray. At the beginning of the table, the CS₂ sample was labeled a “Baseline”, and the actual samples were marked for “Analysis”. At the end of the table, the “Sleep Sim-Dist” method was set to activate, which caused the machine to go into its “Sleep” mode, which closed the gas valves and cooled off the ovens. Once the sample table was prepared, the “Begin” button was pressed, and the program took over. Each sample run lasted for approximately 40 minutes, but the cool-down in between the runs typically took over an hour. After the data had been collected, the chromatograms were then analyzed by the StarSD software, and when compared with the appropriate baseline background (CS₂), boiling point distributions can be obtained. These data can then be

analyzed via differentiation to determine if the peaks in the derivative correspond to the digestion efficiency, air-blown softening point, or coke yield.

3.5 Mesophase Pitch

Mesophase pitch can be synthesized through the processing of petroleum, usually through catalytic cracking. The by-product heavy residue obtained from the cracking of petroleum can then undergo thermal treatment, vacuum or steam stripping, oxidation, or distillation. A specific type of pitch that can be produced, called mesophase pitch, is made when an isotropic pitch is subjected to careful thermal treatment. During this treatment, small pockets of mesophase, a liquid crystal state, form. As the treatment progresses, these pockets grow larger and coalesce. Eventually, the pitch becomes a 100% bulk mesophase pitch. These pitches have the properties of both an ordered solid state and a fluid liquid state, and are often used for high-modulus fibers and composites.

Mesophase pitches can form when isotropic pitch is heated above 350 °C. After melting, the pitch undergoes dehydrogenative condensation to increase the pitch aromaticity. The increase in aromaticity produces larger, more planar molecules, which come together to form tiny anisotropic spheres of liquid crystalline-like material. As these spheres collide, they coalesce to form larger spheres until the pitch becomes 100% bulk mesophase. Such a pitch can be used to produce high strength carbon fibers.

In this chapter, all of the materials and equipment used in the experiments are discussed, along with the processes of catalyst sulfiding, solvent hydrogenation, coal digestion, THF extraction of the products, followed by the scale-up process and the pitch modification (air-blowing), carbonization of the coal digests, as well as the analytical tests performed on the feeds and products. Process flow diagrams for both the small scale (30 cm³) and large scale (one gallon) experiments are given in previous figures.

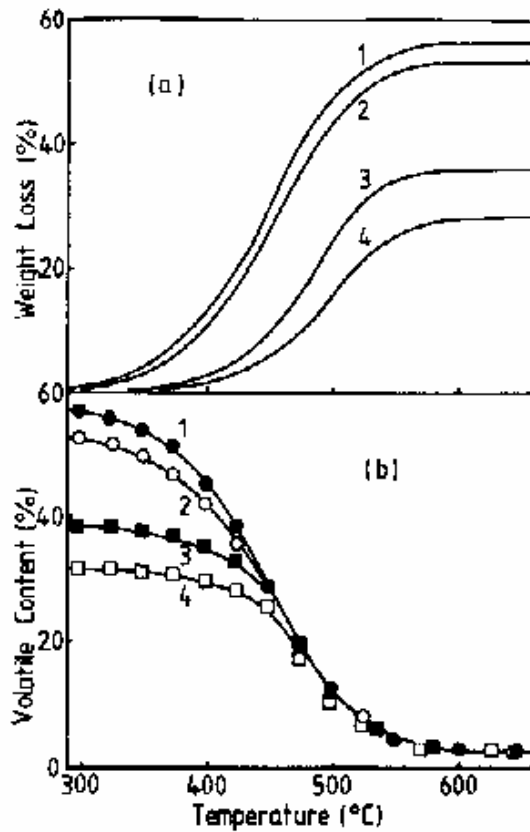


Figure 41. Thermogravimetric (TGA) Data for Pyrolysis Products of A240 Petroleum Pitch, 1 - as received; 2 - 365°C; 3 - 400°C; 4 - 460°C.

4.0 Results and Analysis

4.1 Coal Conversion using Different Solvents

Prior state of the art research has shown that tetralin is a highly effective hydrogen donor solvent capable of dissolving coal at a level of at least 70% by weight. However, tetralin (hydrogenated naphthalene) is already a premium product compared to the cost of either crude oil or coal tar pitch. While in principle it is possible to utilize expensive solvents in solvent extraction products, it is essential that expensive solvents be recovered efficiently. From an economic perspective it is possible to incorporate solvents in the final product if such solvents' cost is lower than the intended final product then the solvent can be successfully substituted for tetralin. Thus, instead of requiring 99% recovery and recycling of tetralin, it might be economically acceptable to carry out protocols with approximately 85% recovery.

The primary focus of the research discussed herein is upon reducing dependence on petroleum as well as coal tar from recovery coke ovens, leading to a desire to recycle solvent. However, it is recognized that the liquid products may be more valuable as a liquid fuel sources (for, example, as blends for gasoline, diesel, heating oil, aviation oil, etc.). Hence if and when this basic process is implemented by industry, it may well be that liquid fuel production could enhance the economics of the process beyond what the recycling-based protocols used at the laboratory and pilot scale.

Generally, aromatic heavy oils can be candidate solvents for coal-based processes. As a rule of thumb, "like dissolves like" would imply that coal-derived solvents might be effective at dissolving coal. However, petroleum derived solvents such as Decant Oil and Maraflex Oil, Slurry Oil were also trialed as control experiments. Three coal derived oils were selected for comparison trials as coal solvents: Heavy Creosote Oil (HCO), Refined Chemical Oil (RCO), and Carbon Black Base (CBB). All three are obtained as distillates of coal tar recovered from metallurgical coke ovens. Hence, all three oils are reasonably low cost and available in large quantities.

The basic protocol to evaluate each oil was to first flush the reactor with solvent to remove residual materials from previous experiments. The nominal five gallon reactor was usually filled with 2.5 gallons, or approximately 588 in³. This volume would fill the reactor up to about 9.1 inches from the bottom of the reactor. Assuming a specific gravity of the warmed solvent of 1.1, the mass of solvent to be charged to the reactor was 27.5lb or 12.49kg. The specific hydrogenation conditions for each solvent are given below.

After initial loading with the solvent, the reactor was purged twice and pressurized with hydrogen gas up to the desired level (in the first run, this was 500 psig H₂ cold). The reactor furnace was then heated to the reaction temperature while the impeller, controlled by the Reliance Electric SP500 VS Drive, rotated at 1000 rpm. The time, furnace temperature, reactor temperature, and reactor pressure were monitored during the entire process. Once the reactor reached the desired temperature, the reaction was allowed to proceed for one hour. At this time the furnace was turned off and the reactor was allowed to cool slowly. This typically took an overnight period, and the reactor temperature was at about ambient conditions when noted the following morning. The change in pressure from before the reaction had cooled to after the reactor had

cooled was recorded, as this is most likely the amount of hydrogen gas consumed. The reactor was then vented, and the furnace and impeller were then turned on again to warm the contents to allow for thorough draining. The contents were drained into 1-gallon tin cans and the mass of the product was noted. For this work there were three “levels” of hydrogenation used on the solvents as shown below.

Simulated distillation and FTIR were performed on both the raw and hydrogenated solvents as part of a standard protocol, in order to observe differences between the raw and processed solvents.

Table 19. Solvent Hydrogenation Reaction Conditions.

Hydrogenation Level	Solvent	Temperature (°C)	Pressure (psig cold)	Time (hr)
1	CBB	275	500	1
2	CBB	350	500	1
3	CBB	375	750	1
4	SO	375	750	1
5	MO	375	750	1

Accordingly, the ability of each solvent to digest coal was evaluated. First, the coal conversions with fresh solvents under standard conditions of hydrotreatment are discussed. Next, the same conversions with process-derived recovered solvents are presented and compared with those obtained from fresh solvents. Then, Mass and ash balances of the reactions are presented, and the reasons for the losses/gains are evaluated. The dependence of process parameters like temperature and reaction atmosphere is presented as well. Nitrogen was used to run the hydrotreating reactions under an inert atmosphere. Temperature was varied in differentials of 50 °C from 350 °C to 450 °C, to investigate the effect of this parameter on the conversion of the coal.

Tetrahydrofuran (THF) was used as a secondary solvent to separate the insoluble material from dissolved coal. THF would likely not be used as part of an industrial system to produce synthetic pitch, but represents a laboratory technique to precisely determine the amount of coal which can be digested in the primary solvents (i.e, hydrogenated HCO, RCO or CBB).

Finally, conversion results from a set of successive hydrotreatment experiments involving only recovered solvents and blends of fresh and recovered solvents are discussed.

Coke yield, ash content, elemental analysis, and optical texture of the resultant pitches are assessed. Based on these results optimum continuous hydrotreatment process parameters utilizing the recovered solvents could be established.

4.1.1 Solvent Hydrogenation

All the hydrogenation reactions were started with initial 500 psig cold gas pressure. Pressure was monitored with time during the course of the reaction and following quenching. The pressure profiles show the maximum pressure under high

temperature conditions, the average rate of rise or fall of pressure during the reaction and the cold pressure at the end of the run. This information gives significant insight into the chemistry of the reaction the rate of pressure drop for a hydrogen atmosphere likely is related to the rate of consumption of hydrogen in the hydrogenation reaction. Conversely, the rate of pressure rise when a nitrogen overpressure is present may be due to volatile gases.

Thus, during hydrogenation, the hydrogen pressure in the reactor initially increases with the increasing temperature. However, once a temperature of approximately 250°C is reached, the hydrogen pressure begins to drop off sharply. Likewise, this effect is associated with a decrease in the final cold pressure of hydrogen. However, only a small amount of hydrogen was actually been added to any of the solvents (maximum of ~0.25% wt.), a consequence of the mild conditions used for hydrogenation. The low level of hydrogenation could imply that the aromatic components were not totally saturated and that concentration of hydroaromatics was increased, which is desirable. This helps to keep the economical and safety concerns for the use of hydrogen gas in this process at a minimum. Hydrogen consumption was calculated using the initial and final cold pressure in the reactor (assuming hydrogen only in the vapor phase) with the ideal gas equation to obtain the initial and final mass of hydrogen gas present, then finding the difference.

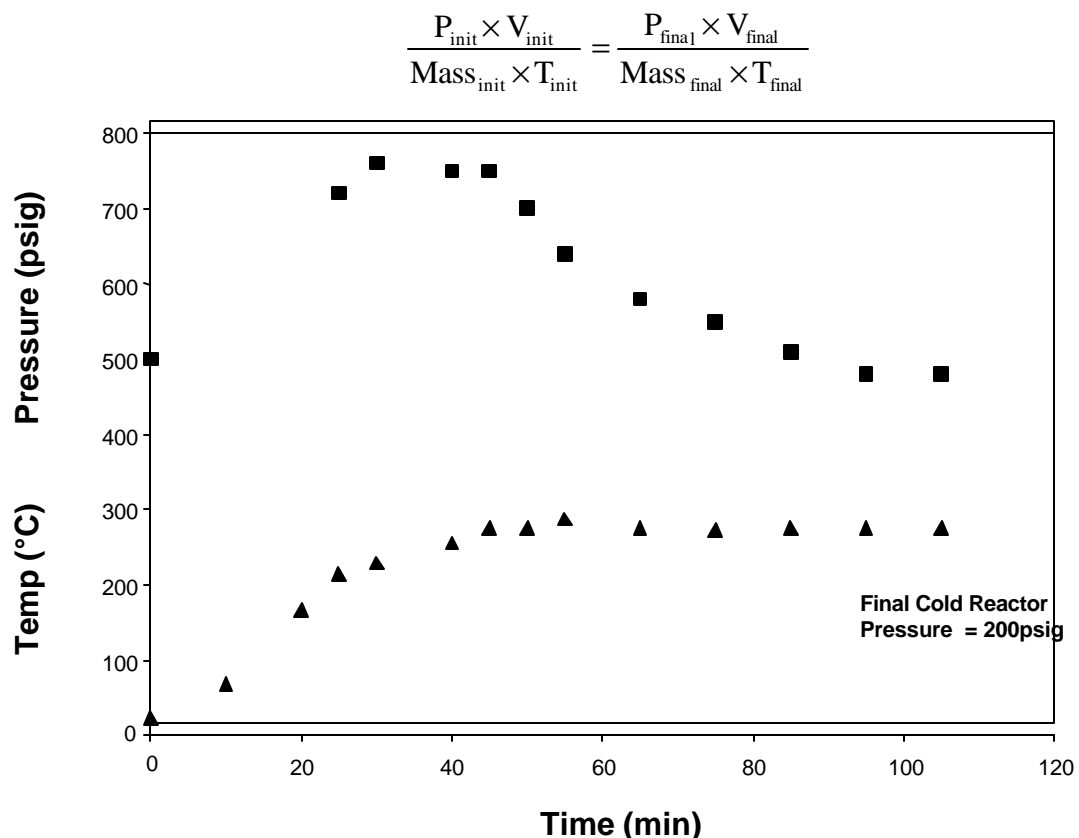


Figure 42. Temperature and Pressure for HCBB Level 1 Hydrogenation

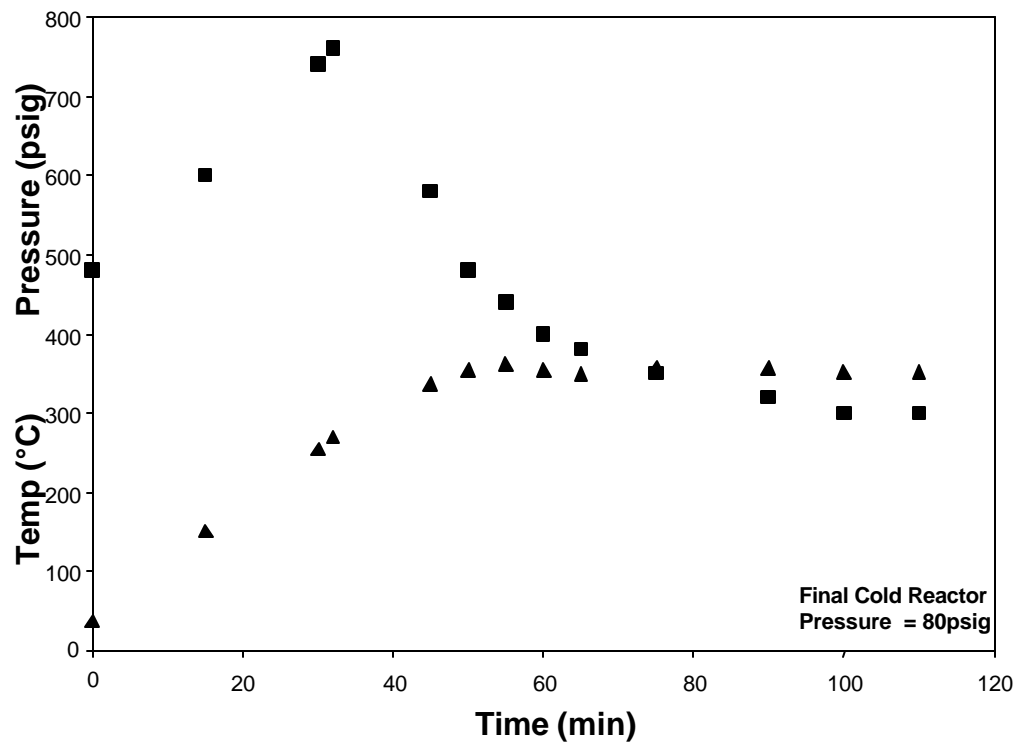


Figure 43. Temperature and Pressure for HCBB Level 2 Hydrogenation

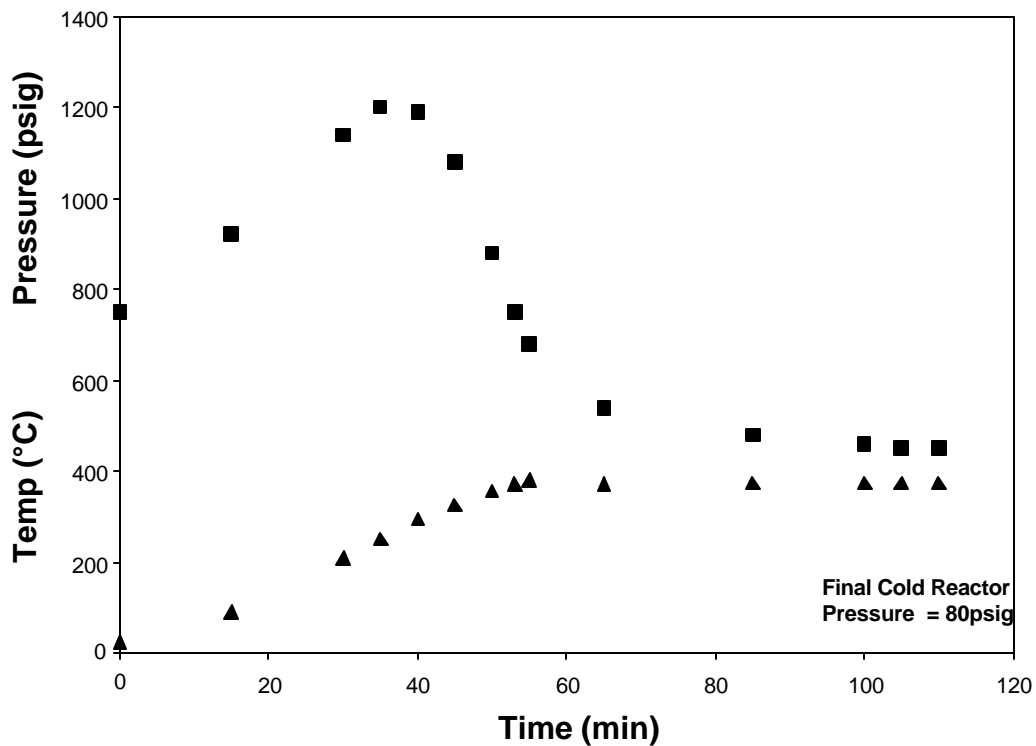


Figure 44. Temperature and Pressure for HCBB Level 3 Hydrogenation

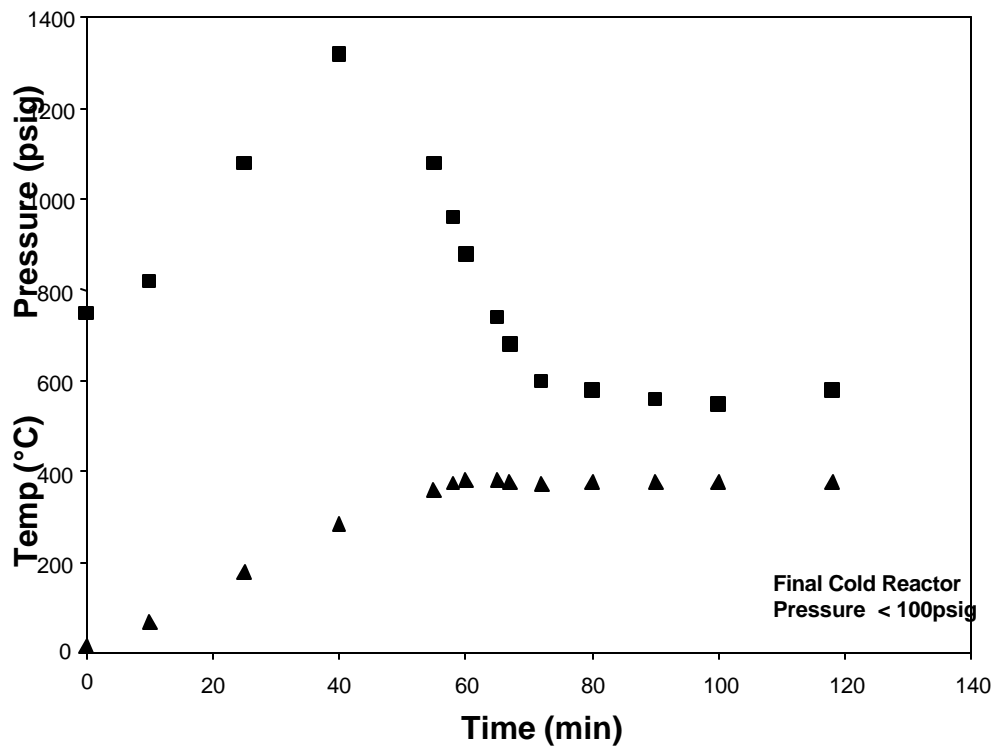


Figure 45. Temperature and Pressure for HSO Level 3 Hydrogenation.

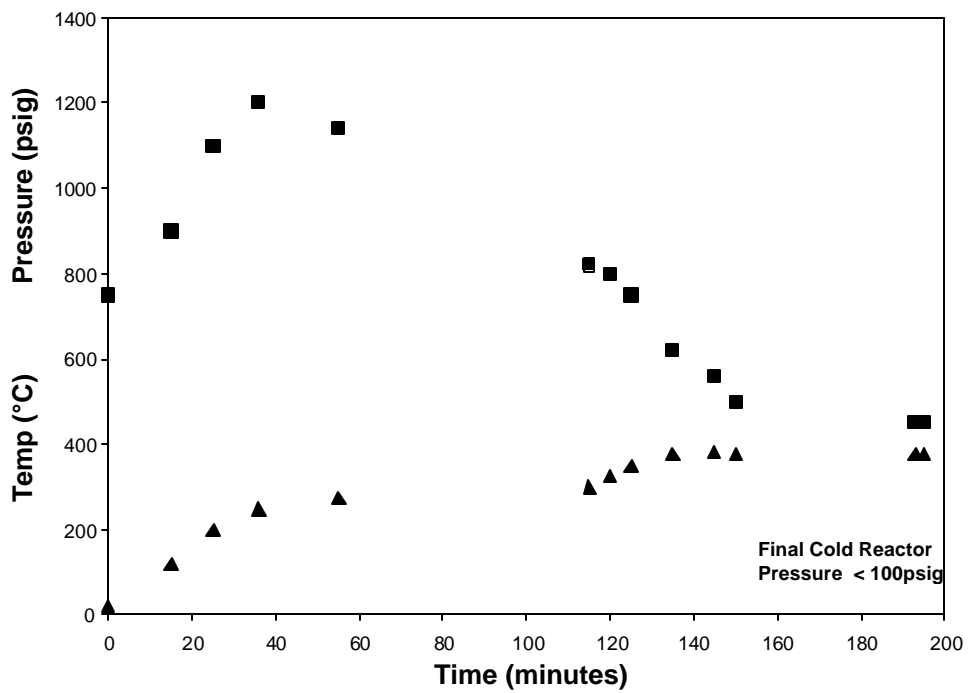


Figure 46. Temperature and Pressure for HMO Level 3 Hydrogenation.

Table 20. Solvent Hydrogenation Results.

Run Description	Mass H ₂ absorbed (g)	Wt% H ₂ absorbed	Reactor T, °C	Initial cold H ₂ Pressure (psig)
CBB Hydrogenation Level 1	12.99	0.10	275	500
CBB Hydrogenation Level 2	16.17	0.14	350	500
CBB Hydrogenation Level 3	28.48	0.24	375	750
Slurry Oil Hydrogenation Level 3	28.64	0.24	375	750
Maraflex Oil Hydrogenation Level 3	28.20	0.24	375	750

Simulated Distillation performed on each of the solvents used in this study shows some distinct changes in the boiling point distributions with hydrogenation. Comparing the raw solvents against each other, one can see the smooth and broad distribution present with the petroleum-derived solvents. The carbon black base (CBB) shows a more narrow distribution range, but a much more erratic curve. This is the result of the fact that this solvent is composed of distinct classes of aromatics, the steps in the curve possibly related to the ring numbers. For example, naphthalene is believed to cause the pastiness the solvent exhibits at room temperature. With hydrogenation, the boiling point distribution shifts, as the compounds become slightly more saturated with hydrogen, or in the case of the slurry oil, the molecules lose some small aliphatic side chains. Each solvent responds to the hydrogenation, but the carbon black base responds in a more significant way. Where there is not only a shift, but a substantial narrowing of the boiling point range, especially for the level 3 hydrogenated carbon black base, HCBB-L3.

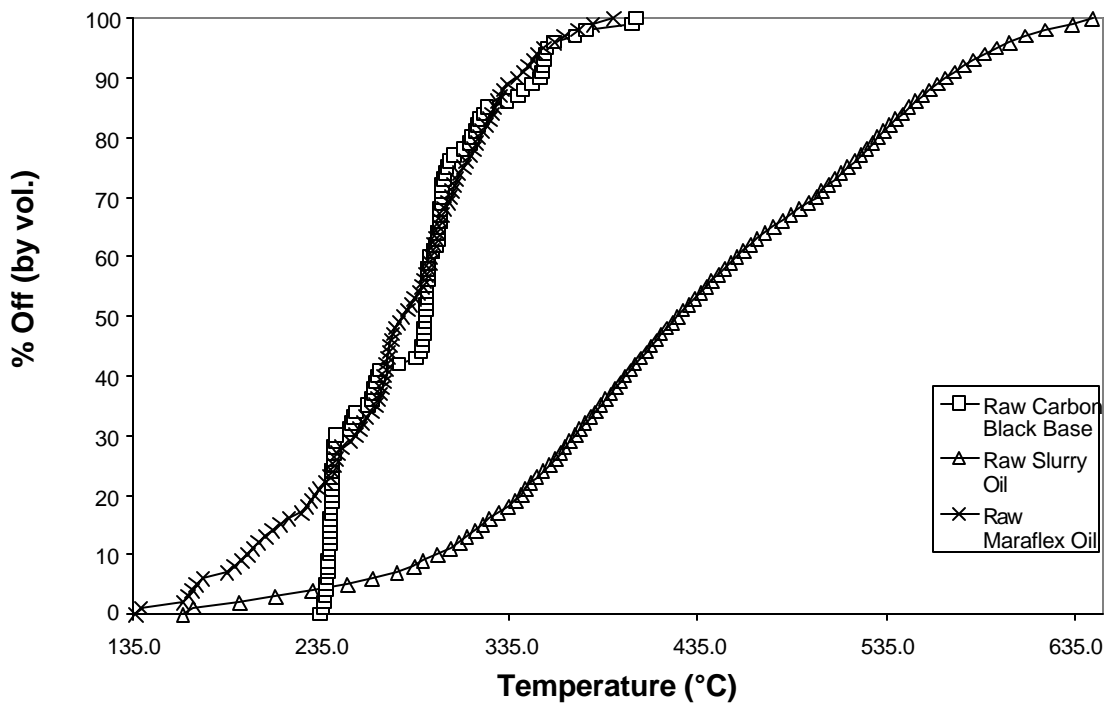


Figure 47. Boiling Point Curves of Raw Solvents.

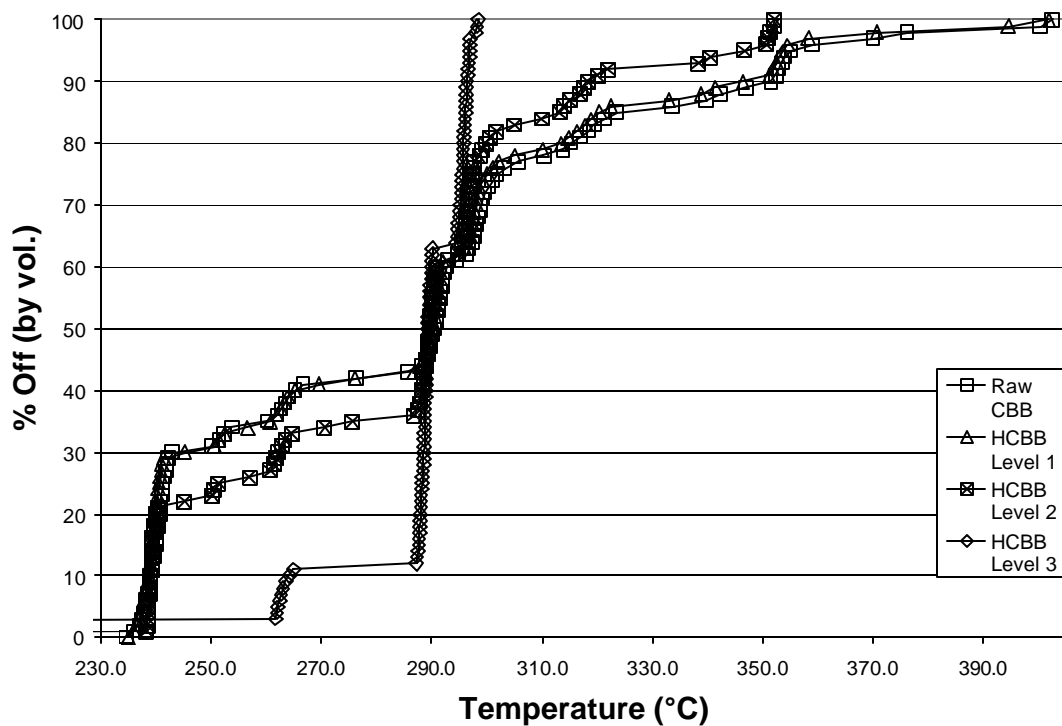


Figure 48. Boiling Point Curves of CBB Solvents.

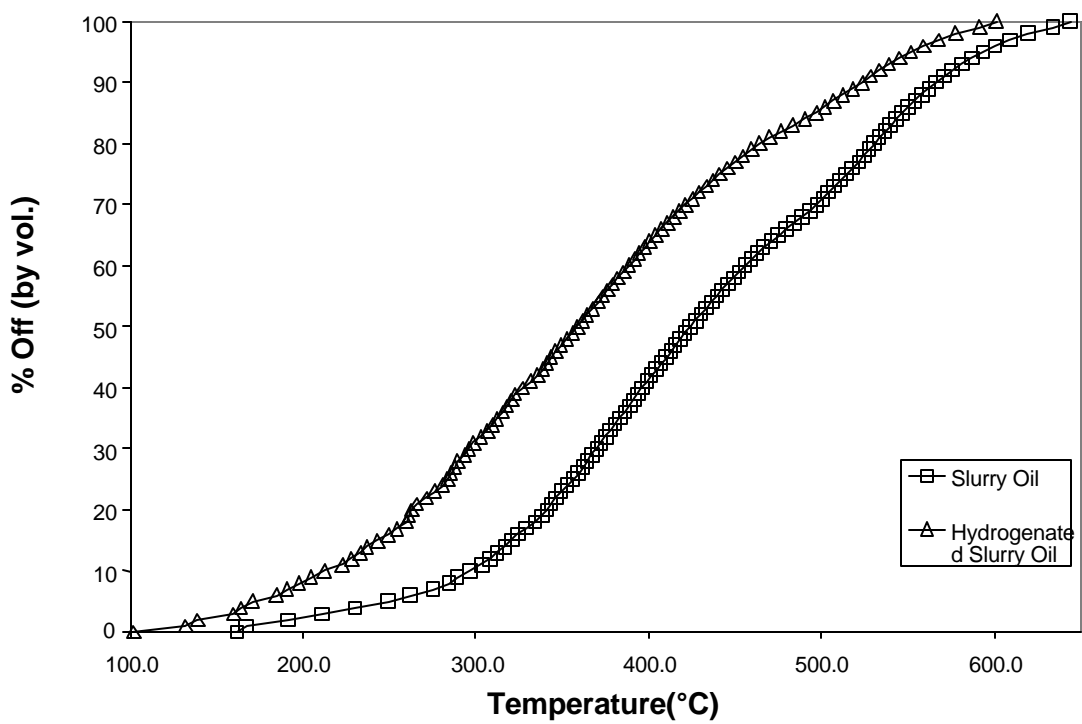


Figure 49. Boiling Point Curves of Slurry Oils.

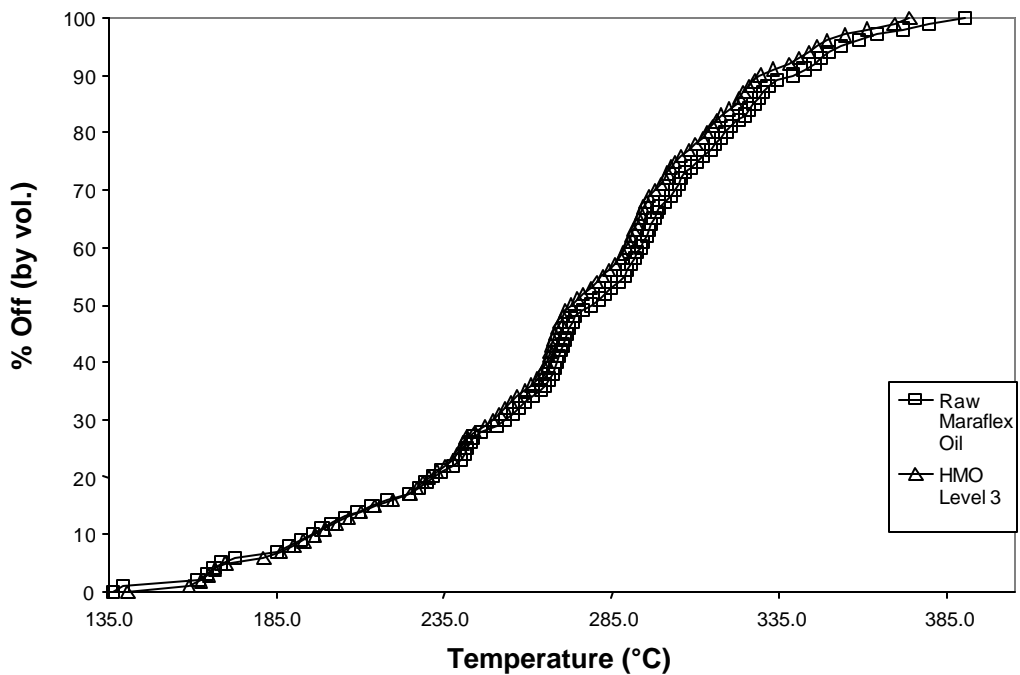


Figure 50. Boiling Point Curves of Maraflex Oils.

The first derivative of the boiling point curves was calculated using a simple slope calculation at each point in the curve (rise / run). Each curve shows the rate of change of the boiling point curves, which were prepared in an effort to see if there is some pattern in the curves for the different solvents. While it is apparent from comparing the curves for the slurry oil and Maraflex oil versus their hydrogenated counterparts, respectively, that a change has taken place (often as significant change), it is not apparent how this might apply to the present study. It is interesting to note that the changes with the carbon black base curves, much like the original boiling point distributions themselves, are erratic and, in fact, the level 3 hydrogenation curve is extremely different from the other CBB curves. The highest peaks in the derivative (corresponding to the largest rate of change), all occur at 10 for the CBB samples; the placement of these peaks simply shifts to higher temperatures. For the slurry oil the height of the highest peaks increases with hydrogenation, indicating a faster rate of change of the boiling point in the range of 350-400°C. For the Maraflex oil, the fastest rate of change of the boiling point curves occurs at a different temperature in the raw solvent than in the hydrogenated solvent.

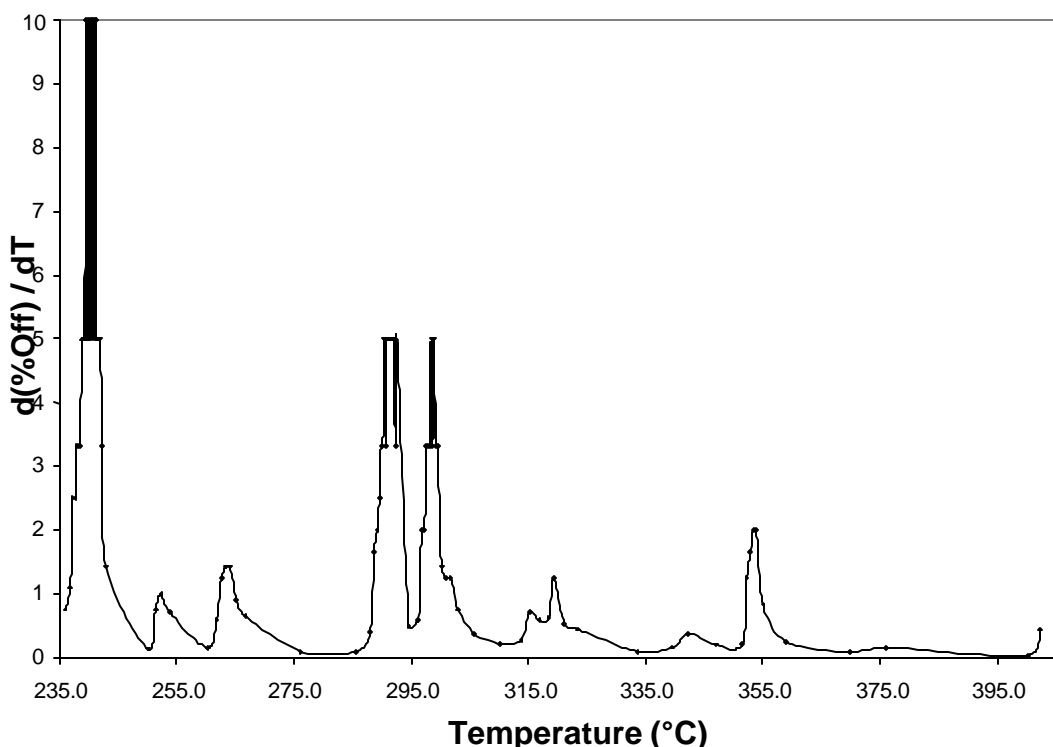


Figure 51. First Derivative of Boiling Point Curve for CBB vs Temperature.

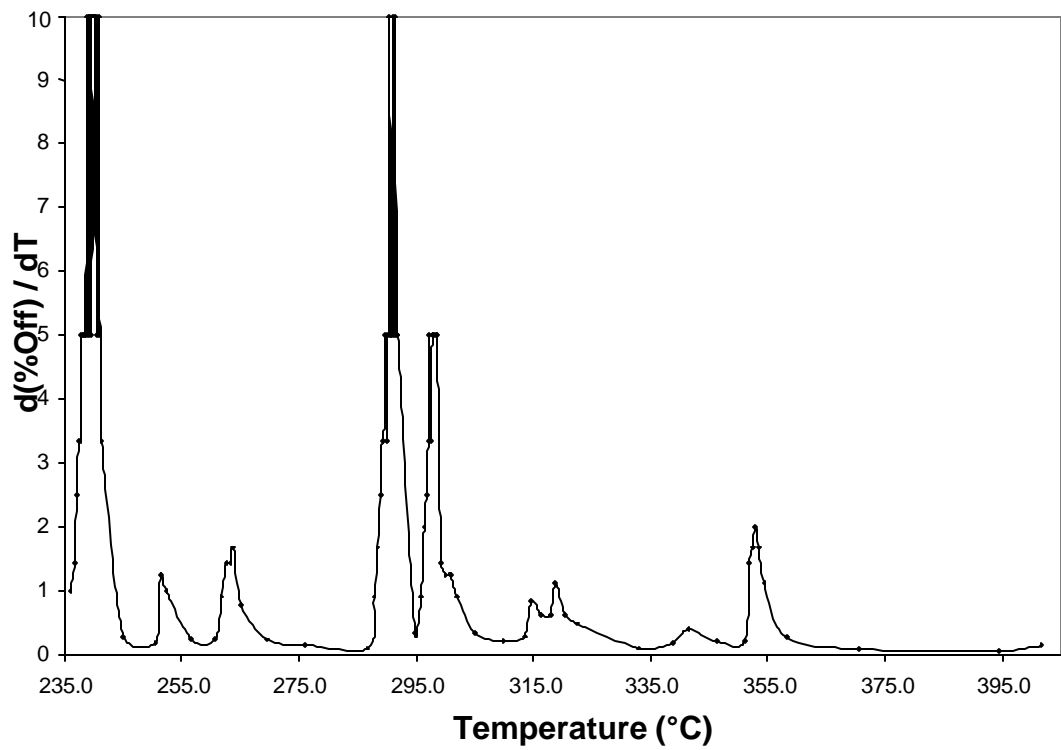


Figure 52. First Derivative of Boiling Point Curve for HCBB-L1 vs Temperature.

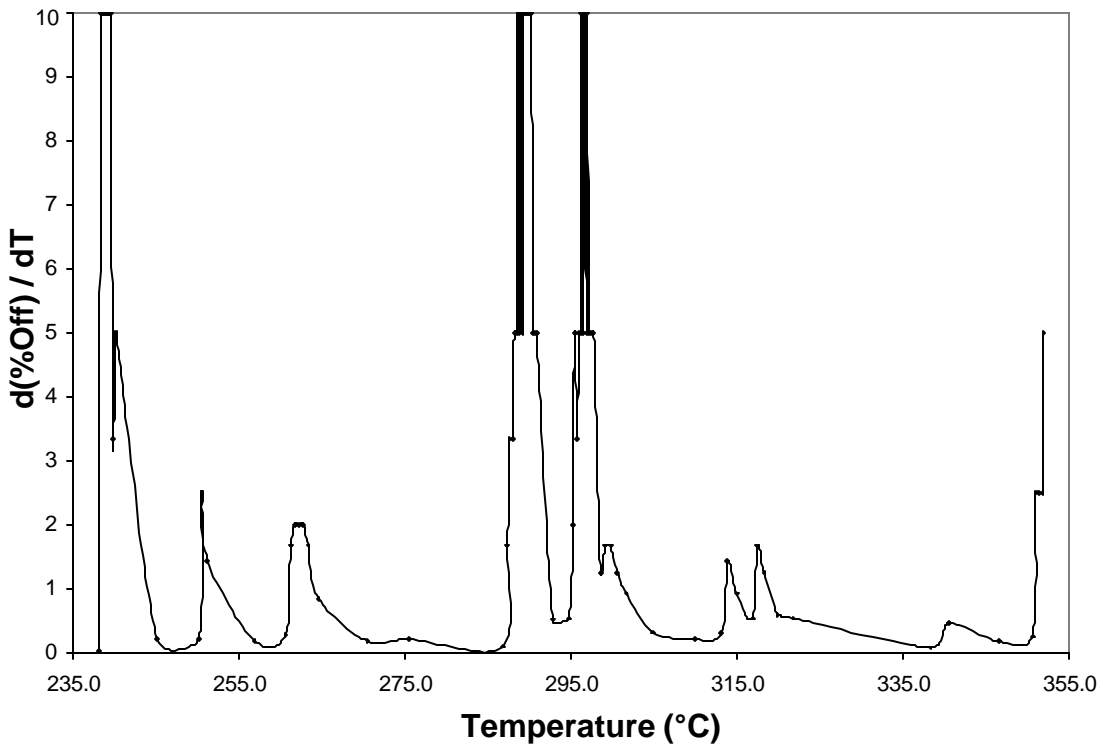


Figure 53. First Derivative of Boiling Point Curve for HCBB-L2 vs Temperature.

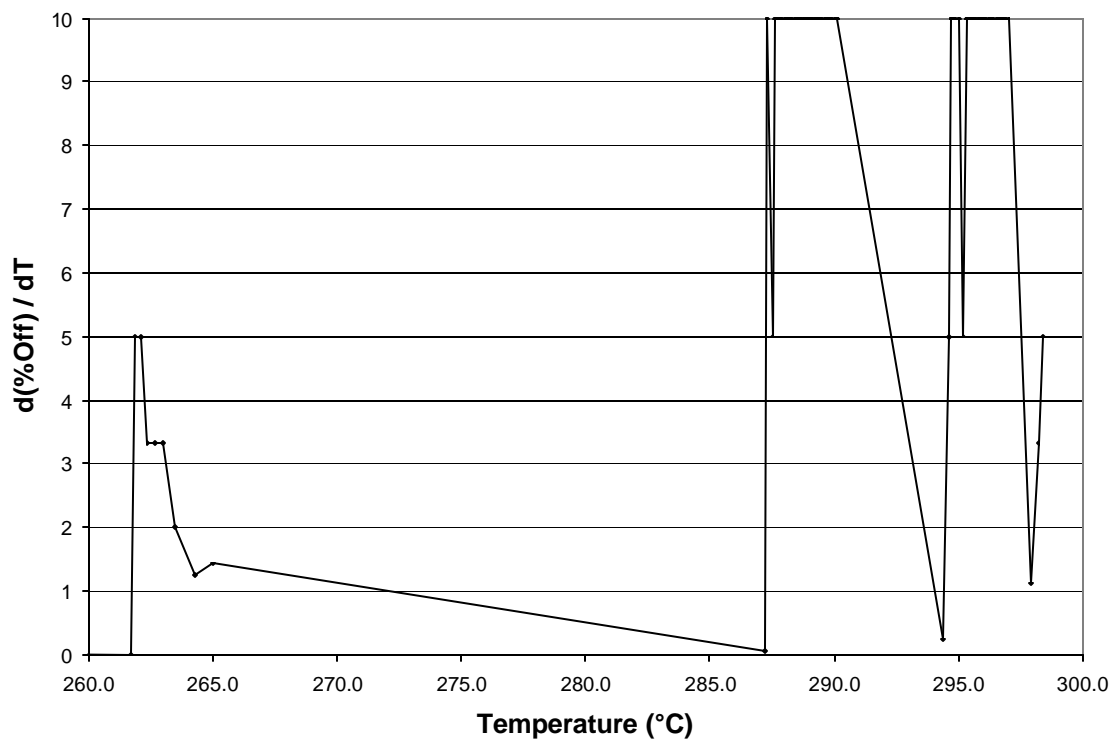


Figure 54. First Derivative of Boiling Point Curve for HCBB-L3 vs Temperature.

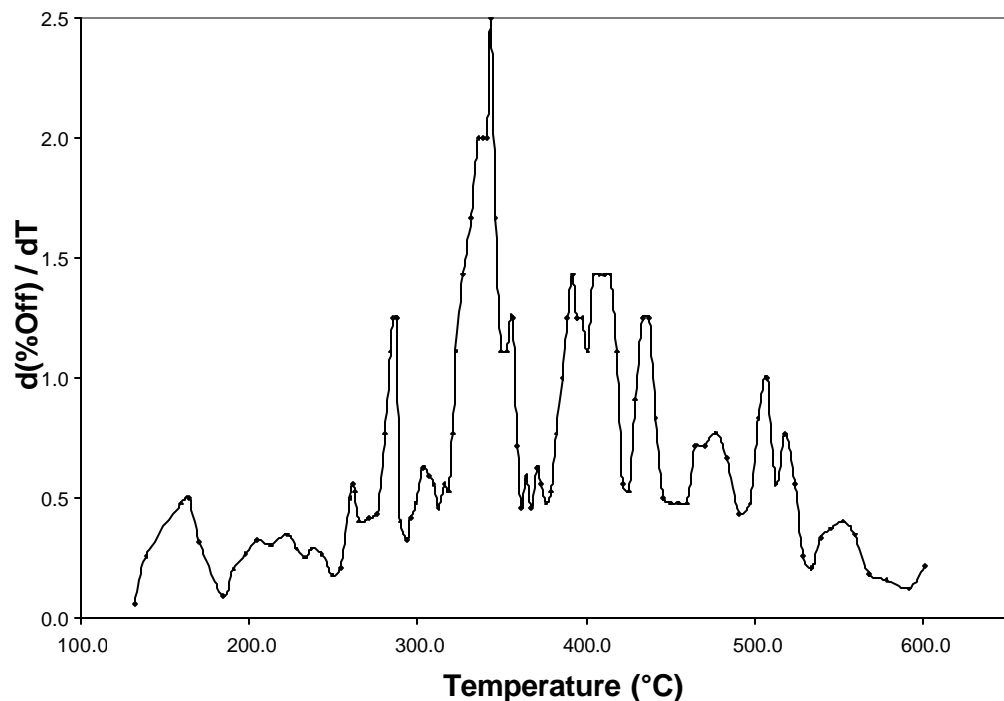


Figure 55. Derivative of Boiling Point Curve for HSO-L3 vs Temperature.

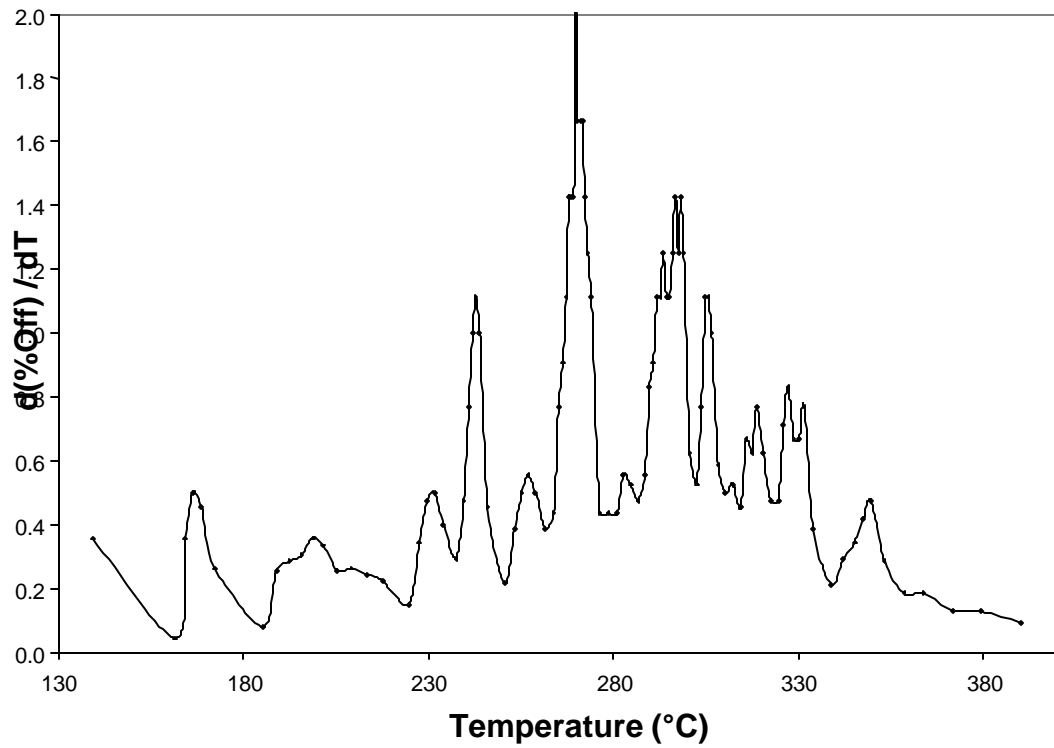


Figure 56. First Derivative of Boiling Point Curve for Maraflex Oil vs Temperature.

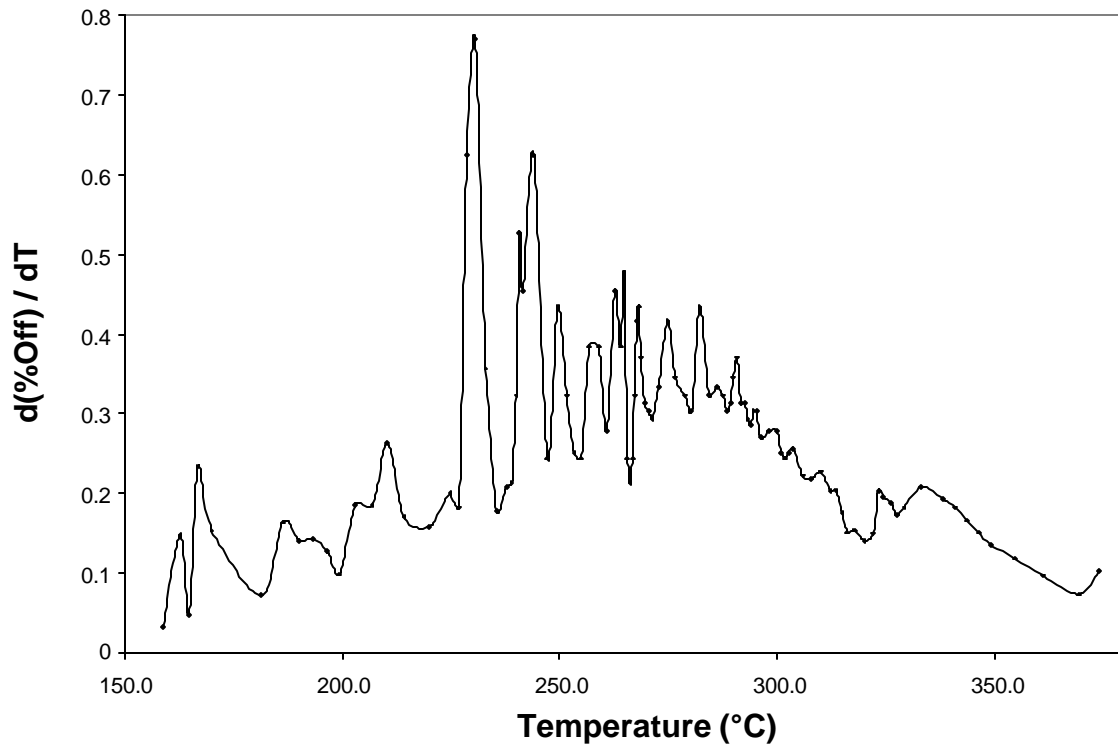


Figure 57. First Derivative of Boiling Point Curve for HMO-L3 vs Temperature.

Elemental Analysis and FTIR were also performed on each of the solvents and hydrogenated variant. The C/H ratio of the solvents provide an indication of what is happening in the solvent hydrogenation. The first observation is the obvious difference in C/H ratios of the coal derived liquids (CBB, AO) and the petroleum derived liquids (SO, MO). In both the carbon black base and Maraflex oil samples, as the hydrogenation level increases, the C/H atomic ratio and aromaticity factor $\{H_{ar} / (H_{ar}+H_{al})\}$ decrease, indicating that hydrogen is added to the solvents and is saturating the ring structures therein. However, for the slurry oil, the C/H ratio, and aromaticity factor increases with hydrogenation. During this reaction, it is hypothesized that in addition to hydrogen being added in bulk to the slurry oil, that perhaps small aliphatic side chains (i.e. ethane, propane) are being broken off of the solvent molecules and released into the vapor phase.

Table 21. Elemental and FTIR Analysis Data for Solvents.

Solvent	% C	% H	C / H atomic ratio	Har	Hal	$H_{ar} / (H_{ar}+H_{al})$
CBB	91.58	5.71	1.336	73.77	50.51	0.594
HCBB-L1	92.15	5.81	1.322	75.11	57.98	0.564
HCBB-L2	91.97	5.82	1.316	70.71	58.57	0.547
HCBB-L3	91.39	5.84	1.303	74.91	70.97	0.514
SO	87.38	9.56	0.762	23.39	362.55	0.061
HSO-L3	87.13	8.98	0.808	28.18	295.39	0.087
MO	92.22	7.77	0.990	56.74	144.03	0.283
HMO-L3	92.19	7.82	0.982	51.11	155.58	0.247
AO	92.41	6.21	1.241	N/A	N/A	N/A

Additionally, the amount of sulfur (S) present in the solvents is affected in this hydrogenation step. The amount of sulfur in all of the solvents is decreased with hydrogenation, as can be seen from the following figure. This is good, especially for the slurry oils, which contain a larger amount of sulfur than any of the other solvents initially. The nitrogen level in these solvents is not appreciably affected in the hydrogenation, but the level is reasonably low in this process, and the nitrogen level in the products is not of importance in this study.

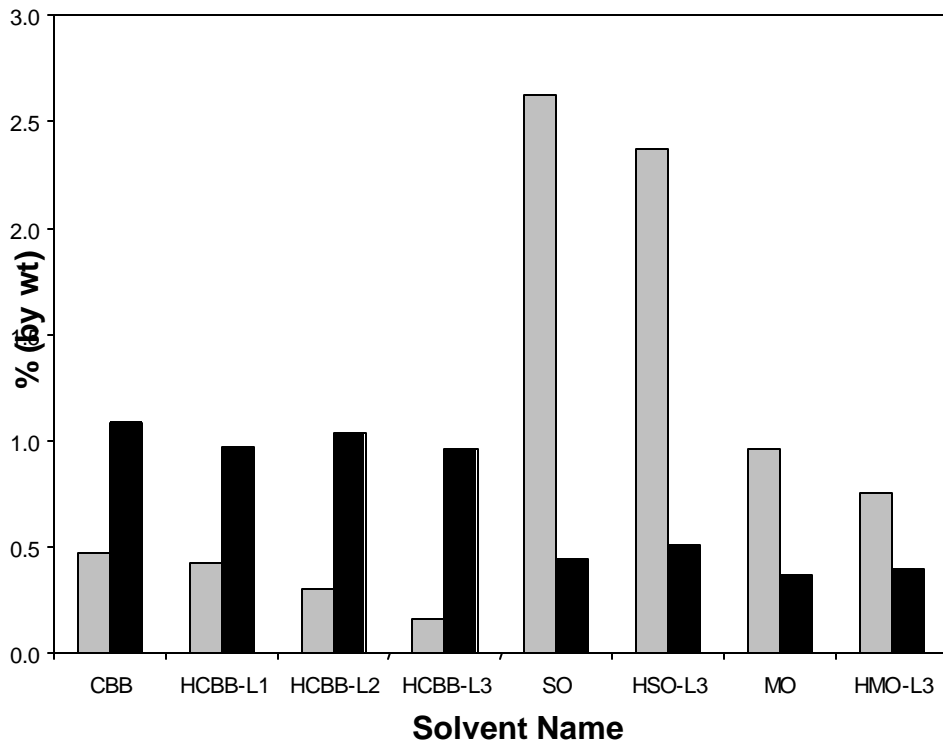


Figure 58. Amount of Sulfur (left) and Nitrogen in Solvents.

4.1.2 Coal Conversion in HCO, CBB and RCO

Heavy Creosote Oil (HCO), Refined Chemical Oil (RCO), and Carbon Black Base (CBB) were screened for their suitability as hydrogen-donor solvents for coal conversion under identical conditions of 400 °C, 500 psig cold hydrogen pressure, one hour reaction time, and a solvent-to-coal ratio of 5:1. This solvent-to-coal ratio is higher than what would be sought for commercial processes. The main reason for using a high solvent-to-coal ratio was to obtain an adequate amount of recovered solvent after separation from the pitch, so as to study these recovered solvents separately as recycle solvents in subsequent digestion runs. These coal-derived liquids are characterized according to their ability to convert coal to THF soluble material. Two different methods of measuring their effectiveness were used: (1) the overall conversion based on the total feed (i.e. coal plus solvent) as given by the first equation and (2) the coal-alone conversion based only on the weight of coal as given by the second equation.

The overall and coal-alone conversion for these liquids at 400 °C and 500 psig H₂ pressure is shown in the figure below. These results show that the most effective solvent for solubilizing coal to THF solubles is CBB with a coal-alone conversion of 43.4 ± 0.9 %, while the least effective solvent is RCO with coal-alone conversion of 31.1 ± 0.5 %. Conversion for the solvent CBB is close to HCO showing a conversion of 42.6 ± 0.7 %. The overall conversion of CBB, HCO, and RCO are 90.2, 90.1, and 88.2 %, respectively.

The absolute value of the conversion for each solvent differs depending on whether the overall or coal-alone basis is used. In other words, the overall conversion

includes solvent in its calculation, while the coal-alone conversion does not. Thus, the coal-alone conversion might seem to be a more appropriate figure of merit. Yet the distinction between coal and solvent is somewhat lost during the digestion, as the final product contains contributions from both feedstocks. Hence both bases ought to be considered.

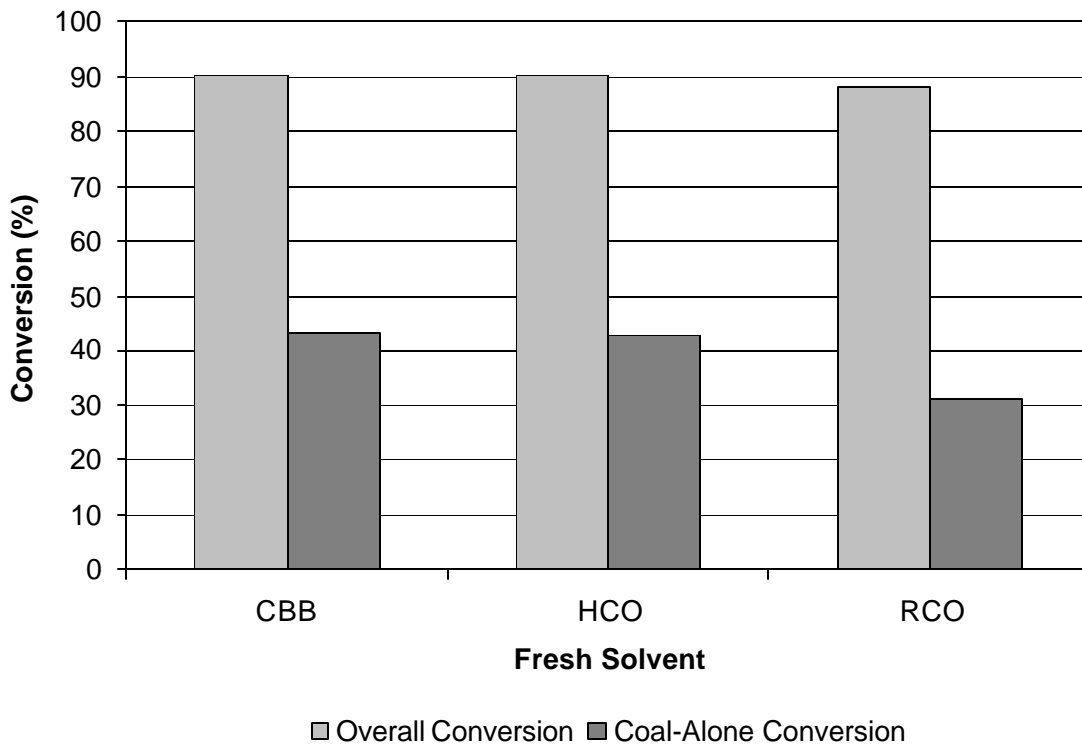


Figure 59. Overall and Coal-alone Conversion Yields with Fresh HCO, CBB and RCO at 400 °C, 500 psig Cold Hydrogen and One Hour Reaction Time

The THF insolubles are derived from the coal and not from the solvent. This was tested initially by dissolving the fresh coal-derived solvents in THF and then filtering the solution to check for any solids. The solution looked homogenous and no residue was found on the filter paper. Since the fresh solvents did not contain any THF insolubles, it was safely assumed that these solvents would not form any such material after hydrotreating. This is an important point since the coal-alone conversion is calculated solely from the weight of the residue which is assumed to originate exclusively from the coal.

4.1.3 Recovered Solvent Evaluation

The effectiveness of the recycled solvent which had been recovered by distillation from the previous hydrotreatment run was measured by comparing the solubility of coal before and after recycling. The following figure shows the overall and coal-alone conversion results for the corresponding recovered solvents. The overall conversion results show 90.4, 90.2, 88.3 % conversion for recovered CBB, HCO and RCO,

respectively. As compared to fresh solvents, the overall conversion is almost the same, because the solvent continues to dominate the amount of coal and hence very little difference in coal conversion was observed. Thus the coal-alone conversion is a more useful figure of merit in this instance.

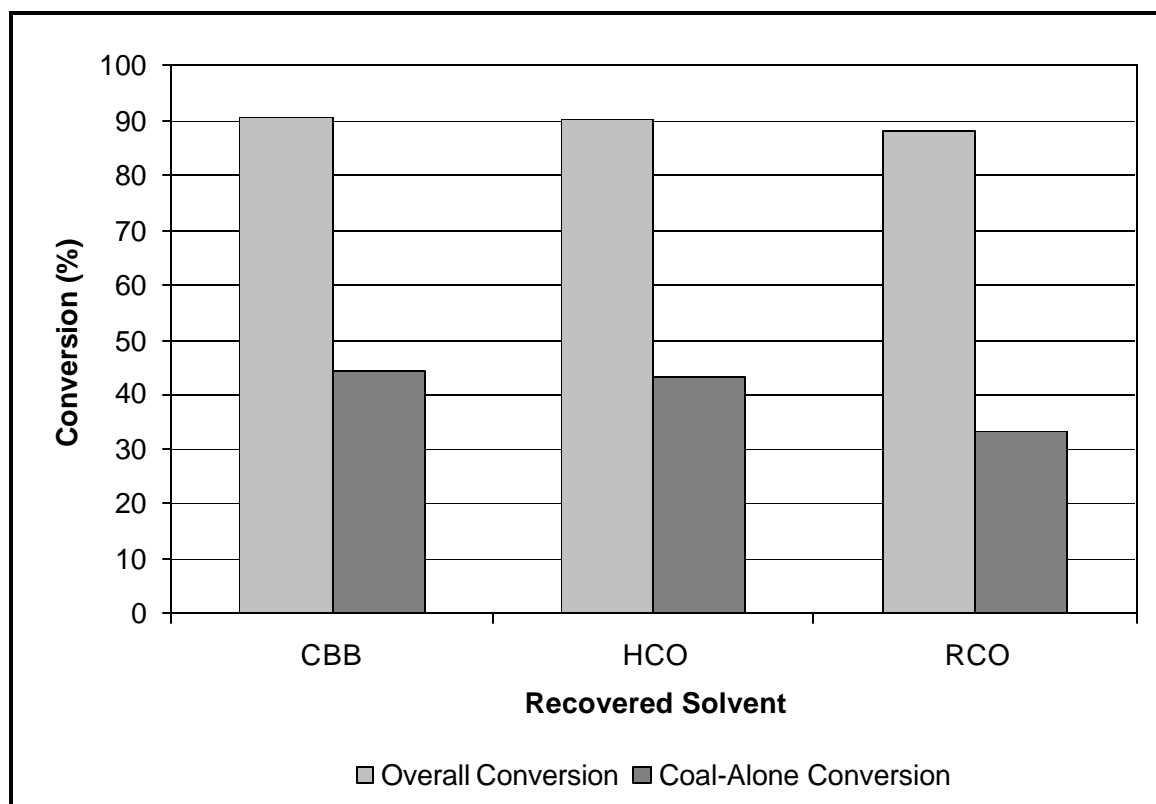


Figure 60. Overall and Coal-alone Conversion Yields with Recovered HCO, CBB and RCO at 400 °C, 500 psig Cold Hydrogen and One Hour Reaction Time.

The results indicate that the coal-alone conversion is $44.2 \pm 0.8\%$, $43.4 \pm 1.1\%$ and $33.2 \pm 1.3\%$ for recycled CBB, HCO and RCO respectively. The coal-alone conversion shows some difference between the fresh and recovered solvents and suggests that the recovered solvents actually behave comparably or better than the fresh solvent. This behavior can be attributed to the fact that the solvent either gets partially hydrogenated in the process of hydrogenating the coal or the distillation concentrates more H-donors in the recovered solvent; hence the recovered solvent is able to perform better in subsequent hydrogenations. In addition, the mineral matter in the coal may be catalytically active in digestion reactions and could support hydrogenation of the solvent along with coal. In fact, this is supported by elemental analysis which shows a higher hydrogen-to-carbon ratio in the recovered solvent compared to fresh solvent.

4.1.4 Mass Balances with Fresh Solvents

A mass balance was performed on each digestion run including the three solvents being tested under the reaction conditions. Mass input includes total coal and solvent

while mass output includes the separated products: THF insoluble residue, pitch and the recovered solvent.

The results of the mass balances with the fresh solvents showed a negative mass balance which means that some mass was lost in each of these digestions. The average mass loss was 7-10 % for the fresh solvents. Several factors could account for the mass loss. First, during the THF separation in a rotary evaporator, very light boiling volatiles may be lost with the recovered THF. In addition, the vacuum distillation step which separated the pitch and the recovered solvent. Since vacuum was used in this separation, some of the lighter boiling compounds would not be condensed at that low pressure. These non-condensables would pass the distillate flask and get trapped in the cold trap of the vacuum pump. This was confirmed by periodically checking the cold trap flask and noting some quantity of liquid. Lastly, some of the lights may have been trapped in the centrifuge glass bottle with THF insolubles, and would eventually get lost in the vacuum oven cold trap during the drying of the THF insolubles. This mass loss could be minimized by washing the residue repeatedly with THF till a clear THF decanting solution appears after centrifugation. The finding though was that even after repeated washings it was very difficult to get a clear THF decant liquid, so it is believed that some of the mass loss could take place in this way.

To minimize the mass loss in the vacuum distillation process, the distillate collection flask was immersed in dry ice in to condense the lighter species that were escaping to the cold trap. In this way the loss during the vacuum distillation step could be minimized, though not eliminated. It was observed in every distillation run that the condenser had a coating of the distillate material, which would not flow even after heating with a heat gun. When the material left over in the condenser was not accounted for, the mass loss estimate was significantly higher. Thus, to account for this material, its mass was found by weighing the condenser before and after the vacuum distillation and incorporating this weight in the mass balances.

Table 22. Mass Balances of Coal Digestion Reactions with Fresh Solvents.

Run ^a	Trial	Coal (g)	Fresh Solvent (g)	Total Input (g)	Pitch (g)	THF Ins. (g)	Rec. Solv. (g)	Total Output (g)	Input - Output (g)	Loss (%)
1	A	4.001	20.02	24.021	2.49	2.3119	17.65	22.452	1.569	6.5
1	B	4.0032	20.1	24.1032	3.01	2.4008	16.87	22.2808	1.8224	7.6
1	C	4.0021	20.2	24.2021	2.88	2.3566	17.1	22.3366	1.8655	7.7
1	D	4.0019	20.1	24.1019	2.72	2.3801	16.55	21.6501	2.4518	10.1
2	A	4.002	20.2	24.202	2.71	2.4201	17.22	22.3501	1.8519	7.6
2	B	4.0056	20.3	24.3056	2.967	2.371	17.29	22.628	1.6776	6.9
2	C	4.0021	19.92	23.9221	3.8	2.3654	16.2	22.3654	1.5567	6.5
2	D	4.0031	20.2	24.2031	3.05	2.4198	16.41	21.8798	2.3233	9.6
3	A	4.0001	20.3	24.3001	3.94	2.8429	15.87	22.6529	1.6472	6.7
3	B	4.0032	20.1	24.1032	3.98	2.8156	15.1	21.8956	2.2076	9.1
3	C	4.0012	20.4	24.4012	4.28	2.8112	14.98	22.0712	2.33	9.7
3	D	3.9988	20.02	24.0188	3.99	2.8256	15.66	22.4756	1.5432	6.4

^a Here run 1 is using CBB, run 2 is using HCO and run 3 is using RCO

4.1.5 Mass Balances with Recovered Solvents

The mass balances with recovered solvents for subsequent runs are shown in the table below. The only difference between fresh and recovered solvent mass balances is that recovered solvents showed a mass loss of 10-13 %. Many of the reasons for mass loss that apply to fresh also apply to the recovered solvents. It is very likely that the recovered solvent is lighter compared to the fresh solvents, as it is a distillate product from the distillation of the mixture of pitch and fresh solvent. This is also suggested by the coloration of the recovered solvents which is less dark than the fresh solvent and also by the hydrogen-to-carbon ratio of the recovered solvent which is greater than the fresh solvent. So, all the factors of mass loss would be even more enhanced for these recovered solvents giving a higher value to the loss.

The errors in mass balance would be transferred to the other calculations which are based on the mass of the reactants and the recovered products. These calculations would include ash balances, carbon balances and hydrogen balances.

Table 23. Mass Balances of Coal Digestion Reactions with Recovered Solvents.

Run ^a	Trial	Coal (g)	Rec. Solvent (g)	Total Input (g)	Pitch (g)	THF Ins. (g)	Rec. Solv. (g)	Total Output (g)	Input - Output (g)	Loss (%)
4	A	4.001	20.1	24.101	2.988	2.3014	16.125	21.4094	2.6916	11.2
4	B	4.0021	20.4	24.4021	3.1088	2.3708	15.58	21.0596	3.3425	13.7
4	C	4.008	20.5	24.508	3.2756	2.3244	15.28	20.88	3.628	14.8
4	D	4.0039	19.92	23.9239	2.878	2.3446	16.4	21.6226	2.3013	9.6
5	A	4.0012	20.2	24.2012	3.2931	2.3431	15.49	21.1262	3.075	12.7
5	B	4.0036	20.1	24.1036	2.656	2.405	16.36	21.421	2.6826	11.2
5	C	4.001	20.2	24.201	2.786	2.3203	16.19	21.2963	2.9047	12
5	D	4.0016	20	24.0016	2.9821	2.3848	16.02	21.3869	2.6147	10.9
6	A	4.0026	20.4	24.4026	2.6822	2.6991	15.98	21.3613	3.0413	12.4
6	B	4.0001	19.9	23.9001	3.2612	2.7691	15.14	21.1703	2.7298	11.4
6	C	4.0039	20.1	24.1039	2.9932	2.7982	16.12	21.9114	2.1925	9.1
6	D	4.0013	20.3	24.3013	2.7899	2.7208	15.66	21.1707	3.1306	12.9

^a Here run 4 used Rec. CBB, run 5 is used Rec. HCO and run 6 is used Rec. RCO

4.1.6 Ash Balance

The ash content is critical in the digestion reactions and it is desired for the pitch product to have as low an ash value as possible. It is not possible to eliminate ash entirely from the pitch but there are steps to minimize it, described later. The recovered solvents were tested for ash and found to be negligible. Hence they were disregarded in the ash balance calculation whereas all the ash is concentrated in the THF insolubles. Similarly, this applies to reactants as well, where all the ash is in the coal and negligible ash is in the coal-derived solvents. Most of the ash from the coal is concentrated in the THF insoluble fraction as the mineral matter is not extracted into the coal-derived solvent. The THF insoluble fraction basically contains the mineral matter and the unconverted organic

matter from the coal. All this mineral matter is converted into ash after oxidation. The ash content is found as a weight percent by the ash test described in a previous section. Then the actual mass of ash in the species is determined by multiplying the ash percentage by the corresponding mass of that species from the mass balance. The ash test had a small relative error of around $\pm 2\%$.

The results of the ash balance for fresh and recovered solvent are shown in the next two tables below, respectively. The results show a random distribution of gain and loss of ash in the species. Since the ash balance is calculated from the mass balance, any errors in the mass balance would propagate in the ash balance as well. The ash content in the coal and the THF insolubles dominates the ash balance calculation as can be seen from the results. The positive ash balance values correspond to the negative mass balance values. This is because, as mass is lost, which is typically the lighter hydrocarbons, the ash in the remaining heavier products would be concentrated thus giving a higher ash value as compared to the actual ash in the original samples. Hence positive values of ash balance are more the norm. Most of the values show a positive balance and are consistent with the negative mass balances. But some do show negative values of ash balance. This can be attributed to the fact that sometimes the separation of THF solubles from the insolubles was not entirely complete. It has already been mentioned earlier, that even multiple centrifugations would not give clear THF decanting liquid, suggesting some solubles trapped in the THF insolubles. This phenomenon would decrease the ash in the dominant THF insolubles fraction, thus giving negative ash balance values. As seen in the below tables, the ash in the recovered solvent is negligible since the starting fresh solvent had a very small amount of ash. So the ash in the recovered solvent is not shown in the below tables and the only ash entering the process is from the starting coal.

Table 24. Ash Balances of Coal Digestion Reactions with Fresh Solvents.

Run ^a	Trial	Coal Ash (g)	Solvent Ash (g)	Ash Input (g)	Pitch Ash (g)	THF Ins. Ash (g)	Ash Output (g)	Input - Output (g)	Loss (%)
1	A	0.2240	0.0120	0.2360	0.0039	0.2138	0.2177	0.0183	7.7
1	B	0.2241	0.0120	0.2361	0.0048	0.2220	0.2268	0.0092	3.9
1	C	0.2241	0.0121	0.2362	0.0046	0.2179	0.2225	0.0136	5.7
1	D	0.2241	0.0120	0.2361	0.0043	0.2201	0.2244	0.0116	4.9
2	A	0.2241	0.0161	0.2402	0.0067	0.2371	0.2438	-0.0036	-1.5
2	B	0.2243	0.0162	0.2405	0.0074	0.2323	0.2397	0.0007	1.7
2	C	0.2241	0.0159	0.2400	0.0095	0.2318	0.2413	-0.0013	-0.5
2	D	0.2241	0.0161	0.2402	0.0076	0.2371	0.2447	-0.0045	-1.9
3	A	0.2240	0.0182	0.24227	0.0110	0.2331	0.2441	-0.0019	-0.8
3	B	0.2241	0.0181	0.2422	0.0111	0.2308	0.2419	0.0003	0.2
3	C	0.2240	0.0183	0.2423	0.0119	0.2305	0.2424	-0.0001	-0.04
3	D	0.2239	0.0180	0.2419	0.0111	0.2316	0.2427	-0.0008	-0.3

^a Here run 1 is using CBB, run 2 is using HCO and run 3 is using RCO

Table 25. Ash Balances of the Coal Digestion Reactions with Recovered Solvents.

Run ^a	Trial	Coal Ash (g)	Pitch Ash (g)	THF Ins. Ash (g)	Ash Output (g)	Input - Output (g)	Loss (%)
4	A	0.2240	0.0047	0.1956	0.2003	0.0236	10.5
4	B	0.2241	0.0049	0.2015	0.2064	0.0176	7.8
4	C	0.2244	0.0052	0.1975	0.2027	0.0216	9.6
4	D	0.2242	0.0046	0.1992	0.2038	0.0203	9.0
5	A	0.2240	0.0082	0.1921	0.2003	0.0236	10.5
5	B	0.2242	0.0066	0.1972	0.2038	0.0204	9.1
5	C	0.2240	0.0069	0.1902	0.1971	0.0269	12
5	D	0.2240	0.0074	0.1955	0.2029	0.0210	9.4
6	A	0.2241	0.0075	0.2132	0.2207	0.0033	14.7
6	B	0.2240	0.0091	0.2187	0.2278	-0.0038	-1.7
6	C	0.2242	0.0083	0.2210	0.2293	-0.0051	-2.2
6	D	0.2240	0.0078	0.2149	0.2227	0.0012	0.6

^a Run 4 is used Rec. CBB, run 5 used Rec. HCO and run 6 is used Rec.RCO

The final cold pressure confirms gas consumption of the reactive gas atmosphere. For example hydrogen consumption in the overall reaction gives a final cold pressure less than the initial cold pressure whereas a reverse trend is observed for the nitrogen atmosphere. The difference of final and initial cold pressure indicates either the extent of hydrogen uptake by soluble species and/or solvent in the hydrogen atmosphere or the amount of non-condensables released from the coal/solvent during the reaction in the nitrogen atmosphere. From this difference in pressures the moles of hydrogen consumed or the moles of non-condensables released could be estimated.

The figure below shows the pressure profiles for the fresh solvents under a hydrogen atmosphere. It can be observed that since the atmosphere is hydrogen, the final cold pressure is less than the initial cold starting pressure. RCO gave the maximum pressure rise under hot conditions, indicating it has a lower molecular weight distribution than the other solvents. The difference between the final and initial cold pressure is maximum for CBB, suggesting that more hydrogen is consumed by it to solubilize the coal and hence more soluble species are produced compared to the other solvents. This is in fact found to be true. For the digestion runs, assuming all the pressure difference is due to consumption of hydrogen, the estimated weight percent of hydrogen consumed was found to be 0.06 % on the total feed basis.

The following figure shows the pressure profiles for recovered solvents obtained from runs using the three fresh solvents. For the most part, the profiles are the same, the only difference being the final pressure is somewhat lower than the corresponding pressure for the fresh solvents. Also it can be observed that the maximum pressure and the rate of pressure decrease are higher for these recovered solvents. It suggests that the

recovered solvents should be lighter and may give higher conversion than the fresh solvents.

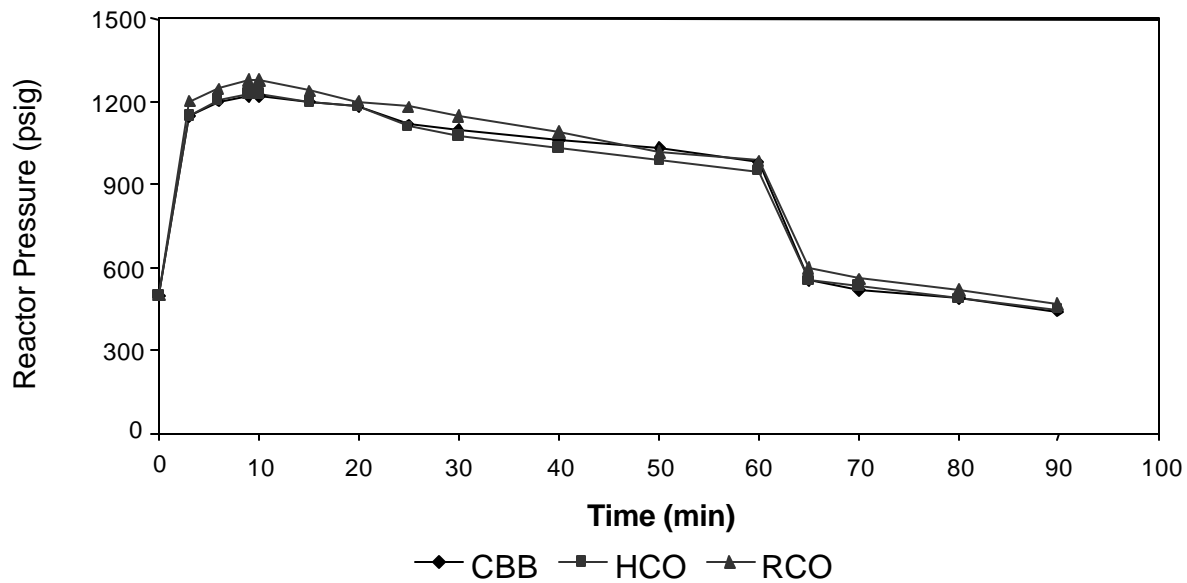


Figure 61. Pressure Profiles for Fresh Solvents CBB, HCO and RCO at 400 °C, 500 psig Cold Hydrogen and One Hour Reaction Time.

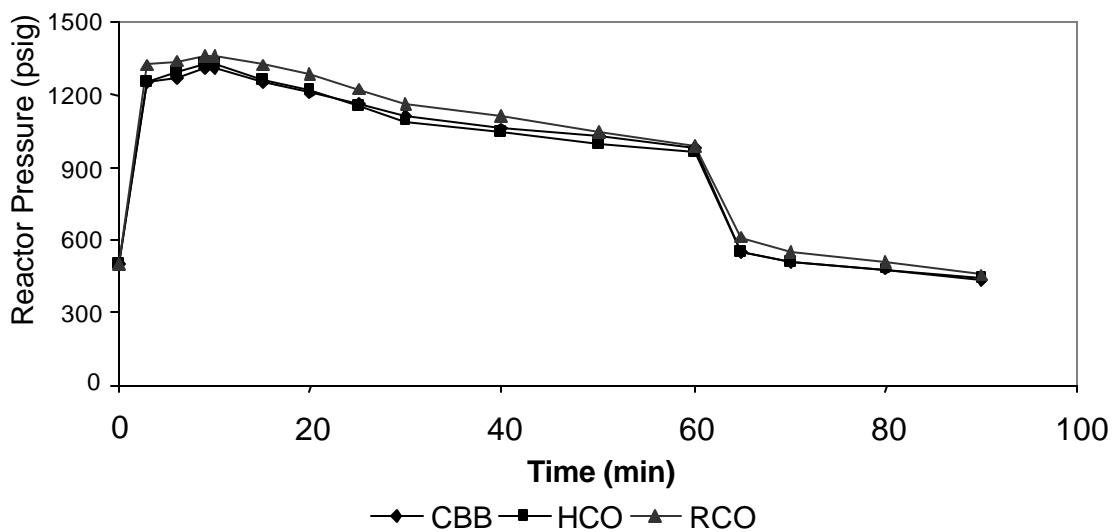


Figure 62. Pressure Profiles for Recovered Solvents CBB, HCO and RCO at 400 °C, 500 psig Cold Hydrogen and One Hour Reaction Time.

4.1.7 Hydrogenation Products

Upon completion of the vacuum distillation, the products of the reaction were separated to form three fractions namely pitch (THF solubles), THF insolubles, and the recovered solvent. The latter two products were considered to be by-products of the process and so are not characterized in as much detail as the pitch product. Elemental analysis and ash content were done on these products so that an elemental balance and ash balance could be made. On the primary pitch product, analytical techniques like softening point, ash content, coke yield, and optical texture were performed to compare pitches obtained from this process to the commercial pitches available on the market. The vacuum distillation conditions were maintained the same for the separations involving different solvents and were 30 mm Hg vacuum and 270-280 °C maximum vapor temperature. It should be noted that the final temperature of the distillation residue left in the pot could be well over 280 °C.

The product distributions for these hydrogenation runs for the three fresh and recovered solvents are shown in the following figure. The product distribution for HCO and CBB appear to be similar while RCO shows some difference. It can be observed that the dominant fraction among the three products is the recovered solvent which accounts for 60-70 % of the original feed amount. The other two fractions, namely the pitch and the THF insolubles, depend upon the coal-alone conversion yields of the corresponding solvents. Since CBB and HCO show similar conversion, these two fractions are close for these two solvents. A general trend is that the quantity of products for runs using recovered solvent is slightly less than that for the fresh solvent. The quantity of recovered solvent is critical here, since the larger the amount the more that is available for recycle.

Also since the recovered solvent is the lightest fraction compared to the other two products, a lower amount of recovered solvent suggests a higher mass loss. For instance RCO shows a low percentage of recovered solvent and hence has a higher average mass loss compared to the other two solvents.

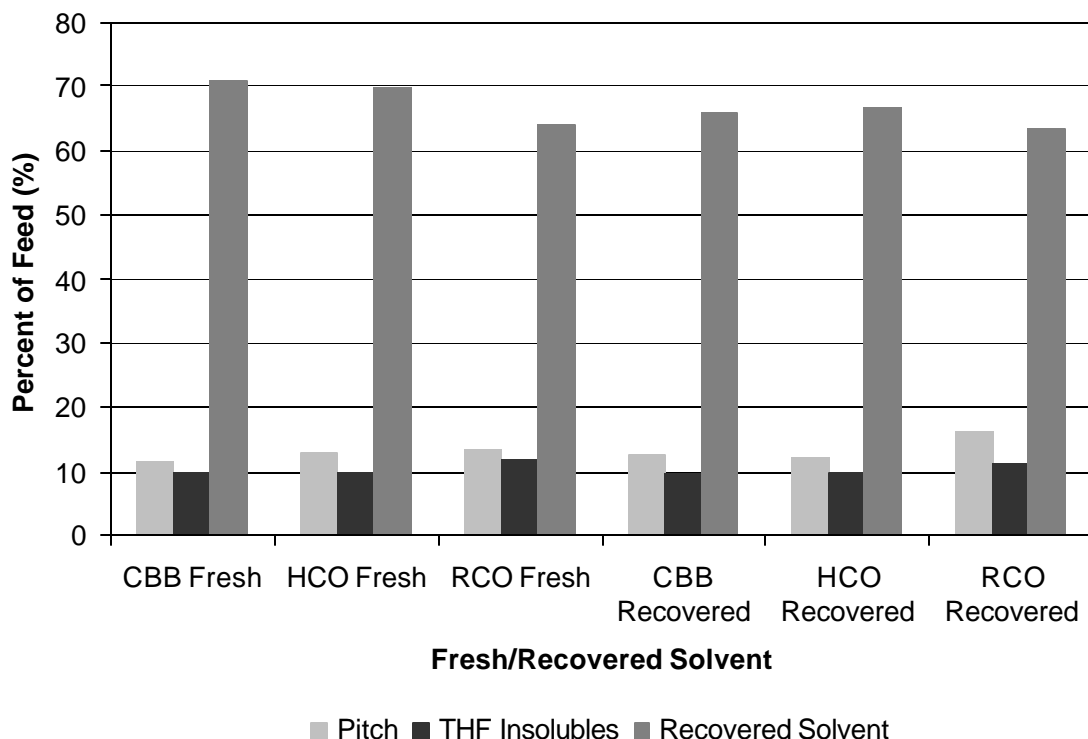


Figure 63. Hydrogenation Product Distribution for Fresh and Recovered Solvents CBB, HCO and RCO at 400 °C, 500 psig Cold Hydrogen and One Hour Reaction Time.

From the above discussion it is clear that a balance must be struck between the amount of solvent distilled and the mass of pitch product. If more pitch product is desired then the amount of recovered solvent decreases, necessitating a larger amount of fresh make-up for subsequent reactions. With very low pitch product, the process might not be economical given that pitch is the primary product. But the fact remains that the balance between these two products is governed by the final properties of the pitch and can be the sole criterion for separation. As discussed in a later section, the pitch properties change depending on the amount of recovered solvent, so in order to obtain a tailor-made pitch, the proper quantity of solvent must be separated.

4.1.8 Parametric Studies in Mini Reactors

From the tubing bomb reactions, the coal conversions obtained indicates that there is an optimal temperature and pressure at which to conduct the scale-up reactions. As can be seen in the next two figures, the optimal conversion is achieved at 400°C. The low conversion obtained at lower temperatures is due to an inability of the solvent to thoroughly digest the coal, while the lower conversion achieved at higher temperatures is likely due to retrograde reactions (polymerizations, combinations) that occur at elevated temperatures, at or near 450°C. Note also that the maximum digestion conversions follow the level of hydrogenation.

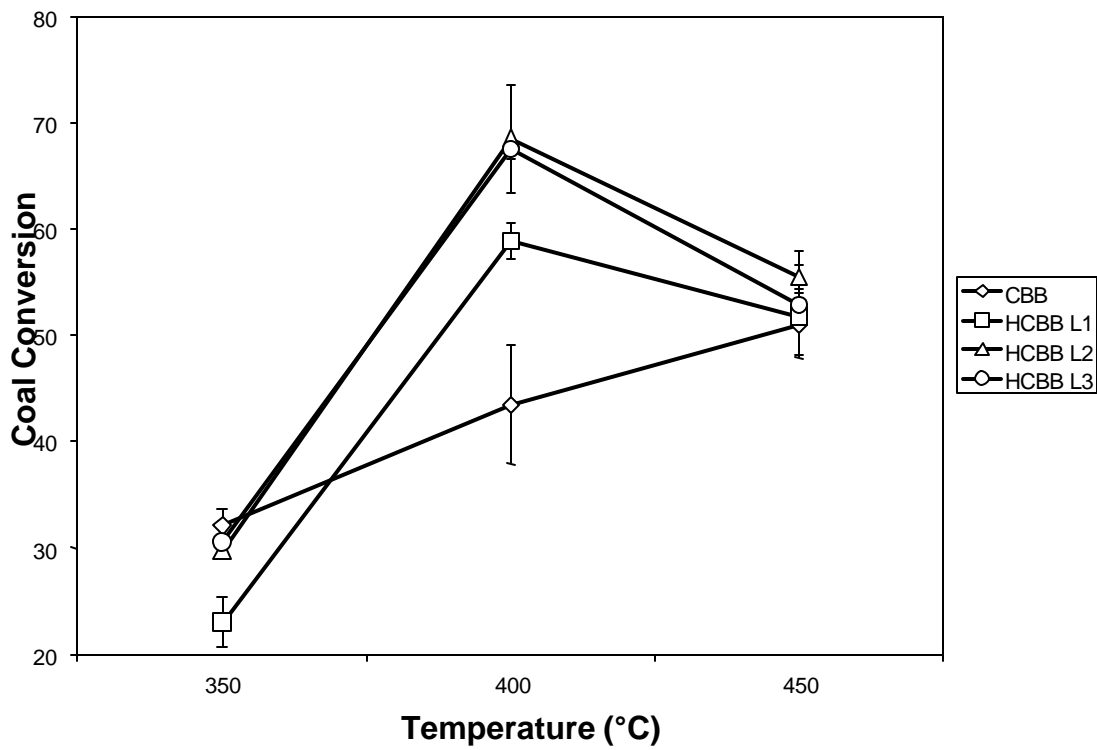


Figure 64. Conversion vs. Temperature at $P = 0$ psig N_2 .

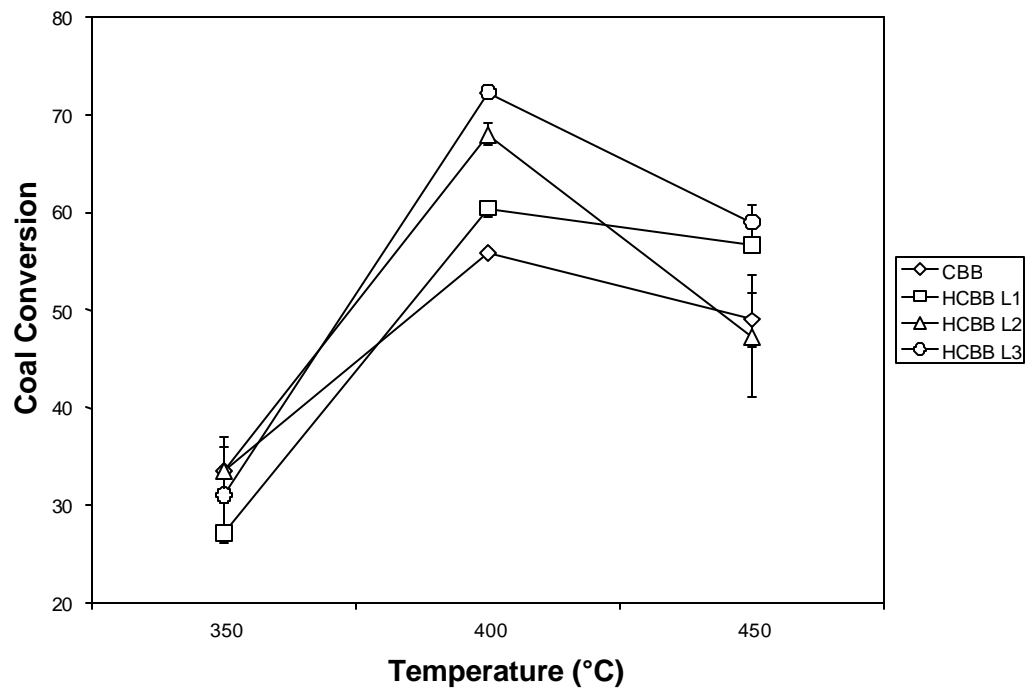


Figure 65. Conversion vs. Temperature at $P = 500$ psig N_2 .

In the determination of the best solvent or solvent combination to use in the scale-up reactions, the first set of data to observe is the conversion of coal in each of the raw solvents as compared to tetralin, which was used for comparison as a standard H-donor liquefaction solvent. It can be seen that the CBB works the best compared to tetralin, followed by the slurry oil, Maraflex oil, and then the anthracene oil. While the anthracene oil is widely reported in the literature to be one of the better industrial by-product oils for solvent digestion of coal, those results were typically at far more severe conditions, and typically the anthracene oil had already been pretreated. The anthracene oil used in this study contained visible solids and may have been out of specifications. As the anthracene oil (AO) performed so poorly, it was eliminated from any further research and discussion.

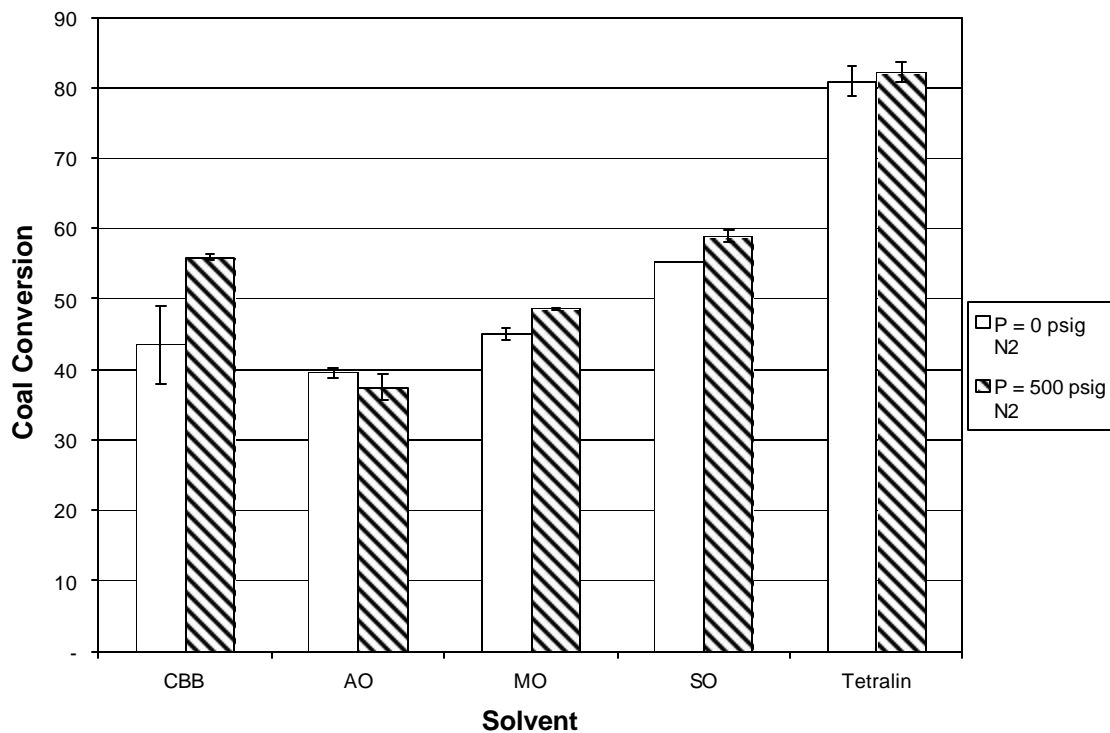


Figure 66. Coal Conversion for Raw Solvents (T = 400°C).

The “level 3” hydrogenation CBB performs the best over the other creosote oil variants. In fact, this solvent works almost as well as tetralin, with tetralin converting only about ten percent more of the coal. It can, however, be seen that the difference between the “level 2” and “level 3” hydrogenations of the CBB is small and they digest the coal to within a close range to each other. This would imply that it would not be necessary to hydrogenate the solvent at the “level 3” conditions. However, for the purpose of this study, the “level 3” hydrogenation was taken to be the best set of conditions.

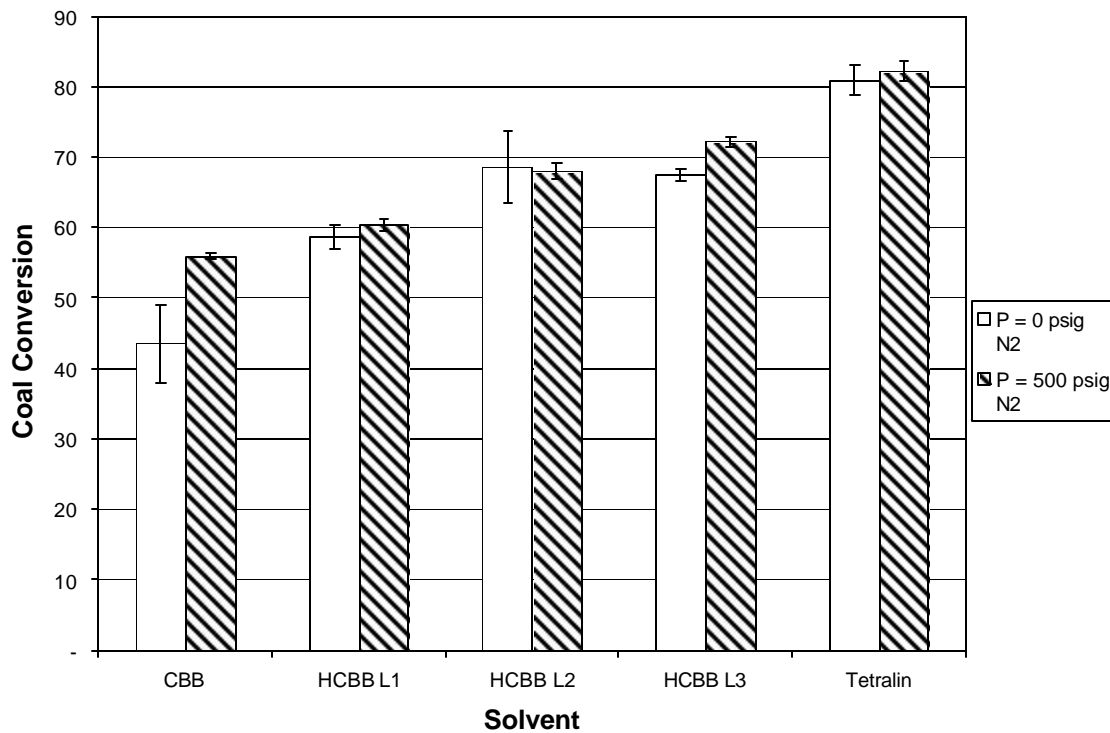


Figure 67. Conversion vs. Hydrogenation Level (T = 400°C).

It can be seen from the previous figure that using combinations of solvents can often result in better conversion than the pure solvents alone. Specifically, the use of HCBB in combination with slurry oil (SO) or hydrogenated slurry oil (HSO) gives better results than the slurry oil alone. This is likely due to the better dispersive effects provided by the coal derived solvent. The runs made with slurry oil alone were often observed to be clumpy and even chunky during extraction from the reactor. This effect was not observed when the solvents were used in combination. It is believed that while the slurry oils might have good hydrogen donor capabilities, they do not have good solvation properties (i.e. it does not keep the coal or coal fragments in solution).

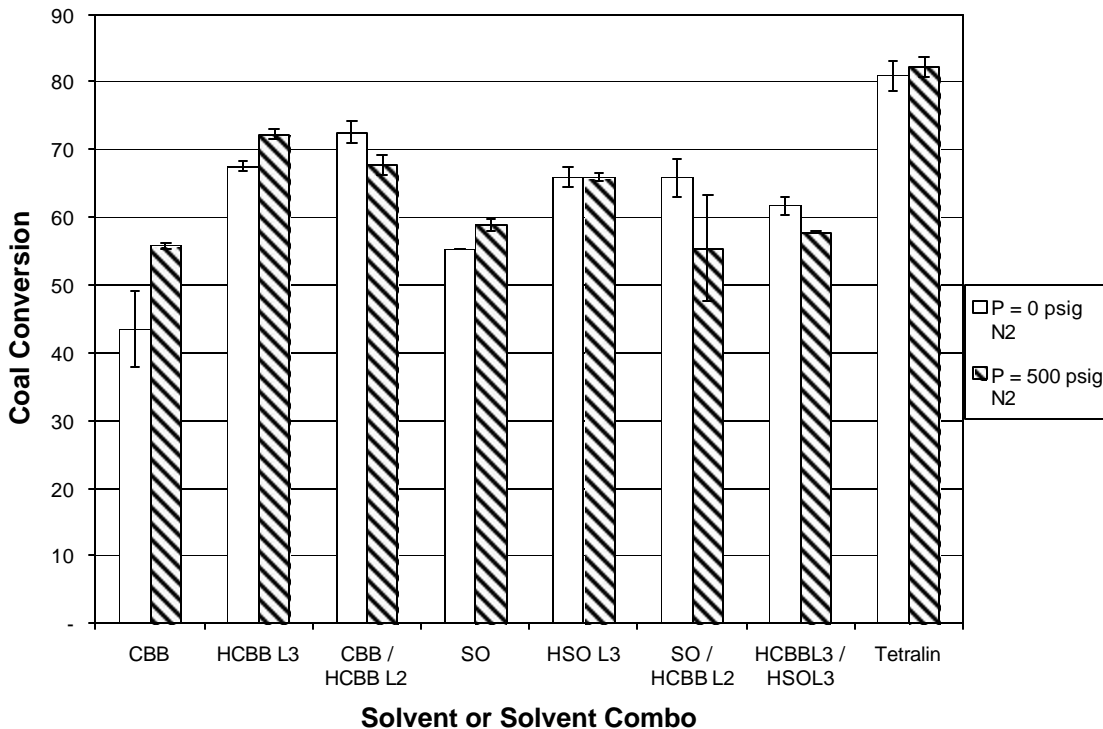


Figure 68. Coal Conversion vs. Solvent Choice (T = 400°C).

The final determination made from the tubing bomb reaction data is the fact that nitrogen pressure appears to have no appreciable effect. As can be seen from each of the figures of data above, the difference between the pressurized and un-pressurized runs is typically insignificant, and it is not consistently better with a nitrogen blanket or pressurized with nitrogen up to 500 psig.

4.2 Scale-Up Studies

After the parametric studies run in the tubing bomb mini-reactors were complete, the best three solvents were chosen for scale-up work. It was decided to also use the Maraflex oil (after hydrogenating it at Level 3) in the scaled-up tests, as this oil was much lighter than the slurry oil, and was comparable with the slurry oil in coal conversion without the “chunkiness” problems associated with processing the products. The description of the six (6) scale-up liquefactions is given in the table below.

Table 26. Scale-Up Digestion Details.

Parameter	A086	A090	A095	A098	A100	B003
Solvent	HCBB-L3	50% HCBB-L3 & 50% HSO-L3	HSO-L3	HCBB-L3	HMO-L3	50% HCBB-L3 & 50% HMO-L3
Temp. (°C)	400	425	425	425	425	425

The first scale-up digestion, operated at 400°C, resulted in a slightly rubbery material after air-blowing. This was believed to be due to the coal fragments not being broken down enough. It was decided for all subsequent digestions that the temperature would be increased to 425°C, to more thoroughly fracture the coal components and more thoroughly digest the coal. This rubberiness was greatly reduced in the second digestion using HCBB-L3 alone (A098). When examining the data from the scale-up experiments, it would appear that the larger reaction volume and more complete mixing causes an increase in conversion for the HCBB cases. The conversion here (A086 & A098) is even better than typically obtained using tetralin (about 94% using CBB vs. about 80% using tetralin in the tubing bombs). However, the slurry oil only case (A095) actually results in a lower coal conversion than was observed in the tubing bombs. As with the tubing bomb studies, it is believed that this lower conversion is a result of the inability of slurry oil to keep the coal particles and fragments solubilized, thus resulting in the formation of solid chunks that resist conversion. The product liquid obtained from this scale-up was extremely difficult to process. The solids still present after stirring at 100°C for an additional few hours (an attempt to dissolve more of the material) prevented removal of the products via vacuum line. Eventually, as much material as possible was removed, then the remaining material in the reactor was thinned out by adding some THF and this material was processed with the centrifuge residue in the THF filtration step. Even including this “unrecoverable” material, the conversion was still below 50%, and the effect of this processing difficulty can be observed from the percent mass balance obtained on that run, which is lower than all other runs (still over 90%). On a more positive note, though, the hydrogenated Maraflex oil seemed to perform better than the slurry oil in the scale-up reactions. It is also important to note that the products from using the hydrogenated Maraflex oil processed much better than the products with slurry oil or even HCBB alone. The hydrogenated Maraflex oil coal digest liquid had a very low viscosity at room temperature, thus was easier to remove from the reactor and process with centrifugation than the other products. Also, the hydrogenated Maraflex oil and HCBB (B003) combination processed easier than the slurry oil runs or the HCBB alone runs. Even though the conversion is lower using hydrogenated Maraflex oil only (A100), the combination of HMO-L3 and HCBB-L3 (B003) gave a comparable conversion to the best case (A086/98).

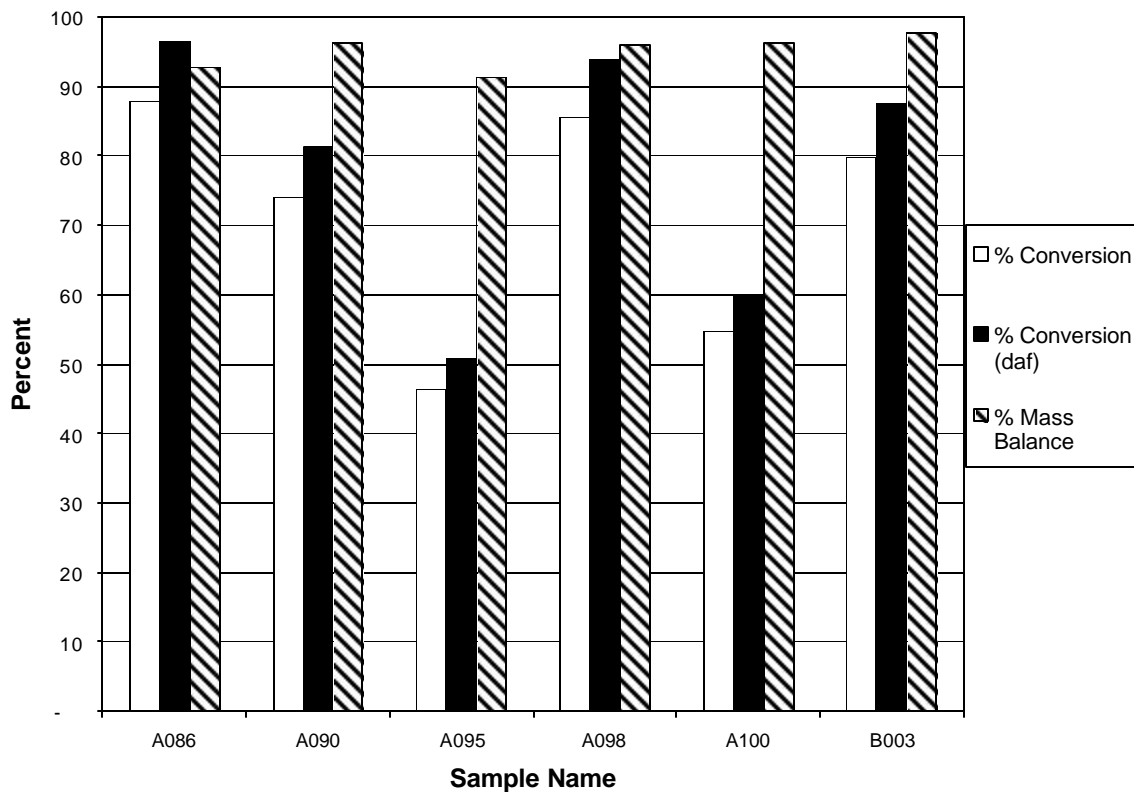


Figure 69. Scale-Up Reaction Conversion vs. Solvent Choice.

To determine how well the digestion has altered the starting coal material, the chemical nature of the coal liquid digests and the feed materials must be studied. The C/H atomic ratio of the coal digests, when compared to the feed coal, decreases with the processing. The lower values are obtained, as would be expected, with the petroleum solvents, while use of the HCBB alone gives only a slightly lower C/H ratio. It is important to keep in mind the coal conversion data when considering the C/H atomic ratio. The petroleum samples converted a much smaller amount of the coal, thus a much smaller amount of the original coal material is incorporated into the final coal liquid digest.

Table 27. Atomic C/H Ratios for Coal Liquid Digests and Feed Coal.

	Kingwood Coal	A086	A090	A095	A098	A100	B003
C/H Atomic Ratio	1.304	1.272	1.121	0.975	1.283	1.052	1.179

The effect of the solvent properties on the conversion and coal digest properties can be seen when the atomic C/H ratio of the solvent used is compared with the digestion conversion. The ratios for the solvent mixtures were calculated by a weighted average of the pure solvent elemental analyses. The digestions with HCBB only (A086 and A098) give the best conversion, and yet have the highest C/H ratio. This must be at least partially attributed to the inability of the slurry oil to properly solvate the coal, but the trend seems to indicate that a solvent with a higher C/H ratio (one closer to that of the feed coal), or a greater aromaticity, will give the best coal conversion in this process. Beyond the total amount of hydrogen present in the solvent, the types of hydrogen present may have an effect on the conversions observed in the digestion. The results of FTIR analysis show the relative amounts of aromatic and aliphatic hydrogen present in each of the solvents, and when plotted against the conversions, it is obvious the type of hydrogen present in the solvent has an effect (shown in the following four figures). The first figure, a plot of the "aromaticity factor" versus conversion shows an increase in conversion as the aromaticity increases. This is substantiated by the second and third figures. The second figure shows that as the ratio of aromatic hydrogen to aliphatic hydrogen increases, so too does conversion. A comparison of the level of aromatic carbon-carbon bonding versus the total hydrogen against the conversion also indicates that a more aromatic solvent will work better in the digestion. In the last figure, it becomes apparent that as the amount of aromatic hydrogen increases, or, conversely, as the amount of aromatic carbon decreases (through the partial/complete saturation of aromatic rings with hydrogen), the conversion increases. This reduction in aromatic carbon results as the rings are partially saturated with hydrogen and this hydrogen is then more labile, and is therefore more easily donated during the digestion process. So there is a point at which the addition of hydrogen ceases to break apart aliphatics and multi-ring aromatics into 2 or 3 - ring aromatics and begins to saturate the aromatics present in the solvent. The conclusion is that aromatic solvents are good digestion solvents, but hydroaromatic solvents are even better.

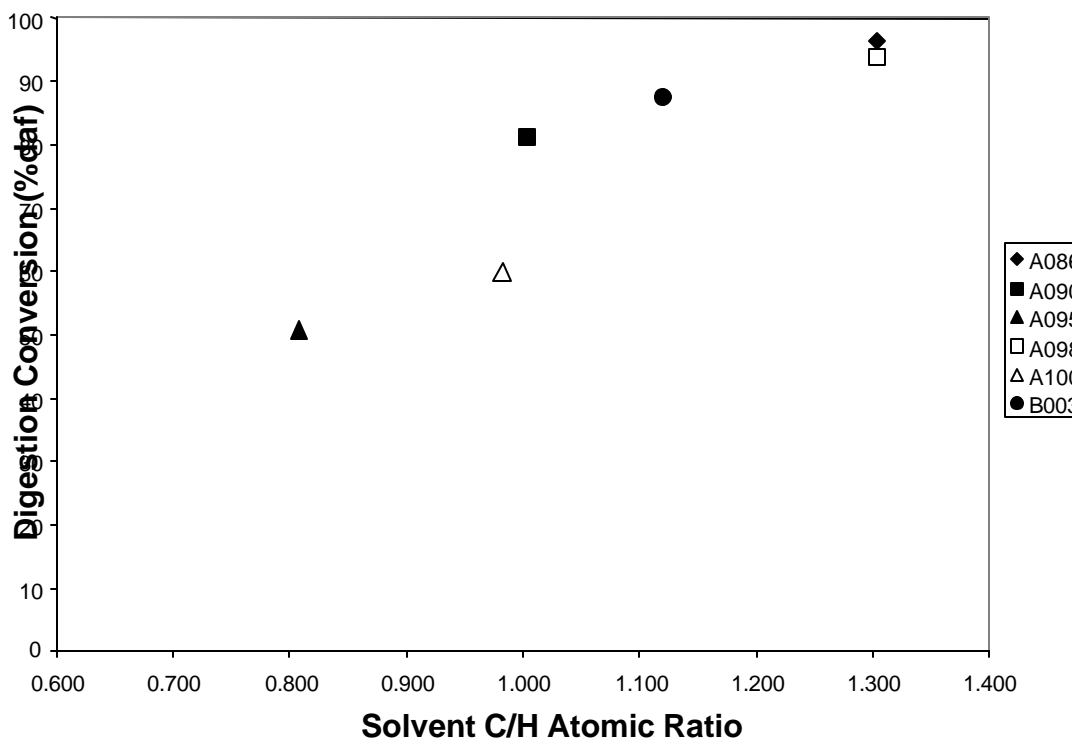


Figure 70. Solvent C/H Ratios vs. Digestion Conversions (daf).

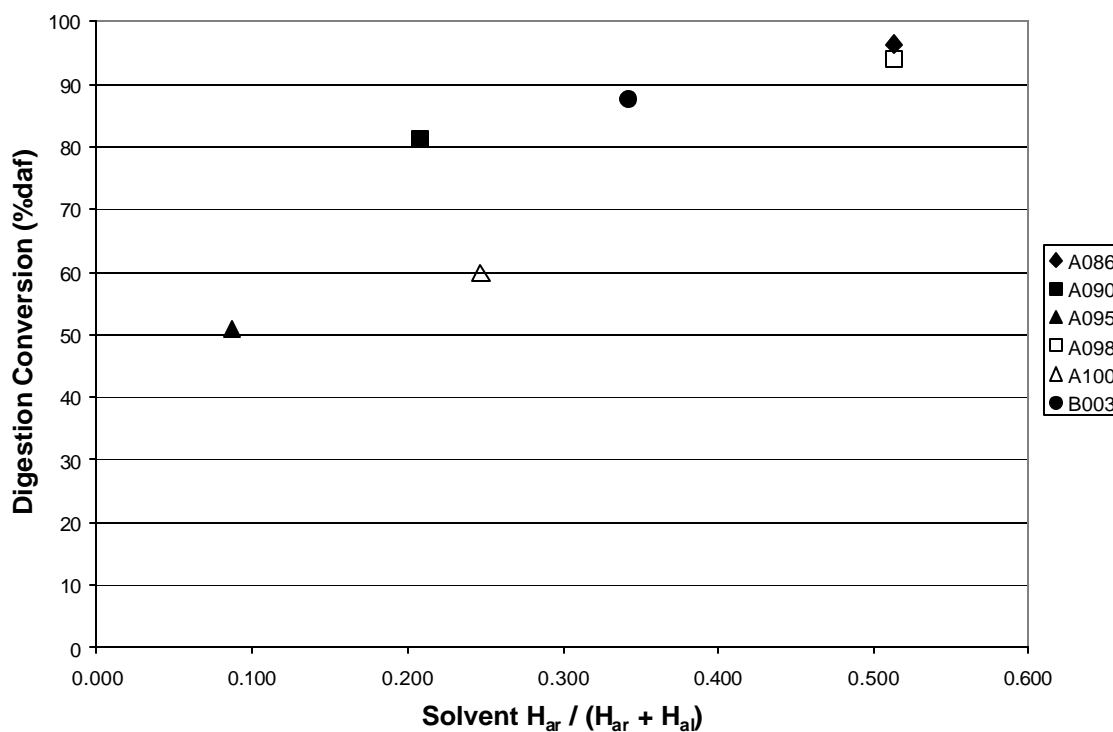


Figure 71. Solvent $H_{ar} / (H_{ar} + H_{al})$ vs. Digestion Conversions (daf).

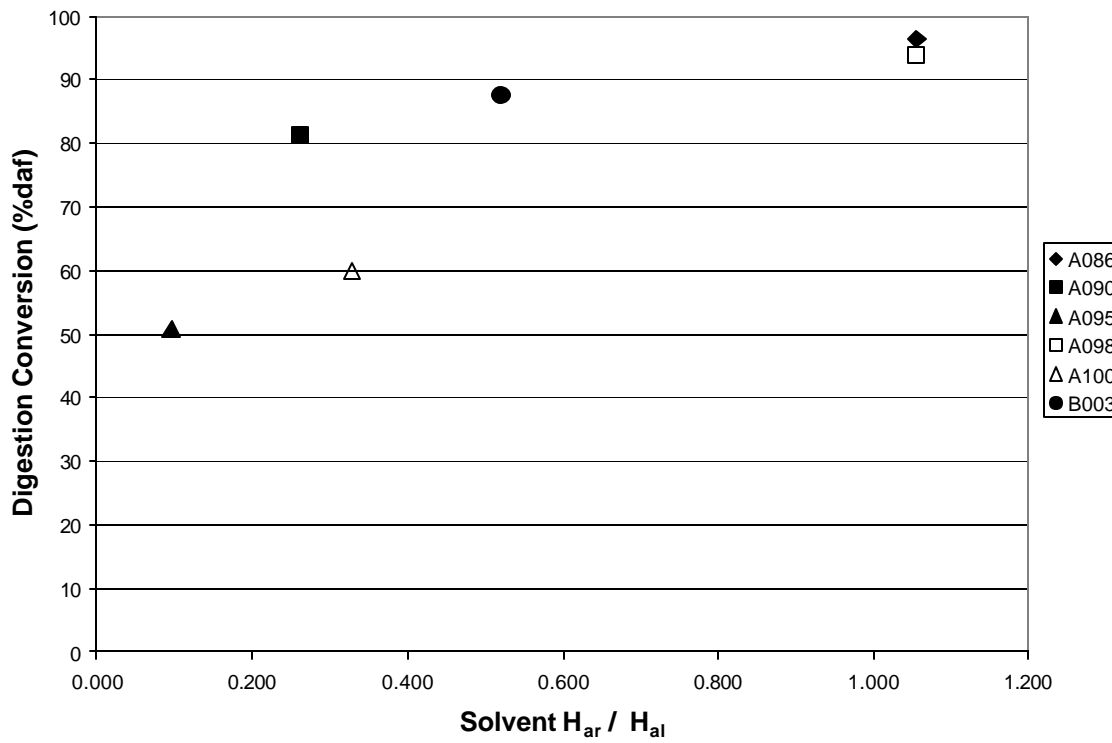


Figure 72. Solvent H_{ar} / H_{al} Ratios vs. Digestion Conversions (daf).

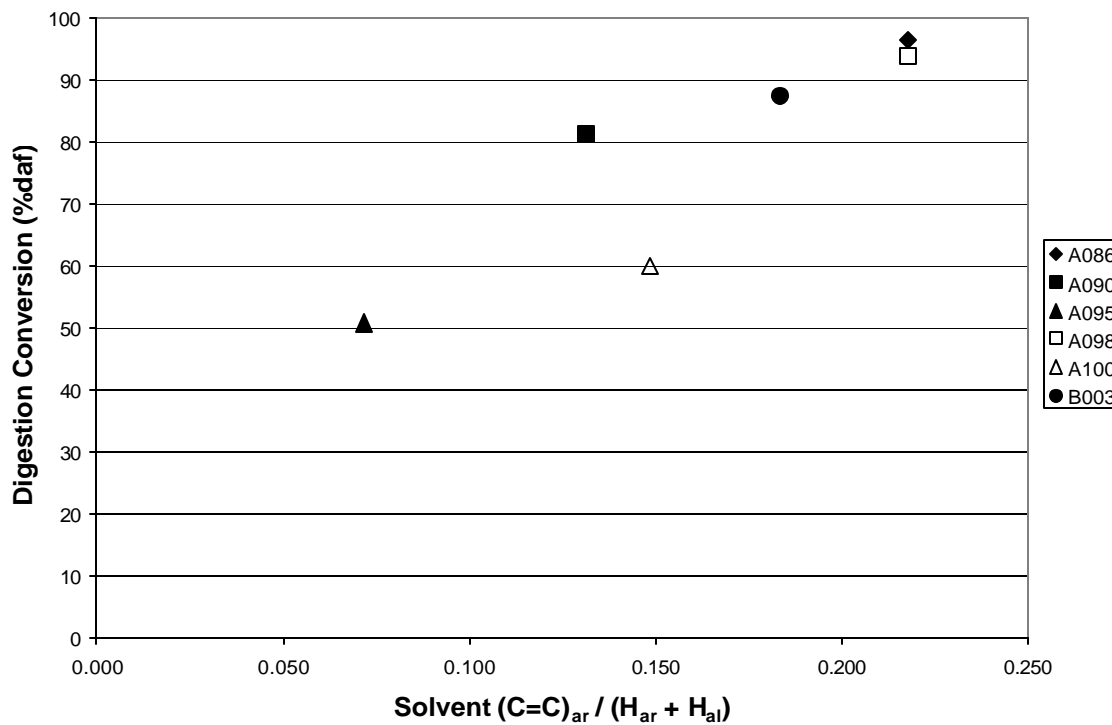


Figure 73. Solvent $(C=C)_{ar} / (H_{ar} + H_{al})$ Ratios vs. Digestion Conversions (daf).

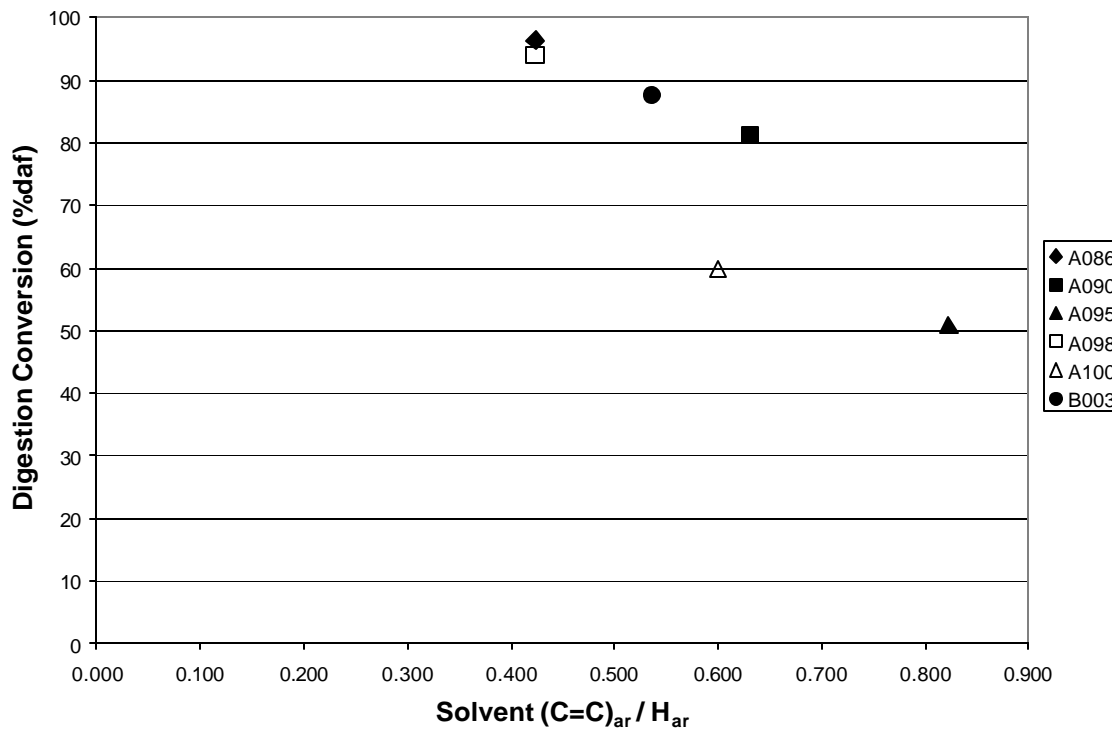


Figure 74. Solvent $(C=C)_{ar} / H_{ar}$ Ratios vs. Digestion Conversions (daf).

4.2.1 Variation of Hydrogenation Parameters

To understand the influence of the reaction parameters on hydrogenation, temperature and reaction atmosphere were varied. The other parameters such as the reaction pressure and the solvent-to-coal ratio were not studied here as they have been previously looked at in a similar work.⁷⁰ Here hydrotreatment was performed at three different temperatures, viz. 350 °C, 400 °C and 450 °C. The reaction atmosphere was changed to nitrogen instead of hydrogen at the same standard pressure of 500 psig cold. A table below gives the details of the runs involving different hydrogenation conditions.

Temperature is an important parameter in hydrogenation as it determines the severity of the hydrotreatment reaction. All the runs in which temperature was varied included CBB as the solvent along with an initial cold hydrogen pressure of 500 psig and reaction time of one hour. CBB was chosen as the solvent to study the effect of temperature as it is commercially available and gave the highest conversion among the three solvents. As mentioned earlier, conversion results were studied at three different temperatures for both fresh and recovered solvents. Temperatures above 450 °C were avoided since higher temperature would give low liquid yield due to excessive gas make by cracking.

The previous figure shows the coal-alone conversion for different temperatures for the fresh and recovered CBB in the hydrogen atmosphere. As expected the conversion goes up with temperature. For the fresh CBB solvent, the lowest conversion is observed at 350 °C which is 32.1 ± 0.8 %, while the coal-alone conversion increases at higher temperatures as seen from the last figure, giving 43.4 ± 0.9 % and 47.8 ± 1.2 % for 400

$^{\circ}\text{C}$ and $450\text{ }^{\circ}\text{C}$ respectively. The last figure also shows the conversion results at the same temperatures but for the recovered solvents. Here the same trend is followed with conversion results of $32.8 \pm 2\text{ \%}$, $44.2 \pm 0.8\text{ \%}$, $49.4 \pm 0.9\text{ \%}$ with corresponding increasing temperatures. It should be noted that the recovered solvents show slightly higher conversion results for each corresponding temperature than the fresh solvents. Also it can be noticed that the difference between the conversion at the same temperature for fresh and recovered solvent increases with temperature. In processes like EDS (discussed earlier) it has been observed that if the severity of the solvent rehydrogenation step is increased, the solvent is able to incorporate more hydrogen due to enhanced reactivity at higher temperatures. These rehydrogenated solvents are then able to perform better when reacted with coal. This trend is noted in the runs here using the recovered solvents. However, there is a trade-off. While high temperature will give high conversion, too high a temperature will cause cracking and hydrogen rich species might be lost to the vapor phase. This phenomenon may be bad as the products would be less rich in hydrogen and the conversion would also suffer. No attempt was made here to assess the effect of temperature on the gas-phase yield or composition.

The table below shows the elemental analysis of the products obtained with CBB at the three different temperatures. The hydrogen-to-carbon ratio increases in the order fresh to recovered first pass solvent to recovered second pass solvent. The interesting point to note here is the difference in the hydrogen-to-carbon ratio between the fresh and successively hydrogenated solvents is less at low temperature than at higher temperatures. The pitch properties do not change much with temperature and exhibit similar hydrogen-to-carbon ratio. Also the THF insolubles have similar properties for different temperatures.

The following figure shows the pressure profiles for fresh and recovered solvent in a hydrogen atmosphere at $350\text{ }^{\circ}\text{C}$ and $450\text{ }^{\circ}\text{C}$. The higher temperature, $450\text{ }^{\circ}\text{C}$, gives the maximum difference between the final and initial cold pressures whereas $350\text{ }^{\circ}\text{C}$ gives a smaller difference. This suggests that the conversion should increase with increasing

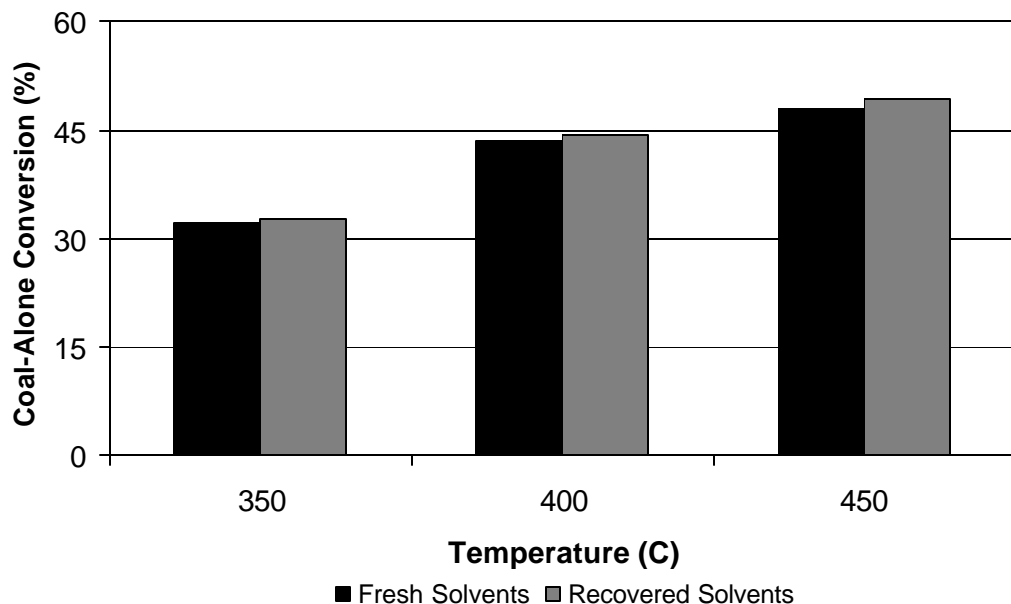


Figure 75. Coal-alone Conversion at Different Temperature For Fresh and Recovered CBB at 500 psig Cold Hydrogen and one Hour Reaction Time.

temperature, due to higher hydrogen uptake by the reactants, and indeed this was found to be the case.

Samples of the corresponding cokes were tested for optical texture under a polarized light microscope. The results show similar texture for samples trialed at both 350 °C and 450 °C. Slightly smaller domains were observed for the 350 °C samples as compared to the 450 °C samples. This suggests that lower temperature might impart less anisotropy. Overall these structures are similar to the samples at 400 °C of CBB. The samples from pass 1 and 2 do not show any difference in the coke structure.

To study the effect of reaction atmosphere on the conversion and the nature of the products nitrogen was used instead of the standard hydrogen atmosphere. The initial cold pressure of 500 psig was maintained for all the reactions and was not varied. The aim here was to study the effect of the gas phase on the reaction and not the pressure.

A figure below shows the coal-alone conversion for the two different atmospheres for both fresh and recovered CBB solvent at 400 °C, 500 psig cold pressure and a reaction time of one hour. It can be seen that the nitrogen atmosphere gave conversion results of 33.8 ± 0.4 % and 34.1 ± 0.7 % for fresh and recovered solvent with the corresponding conversion of 43.4 ± 0.9 % and 44.2 ± 0.8 % for the hydrogen atmosphere. The conversion decreases by around 10 % when the atmosphere is changed to nitrogen.

Table 28. Composition of Hydrogenation Reaction Products for CBB.

Temperature (°C)	Element	Fresh Solvent (%)	Product Fraction (%)			
			Pass 1 Pitch	Pass 1 THF Insolubles	Pass 1 Recovered Solvent	Pass 2 Recovered Solvent
350	C	91.66	92.12	78.71	92.12	92.88
	H	5.78	5.56	3.51	5.91	6.09
	N	0.71	0.88	0.92	0.77	0.75
	S	0.56	0.71	0.93	0.5	0.47
	H/C Ratio	0.75	0.72	0.53	0.77	0.78
400	C	91.66	92.24	78.02	91.79	90.39
	H	5.78	5.46	3.45	5.85	6.16
	N	0.71	0.56	0.86	0.00	0.00
	S	0.56	0.63	0.94	0.45	0.39
	H/C Ratio	0.75	0.71	0.53	0.77	0.82
450	C	91.66	92.15	75.22	90.90	90.56
	H	5.78	5.49	3.49	6.21	6.48
	N	0.71	0.51	0.97	0.73	0.68
	S	0.56	0.74	0.89	0.45	0.36
	H/C Ratio	0.75	0.72	0.56	0.82	0.86

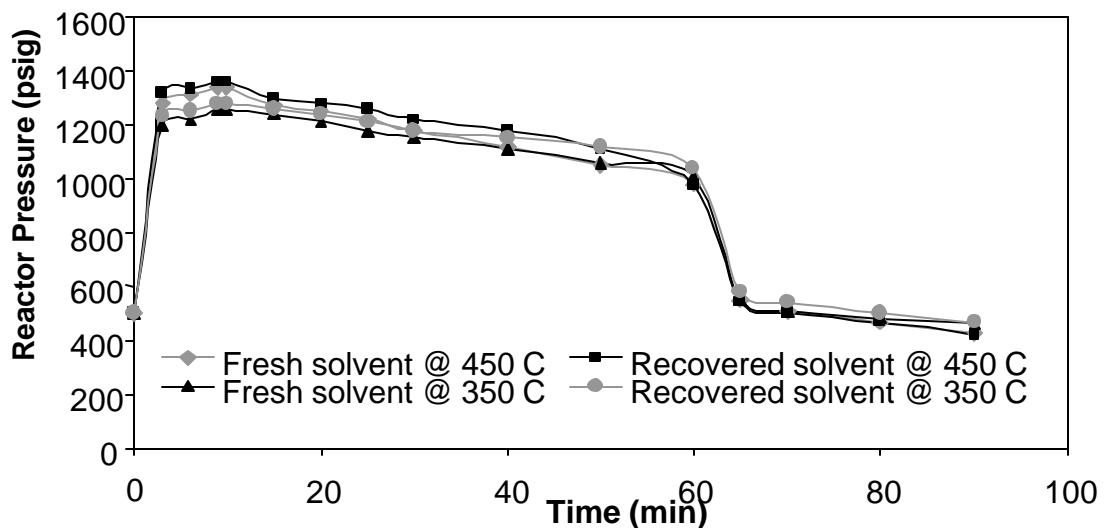


Figure 76. Pressure Profiles at 450 °C and 350 °C for Fresh and Recovered CBB at 500 psig Cold Hydrogen and Reaction Time of One Hour.

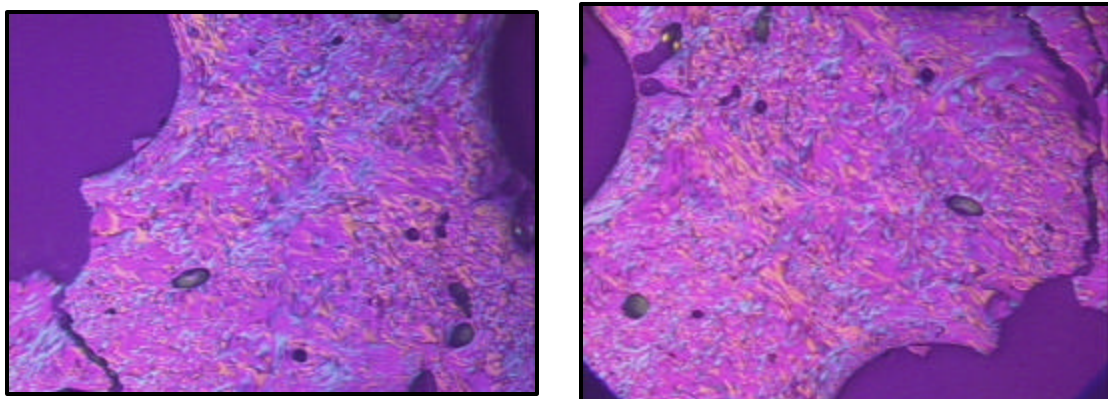


Figure 77. Optical Micrographs of Coke Samples: (A) Pass 1 Coke at 350 °C. (B) Pass 2 Coke at 350 °C.

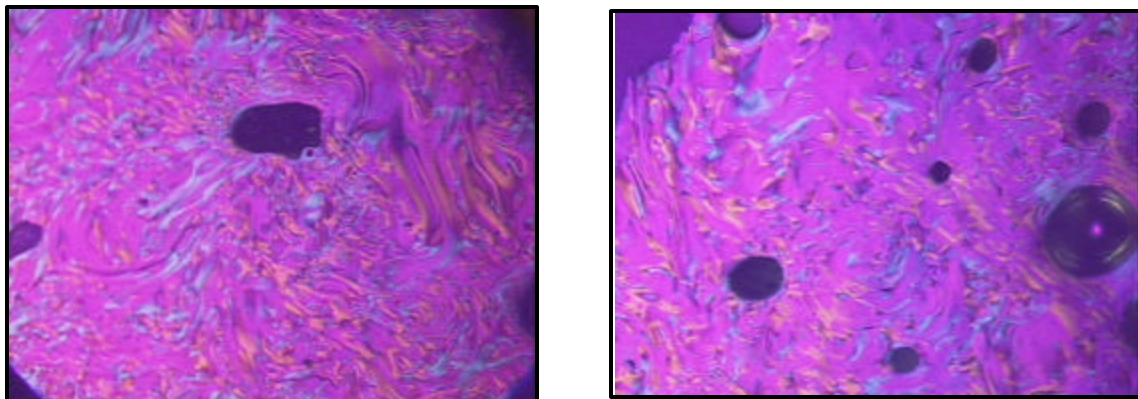


Figure 78. (C) Pass 1 Coke at 450 °C. (D) Pass 2 Coke at 450 °C.

This suggests that hydrogen is critical during these hydrogenation runs. There is also one more important thing to notice here. The conversion with nitrogen at 400 °C is higher than at 350 °C with hydrogen. This means that though the hydrogen atmosphere is crucial, it is the temperature which plays a major role in these types of reactions. Also, here the difference in conversion for fresh and recovered solvent is very small. It is unexpected to see that the conversion is almost the same between fresh and recovered solvents even in the absence of gaseous hydrogen. In reactions such as these, where there is deficiency of hydrogen either by absence of gas phase hydrogen or by absence of hydroaromatic structures in the solvent, the shuttling effect becomes the main mechanism for hydrogen transfer. This effect is described in detail in a previous section.

Though the shuttling effect may be occurring in reactions involving a hydrogen atmosphere, it is not dominant. However, it should become dominant during reaction in the absence of hydrogen. Primarily two or three ring aromatics species like naphthalene, anthracene, and phenanthrene have been found to be responsible for shuttling. These species were found to increase from fresh solvent to recovered solvents under either hydrogen or nitrogen, and even at higher temperatures. These data are shown in a table within this section for fresh and recovered CBB samples under different conditions. The data were obtained from Koppers Industries laboratories and were performed by GC for the polycyclic aromatic hydrocarbons (PAH) content. These data give the content of two, three,

and higher ring aromatic species in the solvents. Based on the data it can be said that the comparable conversion (between fresh and recovered solvents) during reactions with a nitrogen atmosphere is primarily due to the shuttling effect by these aromatic species.

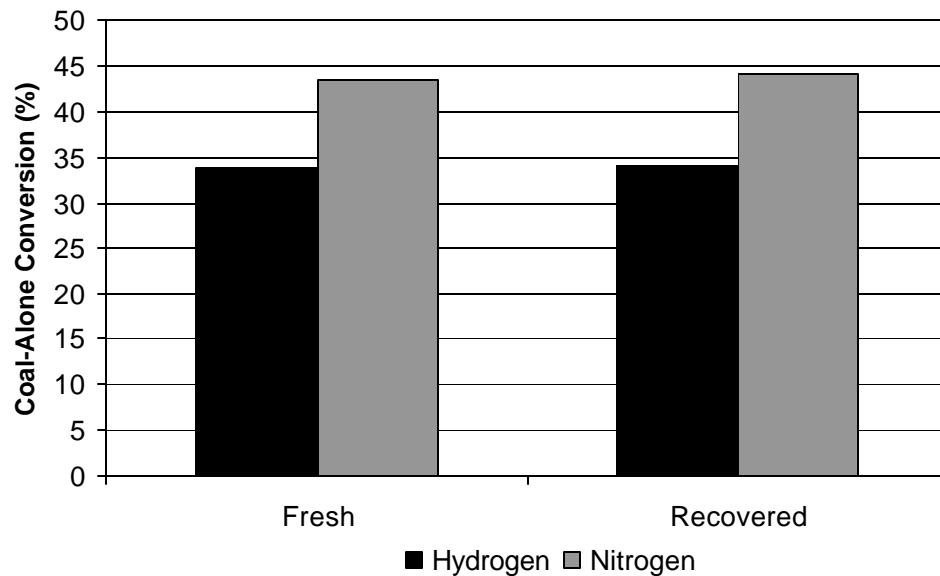


Figure 79. Coal-alone Conversion for Fresh and Recovered CBB under Different Reaction Atmospheres and 400 °C, 500 psig Cold Pressure and a Reaction Time of One Hour.

The next figure shows the pressure profiles for reaction of coal with fresh and recovered CBB solvent under a nitrogen atmosphere. As discussed earlier it shows a rate of rise at the reaction temperature unlike that seen for the hydrogen atmosphere. Here the final pressure is slightly higher than the initial cold pressure as there is no consumption of inert nitrogen. In fact the final and the initial pressures are nearly identical indicating little generation of gas-phase organics.

A previous table shows elemental analysis of the hydrogenation products from reactions involving the nitrogen atmosphere. The recovered solvent here also shows an increase in hydrogen content compared to fresh solvent, which indeed proves that some light organic species must be produced during such reactions even if a reactive atmosphere is not employed. The interesting point to observe is that the difference between the hydrogen content of the recovered and fresh solvent, is far less compared to those involving the reactive hydrogen atmosphere. The pitch and the THF insolubles properties do not change appreciably.

Coke samples from the pitches produced in the nitrogen atmosphere were studied for optical texture. In the figure below, these results are compared with the analogous samples obtained from the hydrogen atmosphere. The domains for the cokes from the nitrogen atmosphere appear smaller than those in the samples reacted under hydrogen. It can be inferred that the domain growth under nitrogen has occurred but to a much lesser extent than that observed for hydrogen. Hence the cokes from the nitrogen atmosphere appear to be more isotropic in nature. This may be important as it allows further control

over the structure of the resultant cokes. The pitch samples shown later in the chapter do not show any appreciable growth of mesophase as observed for the other samples.

Table 29. PAH Species in Fresh and Recovered CBB at Various Conditions of Temperature and Reaction Atmosphere.

Sample	Fresh (%)	Recovered at 350 °C (%)	Recovered at 400 °C (%)	Recovered at 450 °C (%)	Recovered at 400 °C & N ₂ (%)
Naphthalene	2.53	3.79	5.75	7.07	5.47
Acenaphthylene	0.04	0.17	0.37	0.5	0.31
Acenaphthene	4.57	4.22	4.61	4.89	4.32
Phenanthrene	14.63	15.45	15.82	16.05	15.56
Anthracene	1.07	1.09	1.45	1.49	1.15

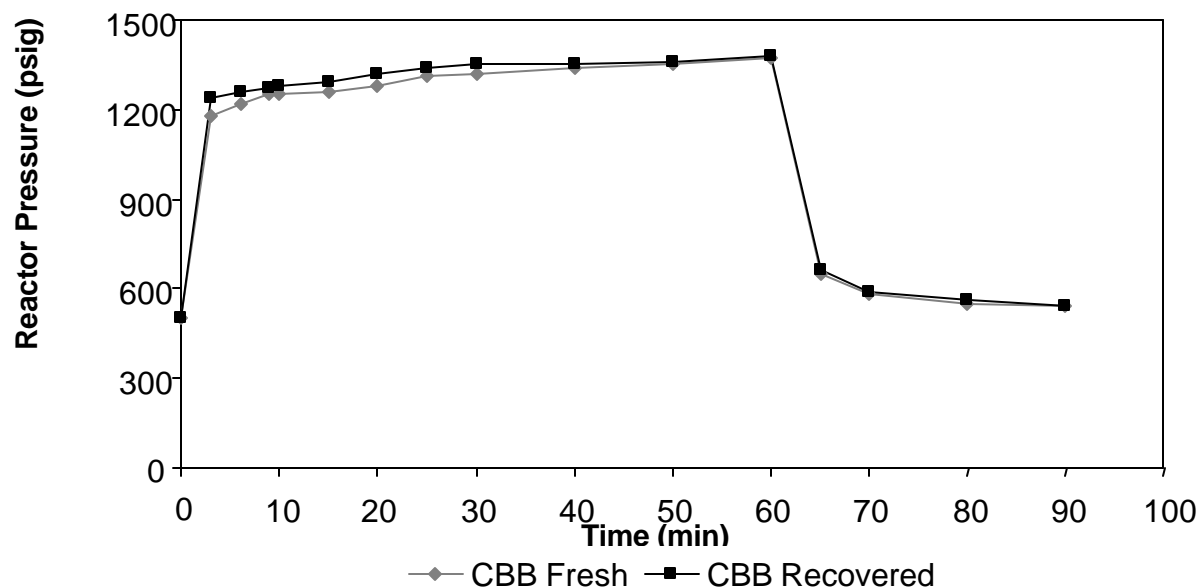


Figure 80. Pressure Profiles for Fresh and Recovered CBB under 500 psig Cold Nitrogen at 400 °C for One Hour.

4.2.2 Successive Hydrogenation Runs

Two different types of successive hydrogenation runs were performed to investigate the effect of successive recycle of the recovered solvent on the process conversion. This can be important industrially where consecutive batches of hydrogenation reactions would be performed in which part of the solvent is recycled. In the first method conversion with only recycled solvents was studied. Since there was a mass loss every time the run was performed, the amount of coal had to be decreased for each subsequent run to maintain the same solvent-to-coal ratio. For this purpose the vacuum distillation was carried out at higher temperatures around 300 °C so as to maximize the amount of solvent recovered as a distillate product.

In the second method, a predetermined fixed quantity of fresh solvent was added to the recycled solvent to maintain both the solvent-to-coal ratio and the mass of solvent for each run. The added quantity of fresh solvent was increased in a predetermined manner with each subsequent run. Here the mass of coal was held constant and did not have to be decreased. These reactions were run at 400 °C and 500 psig cold hydrogen. The rationale for doing these latter experiments was to assess the effect of increasing PAH's (with increasing amount of fresh solvent) on the coal-alone conversion when the original PAH content would decrease with successive recycling in the recovered solvents.

Table 30. Elemental Composition of Digestion Reaction Species for CBB.

Atmosphere	Element	Fresh Solvent (%)	Product Fraction (%)			
			Pass 1 Pitch	Pass 1 THF Insolubles	Pass 1 Recovered Solvent	Pass 2 Recovered Solvent
Hydrogen	C	91.66	92.24	78.02	91.79	90.39
	H	5.78	5.46	3.45	5.85	6.16
	N	0.71	0.56	0.86	0.56	0.44
	S	0.56	0.63	0.94	0.45	0.39
	H/C Ratio	0.75	0.71	0.53	0.77	0.82
Nitrogen	C	91.66	92.56	78.12	92.16	92.91
	H	5.78	5.42	3.56	5.82	5.98
	N	0.71	0.85	0.99	0.64	0.59
	S	0.56	0.74	0.94	0.49	0.47
	H/C Ratio	0.75	0.70	0.55	0.76	0.77

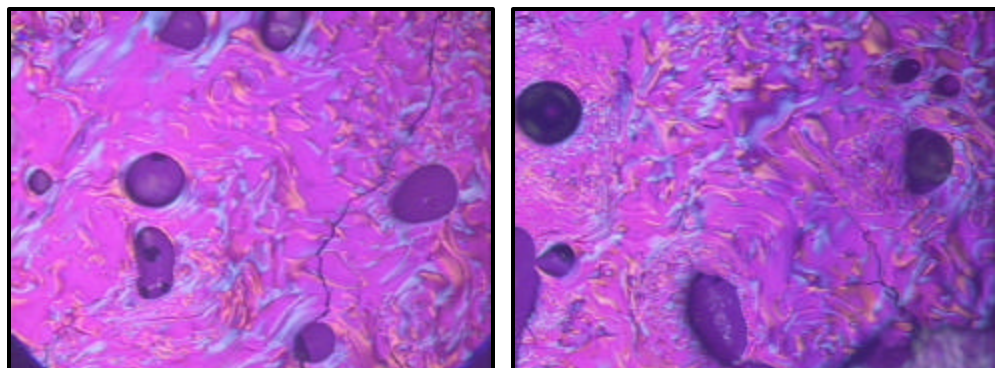


Figure 81. Optical Micrographs of Coke Samples. Left: Pass 1 Coke Under H₂. Right: Pass 2 Coke Under H₂.

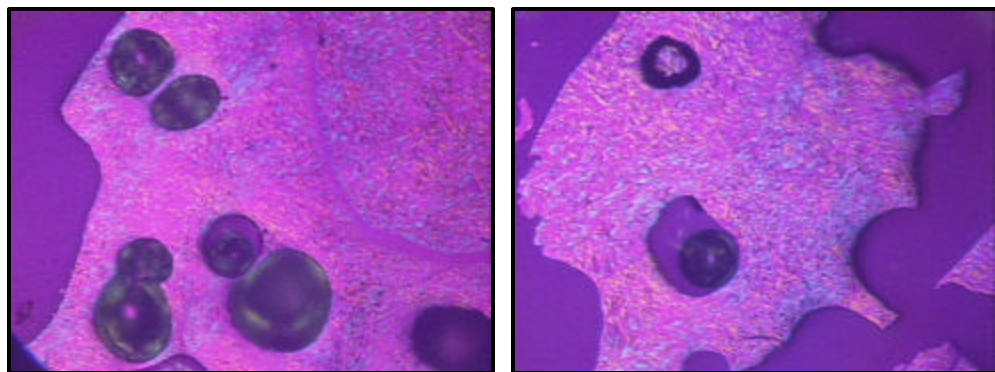


Figure 82. Left: Pass 1 Coke Under N₂. Right: Pass 2 Coke Under N₂.

The figure below shows the conversion results for method one for each subsequent pass from pass 1 (fresh solvent) to pass 5 (recycled through four successive hydrogenation runs). No make-up solvent was added in these runs. The reactions were stopped at pass 5 as with more passes the amount of coal and solvent decreases to a point where accurate conversion results are difficult to achieve. The conversion attains a maximum and then starts to decrease after the third pass. The difference between the last pass (pass 5) and that with the fresh solvent (pass 1) is not great and it is expected that the conversion would continue to drop with more subsequent passes. This can be explained based on the following hypothesis as suggested by A. Awadalla et al.⁷¹ Initially fresh coal-derived solvent contains mostly polycyclic aromatic hydrocarbons (PAH) with some hydroaromatics and alicyclics. It is known that hydroaromatics are good hydrogen donors whereas PAH's are good shuttlers. The initial content of PAH's in such typical coal-derived solvents exceeds that of the content of hydroaromatics. This is the primary reason why these coal derived solvents are poor hydrogen donors and give low conversion compared to standard H-donor solvents like tetralin. During the process of hydrogenation some of the heavy PAH's are converted to corresponding hydroaromatics. Upon repetitive or severe hydrogenation, these hydroaromatics would in turn be converted to alicyclics, which do not serve any purpose with respect to the hydrogenation reactions. So, during the third pass when the conversion peaks, the concentration of hydroaromatics must be maximum after which they start to convert into alicyclics and hence the conversion drops. Thus it is speculated that with further hydrogenations, after the fifth pass, the conversion might drop beyond that of the starting fresh solvent, because most of the PAH's and hydroaromatics would have converted to alicyclics. This hypothesis could be confirmed by GC analysis on the successively recovered solvents but it was beyond the scope of the present work.

The figure below follows the conversion with hydrogen content of the recovered solvent for successive hydrogenations. Here the same maximum in conversion is observed. This shows that when the solvent is going through the conversions of PAH's into hydroaromatics and hydroaromatics to alicyclics, the hydrogen content of the recovered solvents goes up. However, the increased hydrogen content does not guarantee an increase of conversion with subsequent hydrogenation runs since now the hydrogen is bound up in the relatively un-reactive alicyclics. The curve also shows a decreasing trend for the final runs, indicating that the conversion may equalize or even drop below the initial conversion at some point of time upon continued solvent recycle.

In the second method, blends of fresh and successively recovered solvents were used to determine the conversion yields for CBB solvent at 400 °C and 500 psig cold hydrogen pressure. the following figure shows the conversion yield when the successively recovered solvent was blended with fresh make-up solvent to keep the absolute mass of solvent constant in each run. This blend was then incorporated in subsequent hydrogenation runs. The recovered solvent in each subsequent run is obtained from the preceding hydrogenation run and is not a once through recovered solvent. Since each subsequent run had recovered solvent in the blend, the mass losses were observed to first increase and eventually stabilize with increasing amounts of fresh make-up. However the make-up was increased in a predetermined manner from 20 to 80 % to observe if some appreciable conversion changes would occur.

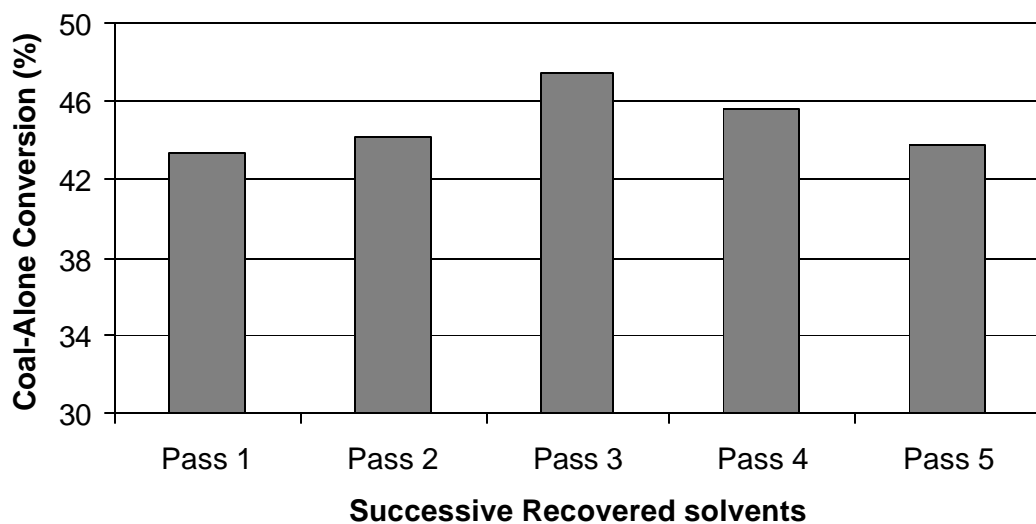


Figure 83. Successive Recovered Solvent Conversion at 400 °C, 500 psig Cold Hydrogen and One Hour Reaction Time and No Make-up Solvent Added.

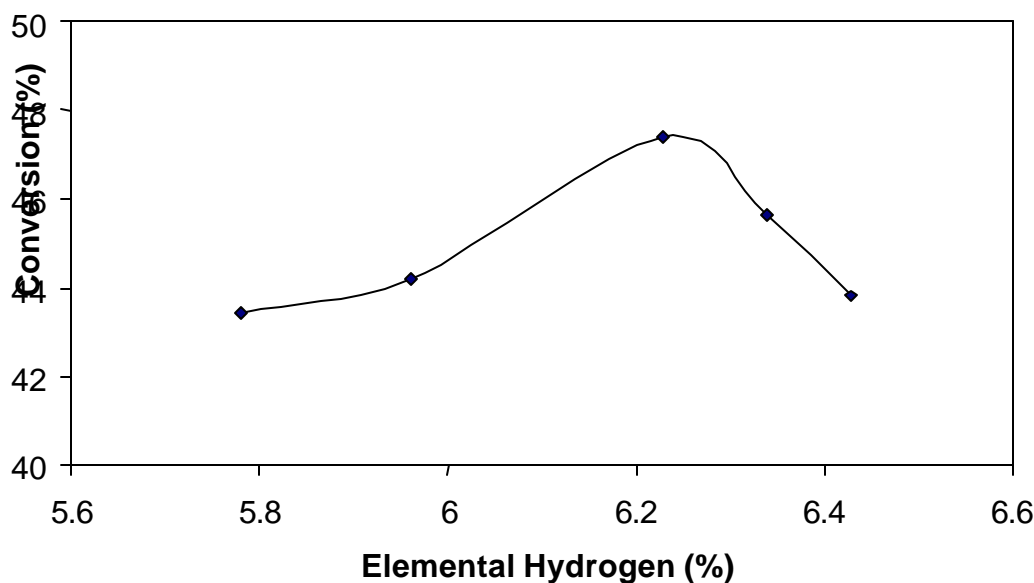


Figure 84. Variation of Successive Recovered Conversion with Elemental Hydrogen Content of the Recovered Solvent.

The figure below shows that the conversion goes through a maximum before starting to decrease as increasing amounts of fresh make-up solvent are added in subsequent runs. Here the conversion in the later runs is not dropping like that in the first method but is flattening out and achieving a steady value. Unlike the results of method one, the introduction of fresh solvent with the recovered solvent is maintaining the concentration of species like PAH's and hydroaromatics roughly constant in the blend giving more conversion at each pass. Also, since the concentration of these important species continues to increase with the introduction of increasingly more fresh solvent, the conversion does not show a decreasing trend but stabilizes to a value close to that found when 100 % fresh solvent is employed. There is one important thing to observe from the following figure where the curve shows a rise in conversion in the 0-20% make-up range. In an actual continuous process, a make-up of fresh solvent between 0 to 20% might be reasonably expected. After the initial variations in the conversion, the amount of fresh solvent make-up in the process will eventually stabilize. If the process is such that the losses are around 20%, a high coal-alone conversion can be expected. This increase of incremental conversion could have a major impact on the economics of such a process.

The figure below shows the conversion profile with the hydrogen content of the blends. It can be seen that the conversion profile follows the same trend as before with increasing hydrogen content. The same argument for method one applies here too, that increasing hydrogen uptake by the blends does not necessarily imply an increase in conversion.

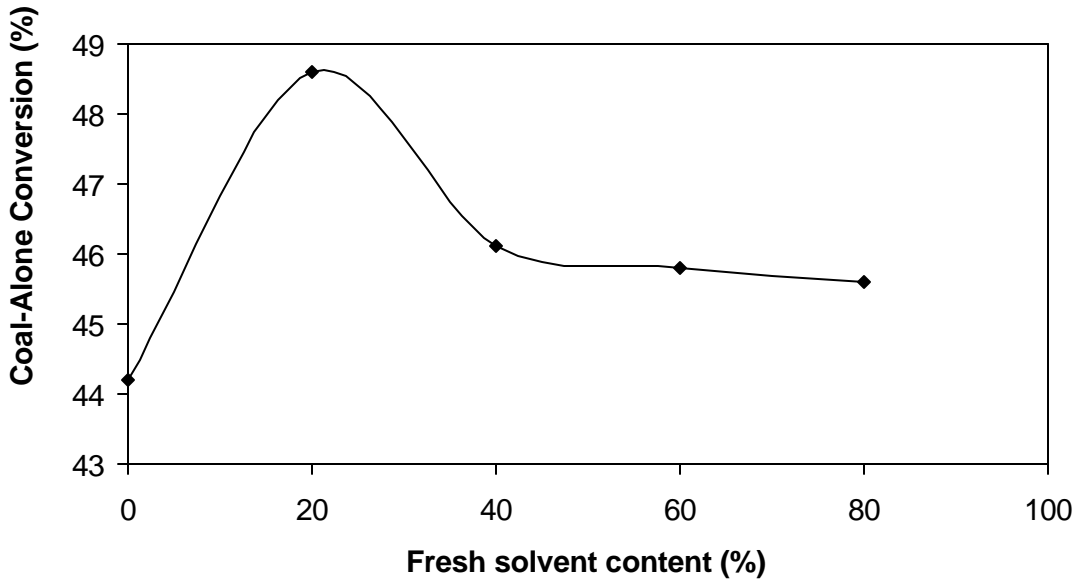


Figure 85. Coal-alone Conversion Results for Fresh and Successively Recovered Solvent Blends at 400 °C, 500 psig Cold Hydrogen and One Hour Reaction Time.

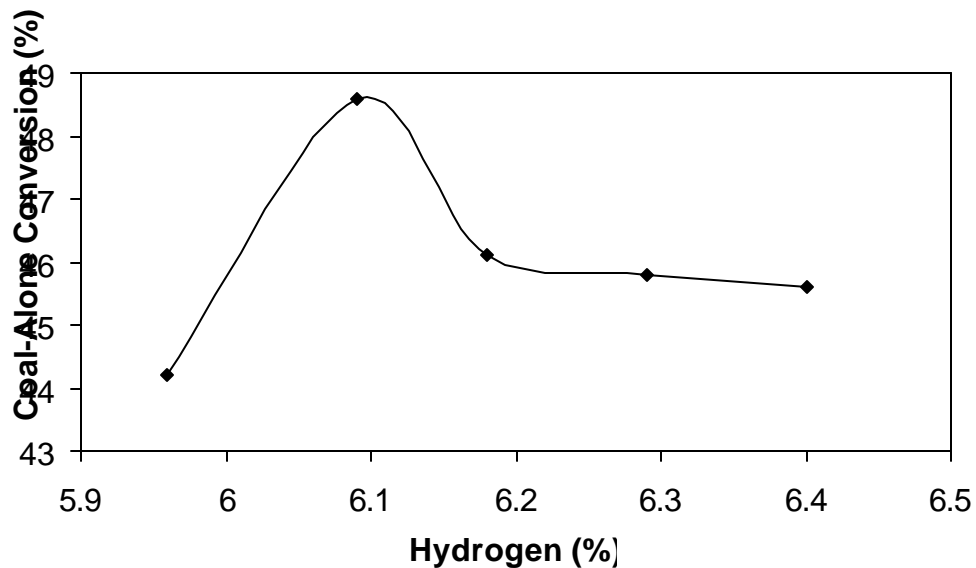


Figure 86. Variation of Coal-alone Conversion for Fresh and Successively Recovered Solvent Blends with Elemental Hydrogen Content of the Blends.

4.3 Pitch Processing

4.3.1 Ash Content

In an industrial process, ash and other insolubles would be removed through a combination of processes such as centrifugation and filtration. However, in the

laboratory environment it is more practical to determine ash content through a secondary solvent extraction. Tetrahydrofuran (THF) is used as a secondary solvent to dissolve pitch, resulting in a low viscosity liquid that can be filtered, resulting in a solution of THF plus THF-soluble material. It is presumed that all the coal dissolved by the hydrogenated aromatic oil-based solvent (i.e., the primary solvent in the process, used to dissolve coal) is also soluble in the THF secondary solvent. THF can then be evaporated, leaving the soluble portion of the coal and industrial byproduct solvent.

The ash content in the pitch is determined by the ASTM method outlined in a previous section. The relative error in determining ash content of the THF insolubles was $\pm 2\%$. In contrast, the relative error of the ash content in the pitch product was found to be $\pm 4\%$. The reason for the high error is the relatively small amount of ash in the pitch as compared to that in the insolubles. Also ash was not found in the recovered solvents as they are the distillate products. So, the two main components of ash content were the pitch and the THF insolubles. The next two tables show the percent ash in these two product fractions for fresh and recovered solvents.

The pitch fraction has a very low ash content of around 0.2-0.3 %, whereas most of the ash is seen in the insolubles. The ash content of the insolubles is around 10% for the all solvents used. As mentioned previously, the solvent which gave high conversion has a higher ash percentage in the THF insolubles. However the pitch product does not follow the expected trend of low ash with increased conversion.

Table 31. Properties of Hydrogenation Products using Fresh Solvent.

Fresh Solvent	Ash Content in THF Insolubles (%)	Ash Content in Pitch (%)	Coke Yield (%)	Softening Point (°C)
CBB	9.2	0.16	81.4	129
HCO	9.1	0.25	79.1	122
RCO	8.2	0.28	84.1	158

Table 32. Properties of Hydrogenation Products using Recovered Solvent.

Recovered Solvent	Ash Content in THF Insolubles (%)	Ash Content in Pitch (%)	Coke Yield (%)	Softening Point (°C)
CBB	8.5	0.15	83.1	132
HCO	8.2	0.24	80.6	125
RCO	7.9	0.27	84.9	156

The ash content in the pitch varies depending on the processing conditions. The ash in the pitches from runs using the recovered solvents is slightly lower than the corresponding runs using fresh solvent. The same applies to the ash in the THF insolubles.

The ash contents of the coal liquids and air blown pitches are shown in the figure below. They have all been decreased significantly from the 8.92% ash present in the feed coal. While these values are much better, they do not quite meet the stringent demands on coke feeds and binder pitches. However, this is not unexpected, as the separation step

in processing the coal liquid would work best at an elevated temperature, which keeps the converted product in a much more fluid state. In this study, the centrifugation used to separate the products from the residues was done with the materials initially in excess of 100°C. Unfortunately, the centrifuge used in this study is incapable of running at elevated temperatures, and the material in the bottles began to cool immediately, thus increasing the viscosity of the coal digest liquids, and hindering the separation of the residue. In a production scale facility, this problem could be eliminated using high temperature liquid-solid separation techniques.

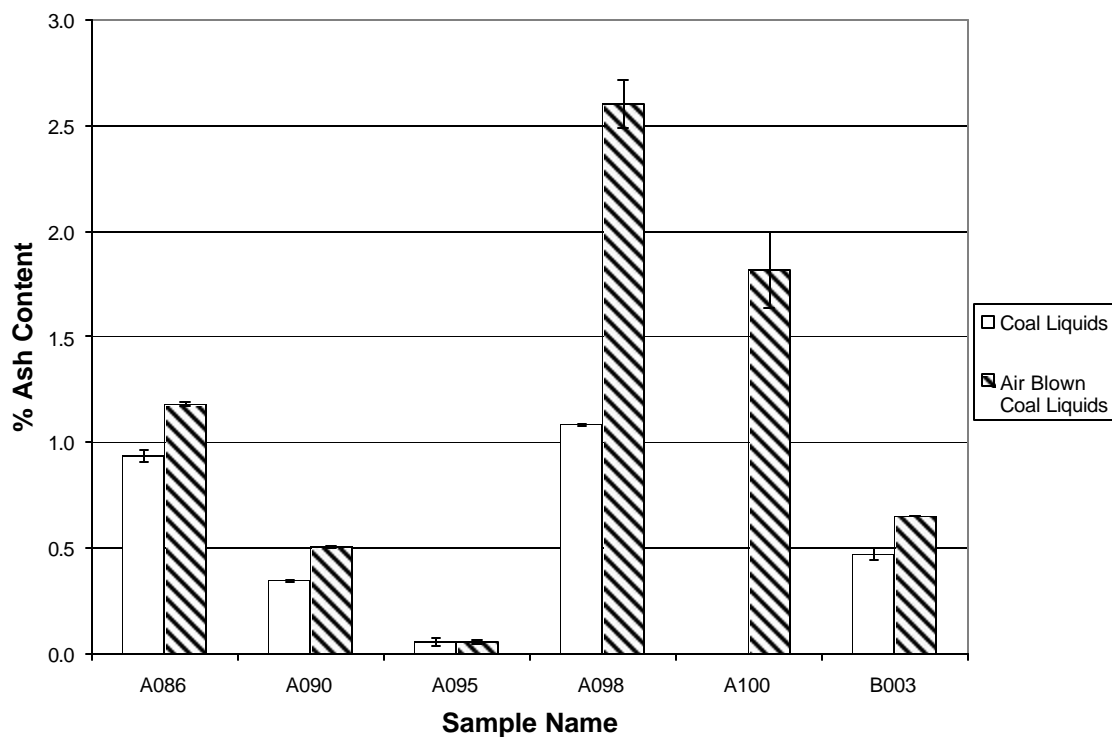


Figure 87. Ash Content in Coal Digest Liquids and Air Blown Digests.

4.3.2 Coke Yield and Softening Point

The softening point of the pitch gives an indication of the temperature at which the pitch melts and is flowable. The coke yield gives the content of non-volatiles in the sample, as described previously. The relative error for the coke test was typically $\pm 1.8\%$ while that for the softening point was $\pm 1.5\text{ }^{\circ}\text{C}$.

The softening point and the coke yield of the pitch samples for fresh and recovered solvents respectively are tabulated below. These values are at a fixed distillation condition of 30 mm hg vacuum and 270-280 °C final vapor temperature. It is important to specify the distillation conditions since the pitch properties are highly dependent on them, as will be discussed below. The coke yields of the pitches are in the range of 80-85% and the softening point is in the range of 130-160 °C. These values are typically higher than those for commercial binder pitches. The optical micrographs of the raw pitches show some development of mesophase due to the rather high temperature the pitch sees in the distillation pot – sometimes higher than 300 °C. Thus the high coke yield

is a consequence of the presence of the mesophase in the pitch. The softening point is rather low for pitches with such high coke yield. This is a result of the continuous isotropic phase which is controlling the softening point. A high coke yield is generally desirable to optimize the yield of the final carbon product. Thus, pitches obtained from this process might be useful for applications such as fiber spinning or coke making which require high softening point and high coke yield.

As mentioned above, changing distillation conditions imparts different properties to the pitch. The figure below shows coke yield and softening point changing for the pitch samples obtained when varying amounts of solvent are distilled. The softening point and coke yield values of these pitch samples are plotted against each other below. It can be observed that a linear trend is followed between these two properties, based on distillation conditions. This can be important commercially, where a variety of tailor-made pitches are required based on the end applications.

The softening point of the air-blown sample is a vital property in the determination of the end use for which the product is suitable. For example, binder pitches typically have softening points around 110°C. After five hours of air blowing, the softening points of the samples produced show softening points in excess of 110°C. This implies that very short air blowing times are required to increase the softening point of the coal digests to the desired level for production of binder pitch. This property is less important for producing coke feeds.

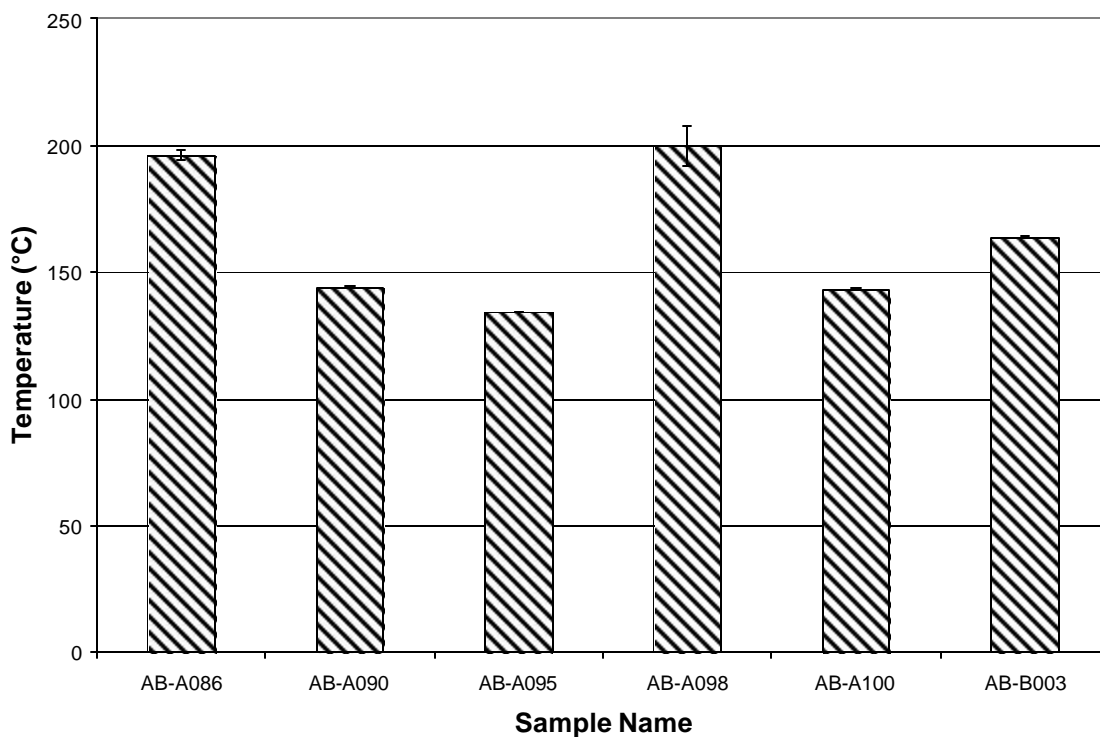


Figure 88. Softening Point (°C) for Air Blown Digests.

4.3.3 Elemental Analysis

Elemental analysis was performed on hydrogenated solvents and reaction products. Only those runs were selected for elemental analysis in which the vacuum distillation conditions were maintained the same. Thus the results could be compared more meaningfully between different solvents. The relative errors in the elemental values for hydrogen and carbon were $\pm 1.8\%$ and $\pm 2.2\%$ respectively. The errors for nitrogen and sulfur were higher, around $\pm 8\%$, due to the low quantities of these elements. The elemental composition and hydrogen-to-carbon ratios of the selected hydrogenation products are shown in the next table. Here pass 1 refers to reaction with fresh solvent whereas pass 2 represents the reaction run with the solvent recovered from pass 1.

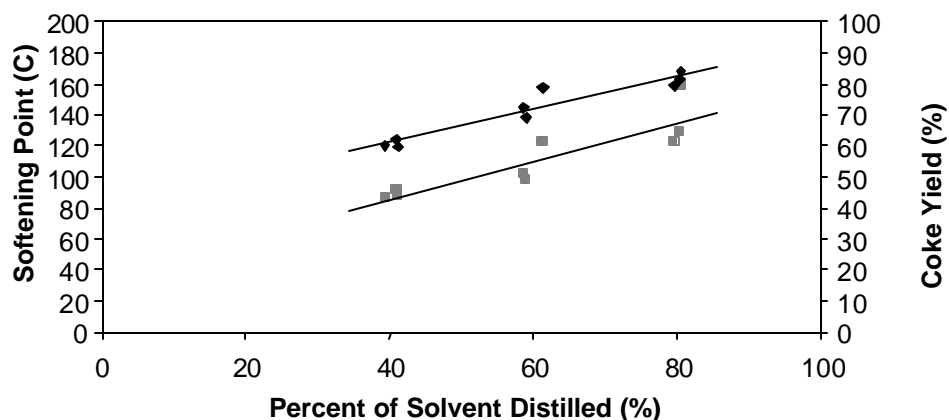


Figure 89. Relation Between Coke Yield and Softening Point for Solvents CBB, HCO and RCO at 400 °C, 500 psig Cold Hydrogen and One Hour Reaction Time.

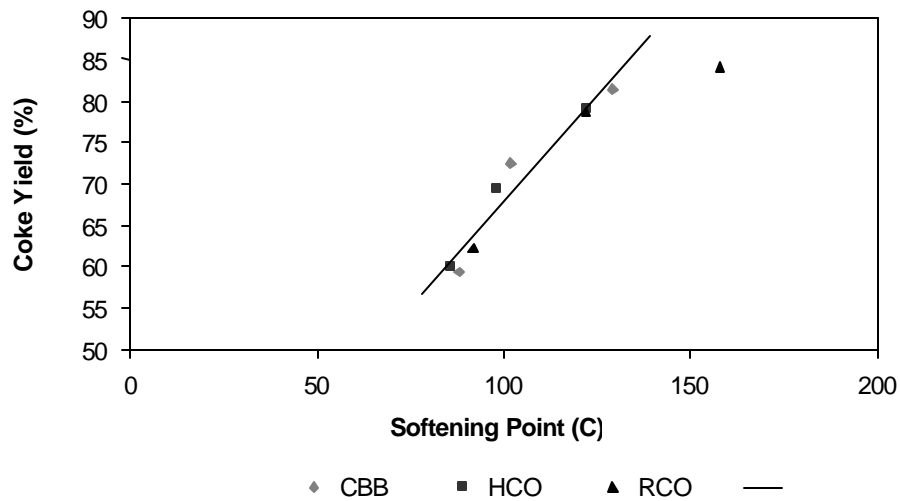


Figure 90. Relation Between Coke Yield and Softening Point for Solvents CBB, HCO and RCO at 400 °C, 500 psig Cold Hydrogen and One Hour Reaction Time.

The hydrogen-to-carbon ratio increases for pass 1 run from THF insolubles to pitch to recovered solvent (see below). This is expected as the solvent is the lightest

fraction among the products obtained. It can be noticed that all pitch products have a higher hydrogen-to-carbon ratio than the starting coal, which means hydrogen has been added to the coal organic matrix by hydrotreatment. Also it can be observed that the pass 2 recovered solvent has a higher hydrogen-to-carbon ratio than pass 1 recovered solvent which in turn has a higher hydrogen-to-carbon ratio than the corresponding fresh solvent. This indicates that some hydrogen rich light material is being produced during the hydrogenation runs. This also explains the fact that higher or comparable conversion is obtained when the recovered solvent from the earlier hydrogenation run is used in a subsequent run. But this is not always true for continued recycling, as will be explained in a later section.

The elemental analysis was also used to perform a carbon and hydrogen balance for the reacting and product species (see below). The carbon balance shows a negative balance suggesting a loss during the process. This is consistent with the fact that the mass balance also shows a negative balance. Since carbon is the dominant element compared to all other elements, the loss of overall mass is reflected in the carbon balance as well. The hydrogen balance also shows a negative balance during the process. This is unexpected due to the fact that a hydrogen uptake is observed during the reaction. The two major reasons for mass loss of hydrogen were neglecting the product gas formed during the reaction and the mass lost during THF evaporation and vacuum distillation. This mass primarily contained lighter species and hence is richer in hydrogen compared to the other elements. As these species are not accounted for in the mass or the elemental balances, a negative hydrogen balance seems reasonable. The last three rows of both upcoming tables (i.e. runs 4B, 5C and 6A) show the carbon and hydrogen balance for the recovered solvents for the same runs as with fresh solvents. It is observed that for the same runs of fresh and recovered solvents, the recovered solvents exhibit higher loss of carbon and hydrogen. This is consistent with the mass balances which showed higher losses for the recovered solvents.

Table 33. Elemental Composition of Solvents at Different Processing Points.

Solvent	Element	Fresh Solvent (%)	Product Fraction (%)			
			Pass 1 Pitch	Pass 1 THF Insolubles	Pass 1 Recovered Solvent	Pass 2 Recovered Solvent
CBB	C	91.66	92.24	78.02	91.79	90.39
	H	5.78	5.46	3.45	5.85	6.16
	N	0.00	0.56	0.86	0.00	0.00
	S	0.56	0.63	0.94	0.45	0.39
	H/C Ratio	0.75	0.71	0.53	0.77	0.82
HCO	C	92.46	92.59	77.99	93.16	93.91
	H	5.76	5.66	3.56	5.95	6.22
	N	0.76	0.85	0.99	0.81	0.74
	S	0.59	0.69	0.91	0.51	0.48
	H/C Ratio	0.75	0.73	0.55	0.77	0.80
RCO	C	91.81	92.15	76.36	89.90	89.66
	H	6.9	6.23	4.21	7.25	7.38
	N	0.58	0.52	0.98	0.72	0.61
	S	0.71	0.79	0.93	0.55	0.51
	H/C Ratio	0.9	0.81	0.66	0.96	0.99

Table 34. Carbon Balance of Select Hydrogenation Runs For all Three Solvents.

Run	Coal C (g)	Solvent C (g)	Total C Input (g)	Pitch C (g)	THF Ins. C (g)	Rec. Solv. C (g)	Total C Output (g)	Input - Output (g)	Loss (%)
1B	3.32	18.42	21.74	2.77	1.80	16.2	20.77	0.97	4.5
2C	3.31	18.42	21.73	3.52	1.84	15.09	20.45	1.28	5.9
3A	3.31	18.64	21.95	3.63	2.17	14.27	20.07	1.88	8.6
4B	3.31	18.72	22.03	2.87	1.85	14.08	18.8	3.23	17.2
5C	3.31	18.82	22.13	2.58	1.81	15.2	19.59	2.54	11.5
6A	3.32	18.34	21.66	2.47	2.06	14.33	18.86	2.8	12.9

Table 35. Hydrogen Balance of Hydrogenation Runs for Three Solvents.

Run	Coal H (g)	Solvent H (g)	Total H Input (g)	Pitch H (g)	THF Ins. H (g)	Rec. Solv. H (g)	Total H Output (g)	Input - Output (g)	Loss (%)
1B	0.20	1.16	1.36	0.16	0.08	0.99	1.23	0.13	9.6
2C	0.20	1.14	1.34	0.21	0.08	0.96	1.25	0.09	6.7
3A	0.20	1.4	1.60	0.24	0.12	1.15	1.51	0.09	5.6
4B	0.20	1.19	1.39	0.17	0.08	0.96	1.21	0.18	12.9
5C	0.20	1.20	1.40	0.16	0.08	1.01	1.25	0.15	10.7
6A	0.20	1.48	1.68	0.17	0.11	1.18	1.46	0.22	13.1

4.3.4 Optical Texture

Optical texture was determined for both the raw pitch and the corresponding cokes, obtained from the pitch in the coke yield test. The pitch samples saw a high temperature during the vacuum distillation. Hence it was speculated that there might be mesophase formation during this process of heat treatment. This was the reason to study the optical texture of the raw pitches. Samples were prepared by embedding them into epoxy and then polishing them for observation under the polarized-light microscope. The optical texture was determined according to the procedure described in a previous section. This technique is very important for the coke samples as the end use of the material is determined based on the structure of the material.

The optical micrographs of the raw pitches are shown below. As can be seen, the majority of the pitches do, in fact, show the onset of some mesophase development. This is a consequence of the high temperature they were exposed to during the vacuum distillation. As mentioned above, the presence of mesophase dispersed in the isotropic pitch matrix explains the high coke yield and moderate softening found for these pitches.

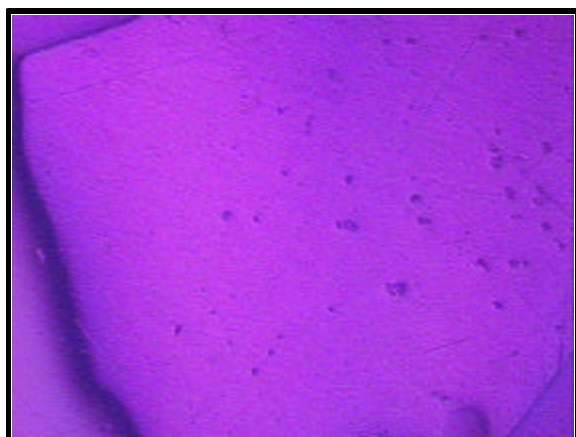


Figure 91. Optical Micrograph of Pitch Sample with Fresh CBB at 400 °C, 500 psig Cold Hydrogen, 5/1 Solvent-to-Coal Ratio and One Hour Reaction Time.

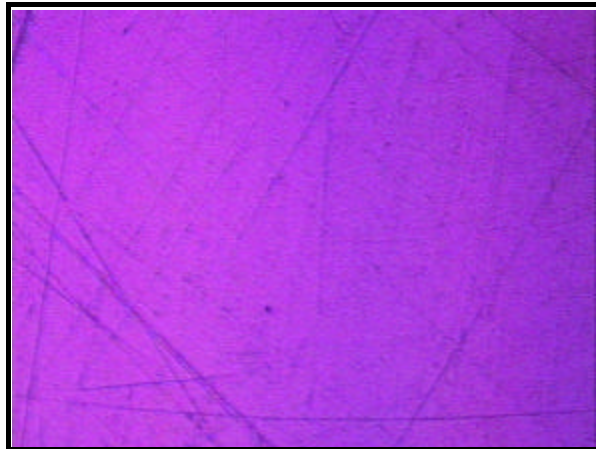


Figure 92. Optical Micrograph of Pitch Sample with Fresh HCO at 400 °C, 500 psig Cold Hydrogen, 5/1 Solvent-to-Coal Ratio and One Hour Reaction Time.

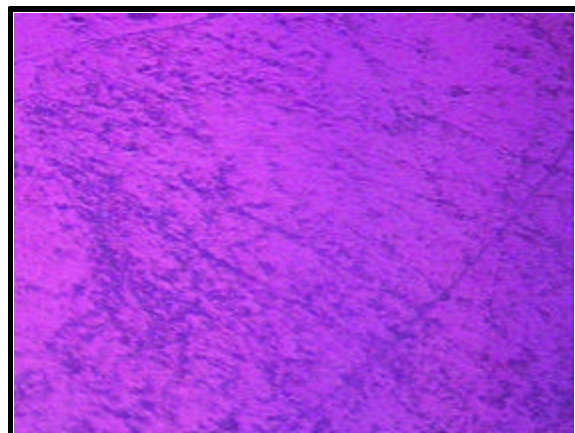


Figure 93. Optical Micrograph of Pitch Sample with Fresh RCO at 400 °C, 500 psig Cold Hydrogen, 5/1 Solvent-to-Coal ratio and One Hour Reaction Time.

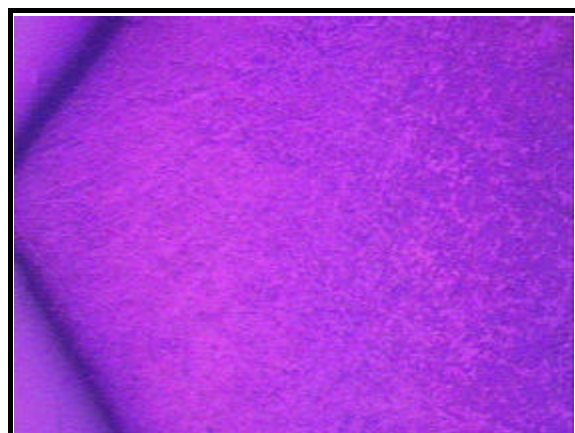


Figure 94. Optical Micrograph of Pitch Sample with Recovered CBB at 400 °C, 500 psig Cold Hydrogen, 5/1 Solvent-to-Coal Ratio and One Hour Reaction Time.

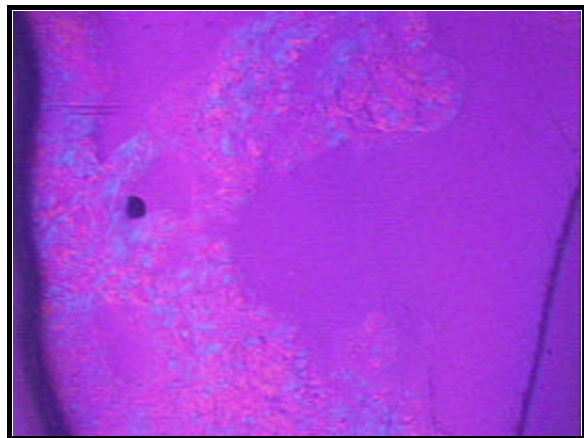


Figure 95. Optical Micrograph of Pitch Sample with Recovered HCO at 400 °C, 500 psig Cold Hydrogen, 5/1 Solvent-to-Coal Ratio and One Hour Reaction Time.



Figure 96. Optical Micrograph of Pitch Sample with Recovered RCO at 400 °C, 500 psig Cold Hydrogen, 5/1 Solvent-to-Coal Ratio and One Hour Reaction Time.

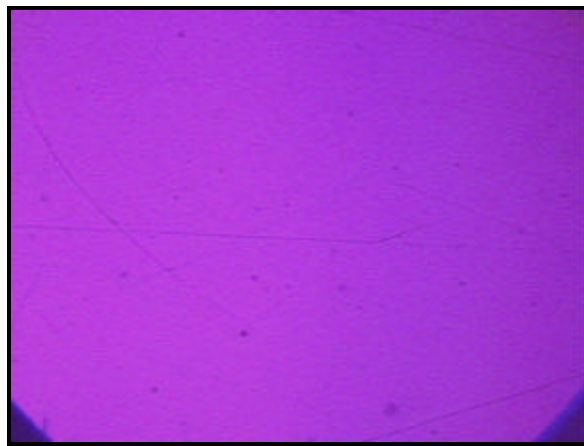


Figure 97. Optical Micrograph of Pitch Sample with Fresh CBB at 350 °C, 500 psig Cold Hydrogen, 5/1 Solvent-to-Coal Ratio and One Hour Reaction Time.

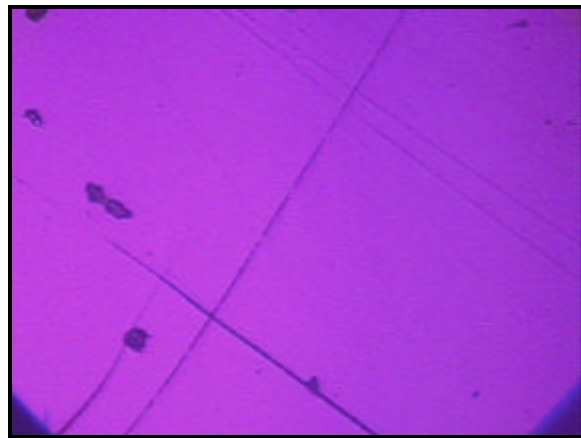


Figure 98. Optical Micrograph of Pitch Sample with Recovered CBB at 350 °C, 500 psig Cold Hydrogen, 5/1 Solvent-to-Coal Ratio and One Hour Reaction Time.

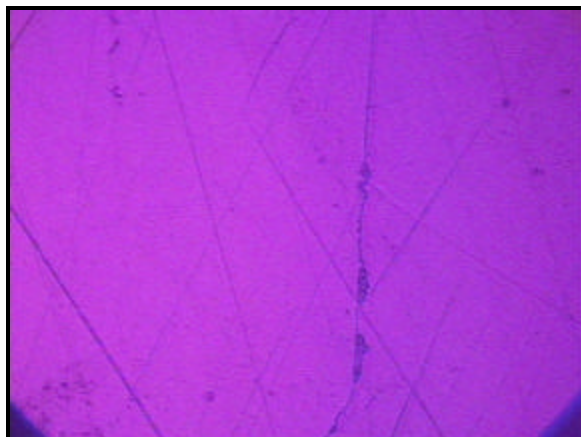


Figure 99. Optical Micrograph of Pitch Sample with Fresh CBB at 450 °C, 500 psig Cold Hydrogen, 5/1 Solvent-to-Coal Ratio and One Hour Reaction Time.

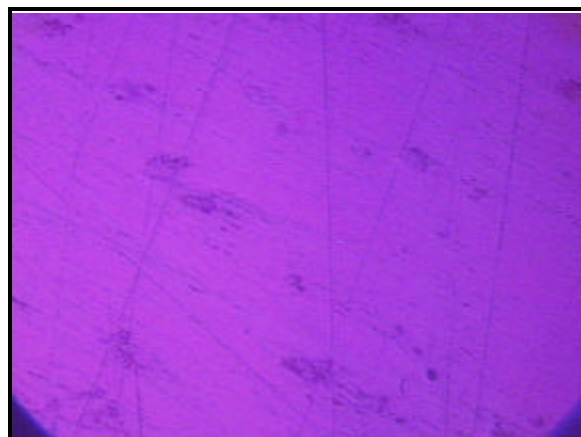


Figure 100. Optical Micrograph of Pitch Sample with Recovered CBB at 450 °C, 500 psig Cold Hydrogen, 5/1 Solvent-to-Coal Ratio and One Hour Reaction Time.



Figure 101. Optical Micrograph of Pitch Sample with Fresh CBB at 400 °C, 500 psig Cold Nitrogen, 5/1 Solvent-to-Coal Ratio and One Hour Reaction Time.

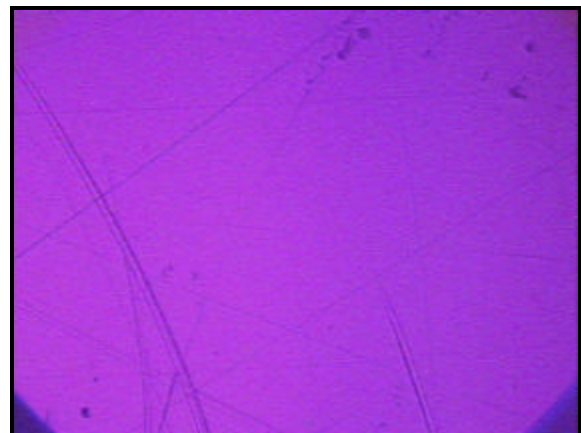


Figure 102. Optical Micrograph of Pitch Sample with Recovered CBB at 400 °C, 500 psig Cold Nitrogen, 5/1 Solvent-to-Coal Ratio and One Hour Reaction Time.

The next series of six figures show the optical micrographs of the cokes samples obtained from the pitches produced using fresh and recovered solvents in the hydrotreatment step. The first, third, and fifth figures show the cokes obtained for pass 1 runs with fresh solvents, while the second, fourth, and sixth figures show the cokes obtained for pass 2 runs for recovered solvents. All the cokes produced from the hydrogenation reactions with CBB and HCO were found to have large flow domains, indicating an anisotropic texture. The domains appear to be smaller and more uniformly distributed in the RCO samples, suggesting a lesser degree of anisotropy as compared to the samples from CBB and HCO. The coke samples from pass 2 runs are very similar to the coke samples of pass 1 runs, suggesting that not much structure related differences are induced by the reaction with recovered solvents.

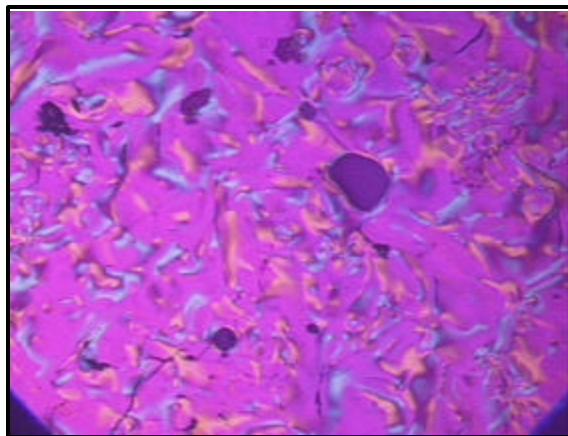


Figure 103. Optical Micrographs of Pass 1 Coke with CBB.

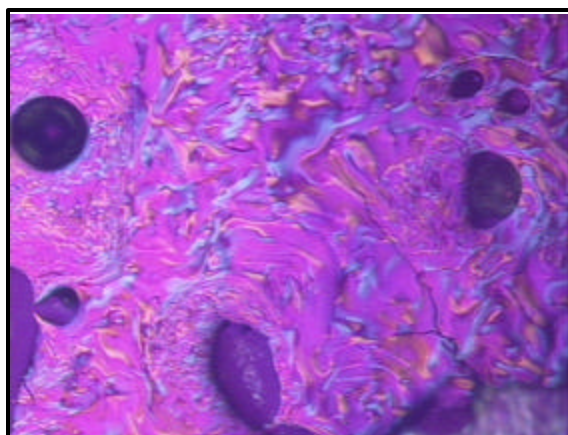


Figure 104. Optical Micrographs Pass 2 Coke with CBB.

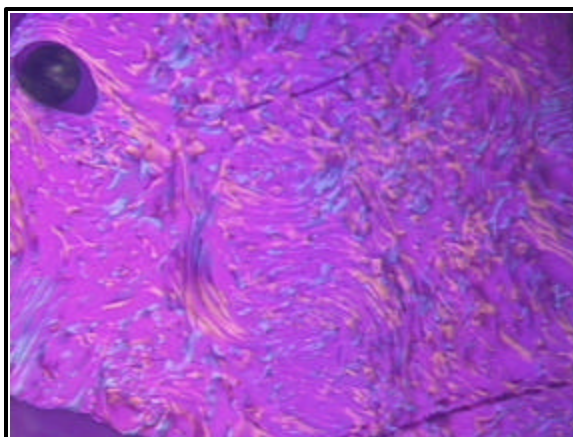


Figure 105. Optical Micrographs of Pass 1 Coke with HCO

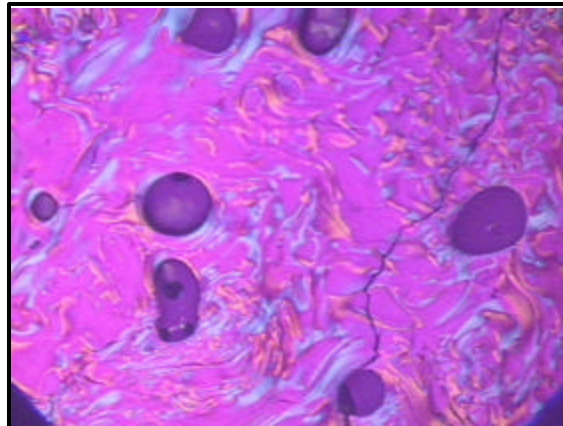


Figure 106. Optical Micrographs of Pass 2 Coke with HCO.

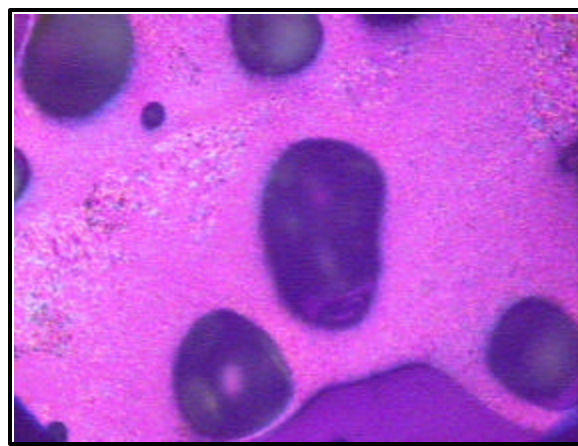


Figure 107. Optical Micrographs of Single-Pass Coke with RCO.

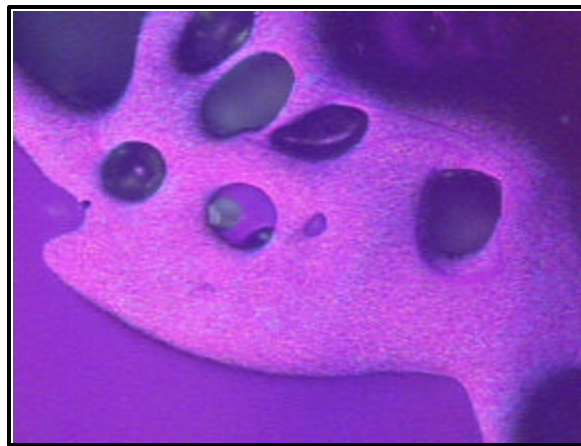


Figure 108. Optical Micrographs of Pass 2 Coke with RCO.

4.3.5 Characterization of Feed Pitches Prior to Air Blowing

As mentioned previously, air blowing is an optional step that can be used instead of (or in addition to) distillation, to raise the softening point and to enhance the coke yield

of hydrocarbon pitches. In the presence of light volatiles, air blowing can diminish the anisotropy of pitches, making it undesirable for the standpoint of producing high quality coke.

The feed pitches were characterized to determine some of their properties prior to treatment, as shown in the following table. All of the feeds were low in ash content, with similar softening point, and coke yield. However, the coal-tar pitch was significantly more dense and contained more pyridine insolubles (PI) than the other two materials.

Table 36. Properties of the Feed Pitch.

	A240 petroleum pitch	Koppers coal-tar pitch (filtered)	Synthetic coal-extract pitch
Ash (wt %)	0.04	0.05	0.01
Mettler Softening Pt. (°C)	116.9	108.1	121.7
Density (g/cc ³)	1.2365	1.3042	1.2465
Alternate Coke Yield (wt %)	50.9	53.7	56.0
Conradson Coke Yield (wt %)	47.1	48.0	52.9
Pyridine Insolubles (wt %)	0.84	11.50	0.15

4.3.6 Air Blowing Effect on Softening Point

Treatment of the feed pitches by air-blowing increases the softening point dramatically compared to blowing with an inert gas such as nitrogen. The A240 petroleum pitch softening point increased from 116.9°C for the parent pitch to about 175°C after air-blowing for 6 hours at 300°C. When the same pitch was subjected to the same conditions, but with nitrogen instead of air, the softening point only increased to about 134°C. The effects on the pitch softening point using air and nitrogen blowing can be seen below.

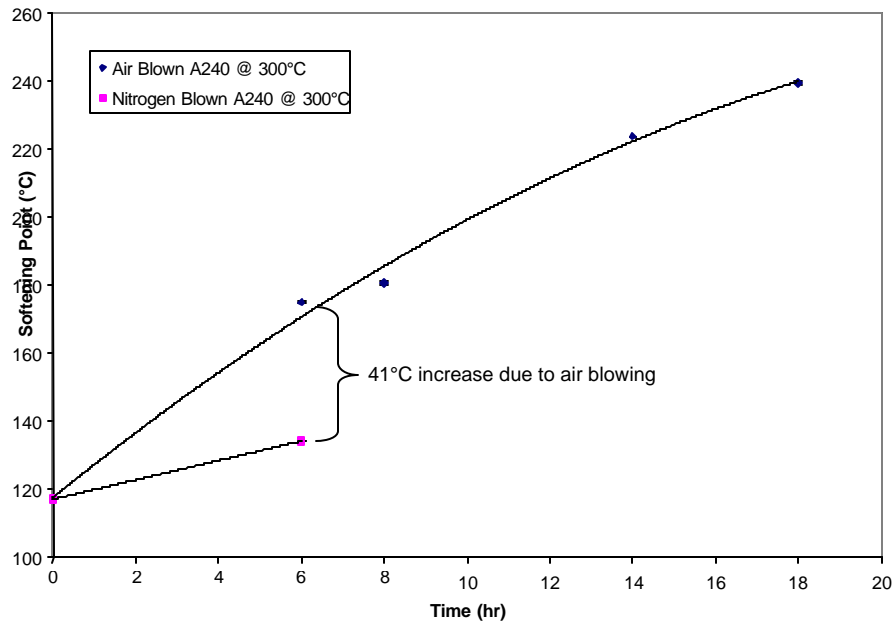


Figure 109. Softening Point Effects of Nitrogen and Air-blowing at 300°C on the Petroleum Pitch, A240.

A similar effect was seen with the coal-tar pitch when subjected to air and nitrogen treatment. The softening point of the coal-tar pitch feed was increased from 108°C to 174°C after 5 hours of air-blowing at 300°C. Nitrogen blowing for the same amount of time and at the same temperature resulted in the increase of the parent pitch softening point from 108°C to 131°C. The air treatment showed a 43°C increase in softening point above that of nitrogen blowing under the same reaction conditions. The effect on the pitch using both air and nitrogen can be seen in the figure below.

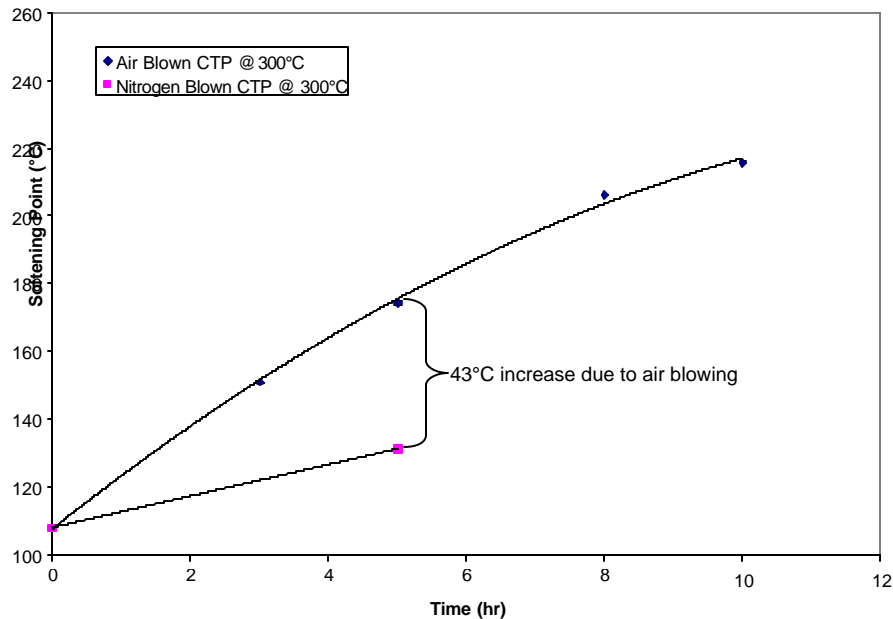


Figure 110. Softening Point Effects of Nitrogen and Air-blowing at 300°C on the Koppers Coal-tar Pitch.

The results from the previous figures show that air-blowing the pitch is more effective than nitrogen in terms of increasing the softening point. The A240 petroleum pitch had a 41°C increase in softening point, while the coal-tar pitch softening point increased by 43°C. Similar results were noted in the literature, as reviewed in Chapter 2. It can be inferred that significantly longer treatment would be required for nitrogen to achieve the same softening point obtained via air blowing.

The results of air-blowing on the softening point can be seen in the figure below. It is clear that softening point increases at shorter treatment times at higher temperatures. These observations are similar to those reported by other researchers, as discussed in the literature review.

The effects of air-blowing on the synthetic coal-extract pitch are shown below. Unlike the other two pitches, the synthetic extract pitch requires much less time to increase its softening point at any given temperature. This shows that coal-extract pitch is more reactive under air-blowing compared to the other two pitches. This can be more easily seen in the upcoming figure, in which the softening points of all three materials, air-blown at 300°C, are plotted together. Here, the coal-extract is evidently more reactive under air-blowing.

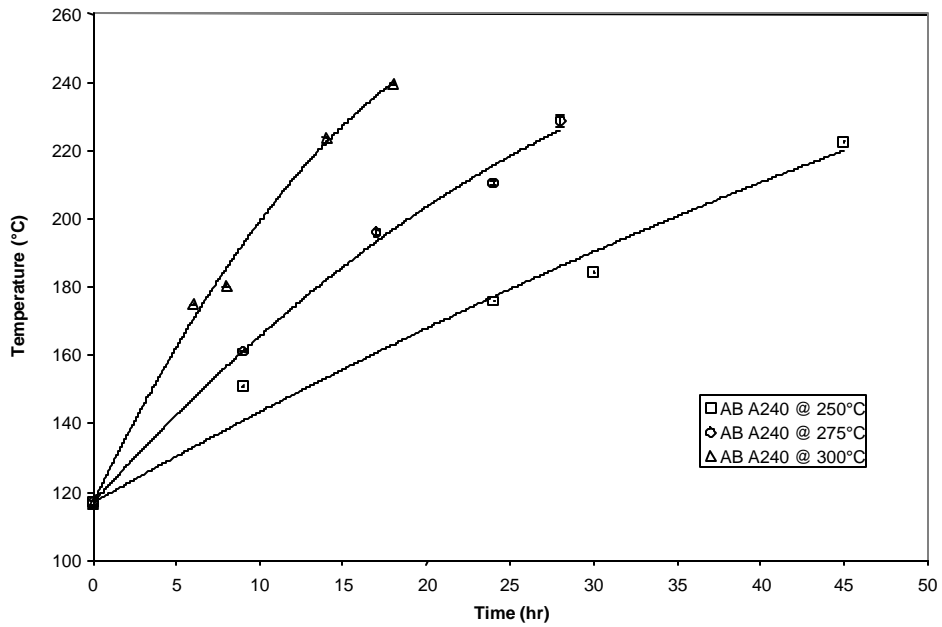


Figure 111. Softening Point Temperatures of Petroleum Pitch Air-blown at Reaction Temperatures of 250°C, 275°C, 300°C.

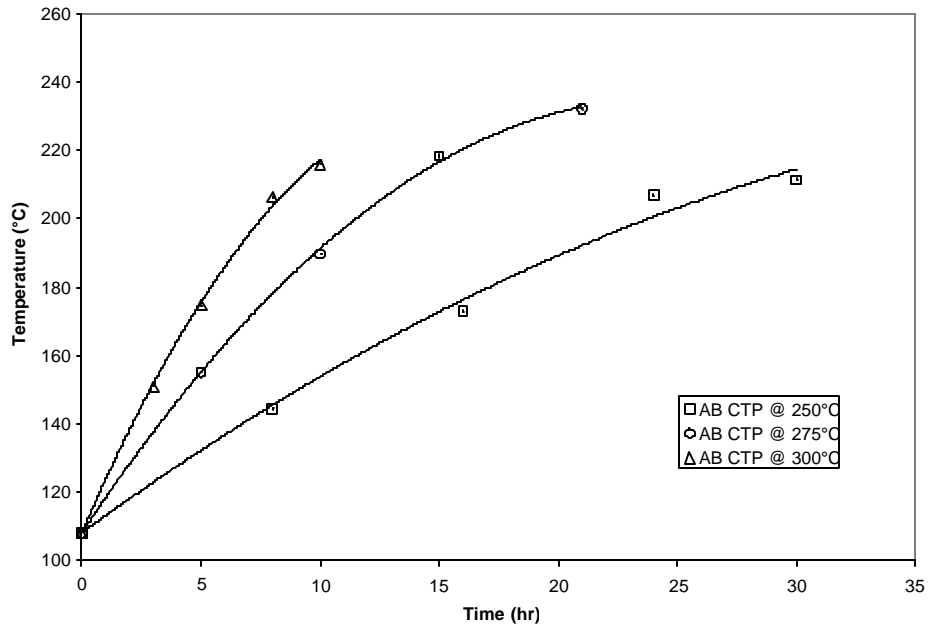


Figure 112. Softening Point Temperatures of Coal-tar Pitch Air-blown at Reaction Temperatures of 250°C, 275°C, 300°C.

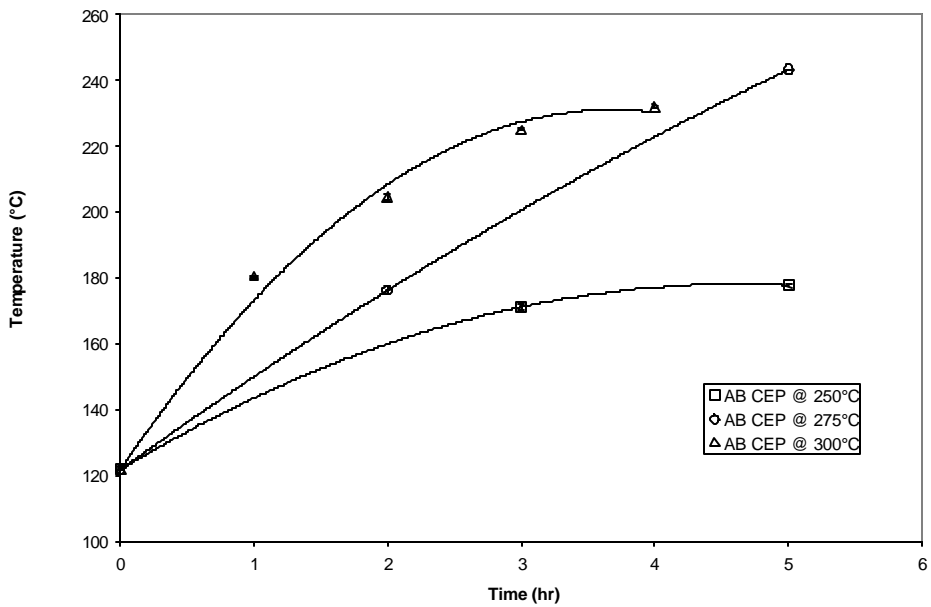


Figure 113. Softening Point Temperatures of Coal-extract Feed Pitch Air-blown at Reaction Temperatures of 250°C, 275°C, 300°C.

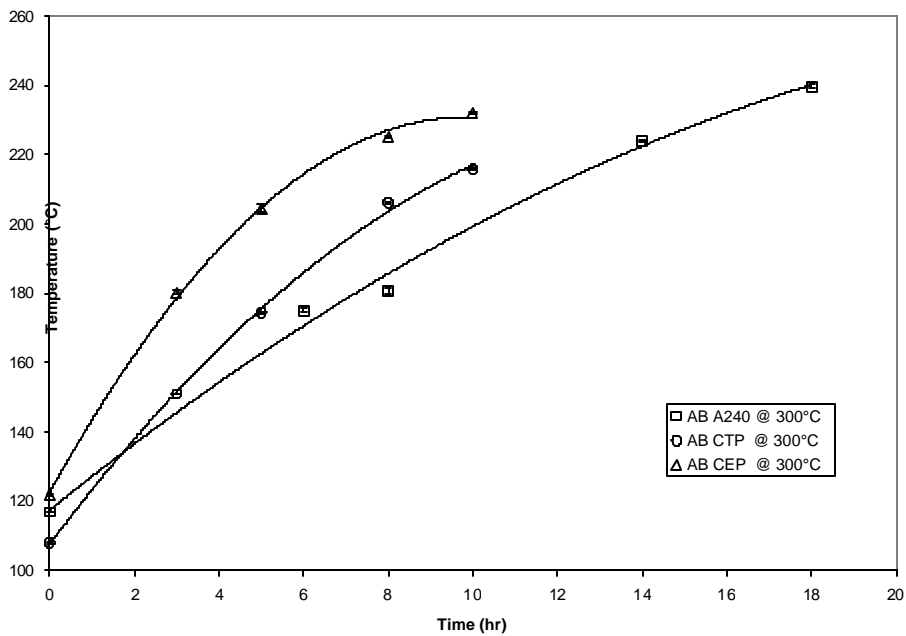


Figure 114. Softening Points of Air-blown Reaction at 300°C for all Three Pitches.

4.3.7 Conradson Carbon and Modified Carbon Determination

The results of air-blowing on the Conradson Coke yield can be seen in the figure below. As expected, the coke yield increases at higher temperatures and longer treatment times, as does the softening point of the pitch. The synthetic extract pitch

requires much less time to increase the coke yield at any given temperature. The modified protocol coke yield can be seen in the figure below. This shows similar trends to the Conradson Coke test.

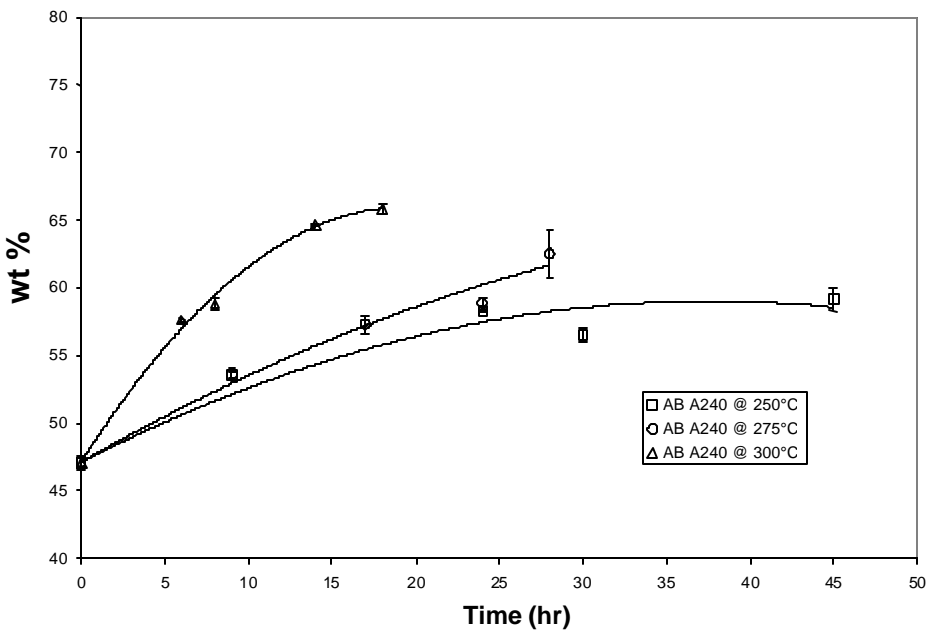


Figure 115. Conradson Coke Yield of Petroleum Pitch Air-blown for Various Periods at 250, 275, and 300°C.

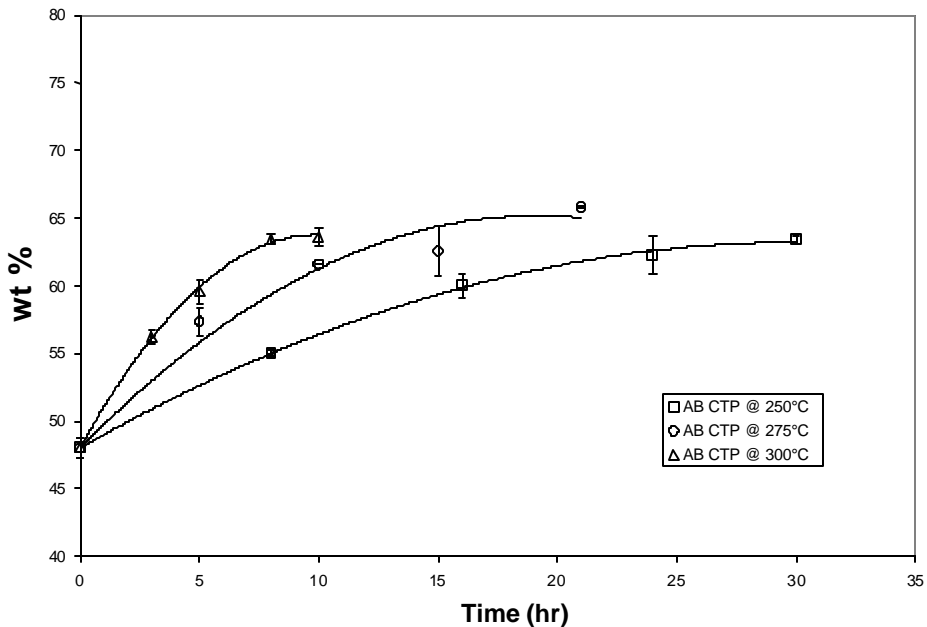


Figure 116. Conradson Coke Yield of Coal-tar Pitch Air-blown for Various Periods at 250, 275, and 300°C.

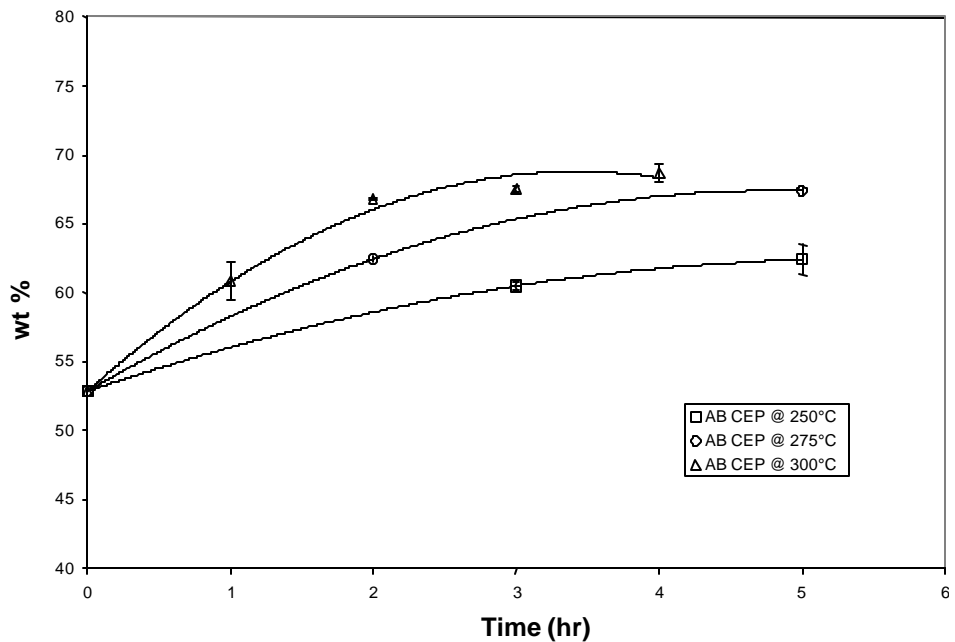


Figure 117. Conradson Coke Yield of Coal-extract Pitch Air-blown for Various Periods at 250, 275, and 300°C.

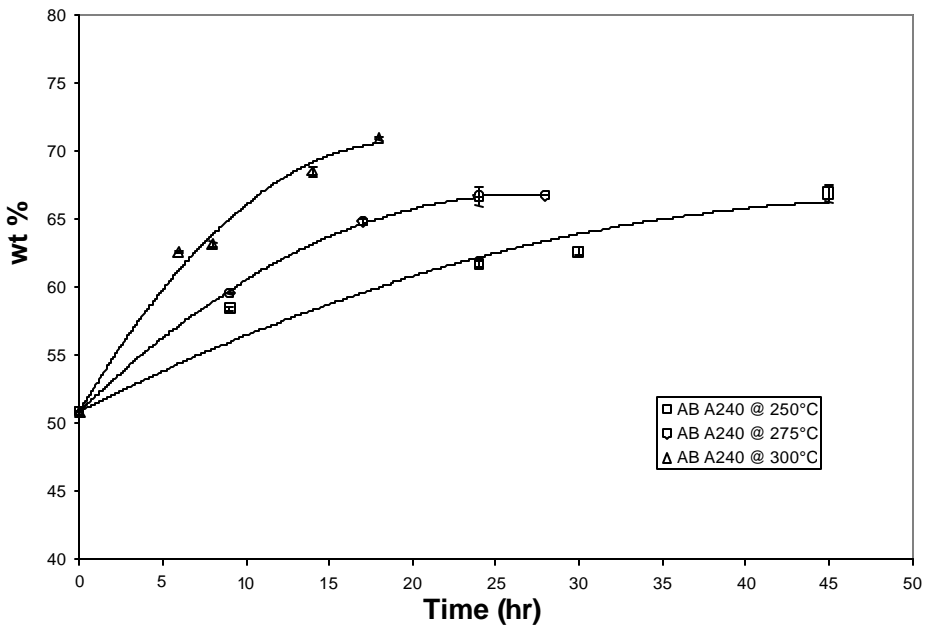


Figure 118. Modified Protocol Coke Yield of A240 Petroleum Pitch Air-blown for Various Periods at 250, 275, and 300°C.

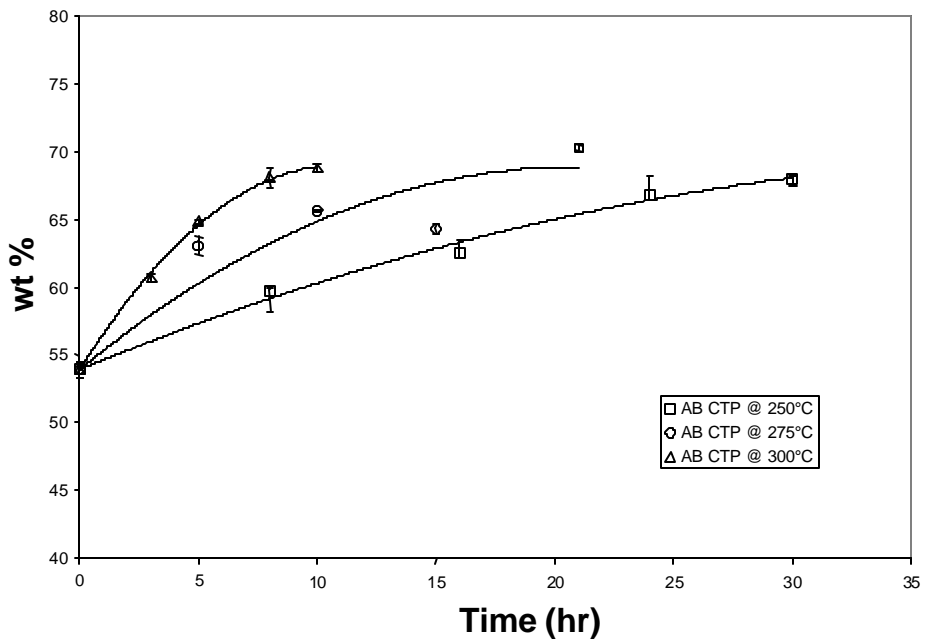


Figure 119. Modified Protocol Coke Yield of Koppers Coal-tar Pitch Air-blown for Various Periods at 250, 275, and 300°C.

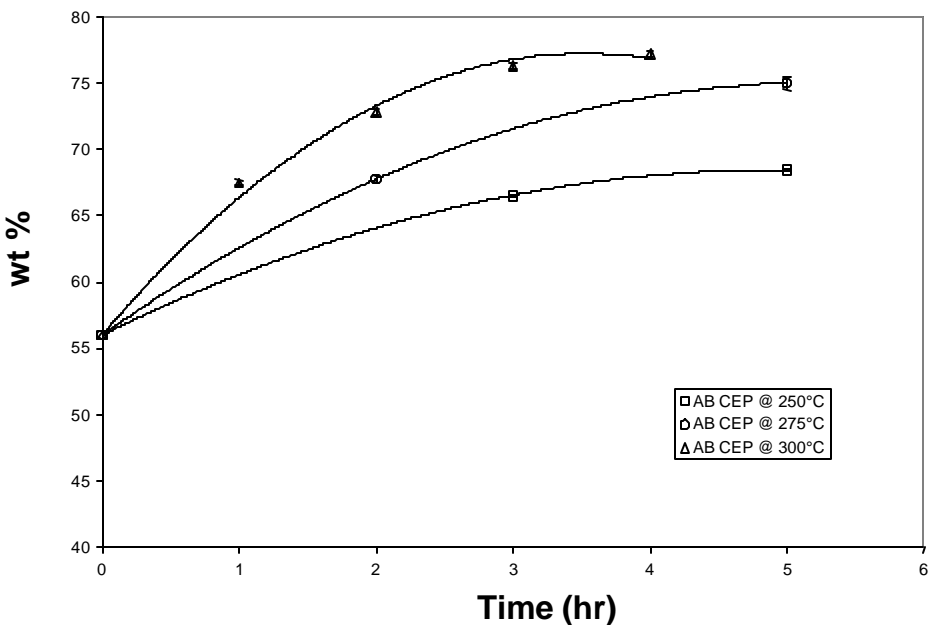


Figure 120. Modified Protocol Coke Yield of Synthetic Coal-extract Pitch. Air-blown for Various Periods at 250, 275, and 300°C.

The coke yields of these products are also essential data. The coke yields of the air-blown digests are greater than that of the liquid digests. This supports the use of air-blowing as a method to alter pitches to fit end uses. However, that the coke yields of the

air blown digests are not as high as would be desirable for coke feeds or binder pitches. Additional air blowing could increase the coke yields, but would also increase softening points, which would negate the use of these materials as binders. This may be solved either through varying the temperature and residence time of the air blowing, or perhaps through some distillation prior to air blowing to remove some of the entrained solvent.

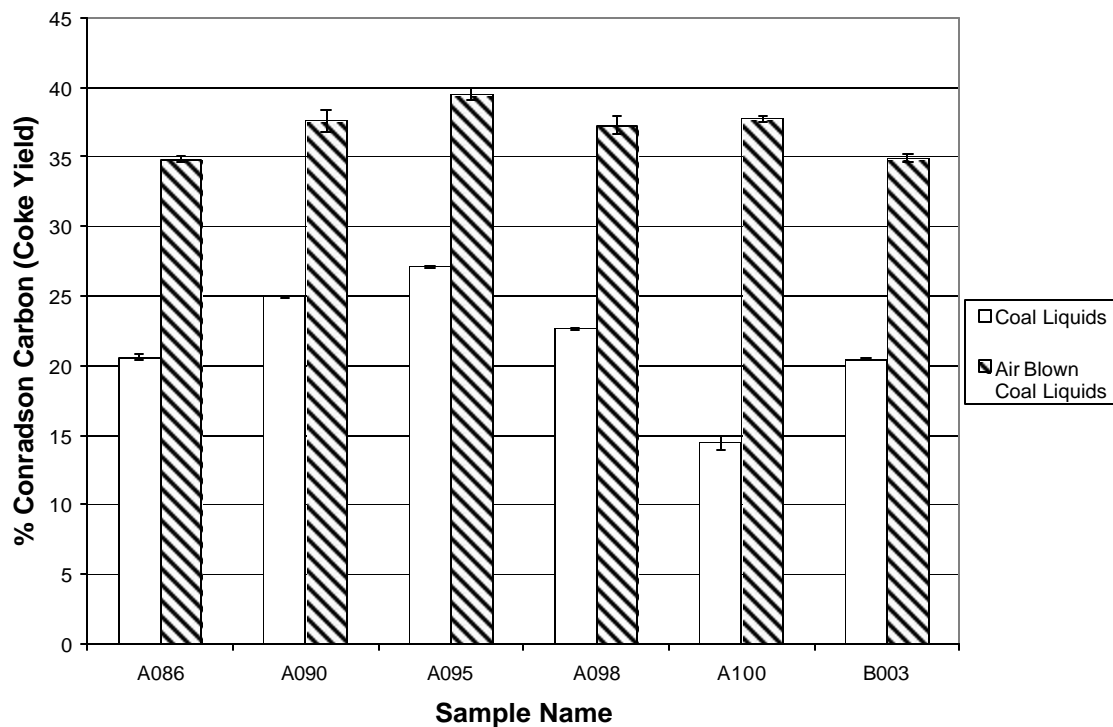


Figure 121. Conradson Carbon Coke Yield of Coal Digests.

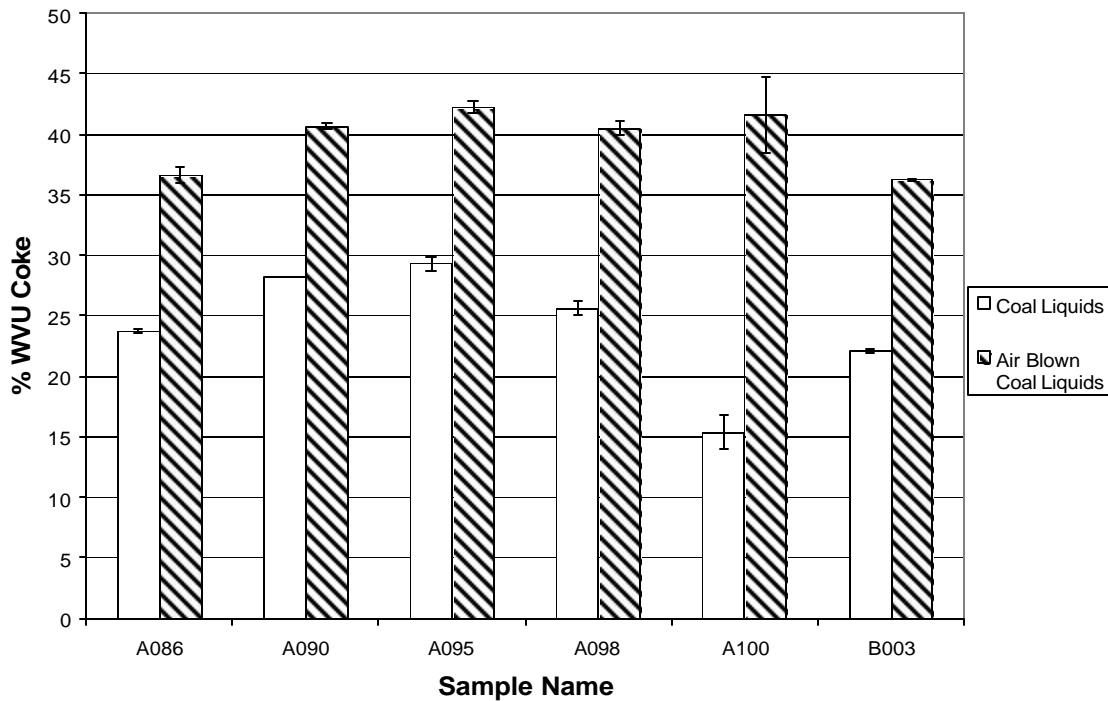


Figure 122. Modified Protocol Coke Yield of Coal Digests.

4.3.8 Effect of Air Blowing on Pitch Density

The density of the three pitches was increased as the air-blowing temperature and time were increased. The results of air-blowing on the density can be seen below. Following the same trends as observed with softening points and coke yields, densities are quite sensitive to air-blowing. The increase in density suggests that air-blowing results in a tighter or more compact ordering of molecules since there is more mass per unit volume.

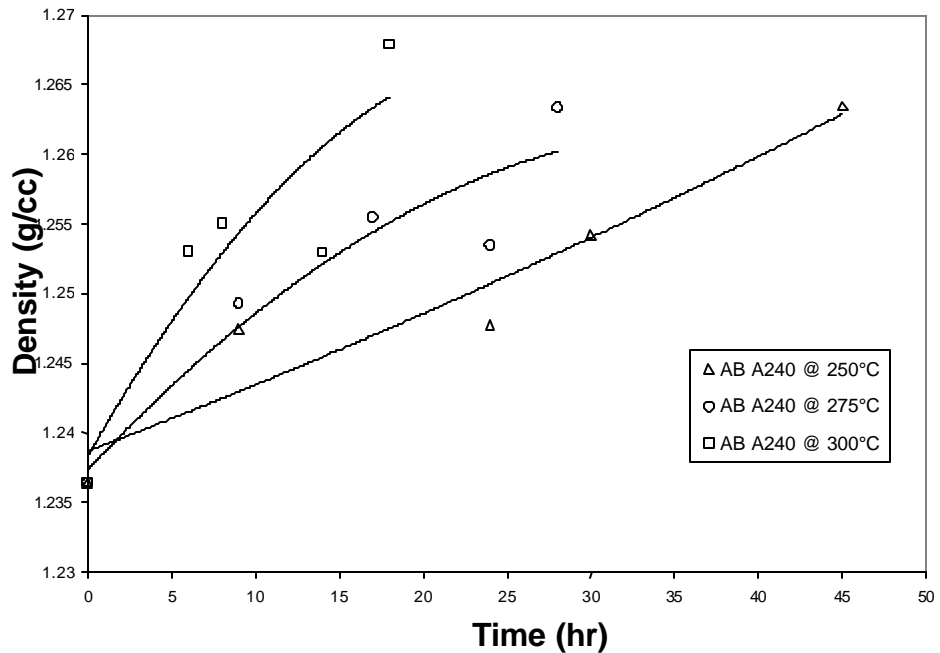


Figure 123. Density of Petroleum Pitches Air-blown at 250, 275, and 300°C.

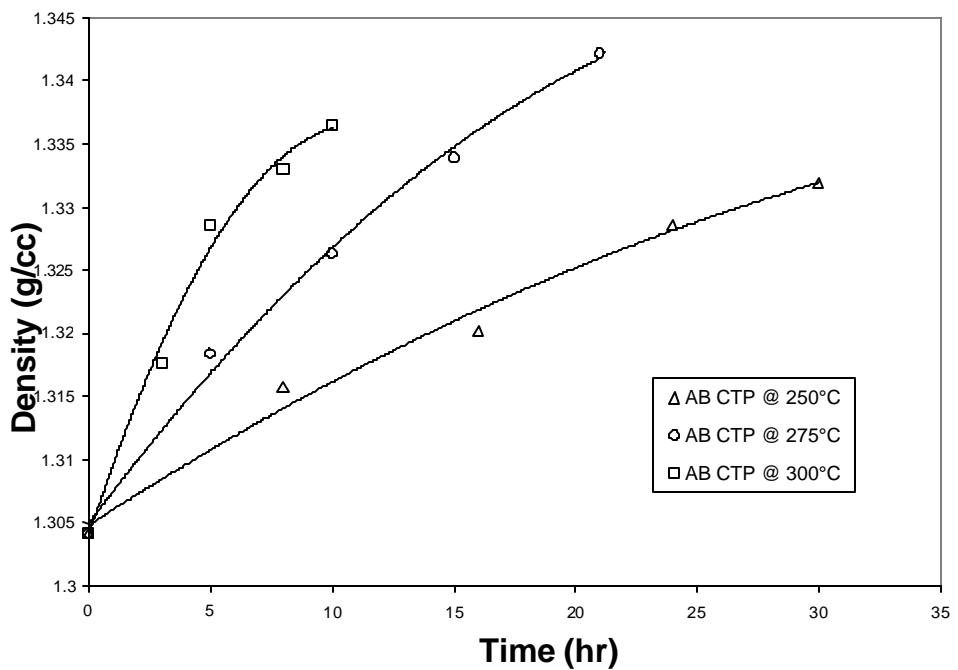


Figure 124. Density of Coal Tar Pitches Air-blown at 250, 275, and 300°C.

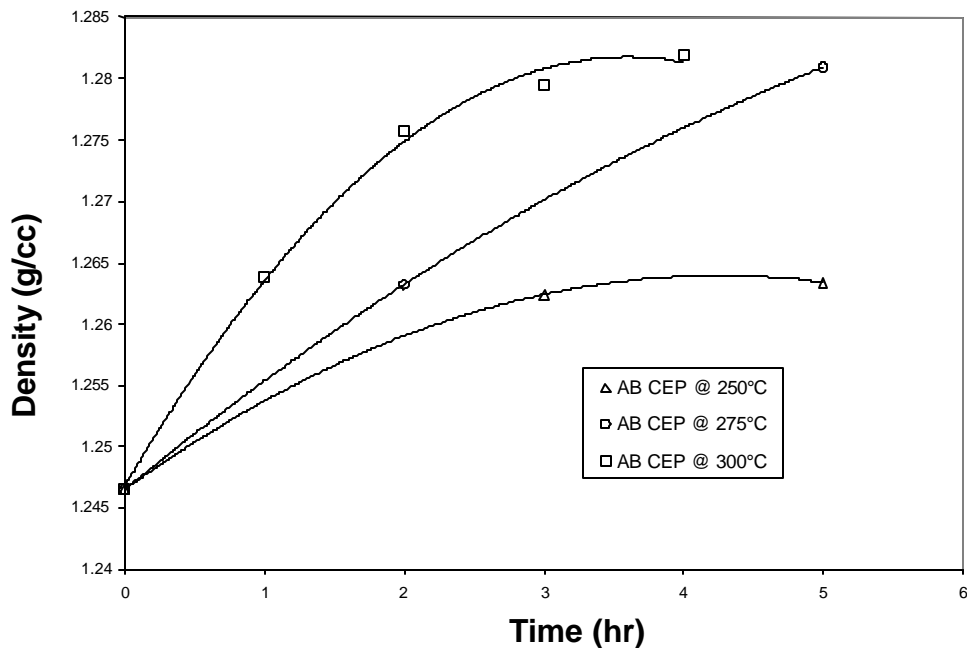


Figure 125. Density of Coal-extract Pitches Air-blown at 250, 275, and 300°C.

The air blowing of the coal digests will also affect the density of the final product. The figure below shows the densities of the air-blown digests. Referring to the table and figure below, it is interesting to note that the air blown A098 digest has a modestly higher density than the A086, even though they were prepared in the same method (only at a temperature of 425°C rather than 400°C). This may imply that the more complete digestion that occurs at higher temperatures resulting in more lower molecular weight compounds that are more readily cross-linked during air-blowing.

Table 37. Sample Identification.

Name	A086	A090	A095	A098	A100	B003
Solvent	HCBB-L3	50% HCBB-L3 & 50% HSO-L3	HSO-L3	HCBB-L3	HMO-L3	50% HCBB-L3 & 50% HMO-L3
Temp. (°C)	400	425	425	425	425	425

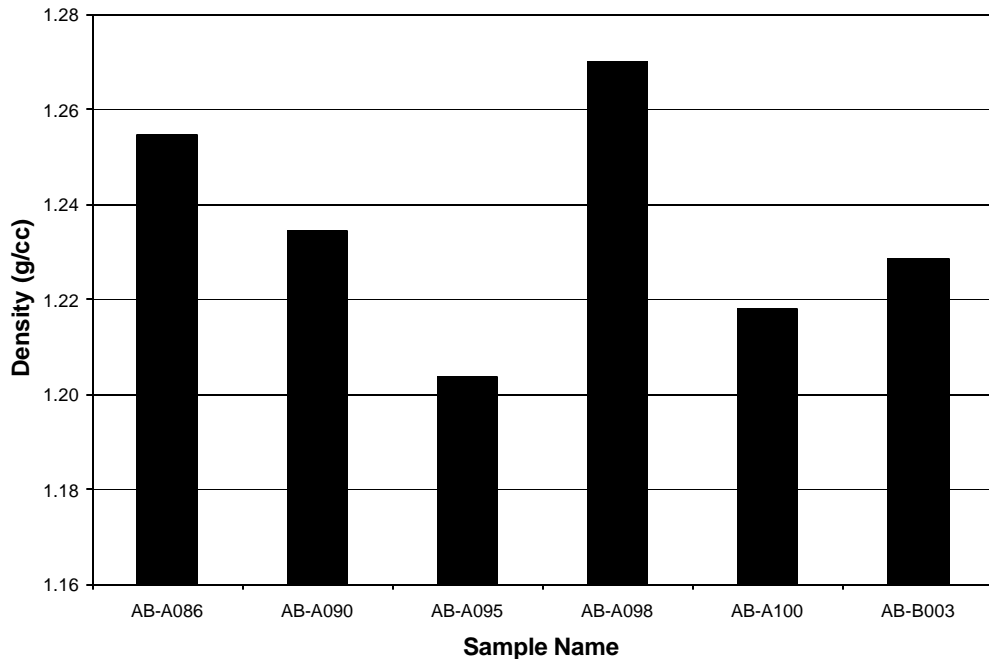


Figure 126. Air Blown Sample Densities.

The viscosity of the coal digests is much lower than the viscosities of the air-blown coal digests. Each digest is affected in a very similar manner, as the viscosity curve shifts to the right (higher temperatures) after air blowing. The important point to take from these figures is that the viscosity of the coal digests, after centrifugation, is in an easily manageable range (100-1000 cP) at temperatures below 100°C. This has positive implications on the potential large-scale production of these materials. The pumping of these materials will not have to be done at very high temperatures, even though some of them are pasty at room temperature. The lone exception is the A095 coal digest, which was produced with level-3 hydrogenated slurry oil only. This coal digest liquid has a viscosity under 1000cP only after heated above 120°C.

4.3.9 Effect of Air Blowing on Pitch Viscosity

The WLF equation was chosen to model the viscosity of the air-blown pitches. Ideally, the glass transition temperature, T_g , should be chosen as the reference temperature. Attempts were made to determine T_g by DSC without success. Only feed pitches exhibited T_g with the air-blown materials showing no transitions. Therefore, a glass transition temperature was estimated as 80 % of the Mettler softening point, as suggested by Barr and Lewis.⁷² Insertion of this calculated T_g into the WFL equation (and assuming $\eta=10^6$ cP at T_g) lead to a great deal of scatter in the data. But since the reference temperature can be arbitrary, the corresponding viscosity can be determined graphically. As can be seen below, all of the curves intersect at a viscosity of 10,000 cP (log 4) for the petroleum pitch. This could also be seen in the coal-tar and coal-extract viscosity measurements, shown below. Each curve was fitted to a logarithmic equation in which the reference temperature was estimated by substituting log 4. From these

equations, the temperature for the reference viscosity could be determined. This temperature and viscosity were used as the reference temperature and reference viscosity, respectively. After the reference temperature and viscosity were determined, the data for all of the treated pitches were modeled using the WLF equation:

$$\text{LOG} \left(\left(\frac{n}{T} \right) \left(\frac{T_R}{n_r} \right) \right) = T - T_R \quad .$$

As can be seen from this information, the data was approximately linear. The relationship indicates that the rheological behavior of both the feed and air-blown pitches behave similarly to other types of conventional pitches and the visco-rheological behavior can be modeled using established theories. The WLF plots for A240, coal-tar, and coal-extract pitches are shown below.

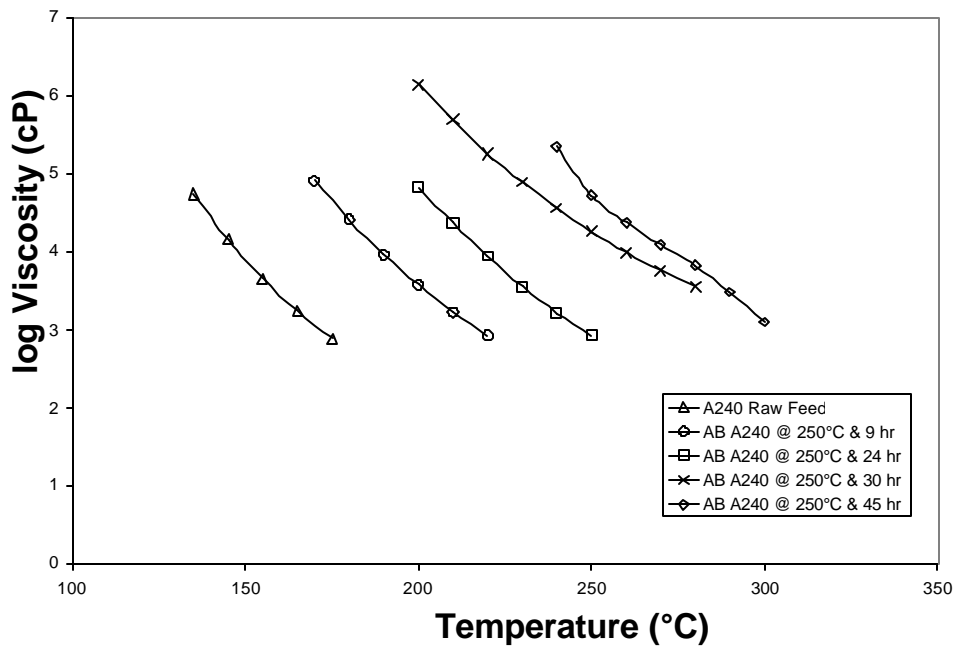


Figure 127. Temperature Dependence of Viscosity for A240 Petroleum Pitch at 250°C.

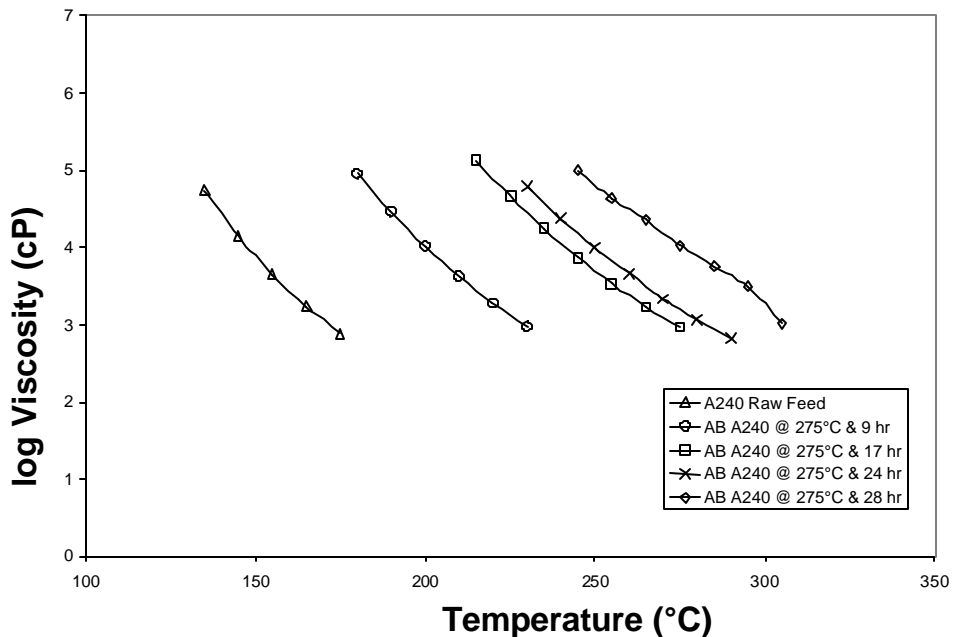


Figure 128. Temperature Dependence of Viscosity for A240 Petroleum Pitch at 275°C.

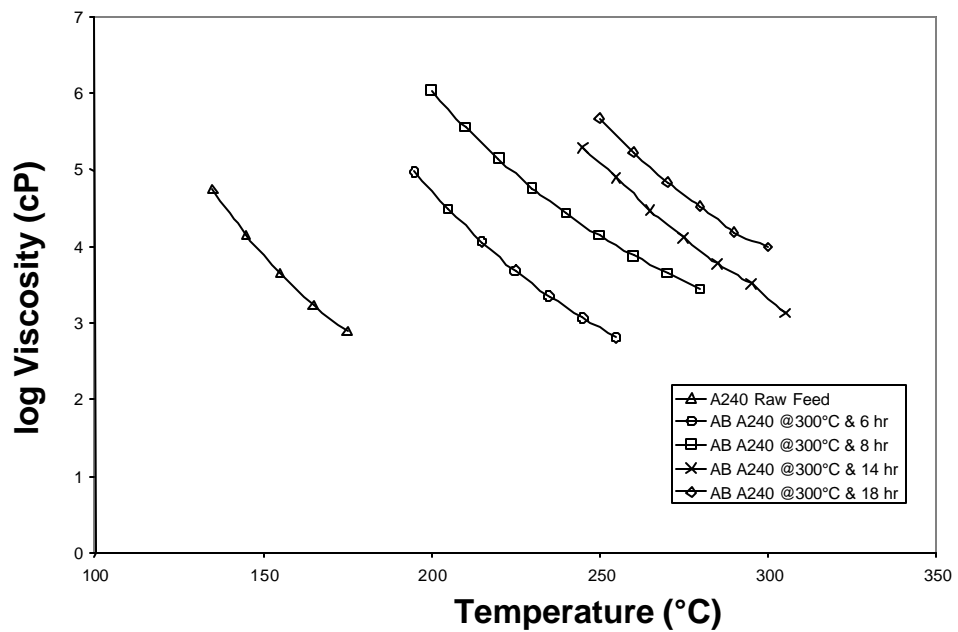


Figure 129. Temperature Dependence of Viscosity for A240 Petroleum Pitch at 300°C.

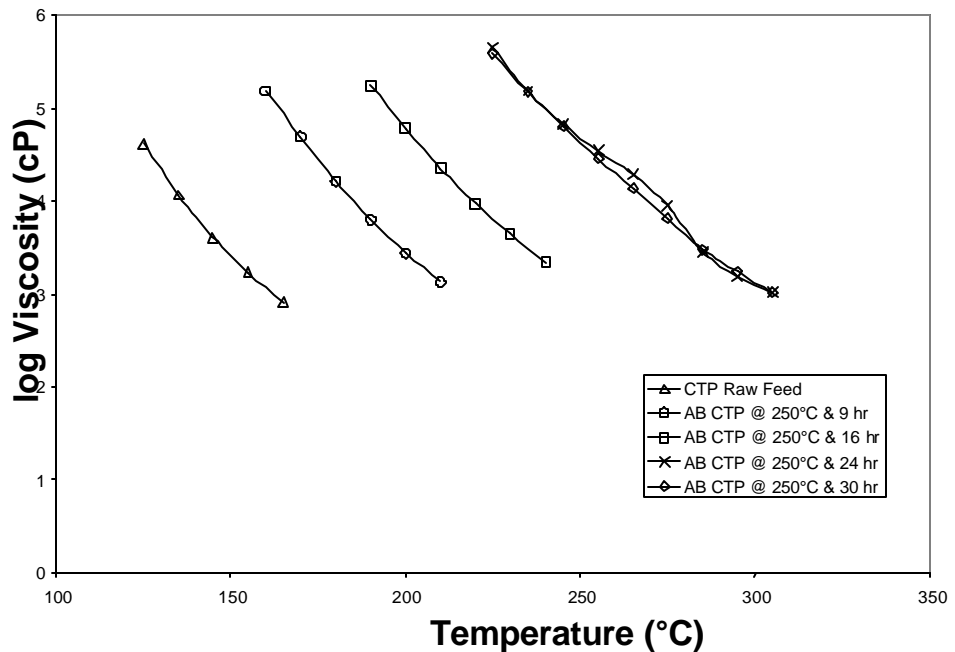


Figure 130. Temperature Dependence of Viscosity for Koppers Coal-tar Pitch at 250°C.

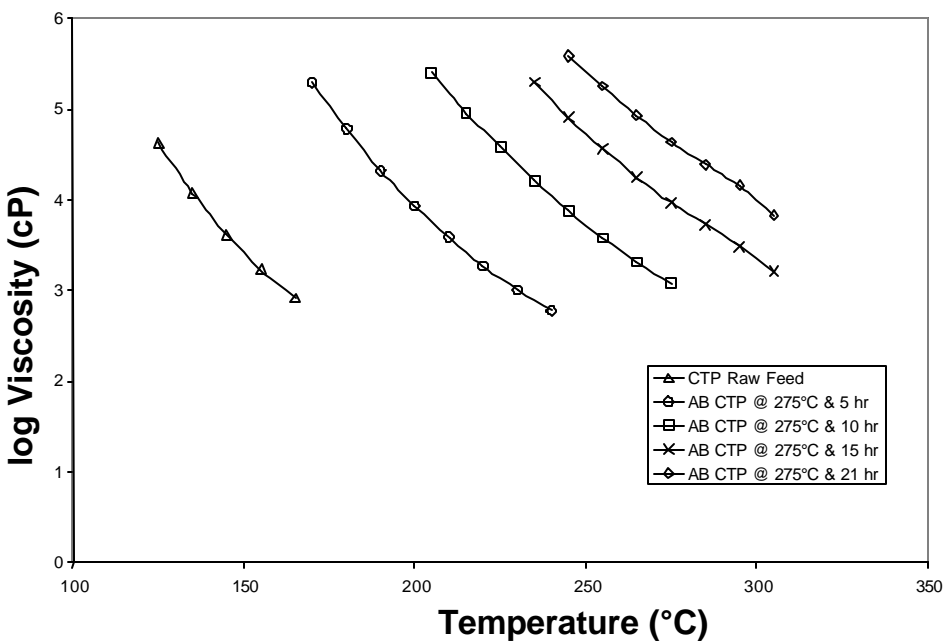


Figure 131. Temperature Dependence of Viscosity for Koppers Coal-tar Pitch at 275°C.

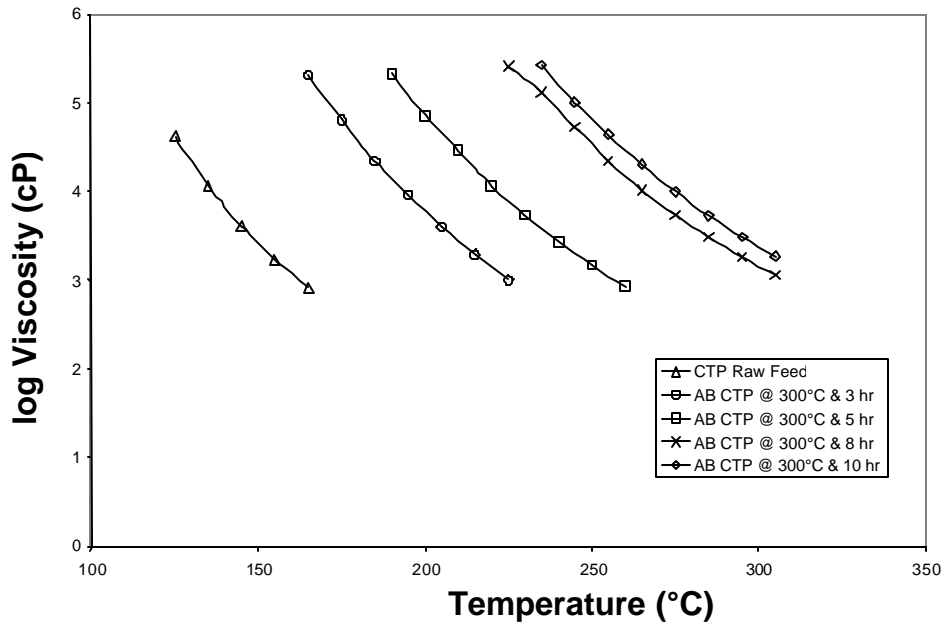


Figure 132. Temperature Dependence of Viscosity for Koppers Coal-tar Pitch at 250°C, 275°C, and 300°C.

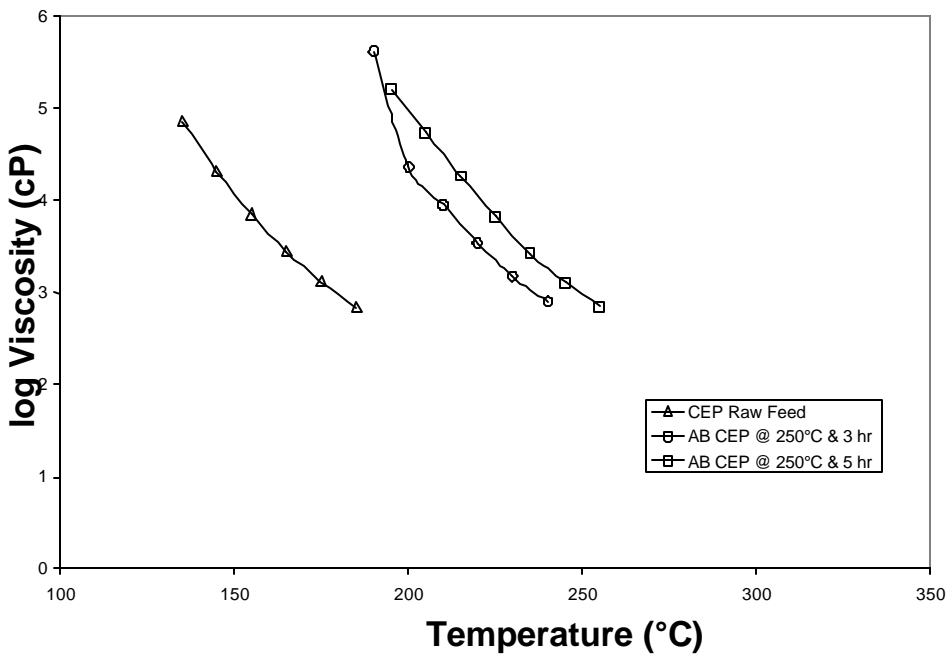


Figure 133. Temperature Dependence of Viscosity for Synthetic Coal-extract Pitch (CEP) at 250°C.

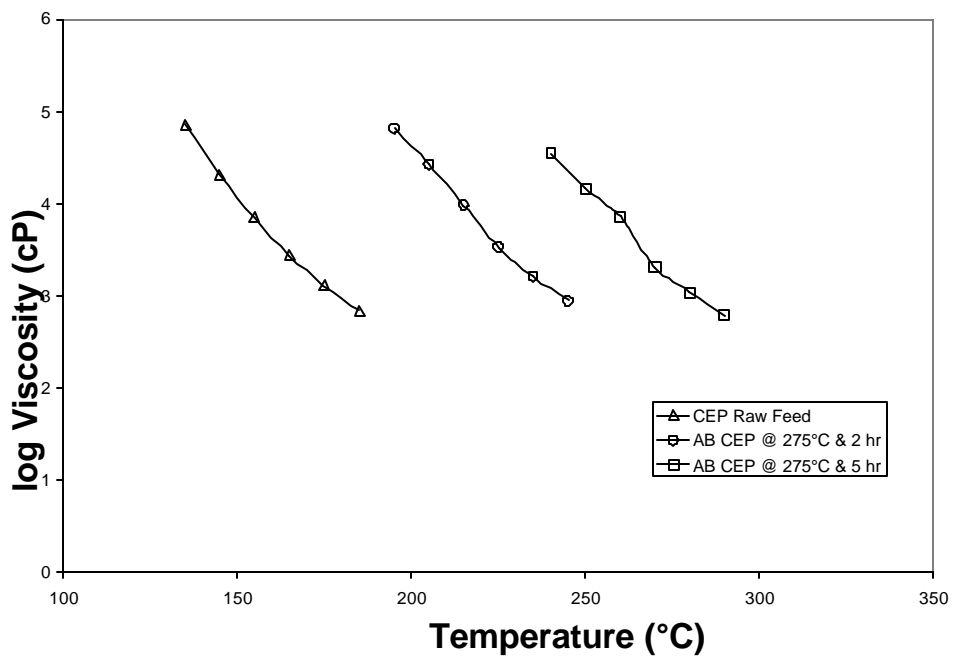


Figure 134. Temperature Dependence of Viscosity for Synthetic Coal-extract Pitch (CEP) at 275°C.

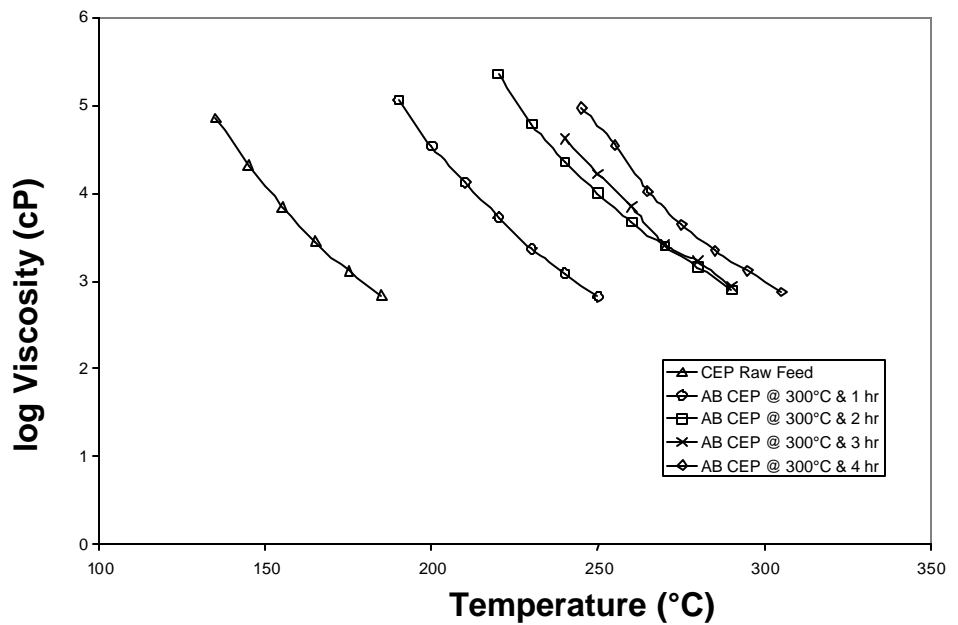


Figure 135. Temperature Dependence of Viscosity for Synthetic Coal-extract Pitch (CEP) at 300°C.

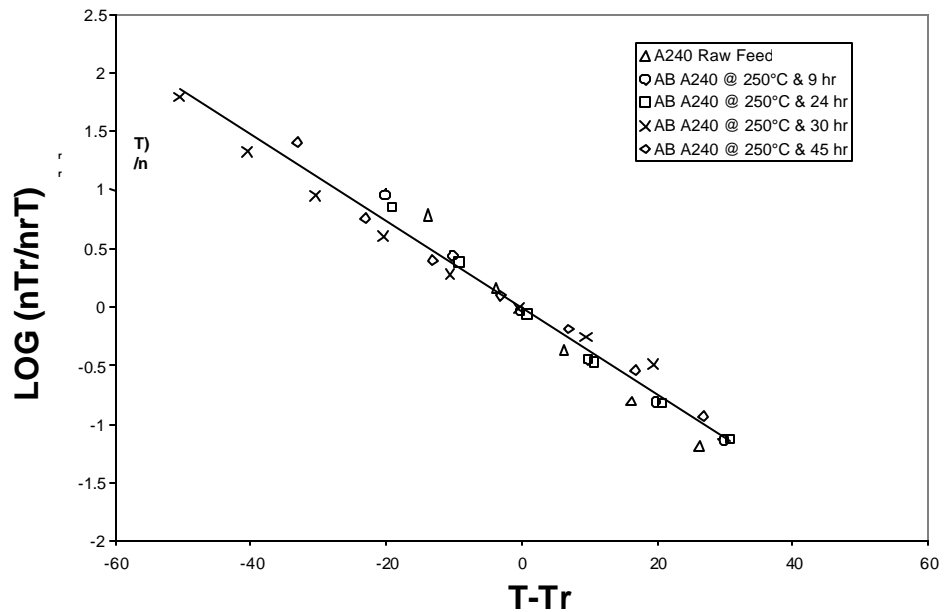


Figure 136. WFL Model of A240 Petroleum Pitch at 250°C.

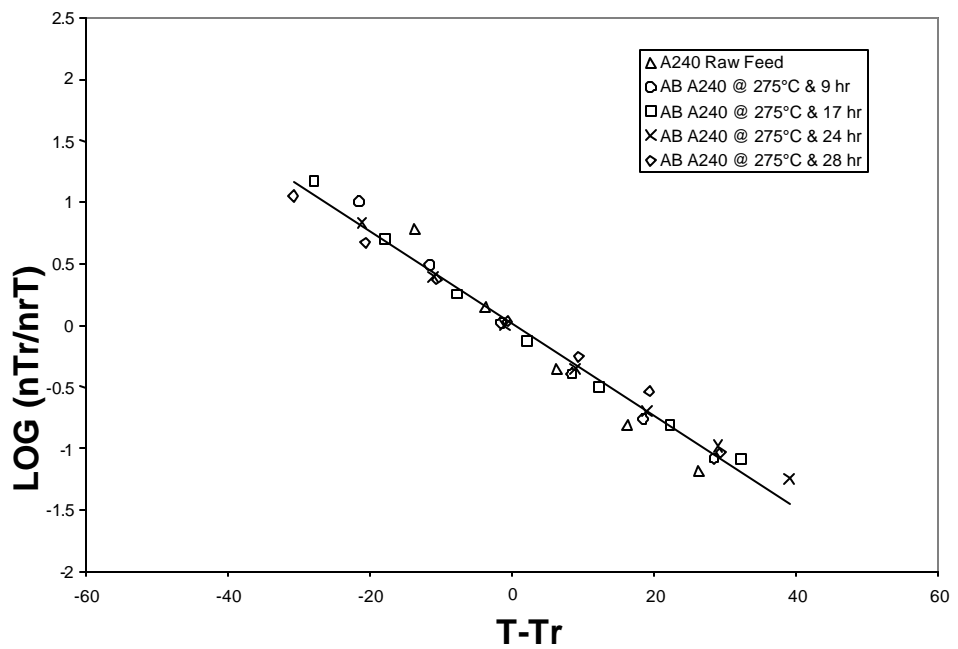


Figure 137. WFL Model of A240 Petroleum Pitch at 275°C.

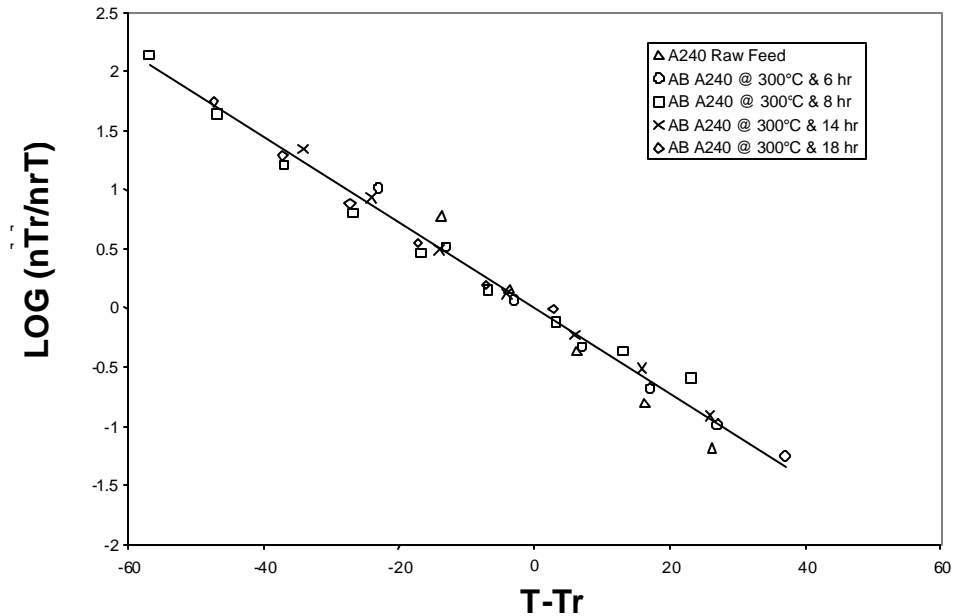


Figure 138. WFL Model of A240 Petroleum Pitch at 300°C.

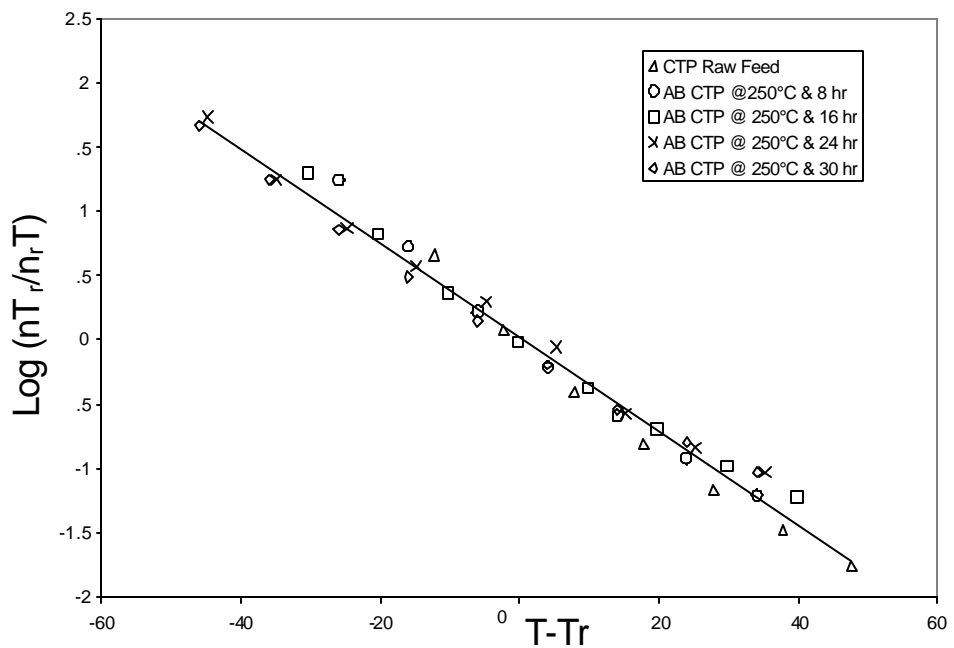


Figure 139. WFL Model of Koppers Coal-tar Pitch (CTP) at 250°C.

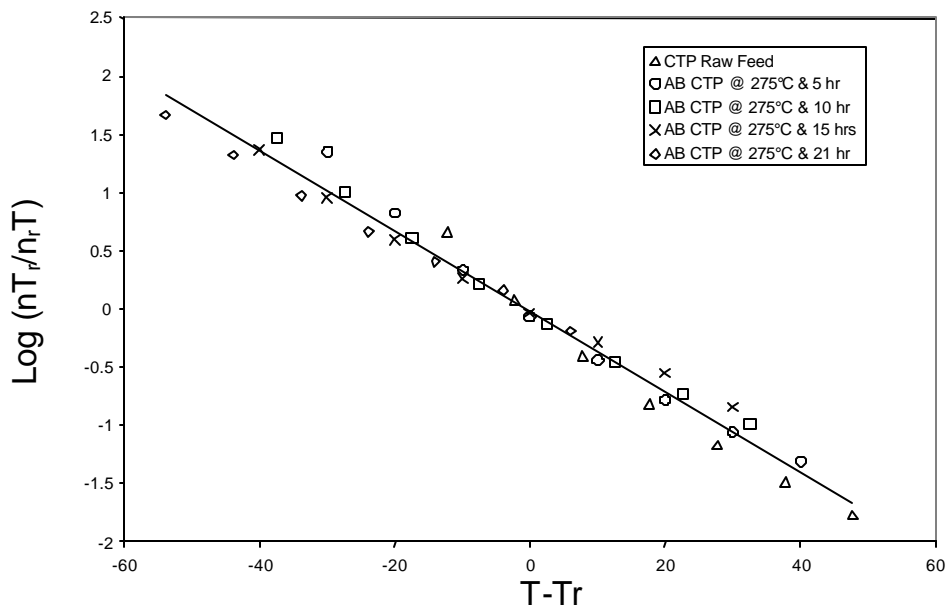


Figure 140. WFL Model of Koppers Coal-tar Pitch (CTP) at 275°C.

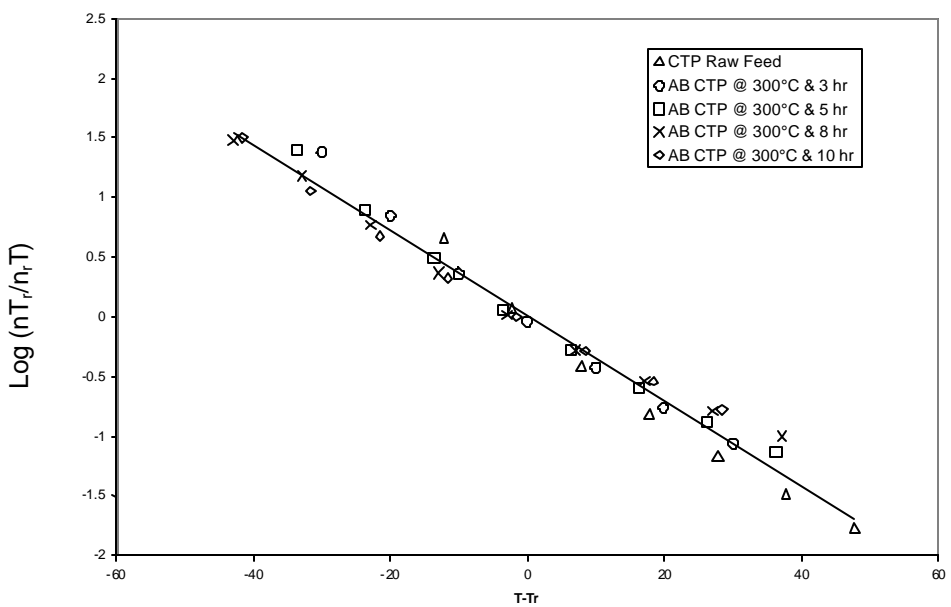


Figure 141. WFL Model of Koppers Coal-tar Pitch (CTP) at 300°C.

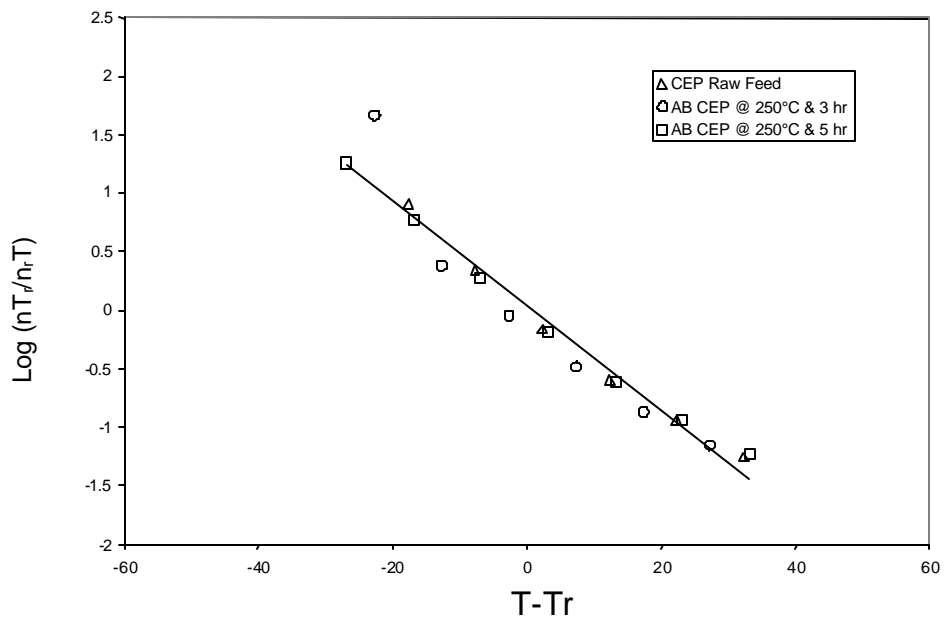


Figure 142. WFL Model of Coal-extract Pitch (CTP) at 250°C.

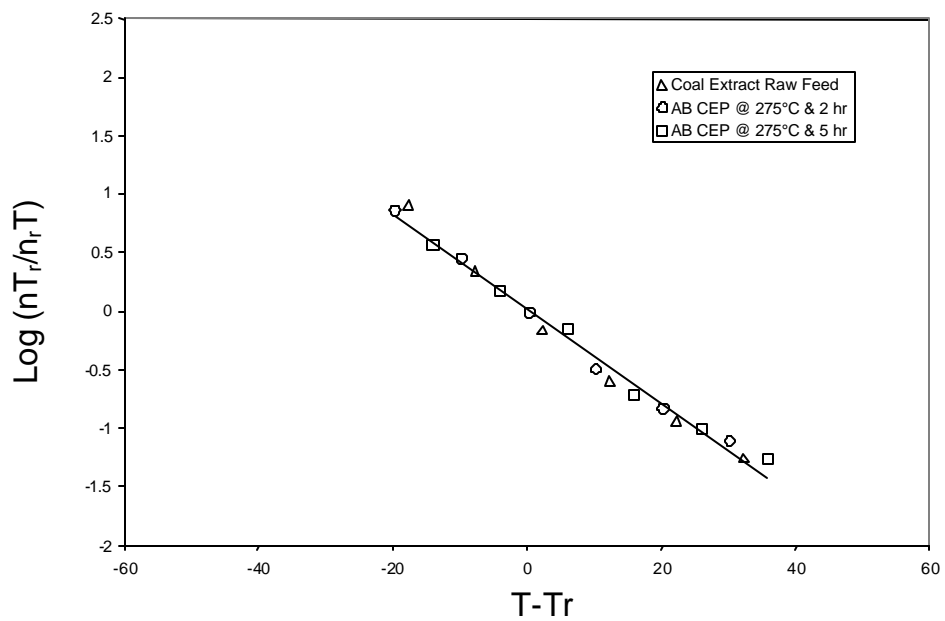


Figure 143. WFL Model of Coal-extract Pitch (CTP) at 275°C.

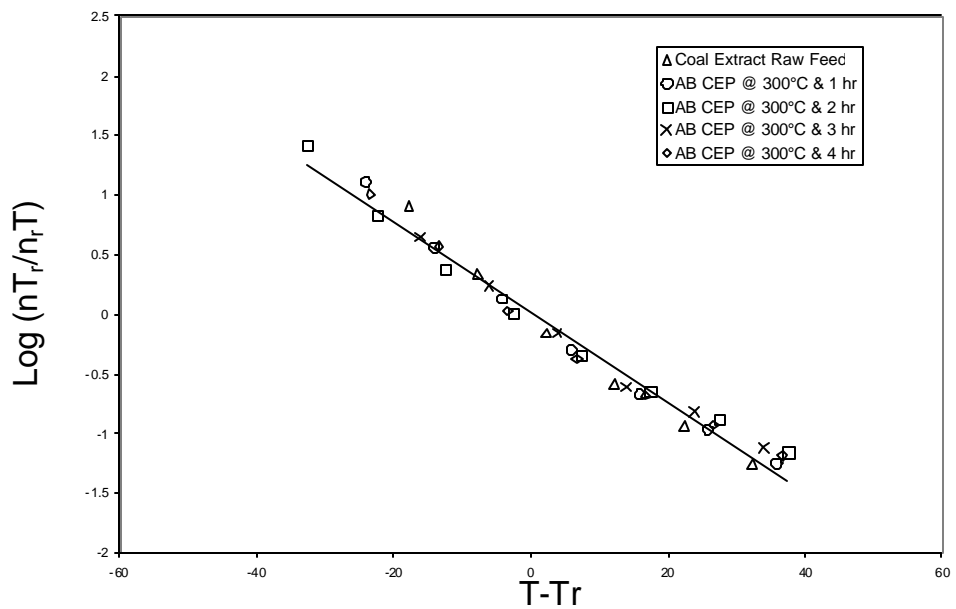


Figure 144. WFL Model of Coal-extract Pitch (CTP) at 300°C.

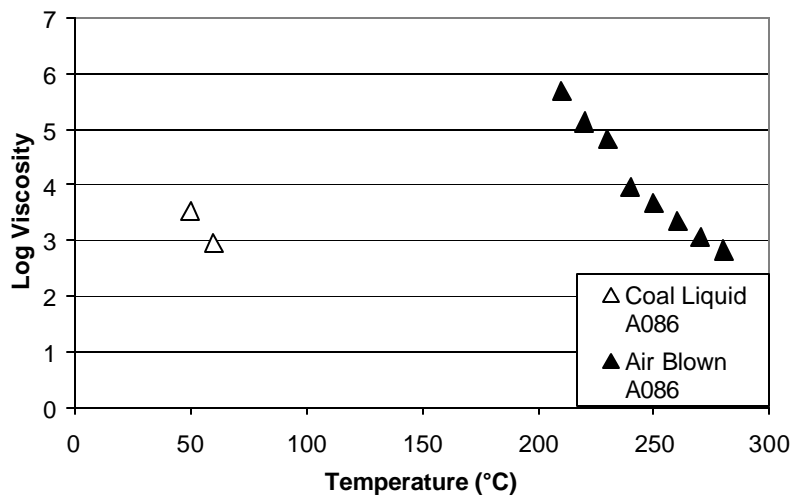


Figure 145. Viscosity Vs Temperature for Air-Blown Coal Digest A086.

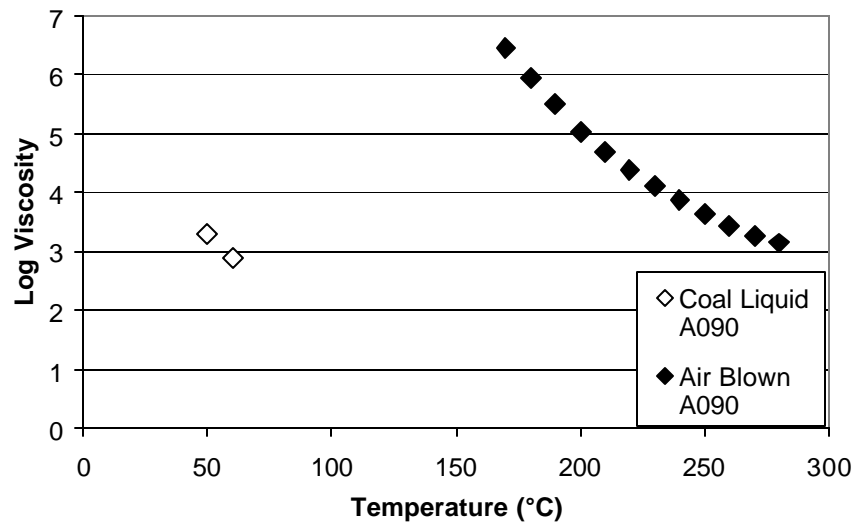


Figure 146. Viscosity Vs Temperature for Air-Blown Coal Digest A090.

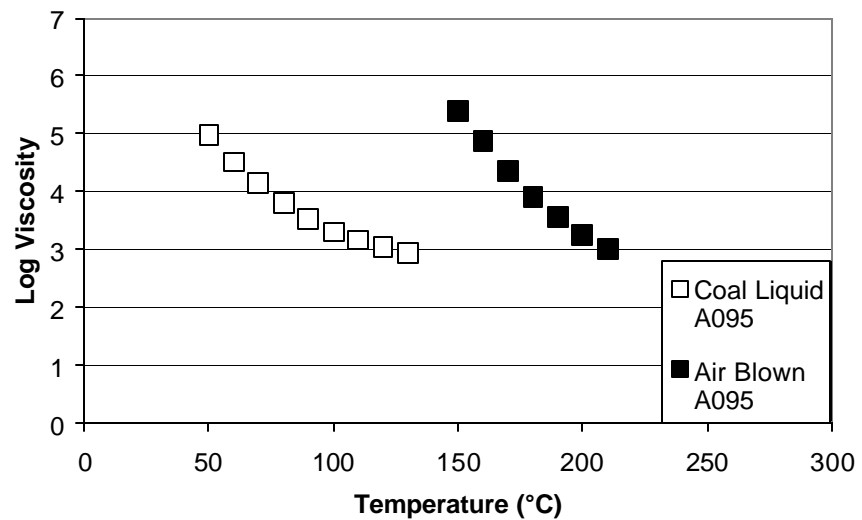


Figure 147. Viscosity Vs Temperature for Air-Blown Coal Digest A095.

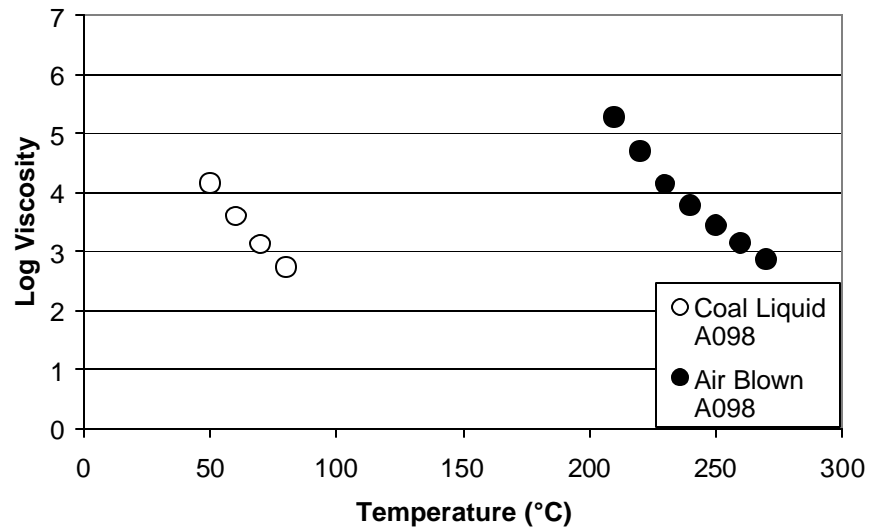


Figure 148. Viscosity Vs Temperature for Air-Blown Coal Digest A098.

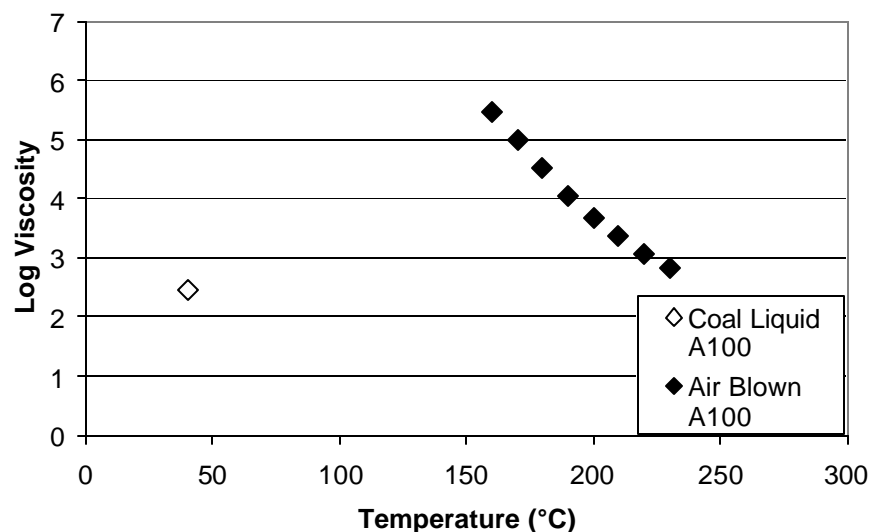


Figure 149. Viscosity Vs Temperature for Air-Blown Coal Digest A100.

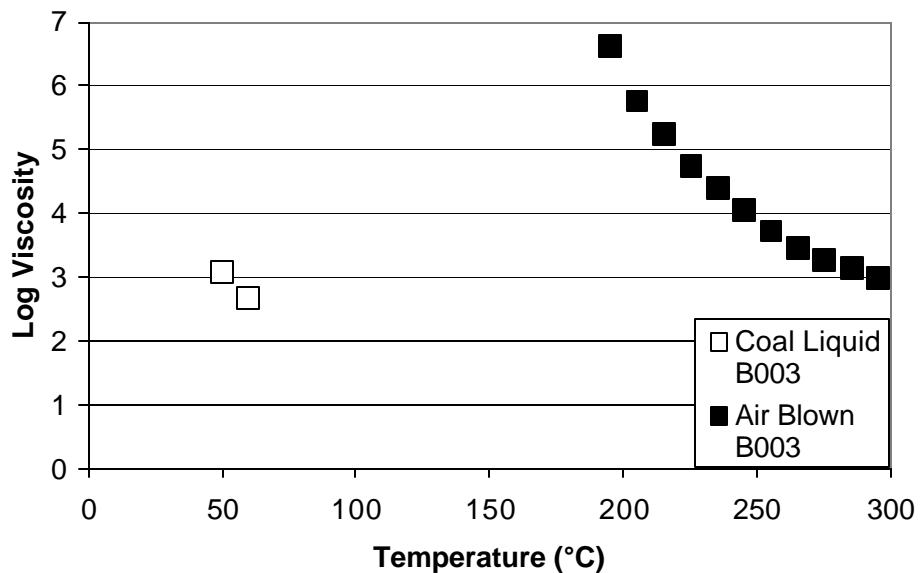


Figure 150. Viscosity Vs Temperature for Air-Blown Coal Digest B003.

4.3.10 Effect of Air Blowing on Pyridine Insoluble Content

Without air blowing, the feed pitches were close to 100% soluble in pyridine, except for the coal-tar pitch with a pyridine insoluble content (PI) of about 11.5 percent. After heat treatment with air, the PI content of all three pitches increased. The PI content of the petroleum pitch continued to increase as treatment time increased for each temperature.

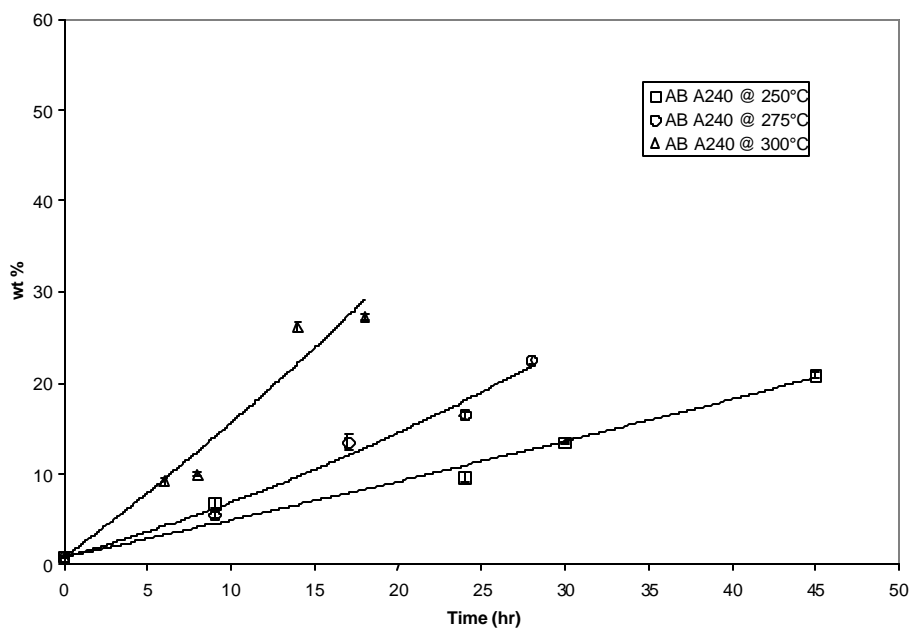


Figure 151. Pyridine Insoluble Content of A240 Petroleum Pitch.

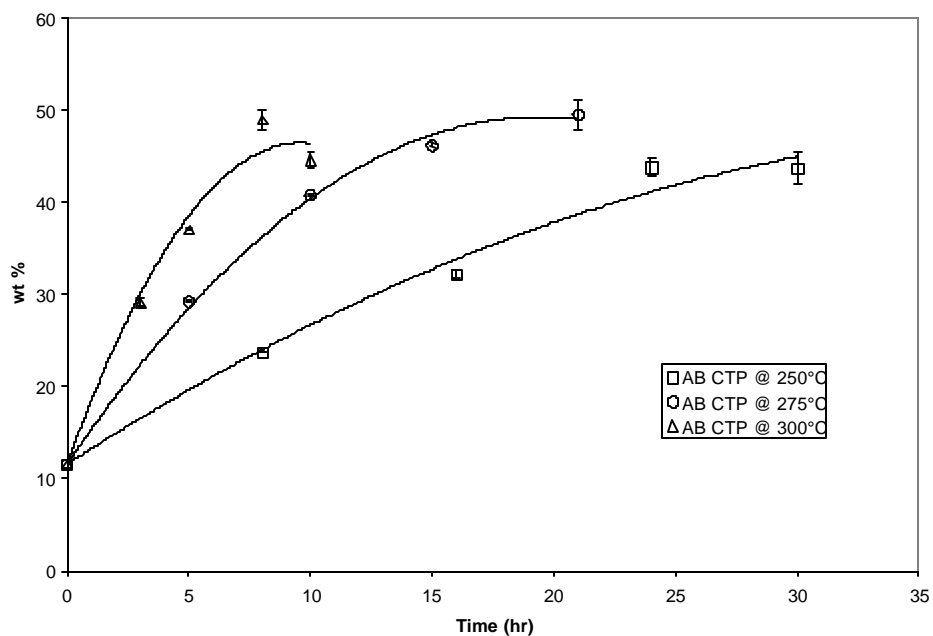


Figure 152. Pyridine Insoluble Content of Koppers Coal-tar Pitch.

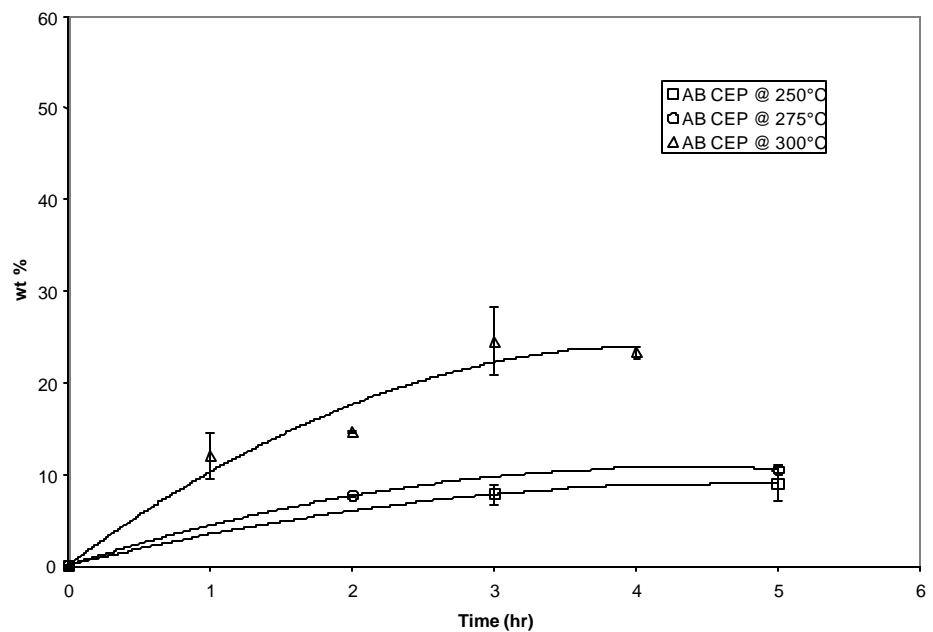


Figure 153. Pyridine Insoluble Content of Synthetic Coal-extract Pitch.

4.3.11 Air Blowing Effects on Toluene Solubility

Air blowing also affects the toluene solubility of the digests. The amount of toluene insoluble material in the air-blown digests doubled in most cases and tripled in

one case. This indicates the amount of higher molecular weight species present in the digest, and is a result of lower molecular weight species cross-linking during the air-blowing, or from the removal of light molecules which are stripped off during the air-blowing, thus concentrating the toluene insolubles. Consequently, this is followed by a reduction in the volatile material present in the digest. This is especially favorable for coke feedstocks, which ideally have a high percentage of fixed carbon.

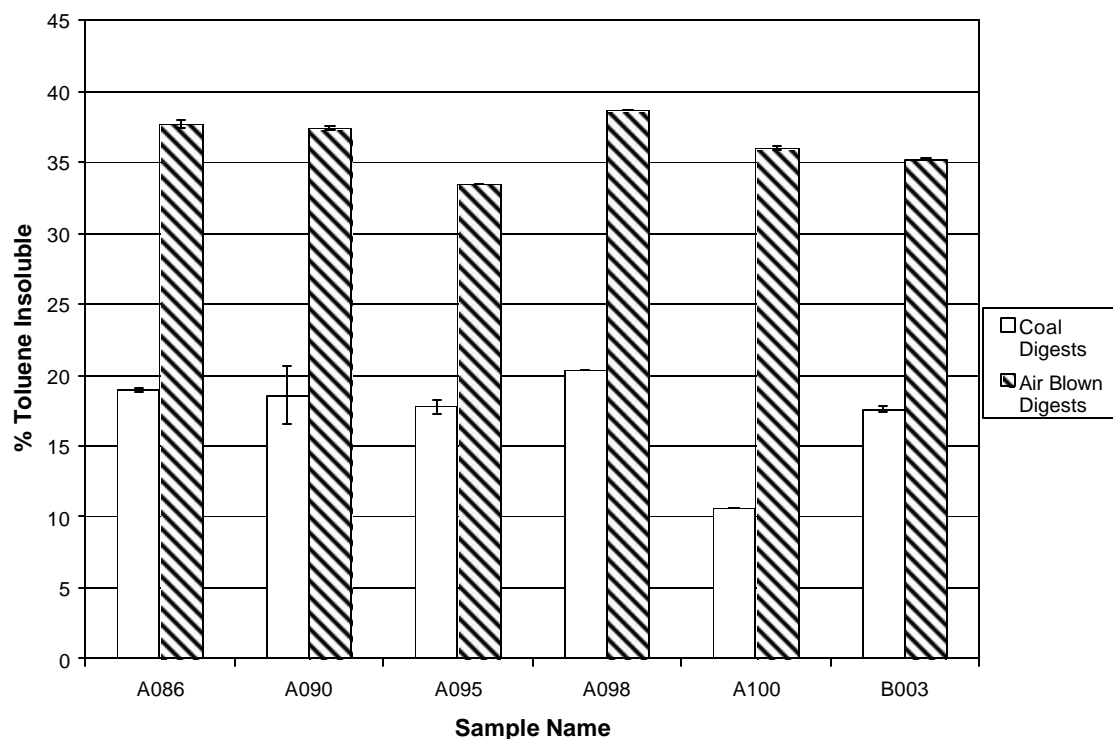
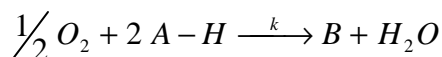


Figure 154. Toluene Insolubles of Coal Digests.

4.3.12 Kinetic Modeling of Chemical Changes due to Air Blowing

Preliminary kinetic modeling of the pitches being air-blown was based on a simplified chemical equation shown below.



This equation shows what may have occurred during the heat treatment of the pitches when air was blown into the pitch. Notice in the equation that the oxygen from the air is not incorporated in the end product of the air-blown pitch, B. Instead the oxygen combines with the hydrogen from the aromatic pitch molecule, A-H, and forms water which exits the reactor in the form of steam. From the above equation, a kinetic equation can be determined assuming second order kinetics,

$$-\frac{d[A-H]}{dt} = k[A-H]^2$$

This equation was integrated from PI wt % A_0 to A and from time 0 hr to each treatment time. Through integration and simplification the equation becomes:

$$\frac{1}{[A]} = kt + \frac{1}{[A_0]}$$

The graphs of this equation for each of the three pitches can be seen in previous figures. The slopes of these lines were calculated for the values of the rate constant, k , at each temperature. From the Arrhenius equation shown below, the activation energy for each pitch can be determined using the rate constants calculated above,

$$\frac{d[\ln k]}{dT} = \frac{Ea}{RT^2}$$

The equation above was integrated and rearranged to produce

$$\ln k = -\frac{Ea}{R} \left(\frac{1}{T} \right) + \ln K$$

The values for the natural log of the rate constants were plotted on a graph versus the inverse temperature in Kelvin to calculate the activation energies for each pitch. Plots for each pitch can be seen in the following figures while the values of the activation energies can be seen in the table below.

Table 38. Activation Energies for the Air-blowing of Three Types of Pitches.

	ln K	K (1/hr)	- Ea/R	Ea (kcal/mole)
A240	10.2	27694.8	-8133.6	16.2
CTP	10.4	32305.7	-7559.8	15.0
CEP	11.8	134995.9	-8271.2	16.4

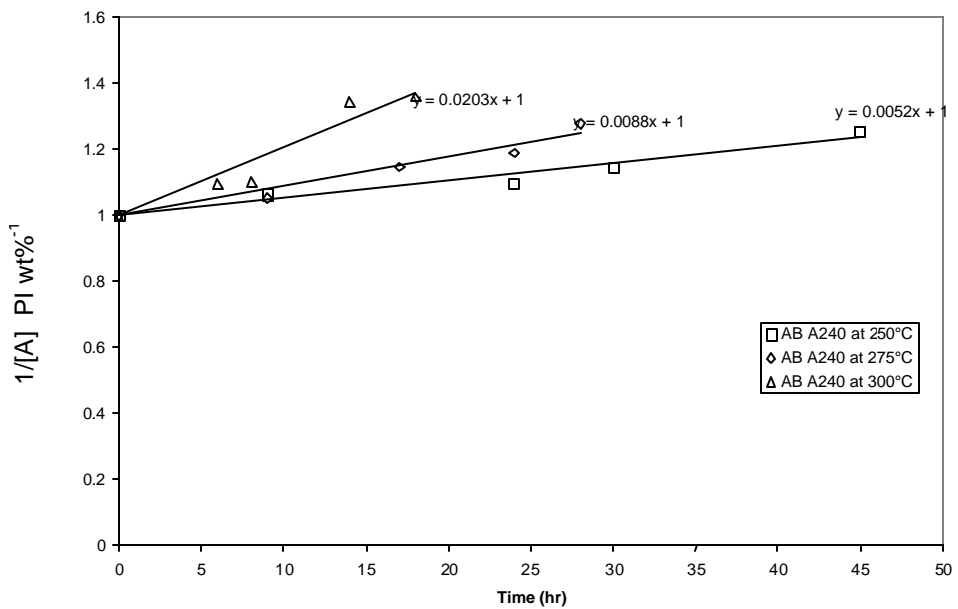


Figure 155. Rate Constant Data for the Air-blowing Kinetics of Petroleum Pitch A240.

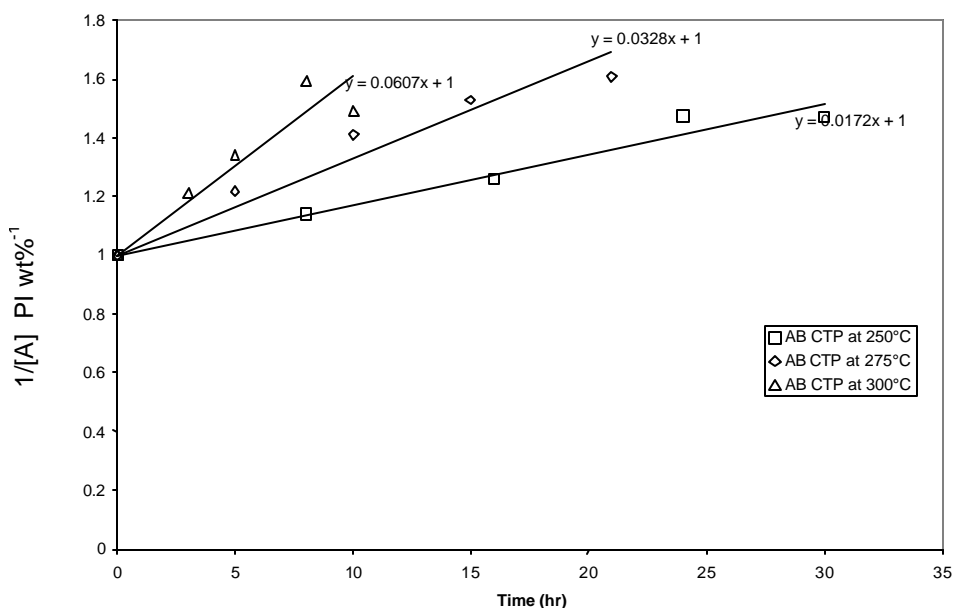


Figure 156. Rate Constant Data for the Air-blowing Kinetics of Coal-tar Pitch.

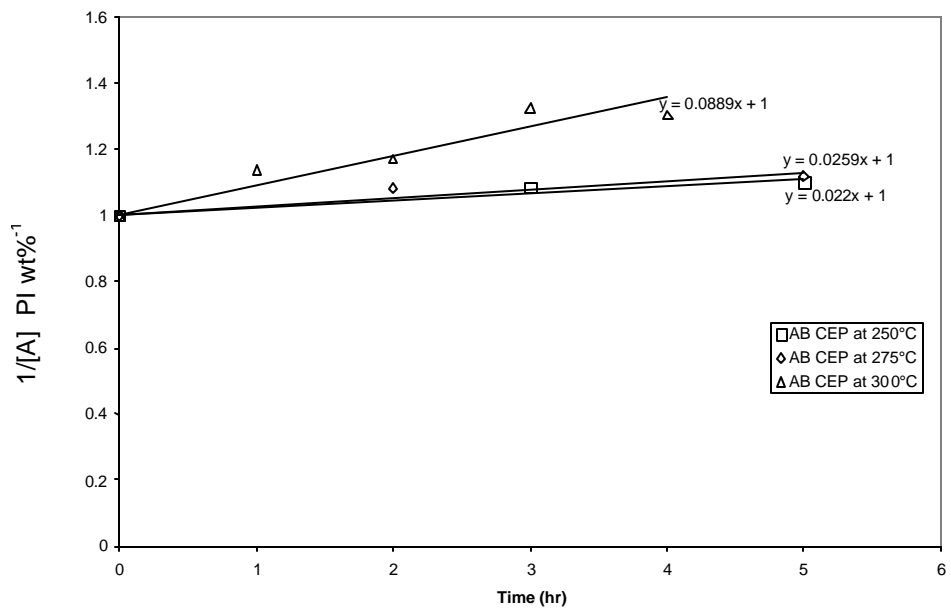


Figure 157. Rate Constant dData for the Air-blowing Kinetics of Coal-extract Pitch.

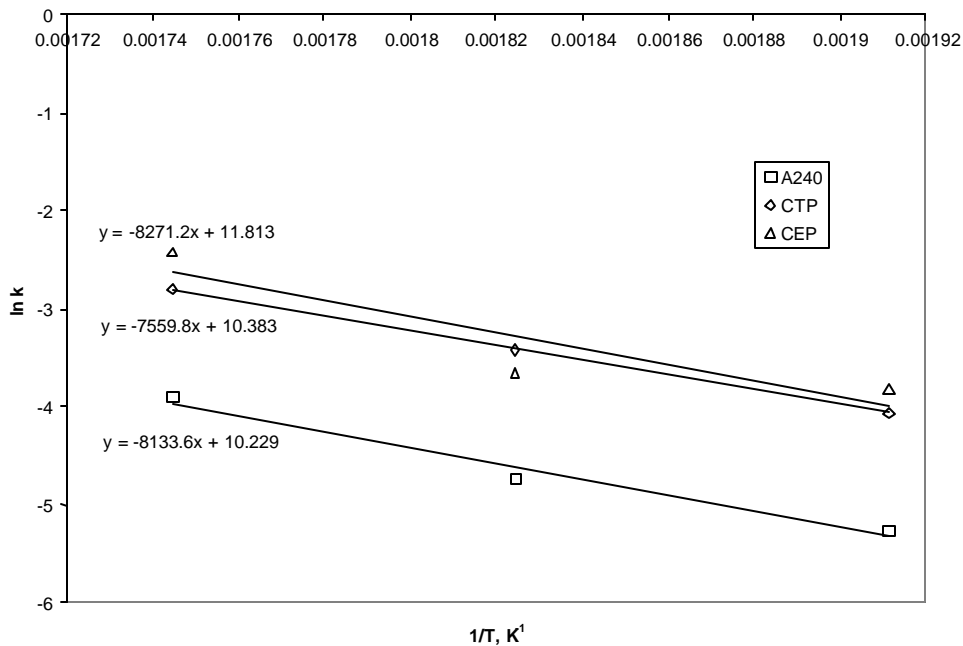


Figure 158. Activation Energies for the Air-blowing of Petroleum Pitch A240, Coal-tar Pitch, and Coal-extract Pitch.

4.3.10 Thermogravimetric Studies on Feed and Air-Blown Pitches

A Thermogravimetric Analyzer (TGA) was used to characterize feed and air-blown pitches. The figures below show the weight loss of the A240 feed and air-blown pitches at various durations for the temperatures of 250°C, 275°C, and 300°C. In these plots, it can be seen that the weight loss of the pitches significantly increases from 250°C until about 550°C. After 550°C, the rate of weight loss becomes asymptotic. From this, it can be concluded that majority of the volatile content was removed before the temperature reaches 550°C.

The figures below show the weight loss of the coal-tar pitches, air-blown at various times, for the temperatures of 250°C, 275°C, and 300°C. In this plot, it can be seen that the weight loss of the pitches significantly increases from 300°C until about 575°C. After 575°C, the rate of weight loss becomes asymptotic. From this, it can be concluded that majority of the volatile content was removed before the temperature reaches 575°C.

The weight loss of the coal-extract pitches air-blown at the various times for the temperatures of 250°C, 275°C, and 300°C is shown below. In this plot, it can be seen that the weight loss of the pitches significantly increases from 200°C until about 525°C. After 525°C, the rate of weight loss becomes asymptotic. From this it can be concluded that majority of the volatile content was removed before the temperature reaches 525°C.

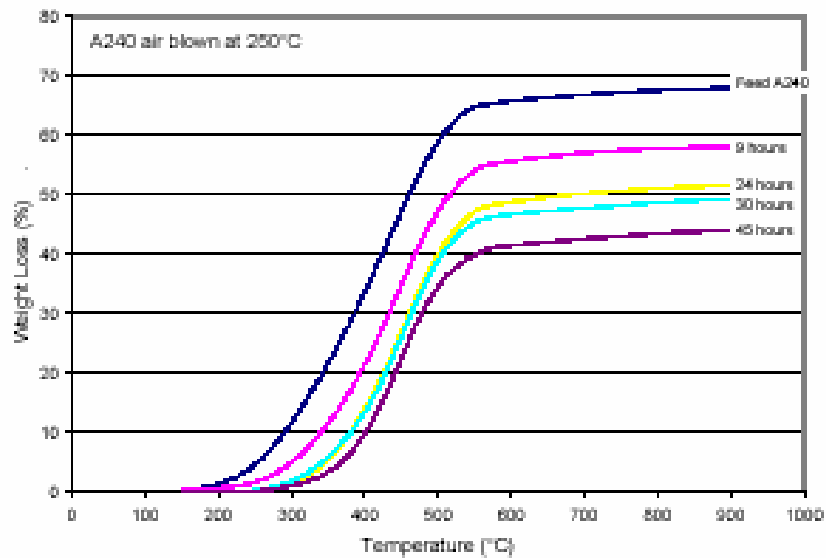


Figure 159. Petroleum Pitch Weight Loss From Air Blowing at 250°C.

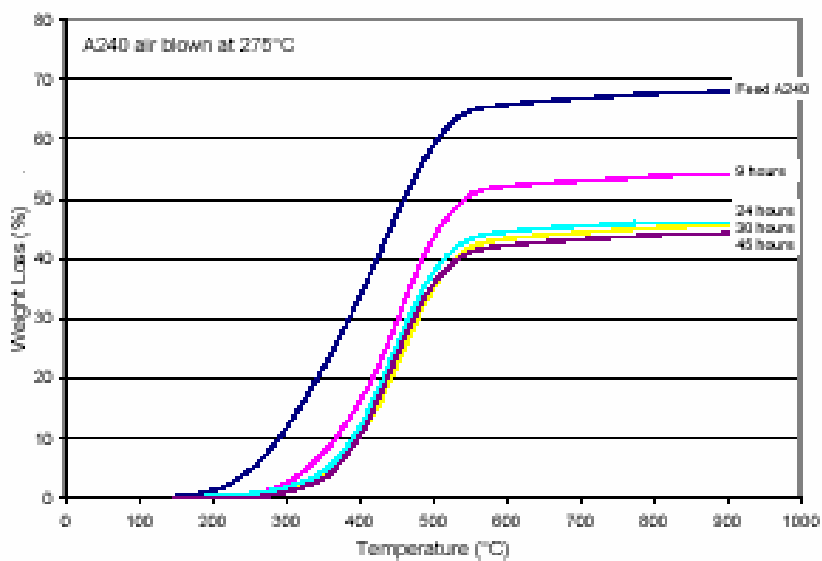


Figure 160. Petroleum Pitch Weight Loss From Air Blowing at 275°C.

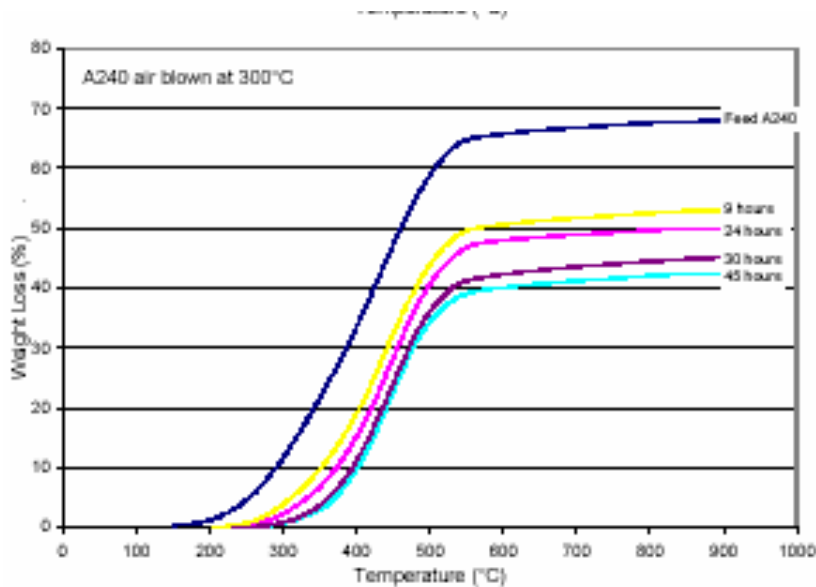


Figure 161. Petroleum Pitch Weight Loss From Air Blowing at 300°C.

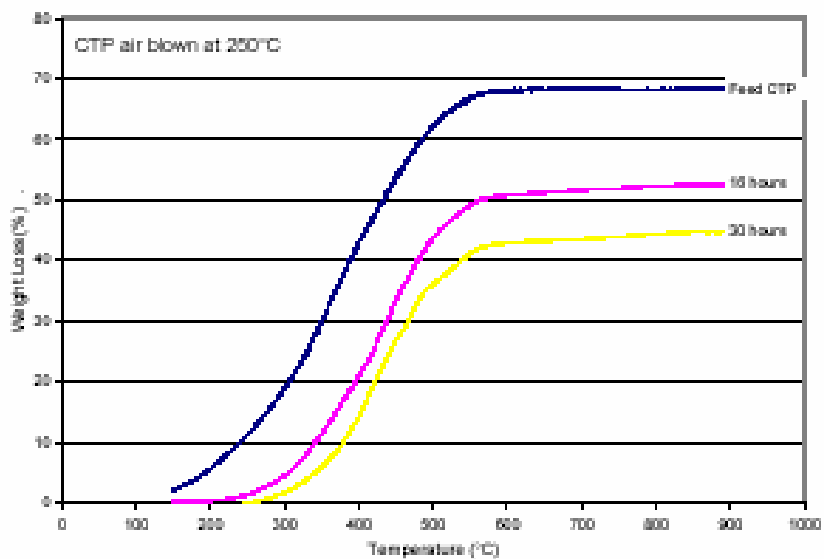


Figure 162. Coal Tar Pitch Weight Loss From Air Blowing at 250°C.

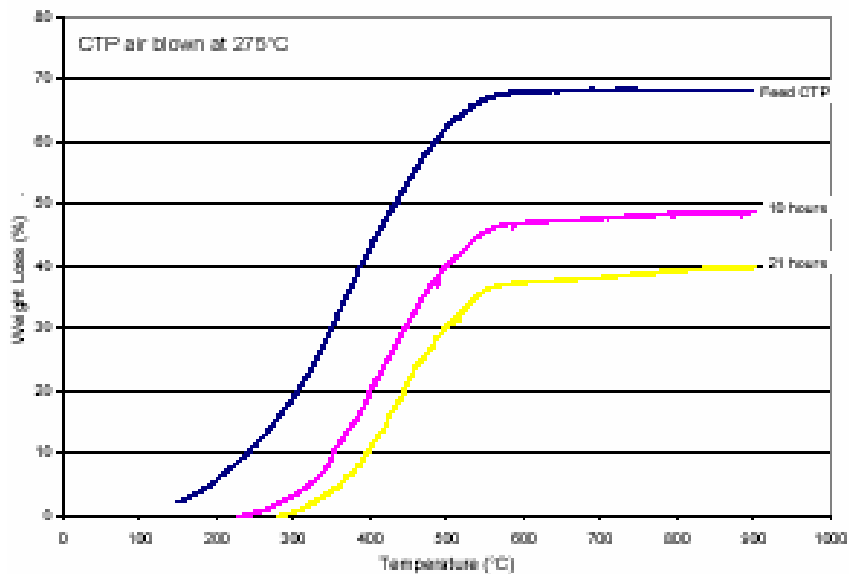


Figure 163. Coal Tar Pitch Weight Loss From Air Blowing at 275°C.

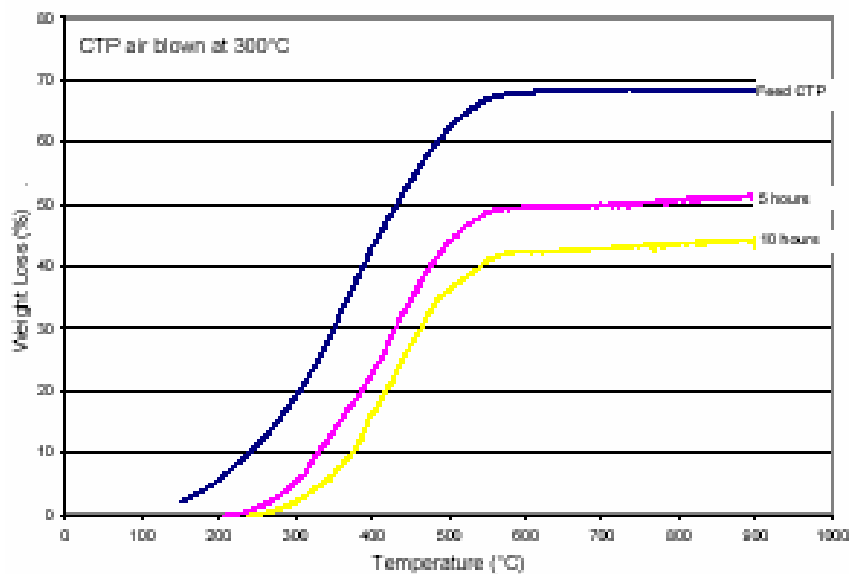


Figure 164. Coal Tar Pitch Weight Loss From Air Blowing at 300°C.

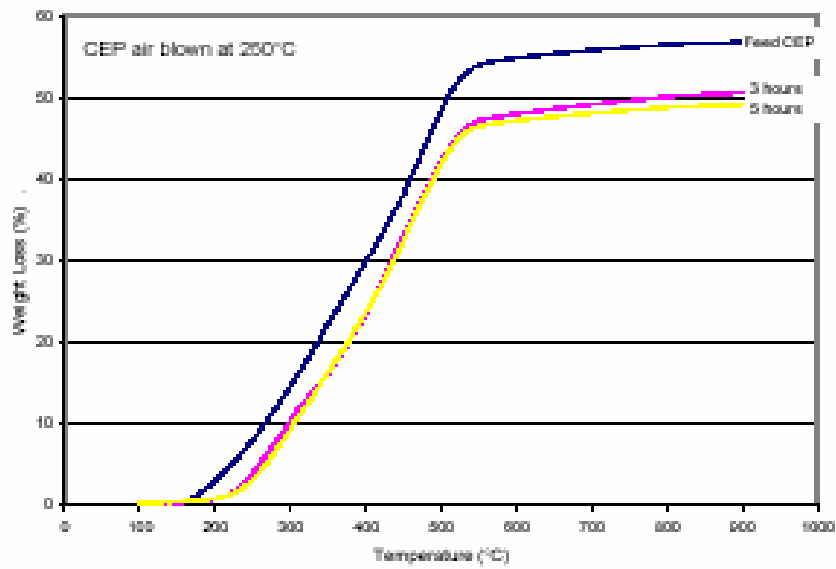


Figure 165. Coal Extract Weight Loss from Air Blowing at 250°C.

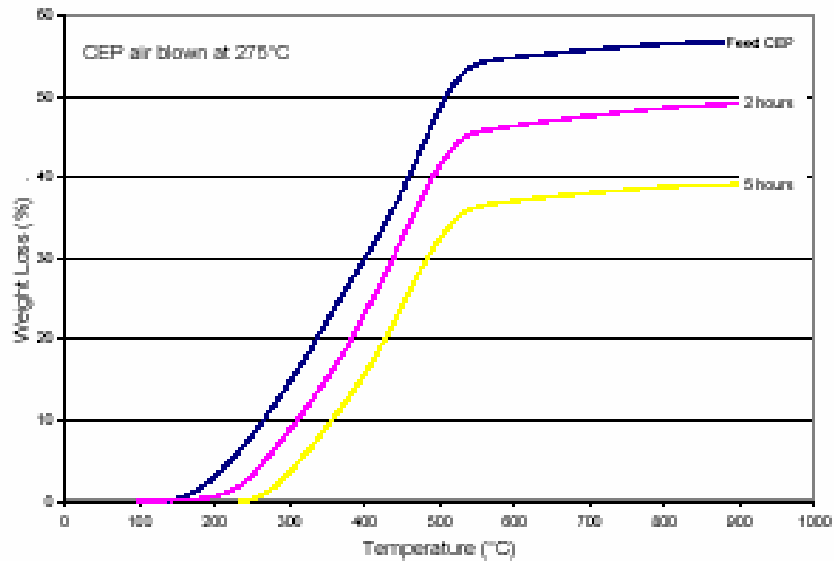


Figure 166. Coal Extract Weight Loss from Air Blowing at 275°C.

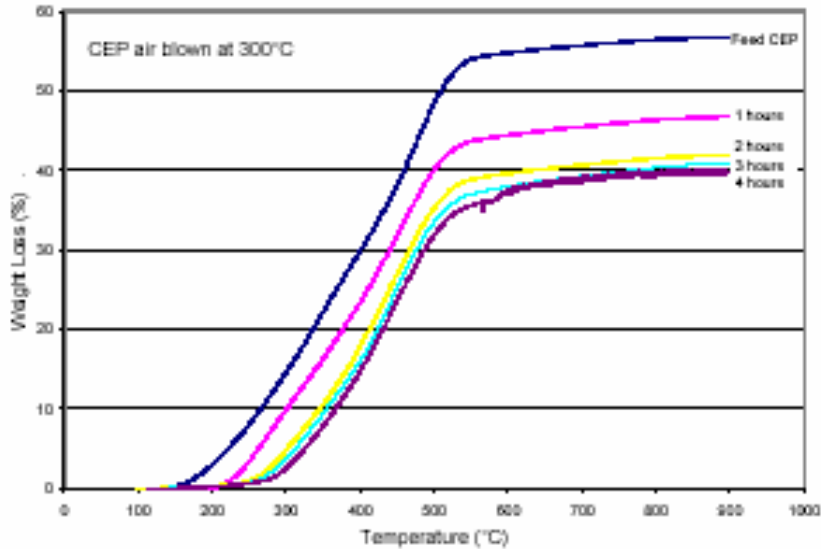


Figure 167. Coal Extract Weight Loss From Air Blowing at 300°C.

Another analysis of TGA data shows the volatile fraction remaining in the pitch. Then figures below illustrate the volatile fraction of the pitch while heated from room temperature to 900°C. The volatile fraction falls off sharply at 250°C, and approaches zero at a lesser rate at 550°C in all of the trials, implying a similar reaction mechanism in all cases.

The volatile fraction remaining in the coal-tar pitch after being heated from room temperature to 900°C is also shown below. These show sharp declines in the amount of volatile matter from approximately 300°C of the heating process up to about 575°C. After 575°C, the volatile fraction of the pitches approaches zero. All experiments with coal-tar pitch show these characteristics, indicating a reaction mechanism independent of time or temperature.

The volatile fractions remaining in the coal-extract pitch after being heated from room temperature to 900°C are also shown below. These figures show a sharp decline in the amount of volatile matter from approximately 200°C of the heating process up to approximately 525°C. After 525°C, the volatile fraction approaches zero. Again, these characteristics are present in all experimental runs of coal-extract pitch, indicating that this pitch also has an independent reaction mechanism. These results do not, however, imply that the same mechanism is operating on these materials, but that each material has a similar mechanism with regard to the loss of volatiles.

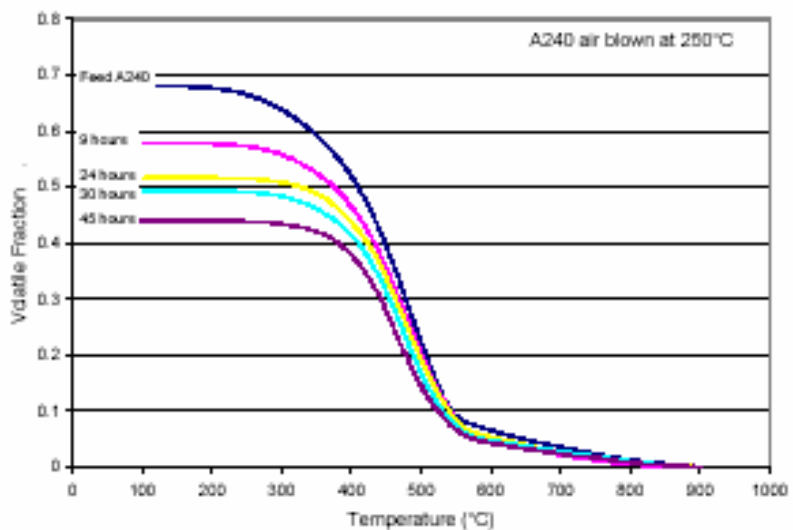


Figure 168. Volatile Fraction Remaining for AB A240 at 250°C.

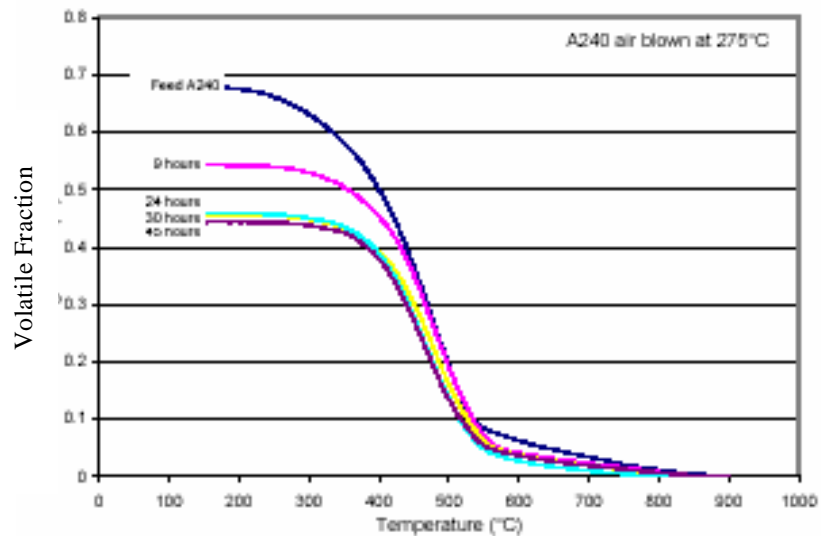


Figure 169. Volatile Fraction Remaining for AB A240 at 275°C.

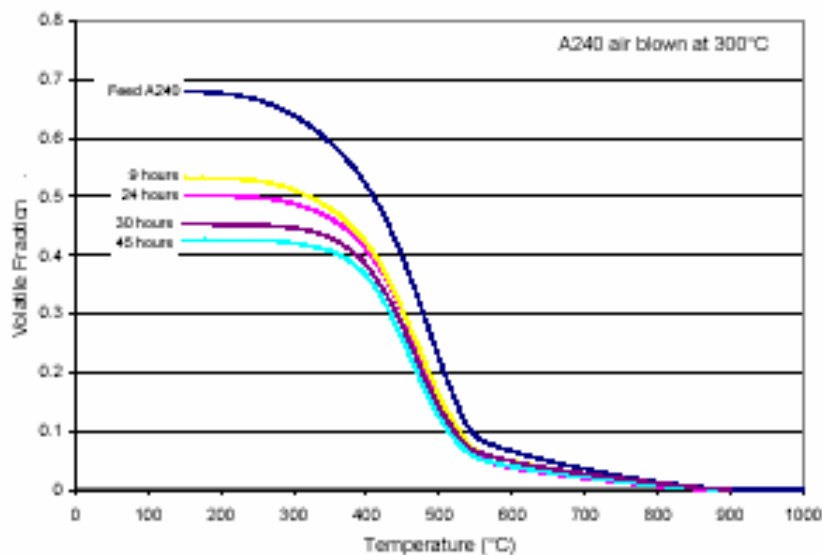


Figure 170. Volatile Fraction Remaining for AB A240 at 300°C.

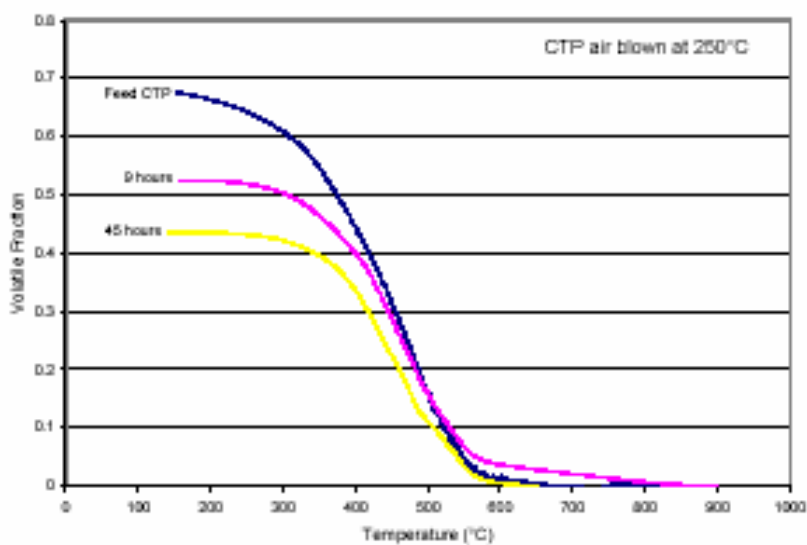


Figure 171. Volatile Fraction Remaining for AB CTP at 250°C.

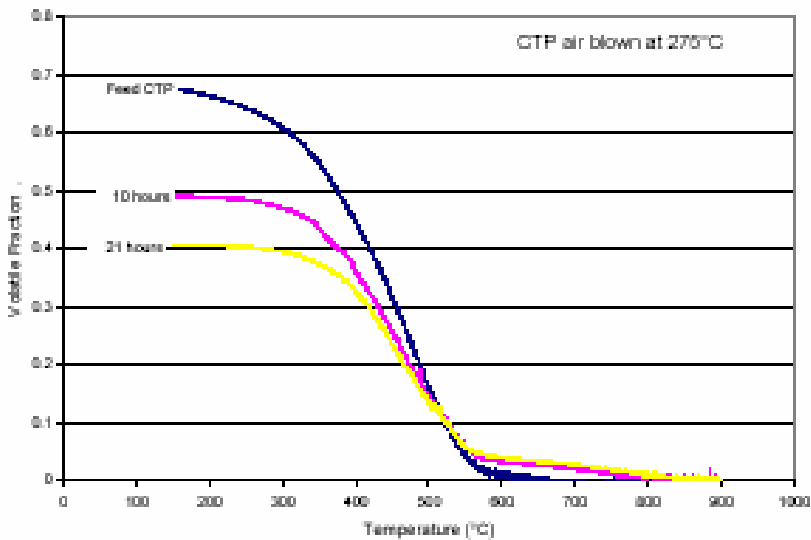


Figure 172. Volatile Fraction Remaining for AB CTP at 275°C.

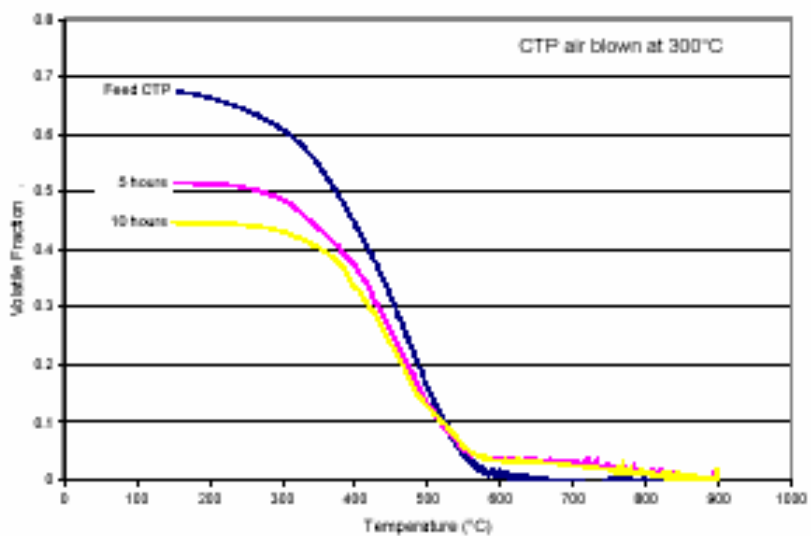


Figure 173. Volatile Fraction Remaining for AB CTP at 300°C.

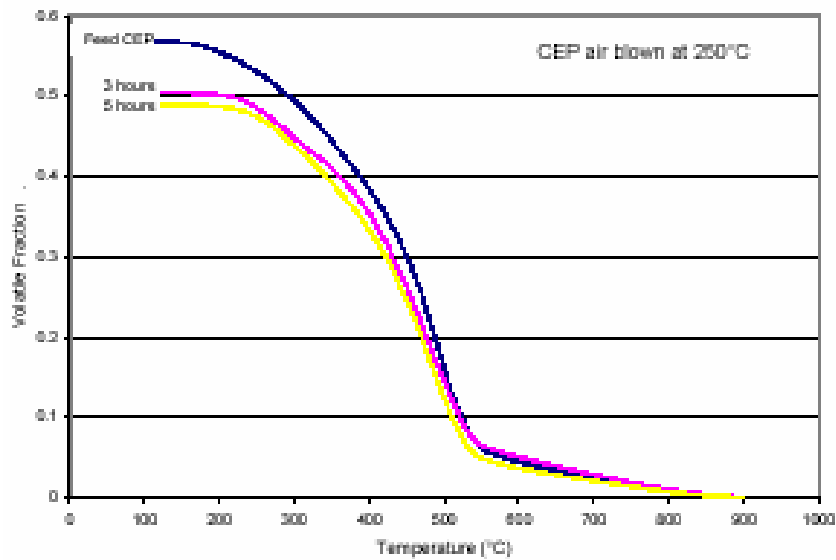


Figure 174. Volatile Fraction for AB Coal Extract at 250°C.

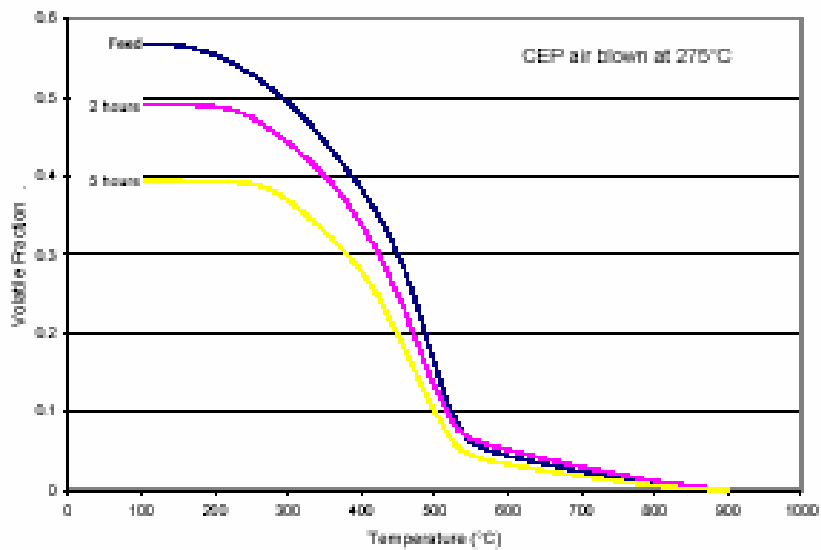


Figure 175. Volatile Fraction for AB Coal Extract at 275°C.

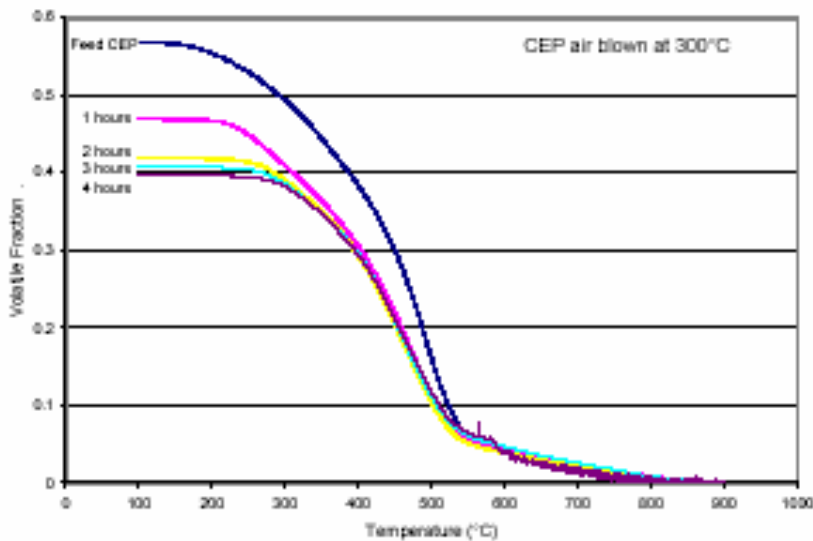


Figure 176. Volatile Fraction for AB Coal Extract at 300°C.

These results concur with the literature reviewed and show that air-blowing is an effective way to polymerize the smaller molecular chains in the pitches. The increase the overall molecular weight results in less volatility. Also, since the volatile fraction plots have consistent characteristics, it can be inferred that a similar chemistry or mechanism is associated with the air-blowing process for each individual feed.

4.3.11 Elemental Analysis and Van Krevelen Plots

An elemental analysis on the pitches can provide insight into the mechanisms of air-blowing. The carbon-to-hydrogen (C/H) atomic ratio increased for the petroleum pitch, while the higher treatment temperatures had a greater increase at a significantly less time, as seen in the figure below. The trends suggest two possible mechanisms. Either an increase in carbon content or a decrease in hydrogen content occurred, resulting in an increase in the C/H atomic ratio. However, the literature suggests the latter effect is more probable.

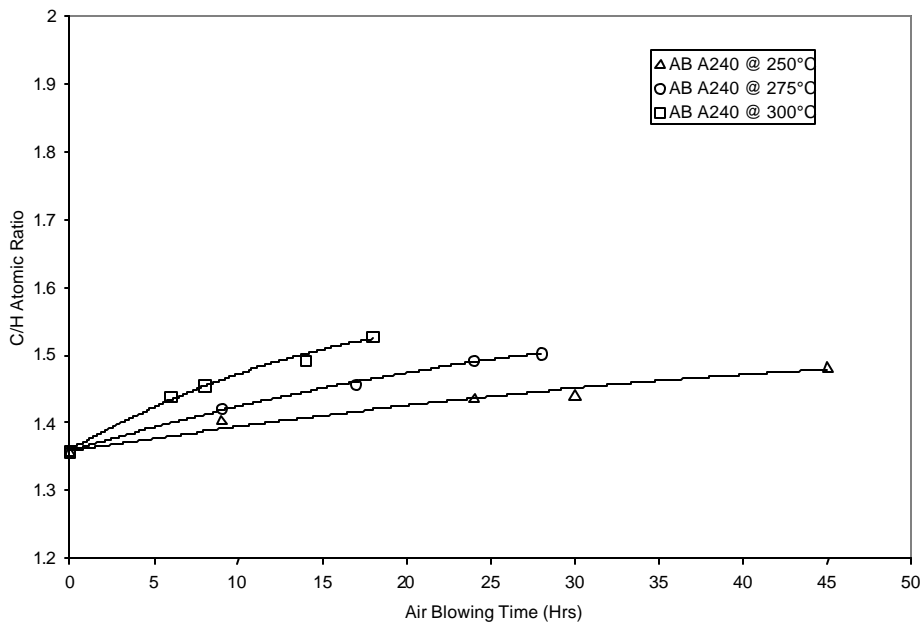


Figure 177. C-H Atomic Ratio vs AB Time A240.

As with the petroleum pitch, the carbon to hydrogen (C/H) atomic ratio increased in the coal-tar pitch, as seen in the figure below. The coal-tar pitch also showed, at higher treatment temperatures, an increase in C/H in significantly less time. The largest increase in C/H occurred in the 21 hour run of air blowing at 275°C and had a value of approximately 0.63%. This indicates that while air blowing does increase the ratio of C/H, the change is small.

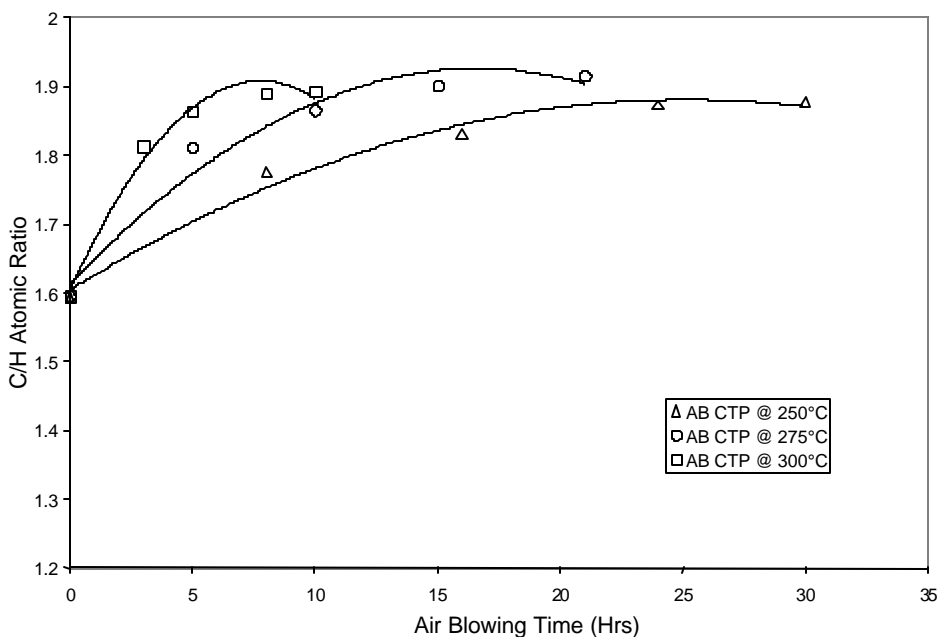


Figure 178. C-H Atomic Ratio vs. AB Time CTP.

The carbon to hydrogen (C/H) atomic ratio also increased in the coal-extract pitch, as can be seen below. The higher treatment temperatures showed an increase in significantly less time. The largest increase in C/H was 0.2%, occurring during the 4 hour experiment at 300°C, indicating that the improvement due to air blowing is slight.

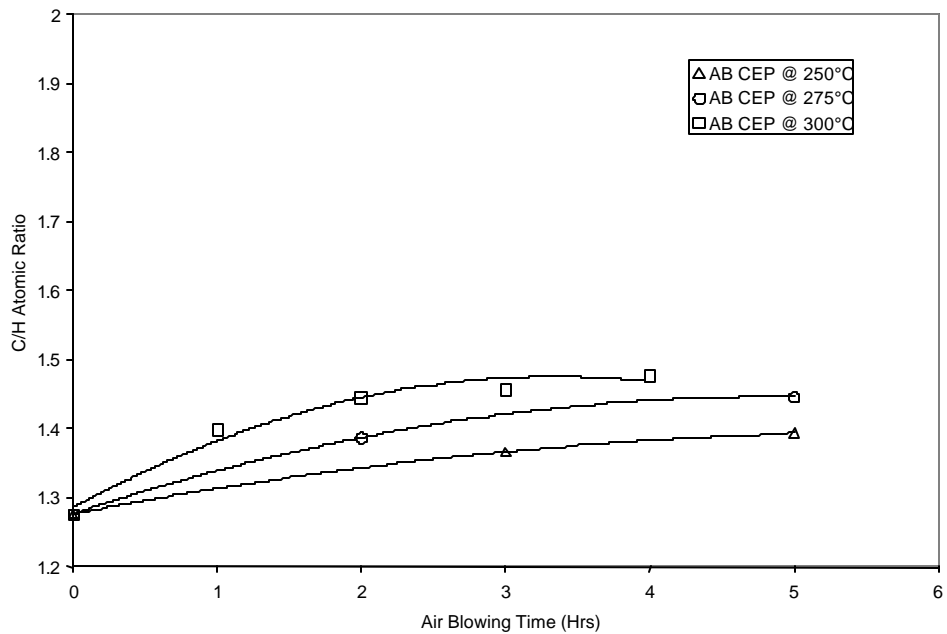


Figure 179. C-H Atomic Ratio Versus Air-blown Time for Coal-extract.

As with the C/H ratio increase in the petroleum pitches, the oxygen content of the pitches increased slightly, as can be seen below. The largest percentage change in oxygen was 0.5%, while the total remained under 1 % oxygen content. This small increase indicated that the air blowing process does not significantly add oxygen to the pitch .

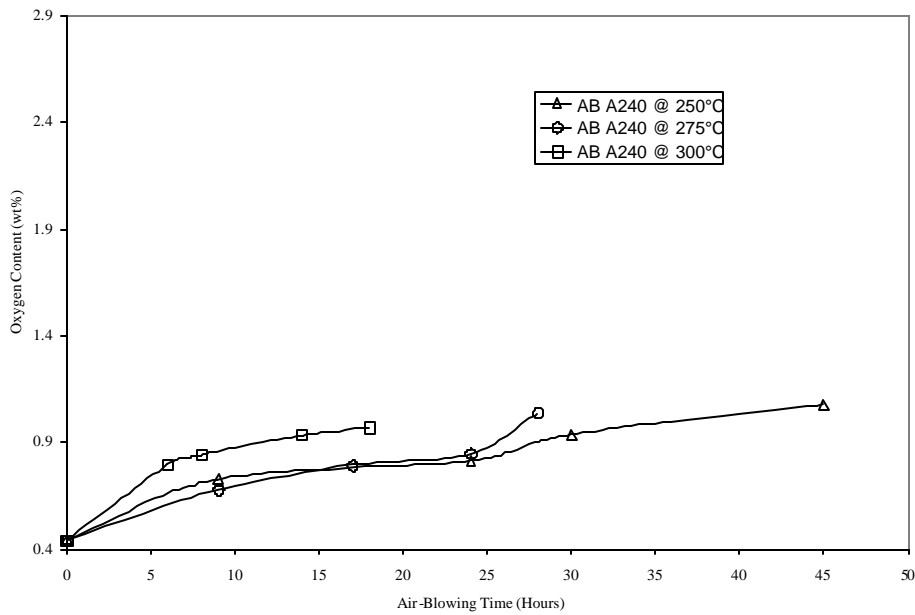


Figure 180. Oxygen Content for Air-blown Petroleum Pitch.

As with the petroleum pitch, the oxygen content in the coal-tar pitch was seen to improve, but only after an initial decrease. The following figure will show that the pitch did not reach the initial oxygen levels, but did regain approximately 0.25% oxygen. These results indicate that air blowing was not a significant source of oxygen for the pitch.

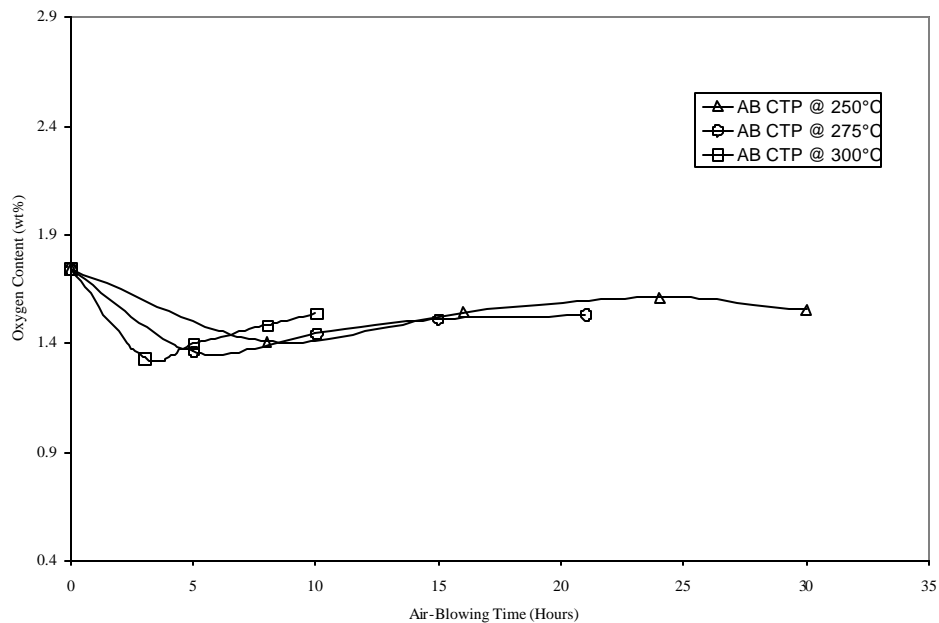


Figure 181. Oxygen Content for Air-blown Coal-tar Pitch.

As seen in the figure below, the oxygen content for coal-extract pitch also decreased. However, there was no subsequent rise in the oxygen level. The loss of

oxygen was approximately 0.1% by weight, further supporting the concept that the air blowing process is not an oxygen source.

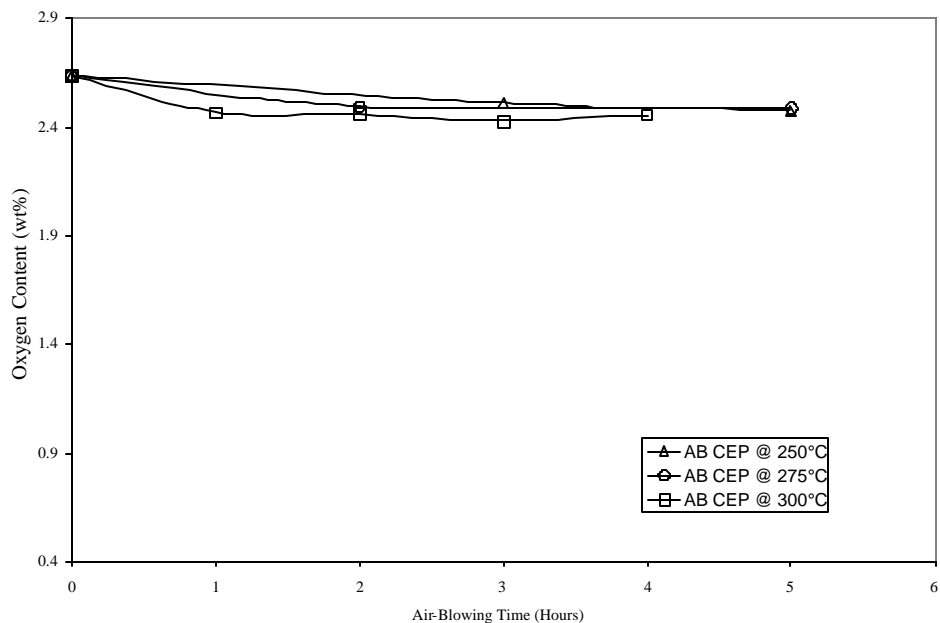


Figure 182. Oxygen Content for Air-blown Coal-extract Pitch.

Van Krevelen plots were constructed to provide insight into the types of mechanisms occurring in the pitch when air-blown. The mechanisms that were employed during the air-blowing process are dehydroxylation, dealkylation, and a combination of both. With the data from the feed pitches and the subsequent air-blown pitches plotted, a mechanism can be predicted for the reaction of each pitch. This will assist in the determination of the mechanisms occurring during the air-blowing of the pitches. A graph of the mechanisms observed in the three pitches can be seen below.

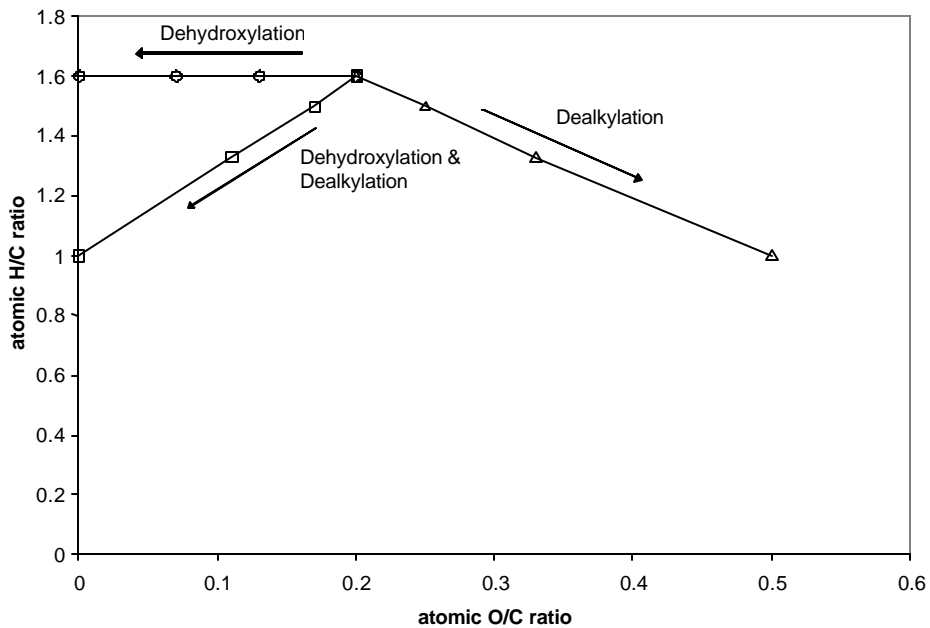


Figure 183. Van Krevelen Plot.

The Van Krevelen plot for the petroleum pitch below shows that a dealkylation type of reaction takes place during the air-blowing of the petroleum pitch.

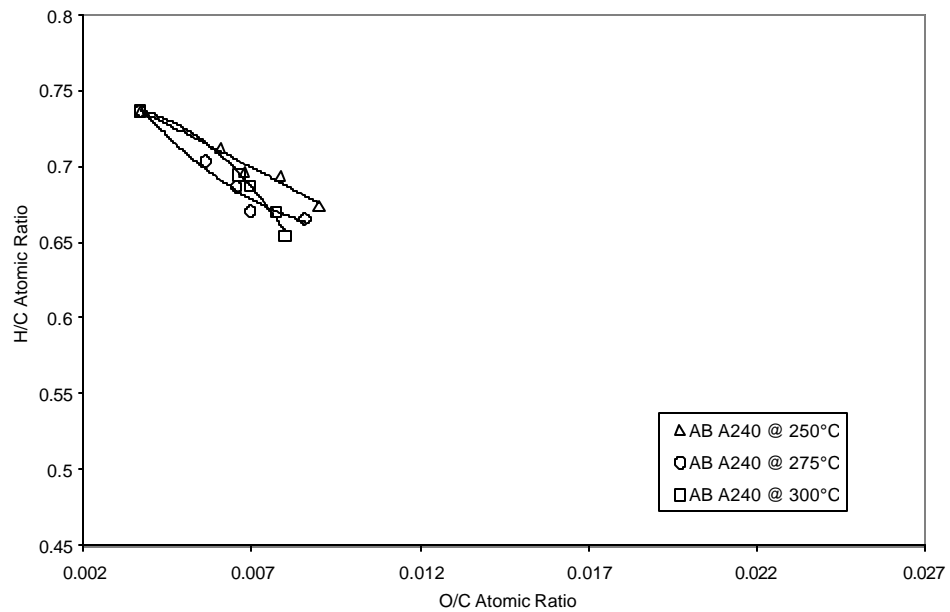


Figure 184. Van Krevelen Plot for A240 Petroleum Pitch.

The Van Krevelen plot was also completed on the coal-tar pitch to estimate the types of changes occurring when air-blown, as seen in the figure below. The Van Krevelen plot for the coal-tar pitch is different from the petroleum pitch. From these data, it shows a combination of dehydroxylation and dealkylation reactions during the air-blowing.

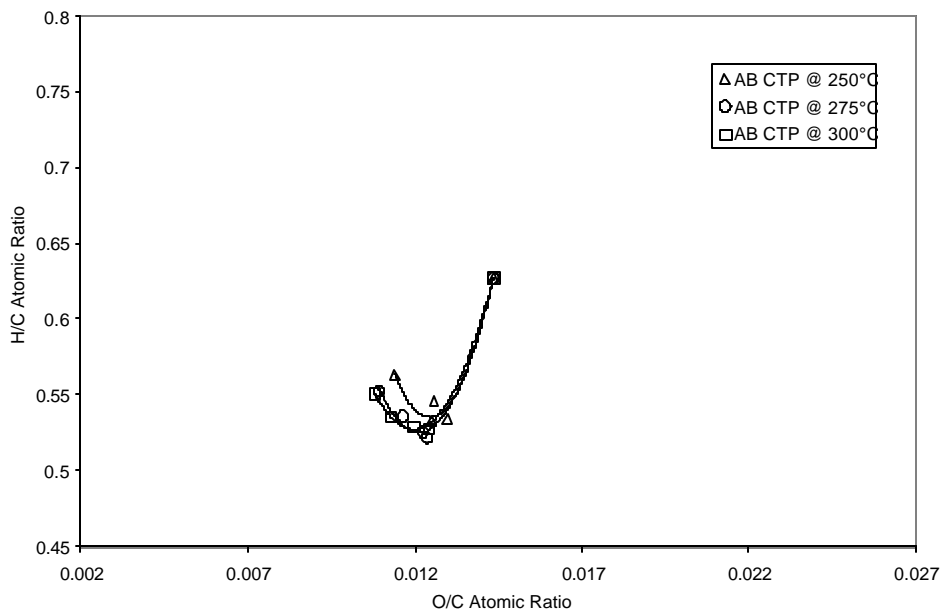


Figure 185. Van Krevelen Plot for Coal-Tar Pitch.

The Van Krevelen plot for the coal-extract pitch, seen in the figure below, exhibits a dehydrogenation mechanism.

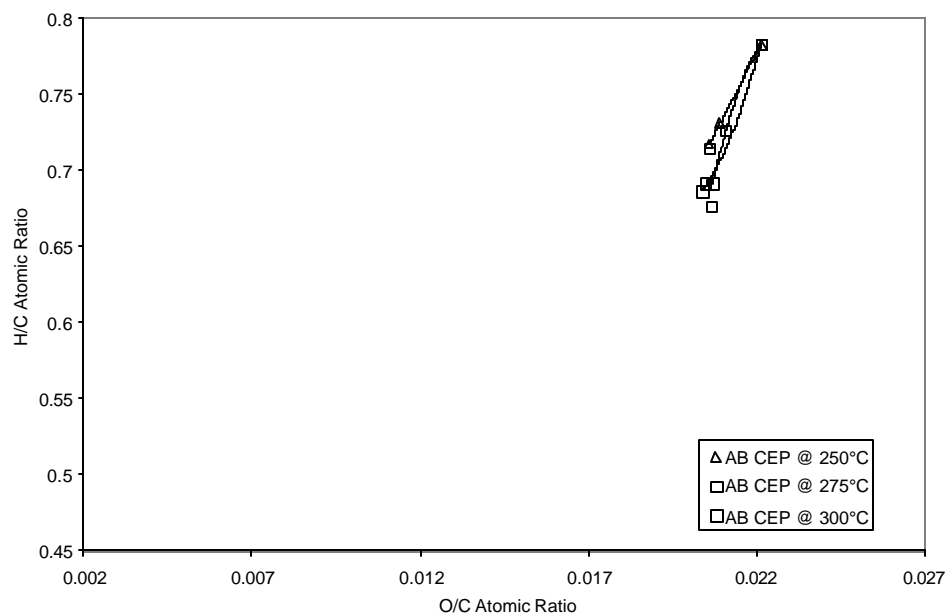


Figure 186. Van Krevelen Plot for Coal Extract Pitch.

From the C/H atomic ratio plots of data and the Van Krevelen plots it can be seen that each type of pitch reacts in a different type of mechanism. The mechanism occurring in the petroleum pitch appears to be dealkylation, while the coal-tar pitch exhibits both mechanisms of dehydroxylation and dealkylation, and the coal-extract pitch shows evidence of dehydrogenation.

4.3.12 Fourier Transform Infrared (FTIR) Analysis on Air-Blown Pitches

Some quantitative observations can be made by comparing FTIR results to changes in oxygen content and carbon-to-hydrogen atomic ratio. The FTIR analysis was developed by integrating the absorbance associated with the aliphatic carbon-hydrogen stretching mode (2900cm^{-1}) and comparing this to the integrated absorbance associated with the aromatic carbon-carbon “breathing” mode (1600cm^{-1}). Drbohlav and Stevenson have shown that the breathing mode does not change significantly during the oxidation of pitches and, thus, can be exploited as an in-situ internal standard.⁷³ It is clearly shown that changes in hydrogen content play an important role during air-blowing and that the C/H atomic ratio increases for all of the pitches. The petroleum pitch contains more hydrogen than the other two pitches, and the coal-tar pitch is the most aromatic. It is also clear that the incorporation of oxygen into the product is minimal. The FTIR spectral interpretation indicates that aliphatic groups are more prevalent in the A240 pitch and that these types of functionality decrease dramatically with the progression of air-blowing, in accordance with changes in C/H atomic. Also, since it is known that coal-tar pitch contains very few aliphatic side chains (primarily methyl), the changes in C/H

atomic ratio must be attributed to reactions not related to these groups, as indicated by the FTIR. These reactions probably take place at hydrogen directly attached to aromatic rings, as supported by the FTIR data. The changes associated with the coal-extract pitch are generally between those of the petroleum and coal-tar pitches.

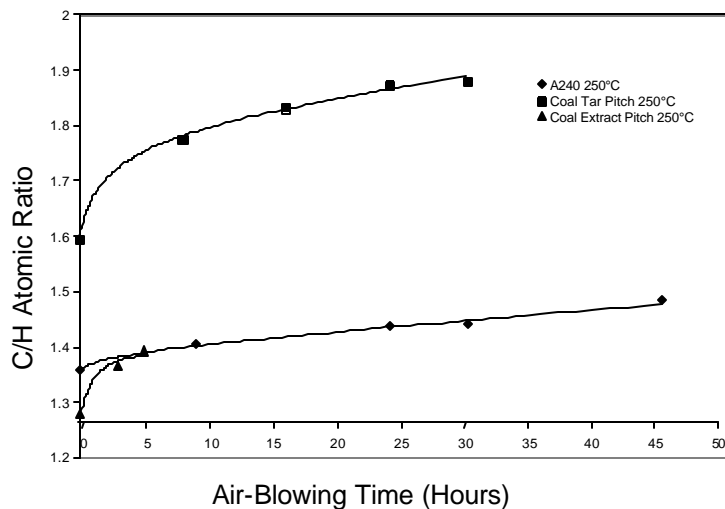


Figure 187. Air Blowing Effect on C/H Atomic Ratio at 250 °C.

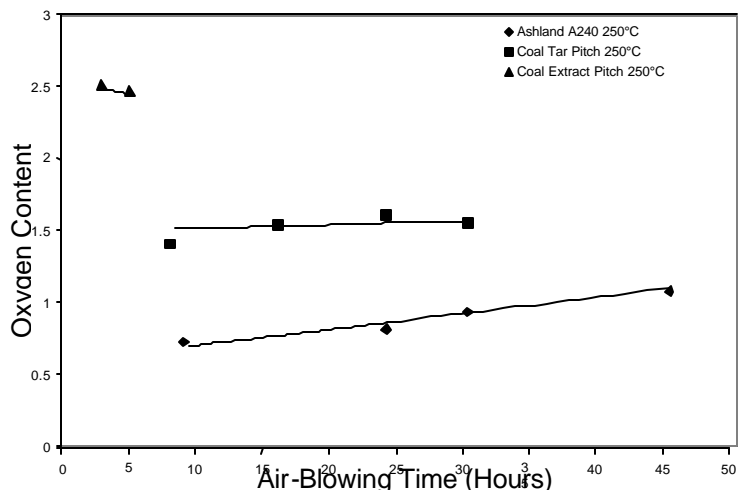


Figure 188. Air Blowing Effect on Oxygen Content at 250 °C.

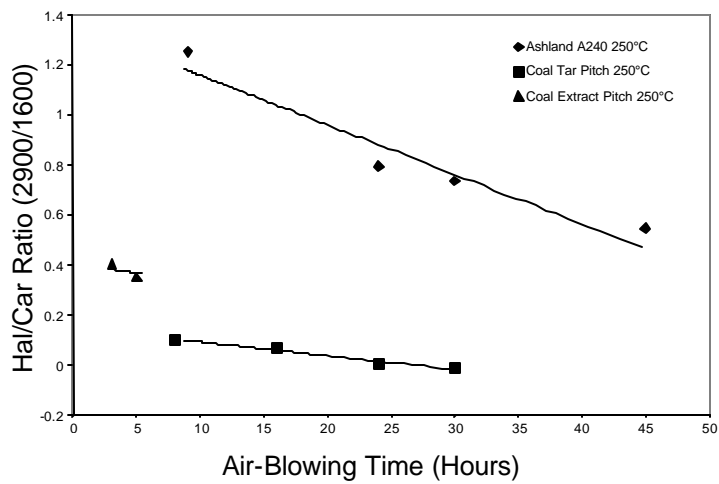


Figure 189. Air Blowing Effect on Aliphatic/Aromatic Ratio at 250 °C.

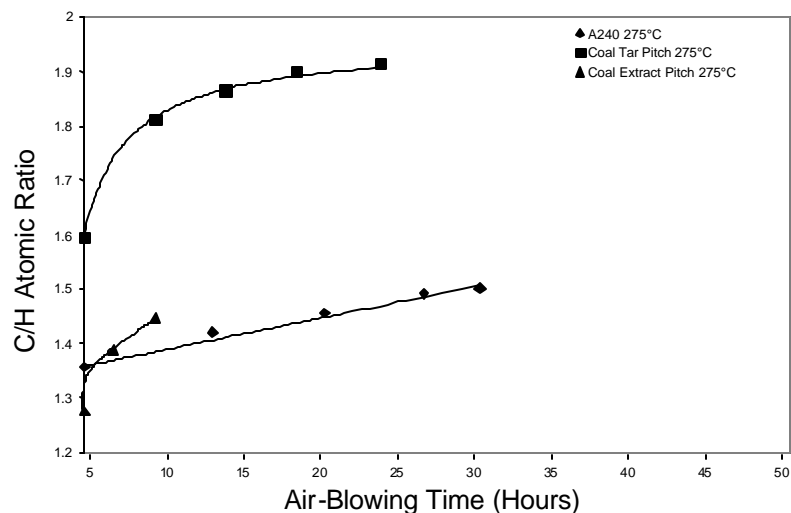


Figure 190. Air Blowing Effect on C/H Atomic Ratio at 275 °C.

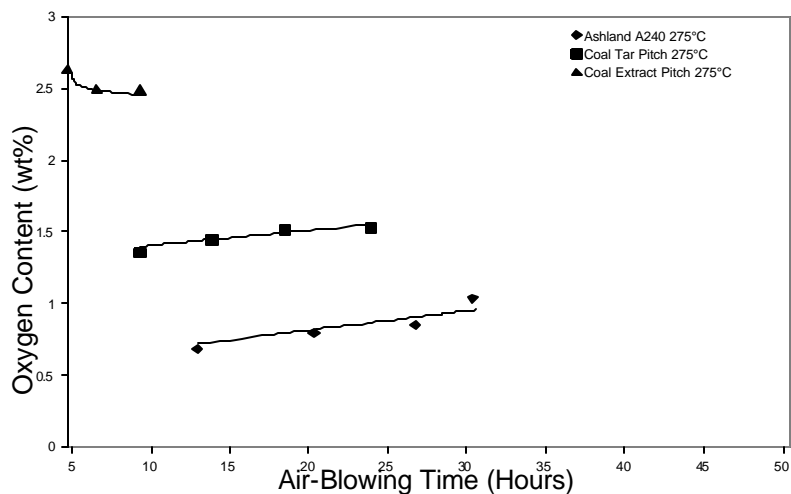


Figure 191. Air Blowing Effect on Oxygen Content at 275 °C.

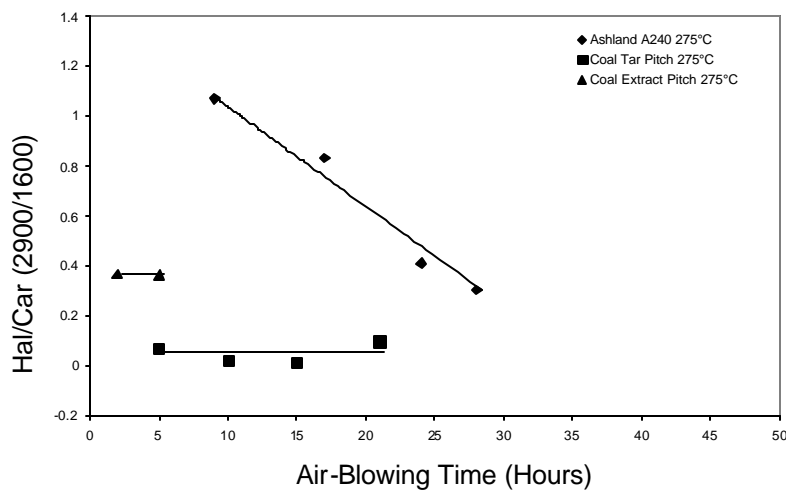


Figure 192. Air Blowing Effect on Aliphatic/Aromatic Ratio at 275°C.

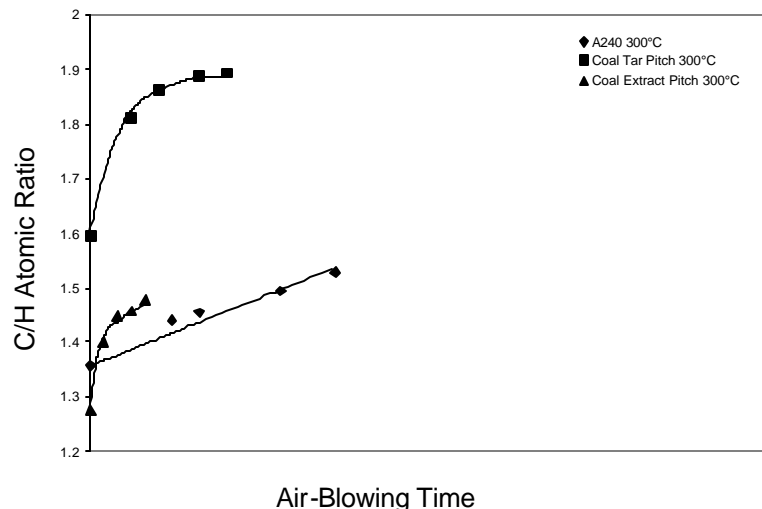


Figure 193. Air Blowing Effect on C/H Atomic Ratio at 300 °C.

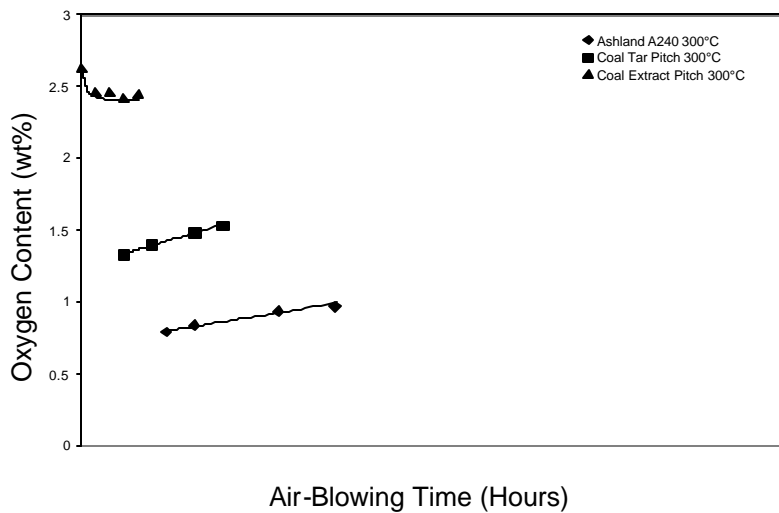


Figure 194. Air Blowing Effect on Oxygen Content at 300 °C.

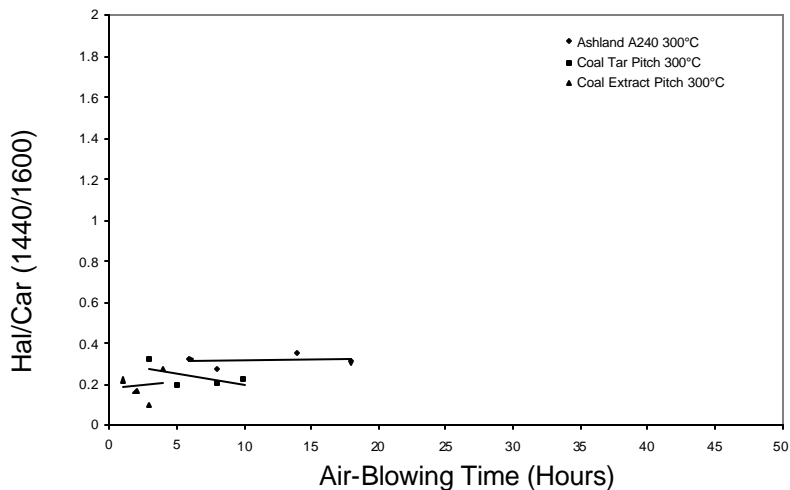


Figure 195. Air Blowing Effect on Aliphatic/Aromatic Ratio at 300 °C.

4.4 Characterization of Cokes from Synthetic Feedstocks

The cokes produced were examined under the microscope to determine the microstructure. The cokes are placed in a plastic cup and then this cup is filled with epoxy and activator (mixed in a 5:1 ratio). After the epoxy hardens, the disks are next polished and cleaned, then placed under the microscope. As can be seen from the photomicrographs below, the carbonized coal digests give a highly anisotropic coke, but after the air-blowing, the coke produced is quite isotropic, even glassy, indicating that the air-blowing has destroyed the ability of the digest to develop anisotropic microstructure in the cokes.

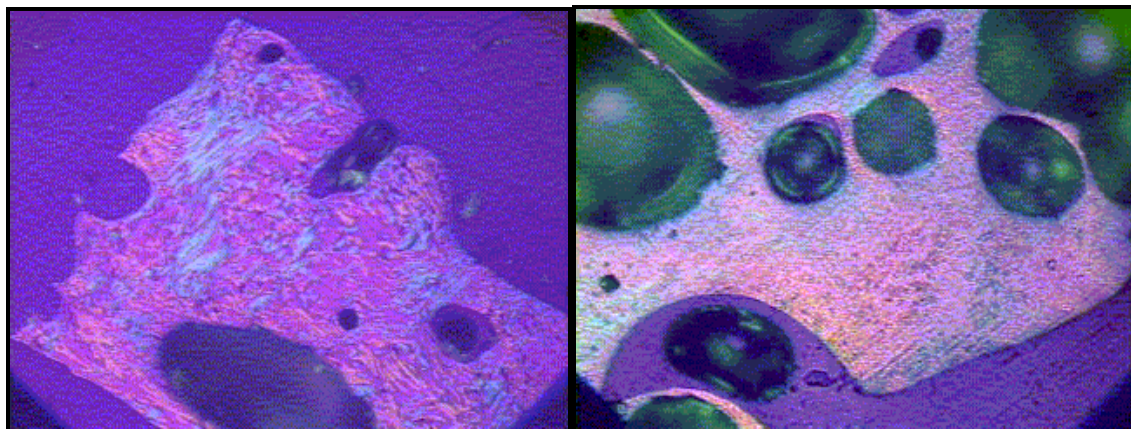


Figure 196. Photomicrographs (160X) of Green Cokes Made From A090 Coal Digest (left) and Air-blown A090 Coal Digest (right).

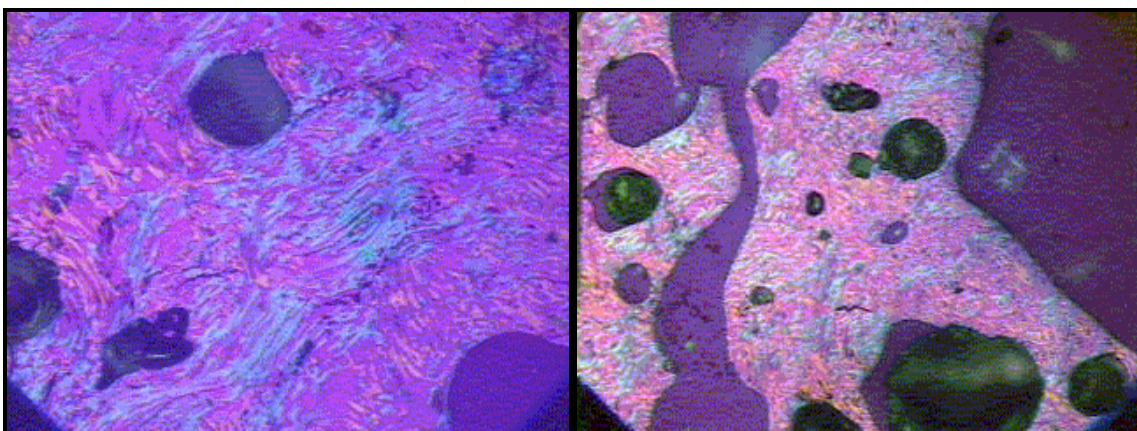


Figure 197. Photomicrographs (160X) of Green Cokes Made From A095 Coal Digest (left) and Air-blown A095 Coal Digest (right).

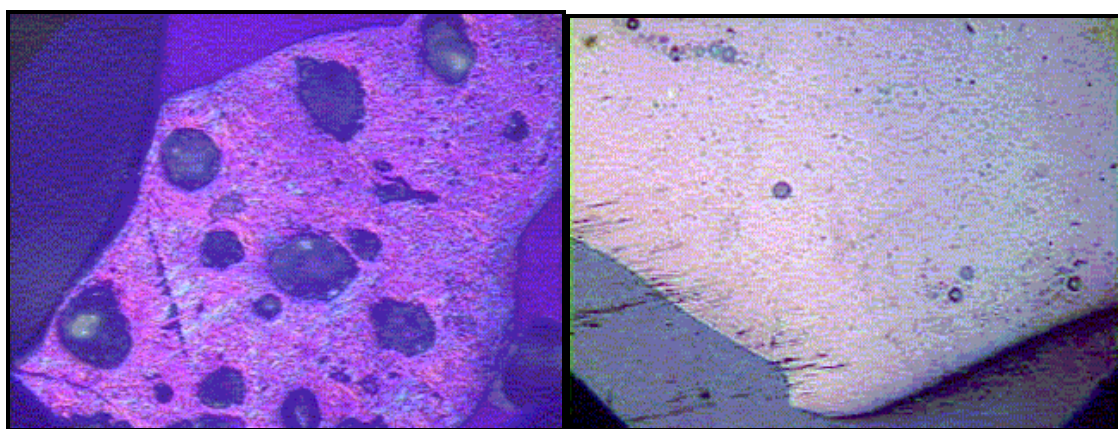


Figure 198. Photomicrographs (160X) of Green Cokes Made From A098 Coal Digest (left) and Air-blown A098 Coal Digest (right).

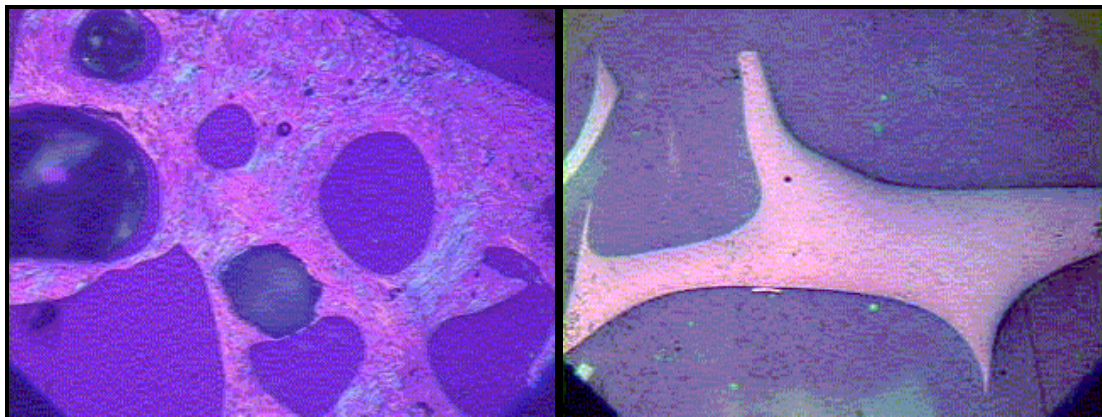


Figure 199. Photomicrographs (160X) of Green Cokes Made From A100 Coal Digest (left) and Air-blown A100 Coal Digest (right).

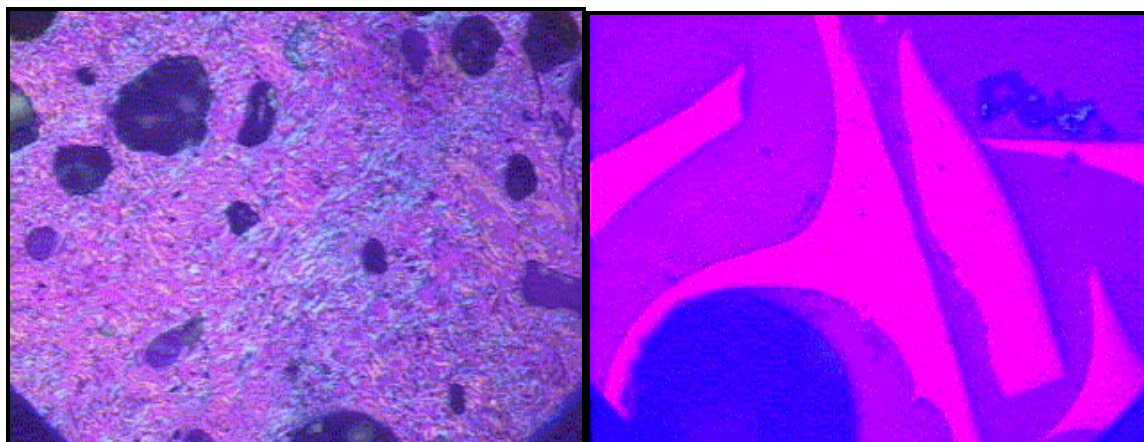


Figure 200. Photomicrographs (160X) of Green Cokes Made From B003 Coal Digest (left) and Air-blown B003 Coal Digest (right).

4.4.1 Atomic Analyses

As these products are intended for use as coke feeds for the carbon anode industry, it would be beneficial to observe how sulfur moves through this process. Sulfur in these processes not only causes the anodes to degrade more rapidly, it can also be introduced into the environment in stack gases and lead to the development of acid rain. A reduction in the sulfur content of the final product will cut down on the corrosion and environmental problems associated with using the carbon products. When compared to the original coal, the concentration of sulfur in most of the final products decreases with the digestion step. Unfortunately, though, the A095 run (hydrogenated slurry oil as solvent) shows an increase in the sulfur concentration. This is a result of the high sulfur concentration present in this solvent. Even after the air-blowing step, the sulfur concentration of the remaining digests is lower than that of the original coal. When using the coal-derived solvent only (A086 and A098), there is over a 60% reduction in the sulfur concentration. This, combined with the reduction in the ash content, makes for a more desirable pitch precursor or potential anode coke feed.

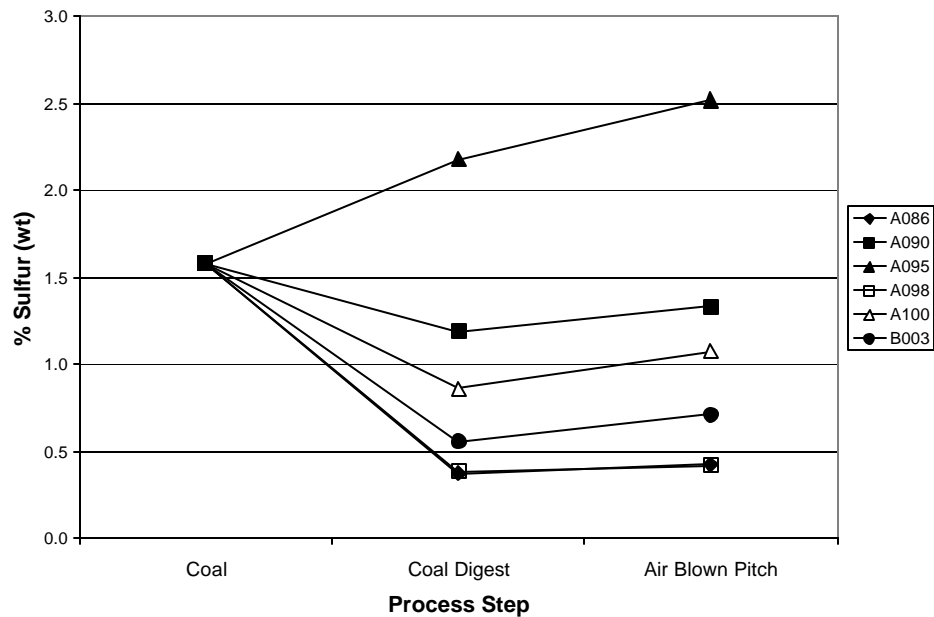


Figure 201. Sulfur Concentrations in Digest Processing.

While the reduction in sulfur is advantageous, there is little change in the nitrogen concentration throughout the process. The runs with HCBB-L3 only (A086 and A098) in fact show an increase in nitrogen, while the samples made with hydrogenated Maraflex oil (HMO-L3) only (A100 and B003) show a marked decrease in nitrogen concentration during the digestion step. The requirements on the nitrogen content of pitches or cokes, however, are not as stringent, so this is not necessarily a disappointing result.

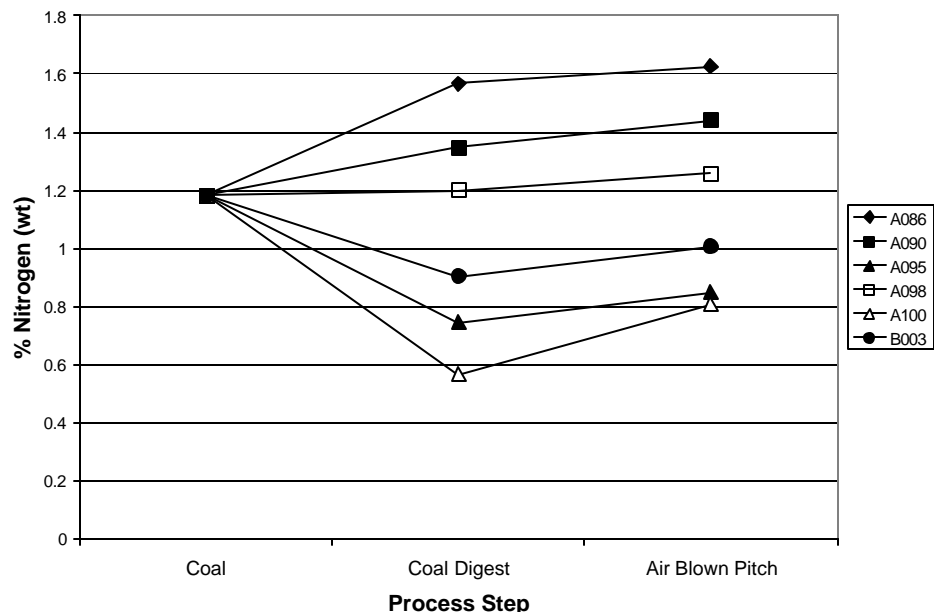


Figure 202. Nitrogen Concentrations in Digest Processing.

The hydrogen concentrations in the process increase dramatically during the digestion, which is the desired result (shown in the figure below). This makes for a better precursor, and even though the carbon concentration in the digests is higher than the feed coal, the atomic C/H ratio is lower in the digests. After air blowing, the pitches show a reduced concentration of hydrogen, and this is likely due to the distilling of lower molecular weight compounds (C₂ – C₈'s) and the cross-linking that takes place during air-blowing. The desired pitch should have a higher C/H atomic ratio than the feed material; this is what increases properties like softening point, coke yield, viscosity, etc.

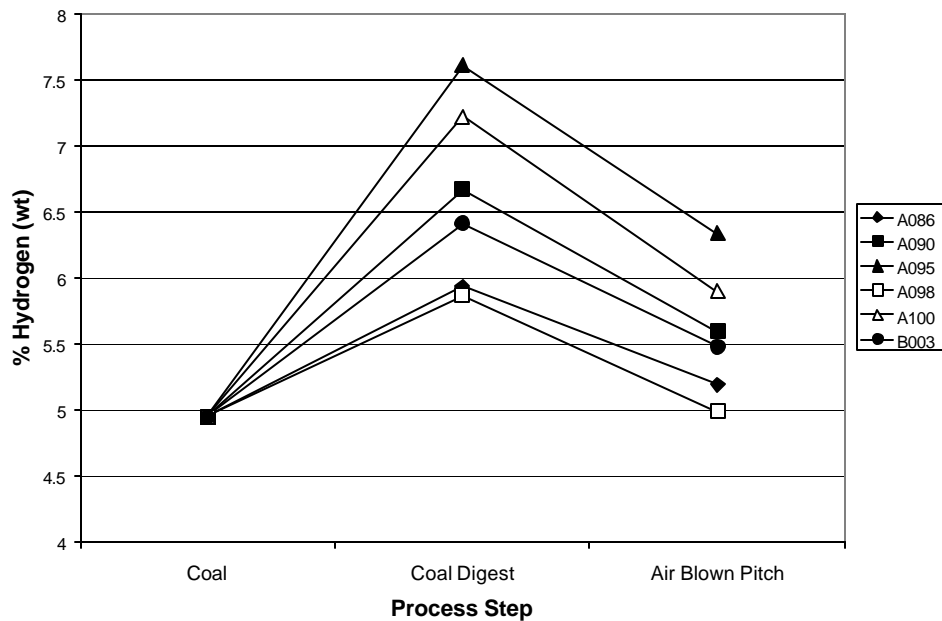


Figure 203. Hydrogen Concentrations in Digest Processing.

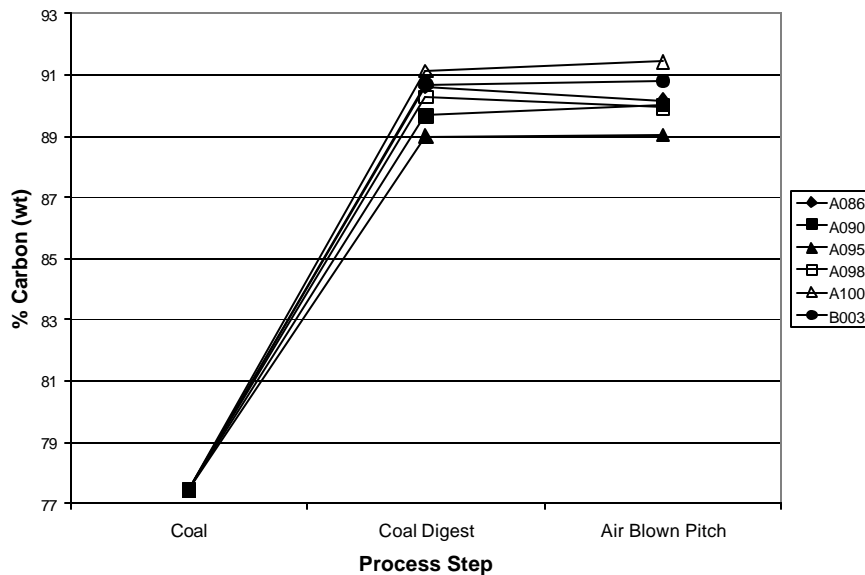


Figure 204. Carbon Concentrations in Digest Processing.

The atomic C/H ratio and the types of hydrogen and carbon present in the solvents and coal digest liquids may have a significant influence on some of the physical properties of the products. An increase in the atomic C/H ratio of the solvent yields an increase in the final softening point of the air-blown digest. The ratio of aromatic hydrogen content to total hydrogen content (the “aromaticity factor”) versus the softening point show that as the aromaticity of the solvent increases, so does the softening point of the air-blown digest (shown in the accompanying figures). Thus, high concentrations of carbon and aromatic hydrogen in a solvent should lead to a high softening point pitch. For a lower softening point pitch (for instance, a binder pitch), the opposite should hold true. These results are most encouraging, since even though the solvents used are derived from both coal and petroleum, and have many differences, the results are relatively consistent.

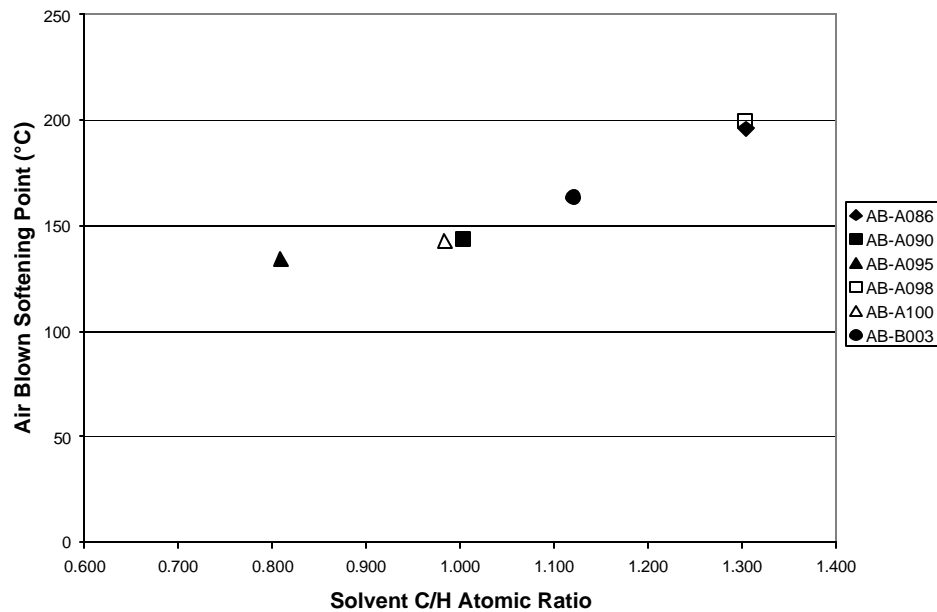


Figure 205. Solvent Atomic C/H Ratio vs. Air-Blown Softening Point (°C).

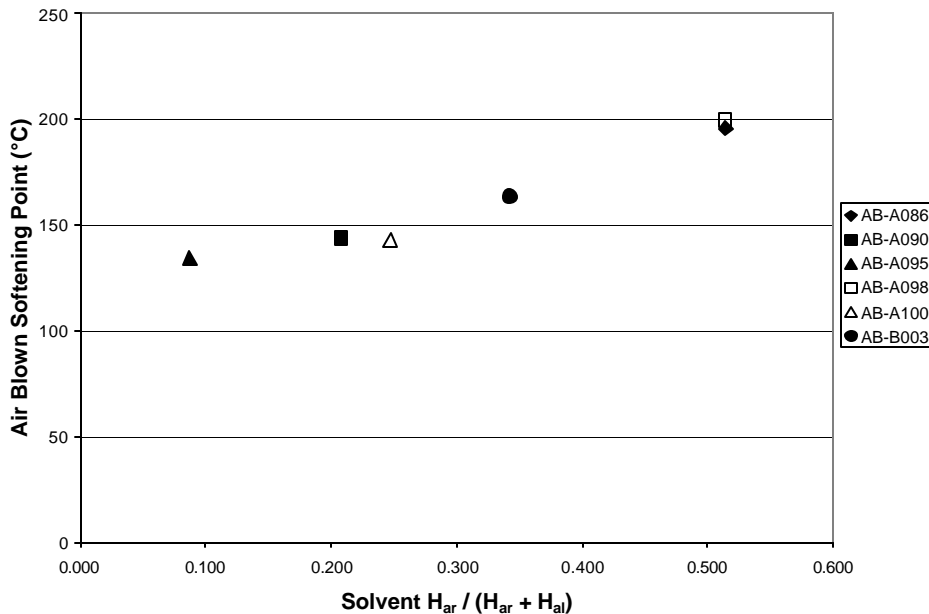


Figure 206. Solvent Aromaticity vs. Softening Point (°C).

This tendency for materials with higher aromaticities and C/H atomic ratios giving higher softening point air-blown materials carries over into the coal digest liquids. Examination of the coal digest C/H atomic ratio vs. air-blown softening point shows nearly the same relationship as with the solvent. The aromaticity of the coal digest liquids also influences the air-blown softening points. As with the atomic C/H ratio, as the aromaticity of the digests increases, so to do the air-blown softening points (shown in the next two figures).

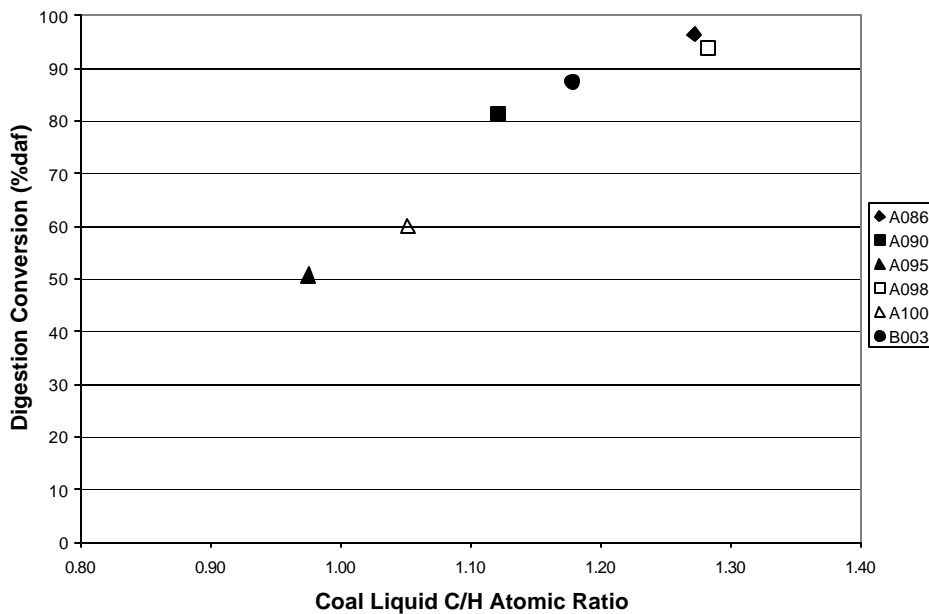


Figure 207. Coal Digest C/H Atomic Ratio vs. Air-Blown Softening Point (°C).

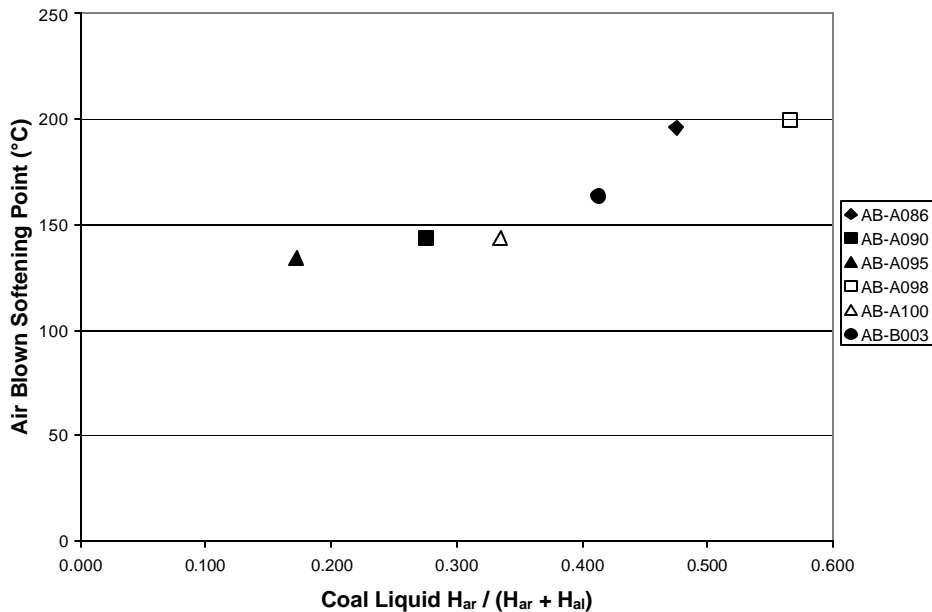


Figure 208. Coal Digest Aromaticity Factor vs. Air-Blown Softening Points (°C).

4.4.2 Vacuum Distillation of Coke Precursors

While most of the results of the reactor scale-up studies are positive, and even though air-blowing in the past has proven an effective method of altering pitch properties, the coke precursors produced in this study are not affected by the air-blowing in as positive a manner. The process has effectively eliminated the possibility of using the air-blown digests as coke feeds, since the cokes made from them are mostly isotropic in nature or very nearly glassy. This observation is in sharp contrast to King, who showed that air blowing had little affect on diminishing the optical microstructure.⁷⁴ The reason could be the presence of the solvent in the coal digest. King had worked with pitches in which the low molecular weight material was absent.

Vacuum distillation on the coal digest liquids was performed to remove most of the solvent. The use of vacuum distillation is based on the theory that part of the problem with the coal digest liquids is that there is too much solvent still left in the digest. This solvent is much more reactive to air-blowing than the converted coal matter, and cross-links more rapidly so that only isotropic, glassy, carbons are formed upon carbonization.

A sample of each coal digest liquid was vacuum distilled, until about half of the original sample volume was distilled off. As this was still at temperatures below 300°C, any distillate should be mostly or completely made up of the original digestion solvent, and since the original solvent to coal weight ratio was 2.5:1, this process lowers this ratio to approximately 0.75:1. The bottoms should be mostly converted coal with some entrained solvent. The details of the distillations are given in the table below. After the distillation, the bottoms, all now solids at room temperature were weighed, and a sample of each was carbonized, using the Alternate coke protocol process. The softening point of each one was found, and these along with the coke yield results are shown in the figures below. The softening points of the three of these vacuum distilled coal digests are more in line with the production of a binder pitch, approximately 110°C (A086, A100

and B003). The vacuum distillation does a much better job of increasing the coke yields of the coal digests. Also, the synthetic cokes of these vacuum distilled coal digests were examined under the microscope, and photomicrographs of each are shown next to the corresponding air-blown coal digest cokes (Below). As can be seen, the vacuum distilled cokes are more anisotropic than the air-blown coal digest cokes. This shows that vacuum distilling some of the solvent off of the coal digests will produce a good pitch precursor, and potentially a coke feed. These vacuum distillations were done at the end of this study, and more research on these should be conducted to better characterize the types of cokes that could be made when combining vacuum distillation and air-blowing.

Table 39. Details of Vacuum Distillation of Coal Digests.

	A086	A090	A095	A098	A100	B003
Sample Wt. (g)	670.78	514.10	521.52	510.91	512.38	516.69
Max Temp. (°C)	195	260	275	235	231	225
Bottoms Wt. (g)	320.05	345.40	296.15	212.04	141.29	235.08
Distillate Wt. (g)	350.73	279.88	252.85	292.37	277.00	268.38

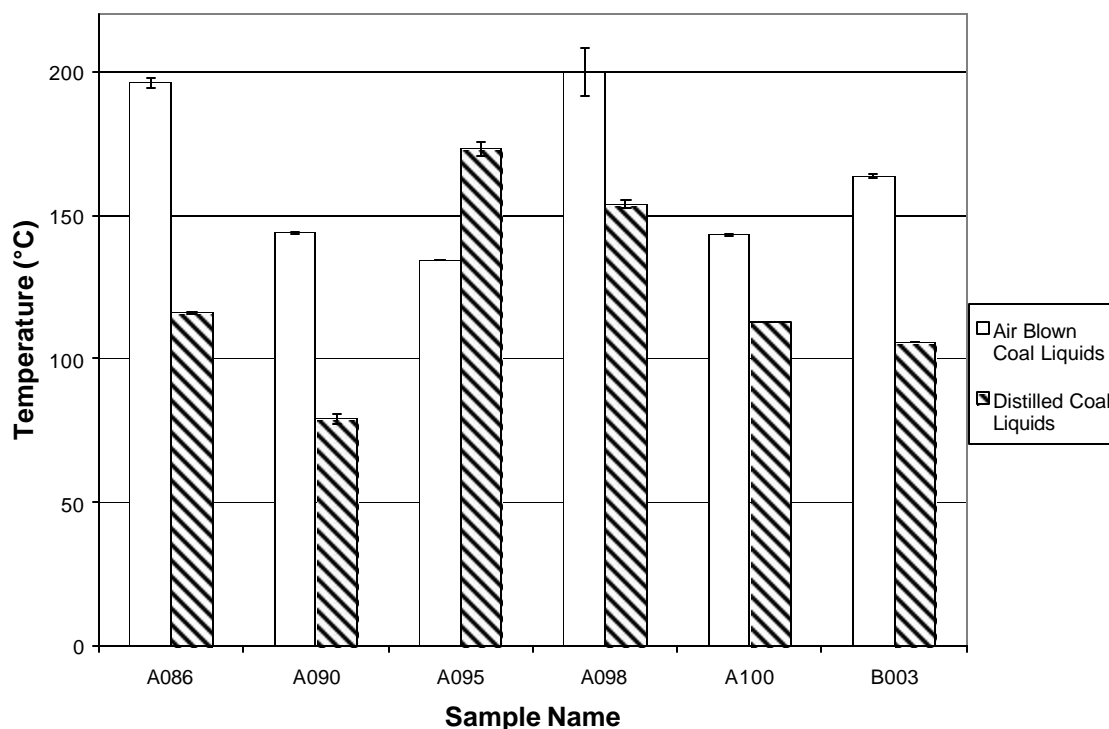


Figure 209. Softening Point (°C) for Air Blown and Distilled Samples.

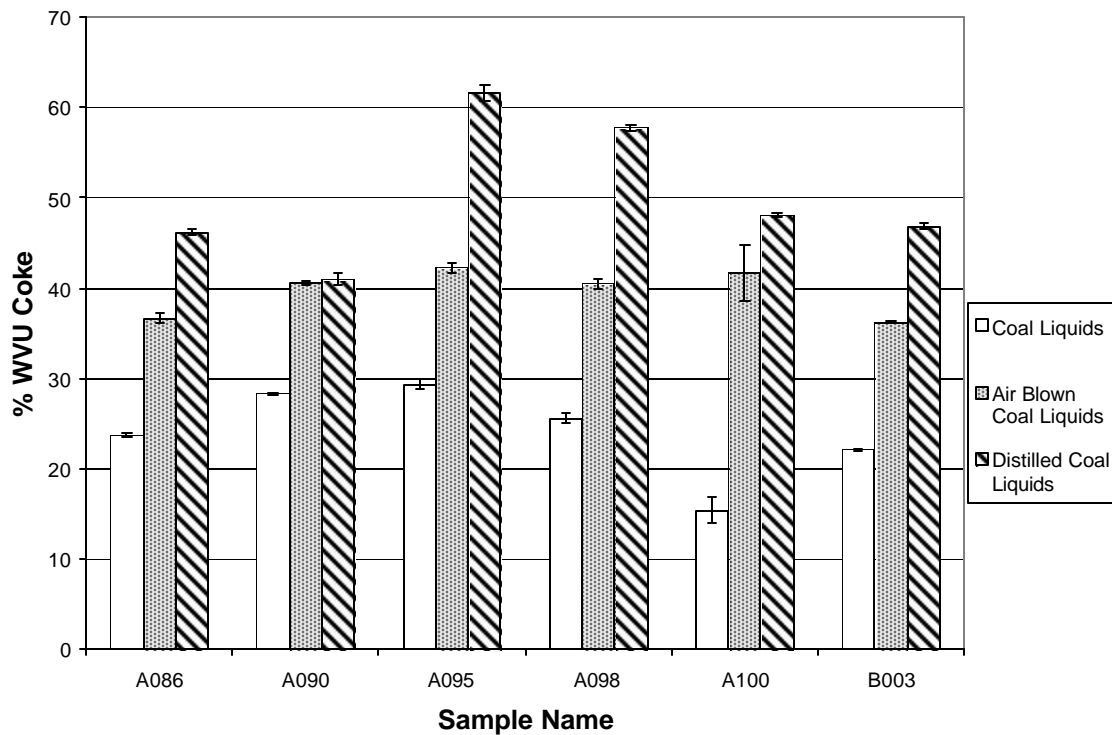


Figure 210. Alternate Protocol Coke Yield (w/ Distilled Coal Liquids).

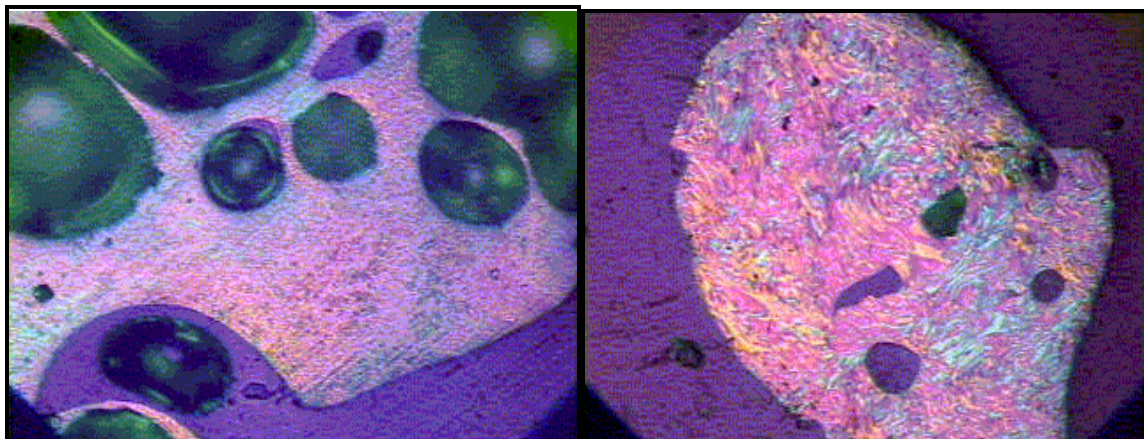


Figure 211. Photomicrographs (160X) of Green Cokes Made From A090 Air-blown Coal Digest (left) and Vacuum Distilled A090 Coal Digest (right).

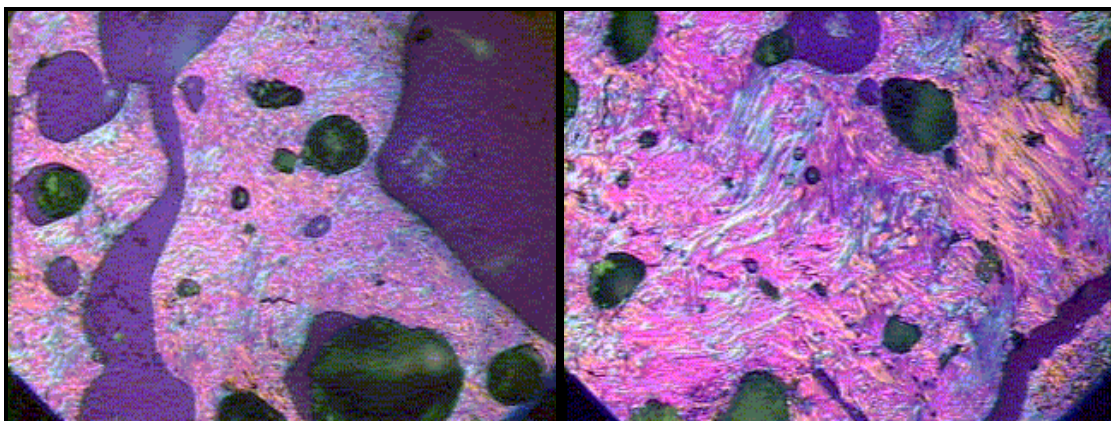


Figure 212. Photomicrographs (160X) of Green Cokes Made From A095 Air-blown Coal Digest (left) and Vacuum Distilled A095 Coal Digest (right).

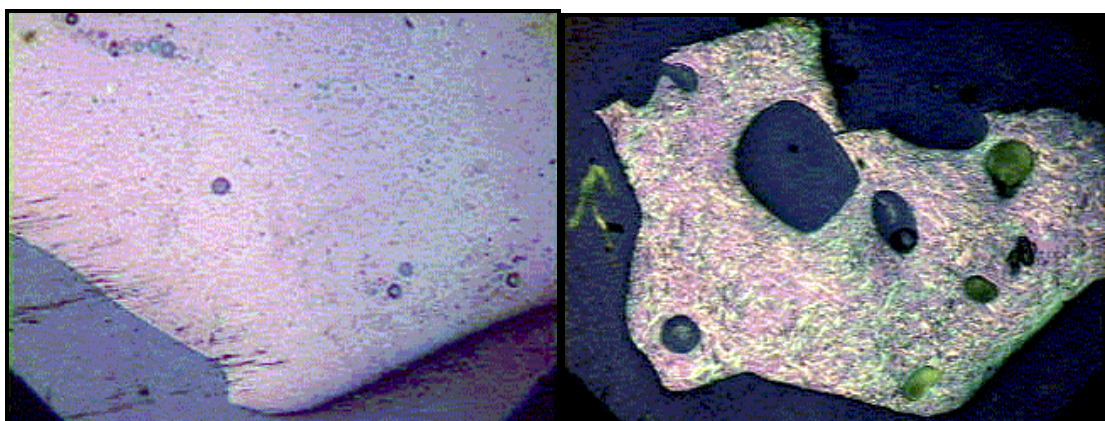


Figure 213. Photomicrographs (160X) of Green Cokes Made From A098 Air-blown Coal Digest (left) and Vacuum Distilled A098 Coal Digest (right).

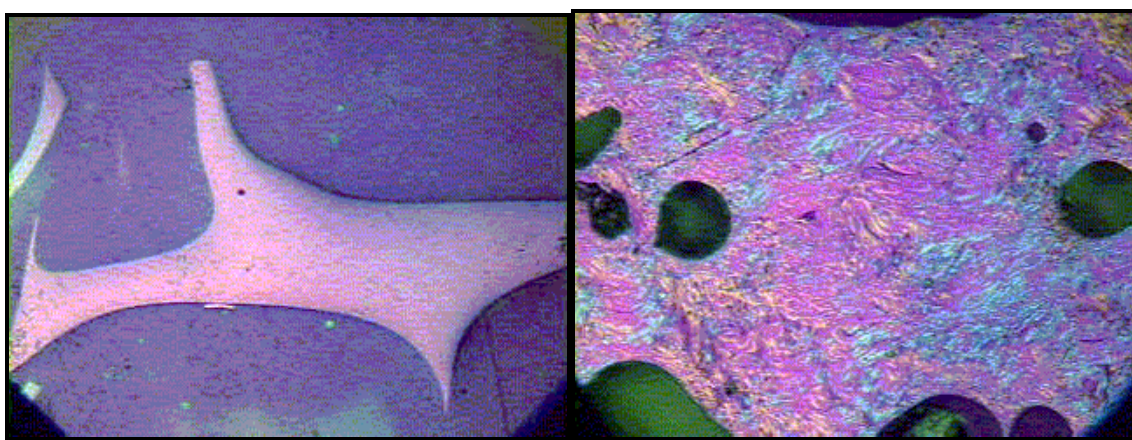


Figure 214. Photomicrographs (160X) of Green Cokes Made From A100 Air-blown Coal Digest (left) and Vacuum Distilled A100 Coal Digest (right).

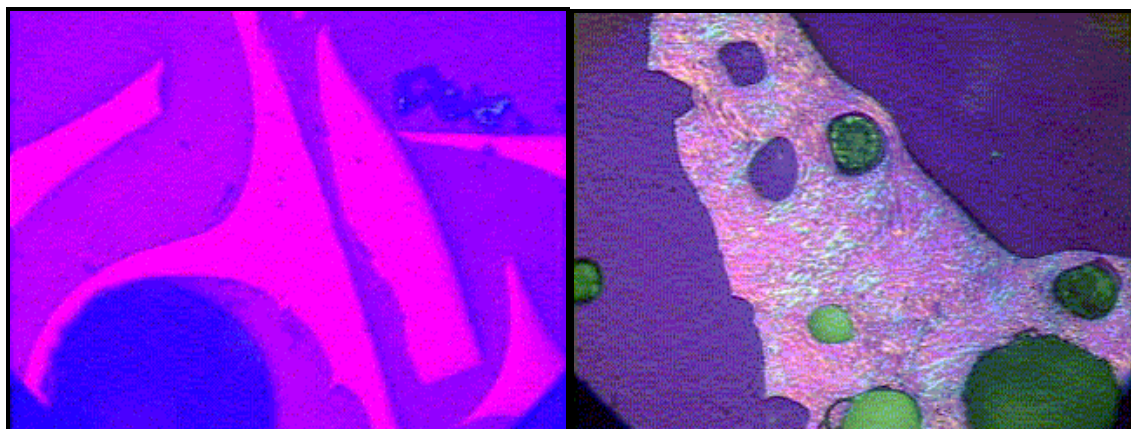


Figure 215. Photomicrographs (160X) of Green Cokes Made From B003 Air-blown Coal Digest (left) and Vacuum Distilled B003 Coal Digest (right).

4.5 Coal Derived Carbon Foam

Carbon foams can be produced from a variety of carbon sources including bituminous coals. Some foam is made from raw coal directly. The coking of raw or hydrogenated coal under controlled conditions of temperature and pressure causes controlled expansion (swelling) and results in the formation of carbon foam which in some cases can be subsequently graphitized. Carbon foams are light-weight materials and their properties can be tailored through the selection of appropriate bituminous coal precursor, foaming conditions and heat treatment conditions. Carbon foams have been made from raw coal, coal extracts, mesophase pitches from petroleum and naphthalene. Calcined carbon foams with low thermal conductivity can be used to provide thermal insulation. On the other hand, graphitized carbon foams with high thermal conductivity have applications in thermal transfer systems like heat exchangers. Heat-treating at a higher temperature increases graphitic ordering and foams with high electrical and thermal conductivity and high elastic modulus can be obtained. The carbon foams can also be infiltrated with polymers or metals to form composite materials.

A series of carbon foams were synthesized using low-cost precursors such as coal, petroleum pitch, coal tar pitch, and hydrogenated coal solvent extracts (coal-based SynPitch)^{75,76,77,78}. The properties of carbon foam can be controlled by adjusting the thermal plastic behavior of precursors and the foaming conditions. The resultant carbon foam could be either a strong structural material or a highly thermal/electrical conductive material, moreover either open or close cell structures are possible. In addition, no foaming agent and stabilization step are required in this method, which simplifies the foaming process and lowers the cost of production.

Unlike Mitsubishi mesophase AR pitch, which can be foamed directly without pretreatment, most coal and petroleum-derived pitches need to be tailored before foaming can be achieved. The major problem with these untreated precursors is that their plastic properties do not normally meet the foaming requirement. The pretreatments mainly involve the polymerization/condensation of pitch using thermal treatments to control the degree of anisotropy of the foaming precursors. For example, to obtain a high-strength structural carbon foam, the desired foaming precursor is isotropic in nature (after carbonization). However, for highly thermally and electrically conductive carbon foam, an anisotropic pitch precursor is required. Thus raw coal and coal solvent extracts usually generate strong isotropic carbon foam, but pitch-based carbon foam can be either mechanically strong foam or highly conductive depending on the degree of anisotropy present.

Samples. Precursors used for foaming in this work include bituminous coals, coal tar pitches (Quinoline insoluble, QI, content 12.8wt%), QI-free coal tar pitch, petroleum pitch(A240) N-methyl-2-pyrrolidone solvent extracts, as well as synthetic pitches produced by hydrogenating coal using a hydrogen donor solvent process to produce a synthetic pitch (Synpitch). The precursors were typically ground to the 50-200 mesh and charged into a mold for foaming.

Pretreatment of pitch precursors. In order to tailor the foaming performance of the pitch precursors such as coal tar pitch, synthetic pitch or petroleum pitch, heat treatment was accomplished in an 1 L autoclave between 200 to 400°C under a N₂ atmosphere.

Foaming method. Foaming was carried out in a pressure vessel by heating the foaming precursor up to 500°C in a N₂ atmosphere, pressure up to 500psi. The resultant green foams were calcined at 1000°C in inert atmosphere to increase the strength and further remove the volatiles.

Characterization. A Gieseler Plastometer P31 and a Dilatometer D34 from Preiser Scientific were used to measure the Gieseler fluidity and dilatation characteristics of foaming precursor in the temperature range up to 540°C at a heating rate of 3°C/min. A Thermo Cahn TG151 TGA was also used to measure the weight loss as a function of temperature. Compressive strength measurement was carried out on an Instron 5869 by using a stainless steel cylinder sample holder and a matched piston (diameter, 25 mm). Sample size is 25 mm diameter by 20~30 mm height. A Hitachi S4700 Field-emission SEM and a Zeiss EL optical microscope were used to observe the structure of carbon foam. Gas adsorption was carried out by means of a Micromeritics Gemini 2375 gas adsorption analyzer by measuring N₂ adsorption at 77K.

The foaming process involves the controlled heating of foaming precursors under the certain pressure in an inert atmosphere. During heating, the evolving volatiles from the light fractions and the thermally decomposed products from the viscous precursor material serve as bubble agents to create foam cells. As a result, the volume of foaming precursor expands. Further heating results in cross-linking and additional outgassing, thereby, solidifying the precursor, which fixes the foam matrix. Therefore, the viscosity and volume swelling of foaming precursors at the foaming temperature are the two main factors affecting the foaming and foam cell structure. Thus, Gieseler fluidity, which is proportional to the inverse of the viscosity, and the dilatation, which is proportional to the volume swelling, can be used to describe the plastic properties of foaming precursors.

The figure below shows the Gieseler fluidity, dilatation and TGA results of a raw coal. As the temperature increases, the material first softens and then turns fluid. The fluidity increases with the increase of temperature, reaches a maximum value, and decreases before final re-solidification at higher temperature. During the heating, the volume of the fluid material expands because of the gas evolved from the pyrolysis of the precursor. Maximum dilatation corresponds to the temperature of maximum fluidity. The TGA curve indicates that the maximum rate of weight loss occurs around 440°C, which corresponds with the maximum fluidity and dilatation condition. The TGA data also indicate that the volatiles continue evolving even after the re-solidification temperature of the material has been reached. This implies that the resultant foam is an open-cell structure. However, in the case where the weight loss ends before the re-solidification temperature, a closed-cell foam will be generated.

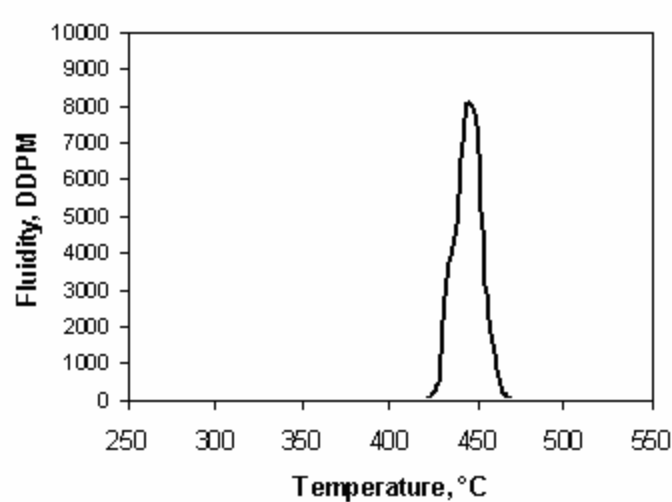


Figure 216. Giesler Fluidity Curve of a Typical Foaming Precursor(coal).

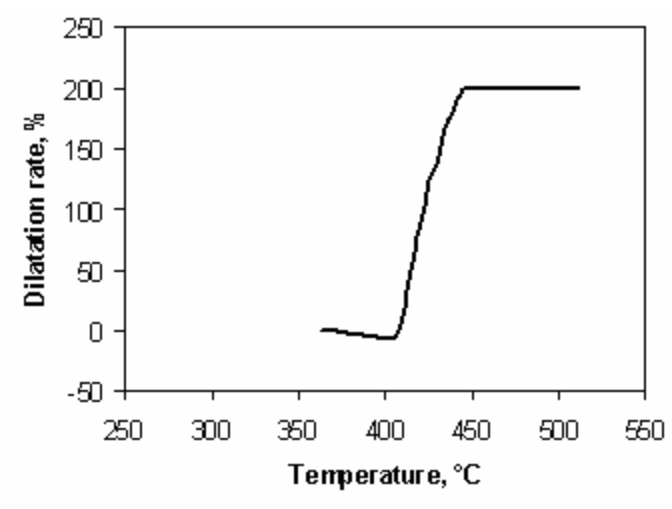


Figure 217. Dilatation Rate Curve of a Typical Foaming Precursor (Coal).

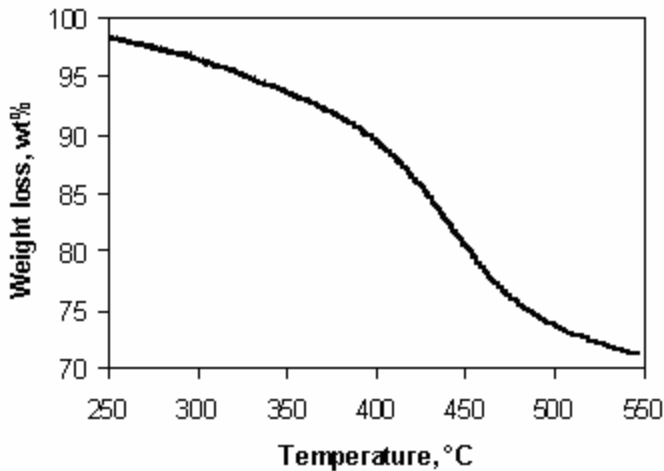


Figure 218. TGA Curve of a Typical Foaming Precursor (Coal).

The dilatation curve reveals the volume expansion at atmospheric pressure. It is obviously too much dilatation for generating the normal carbon foam. Therefore, an external pressure was applied to decrease and control the dilatation. The external applied pressure decreases the dilatation but not the fluidity. Fluidity is increased in this case, because more volatiles and lighter fractions are kept in the system. Accordingly, the fluidity, dilatation and weight loss of the precursor during the foaming stage are the key factors controlling the foaming performance and foam structure. Therefore, the adjustment of the plastic properties of the precursor is crucial to control the characteristics of carbon foam.

The properties of coal very widely, and thus some coals are suitable as foaming precursors and others are not. The foaming behavior of coal precursors is strongly related to their plastic properties, which are dependant on the maceral composition of the coal. Liptinite exhibits strong dilatation power but inertinite does not, while vitrinite is intermediate.⁷⁹ Therefore, the selection of the appropriate coal precursor is important to maintain quality of carbon foam.

The figure below reveals the relationship of the foam bulk density with the dilatation and Gieseler fluidity of the feed coal. It is clear that high dilatation and fluidity generate low-density foams, and vice versa. Therefore, the density of carbon foam can be controlled by adjusting the fluidity and dilatation characteristic of the precursor. Although the two parameters are mainly determined by the nature of coal, they can also be modified by devolatilization and solvent extraction.^{80,81} The light fraction removed by solvent extraction and devolatilization is rich in transferable hydrogen, which will stabilize free radicals generated by pyrolysis.⁸² Removal of the transferable hydrogen will cause the formation of the larger condensed aromatic molecules, therefore decreasing fluidity. The data in the following table indicate that the removal of 2.7% volatile matter results in a significant decrease of maximum fluidity (at higher corresponding temperature) and a slight increase of softening temperature. The results demonstrate the importance of the volatile matter on foaming behavior. In addition, the bulk density of carbon foam can also be controlled by applied external pressure. The higher pressure results in a more dense foam.

Table 40. Effect of Devolatilization on Maximum Fluidity and Softening Point.

Wt% loss during devolatilization	Softening point, °C	Max. fluidity, DDPM
0	434	238@455°C
2.7	438	136@465°C

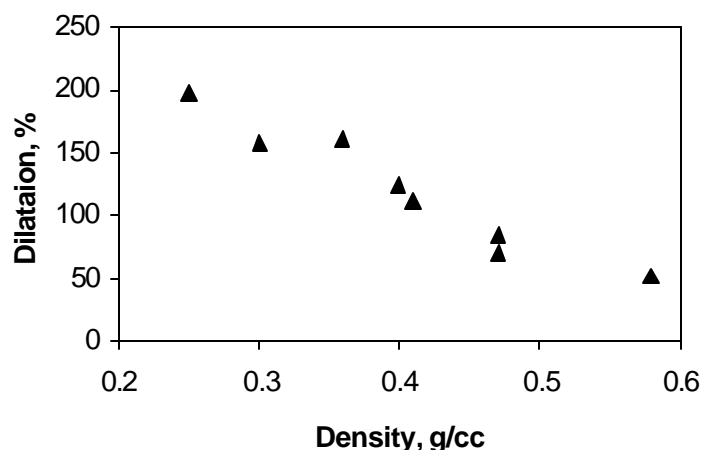
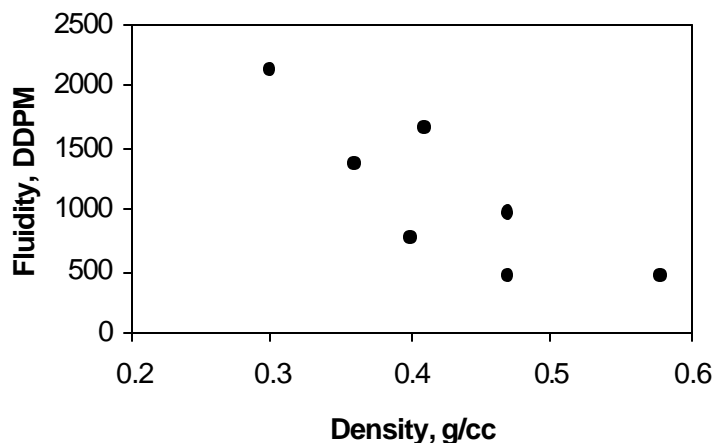


Figure 219. Relation of Fluidity and Dilatation of Coal Foaming Precursors with the Bulk Density of Carbon Foam.

Pitch is another type of foaming precursor, which can be either anisotropic or isotropic in nature. Highly anisotropic pitch can be graphitized, resulting in graphitic foam. Such foams are good thermal and electrical conductors. Pitches with large anisotropic domain sizes yield highly graphitizable carbon, while pitches with small anisotropic domains are less graphitizable. In general, the resultant foam from small anisotropic domains is mechanically stronger (see the discussion that follows). Commercially available pitches, such as petroleum pitch (Ashland A240) and Koppers coal tar pitch are not suitable for making carbon foam directly using our current methods.

The key problem is the viscosity is too low to hold the foam cell shape. Therefore, the pitch properties of these materials have to be tailored to meet the foaming requirements.

Heat treatment of pitch in N₂ induces polymerization and condensation through de-hydrogenation of polyaromatic molecules. This treatment results in the formation of larger condensed and more planar molecules in pitch, which exhibit some anisotropy when coked.^{83,84} The viscosity and softening temperature of treated pitch are thus increased. The following table lists the properties of three pitch samples before and after heat treatment at 400°C under N₂ atmosphere. Heat treatment significantly increases the softening temperature and the content of THF insolubles, which implies the increase of molecular weight and the degree of polymerization and condensation of pitch. An increase in softening temperature reflects an increase in viscosity. In addition, heat treatment increases the thermal stability of the pitch, and thus decreases the weight loss in the foaming stage. The amount of bubble agents is related to the weight loss caused by the evolving volatiles in foaming stage. Therefore, the foam cell size can also be controlled by releasing the right amount of volatile.

Table 41. Effect of Heat Treatment on Foam Precursor Properties.

Samples	Method of treatment	Softening temperature, °C	THF-insolubles, wt%	Weight loss, wt%, 25-500°C at 500psi
A240	none	117*	<20%	22.8
Treated A240	Heat treatment	350**	94.6%	3.3
SynPitch	none	110*	<20%	39.2
Treated SynPitch,	Heat treatment	320**	74.5	4.8
Coal tar pitch	none	110*	<30%	18.2
Treated coal tar pitch	Heat treatment	350**	91.3	2.7

*Mettler Softening point, **From lactometer

The following table lists the general properties of carbon foams derived from different precursors, including raw coal, N-Methyl-2-pyrrolidone solvent-extracted coal, quinoline insoluble-free coal tar pitch (coal tar pitch-I), coal tar pitch containing quinoline insolubles (coal tar pitch-II), Ashland-Marathon A240 petroleum pitch and coal-based synthetic pitch. The bulk density of the corresponding foam ranges from 0.25 to 0.7g/cc. Most of these carbon foams have over 95% open cell structure with porosity of around ~80% according to the helium pycnometry.

The following table also summarizes the compressive strength of carbon foam derived from the various precursors. The compressive strength of the coal-based foams (Kingwood, Lower War Eagle and Bakerstown coal) ranges from 3 to 10 MPa depending on the density of foam. The two coal solvent extract-based foams (Powellton extract-01 and Powellton extract-02) are quite different. The carbon foam with 60% closed-cell structure is much stronger than the other with only 5% closed-cell structure. The strength of pitch-based foam also covers a wide range. Strength depends not only on the structure of foam, but also on the property of precursor material, such as the anisotropic domain size, which will be discussed later.

Table 42. General Properties of Carbon Foam Derived from Different Precursors.

Precursor of carbon foam	Bulk density, g/cc	Porosity, %	Open-cell, %	Compressive Strength, MPa
Kingwood coal	0.32	84.1	96.8	2.9
Lower War Eagle coal	0.33	82.7	98.4	5.5
Bakerstown coal-01	0.38	80.3	98.0	8.0
Bakerstown coal-02	0.40	79.3	97.7	9.9
Powellton extract-01	0.25	87.0	97.1	2.5
Powellton extract-02	0.31	83.6	39.1	18.7
Coal tar pitch-based-I QI-containing	0.67	64.8	83.5	18.2
Coal tar pitch-based-II QI-free	0.56	72.0	98.2	8.0
Coal SynPitch-based	0.42	79.7	95.6	2.8
Petroleum pitch-based	0.34	82.9	97.2	3.9

Although the relation of foam strength with structure is still under investigation, for the open cell foam, the cell size significantly affects the foam strength. The thickness of cell-wall, t , and the length of the cell edge, l , are used to described the foam structure. The measurement of t and l of the foam seems to be difficult, but, for a regular foam structure, its relative density has been related to these structural parameters as:

$$(t/l)^2 \propto (D^*/D_s)$$

where D^* , bulk density; D_s , true density of foam, D^*/D_s relative density.⁸⁵

Unfortunately, since coal and pitch-based foams do not have a perfect and regular cell structure, the relation of relative density with structural parameters may be more complicated. But to a first approximation, relative density can still be used to describe the foam cell structure.

The figure below exhibits the relation of foam strength with the corresponding relative density of four foam samples derived from very similar bituminous coals. The compressive strength increases with the relative density. The increase of relative density implies an increase of the thickness of cell wall, t , or decrease of the length of the cell edge, l . A thicker cell wall and shorter cell edge promote higher compressive strength.

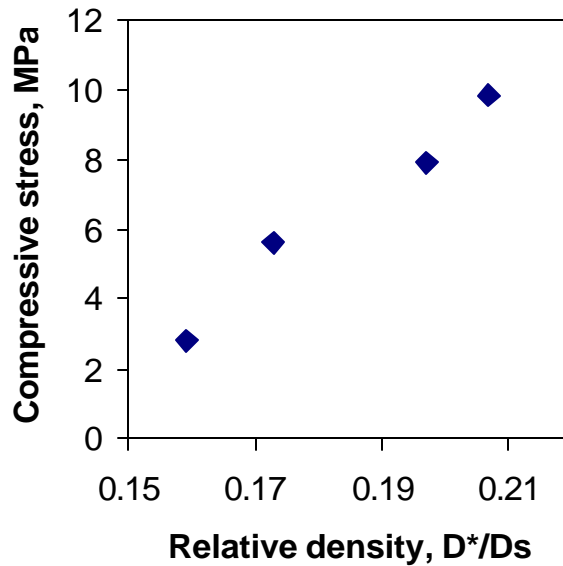


Figure 220. Relation of Compressive Strength with Relative Density of Coal-based Carbon Foam.

However, for the foam derived from the other precursors in the table, the experimental data does not correlate well with the model. Moreover, for closed-cell foam, the situation is much more complicated. Hence, at least one more parameter should be involved in describing the foam strength, i.e., the membrane of closed cell. During crushing, the strain of membrane also prevents the foam structure from collapsing. This may be one of the reasons why closed-cell foam is stronger. However, a cracked membrane will not be effective.

In addition, the strength of carbon foam is also related to the properties of the precursor material, such as the fluidity under the foaming condition. The comparison of the strength of foam derived from precursors with different fluidity is shown in the table below. The data are from two set of samples, all with close relative density and all derived from raw coal. The results clearly indicate that the precursor with the higher fluidity generates the stronger foam.

Table 43. Compressive Strength of Carbon Foams from High and Low Fluidity Precursors.

Foam precursor	Fluidity, DDPM	Relative density	Compressive strength, MPa
Coal-I a	<1000	0.22	3.8
Coal-I b	>10000	0.21	9.9
Coal-II a	<1000	0.20	5.4
Coal-II b	>10000	0.20	8.0

The isotropic and anisotropic nature of pitch significantly affects mechanical, thermal and electrical properties of the subsequent foam. Isotropic material has similar properties in all the direction, while an anisotropic material has dependence on the orientation of the anisotropic flow domain^{86,87,88}. The mechanical strength and the thermal/electrical conductivity are higher for the in-plane than out-of-plane directions, while the coefficient of thermal expansion (CTE) is smaller in-plane than out-of-plane.

The next series of figures show the optical texture of carbon foam under polarized light in the optical microscope. The coal and extract-based carbon foams show a very fine grained anisotropic texture, although they are hard to be recognized in the first two pictures, while pitch-based carbon foams show anisotropic flow texture, as shown in the third and fourth pictures. Petroleum pitch A240, SynPitch and QI free coal tar pitch derived carbon foams exhibit large anisotropic flow domain aligned parallel to the cell wall. However, QI containing coal tar pitch derived foam shows a smaller anisotropic domain size. This is because the QI prevents the coalescence of the mesophase sphere during heat treatment. The flow direction of the anisotropic domains is found mostly parallel to the cell surface, which suggests that during the formation of foam cell, shearing stress from the released gases forces the anisotropic domain to align along the cell wall. This alignment will affect the structure and properties of the carbon foam. Further SEM observation provides more evidence for this effect.

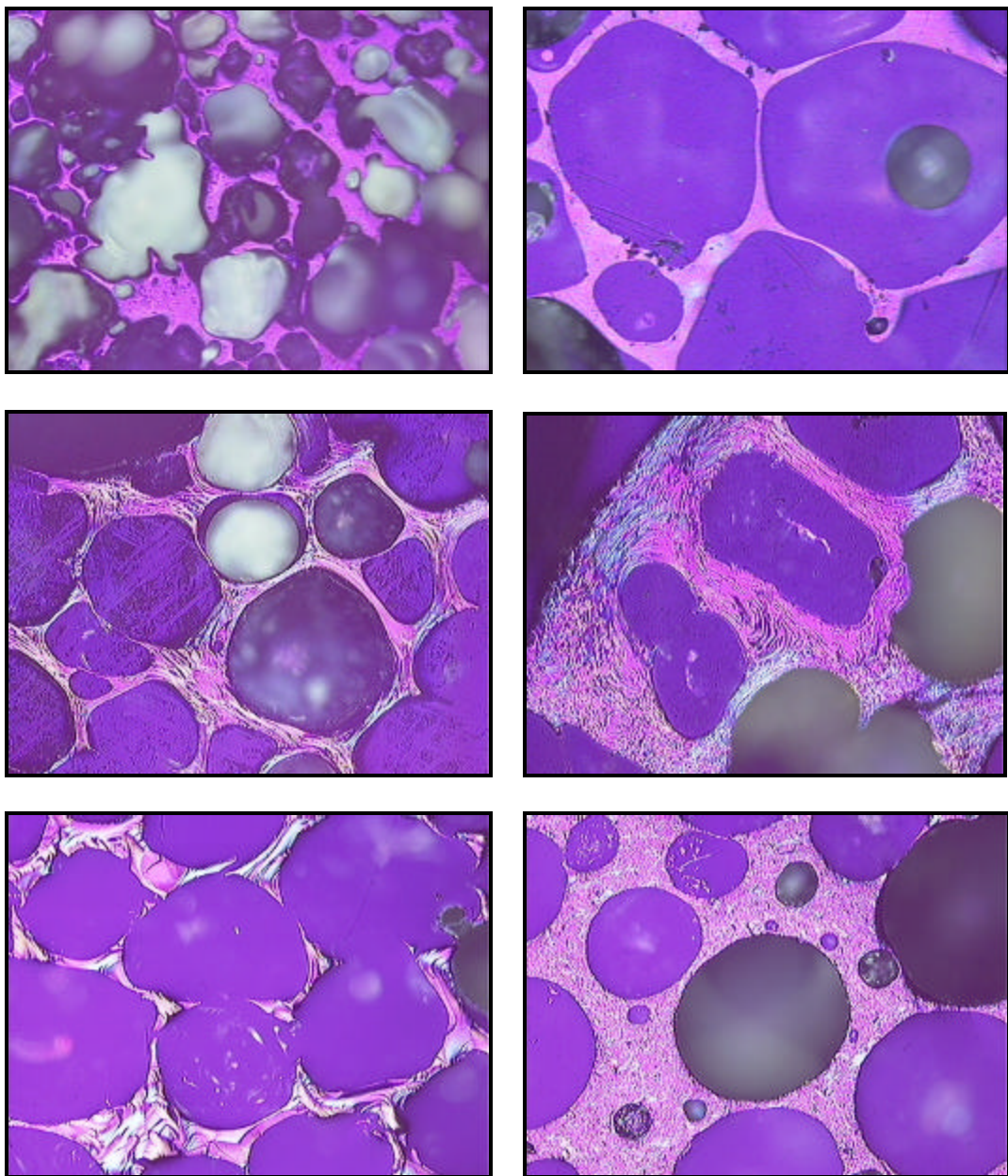


Figure 221. Optical Texture of Carbon Foam Derived from Coal(a), Coal Solvent-extract(b), Petroleum Pitch (c), SynPitch(d), Coal Tar Pitch-II, QI-free (e) and Coal Tar Pitch-I, QI Containing(f).

For applications dependent on the surface properties of carbon foam, surface area and pore structure need to be determined. Unlike the foam cell structure, which is usually observed by SEM, the surface area and pore structure in the foam matrix are investigated by gas adsorption behavior. The micro/mesopore structure in the foam matrix affects the surface adsorption properties of carbon foam and may also affect the strength of the carbon foam. The gas adsorption behavior of a series of carbon foams derived from coal precursors with different properties is discussed below.

According to the adsorption isotherm curve and the corresponding t -plot, the type of porous material could be determined.^{89,90} In the t -plot, a downward deviation from a standard nonporous material is observed when micropores are present in the solid, while an upward deviation indicates the presence of capillary condensation in the meso or macropore.^{91,92} The next series of figures show the isotherms and the corresponding t -plots of three typical carbon foams derived from coal precursors with different plastic properties. From (a) to (c), the Gieseler fluidity decreases from >10000 DDPM for (a), to 1000~10000 DDPM for (b) and <1000 DDPM for (c). The isotherm of sample (a) follows a Type II adsorption. Its t -plot is very close to a straight line passing through the origin, which confirms that the isotherm is a Type II. The results suggest that sample (a) is very close to a nonporous material. Its total surface area is as small as $0.16\text{ m}^2/\text{g}$ (BET), with a micropore area of $0.037\text{ m}^2/\text{g}$ (t-method). The result implies that sample (a) has a solid and rigid foam matrix. Sample (b) is the foam derived from coal with an intermediate fluidity. Its isotherm curve shows a significant increase of the amount of adsorption at very low P/P^0 , which may correspond to the micropore filling. Its corresponding t -plot shows a downward deviation at low-coverage part of t -plot, which indicates sample (b) to be a porous material with some micro structure in the foam matrix. Its higher surface area($0.7\text{ m}^2/\text{g}$ total area, $0.4\text{ m}^2/\text{g}$ micropore area) suggests that sample (b) may be more porous than sample (a) in the foam matrix. Sample (c) is the foam derived from coal with the lowest fluidity. Its isothermal adsorption curve and t -plot clearly indicate a Type I isotherm for micropore structure with a larger total surface area of $3.26\text{ m}^2/\text{g}$, and a micropore area of $2.14\text{ m}^2/\text{g}$. The total surface includes micropore, mesopore and external surface area. The increase of surface area as the fluidity of foaming precursor decreases implies that the pore structure in the carbon foam matrix is related to the fluidity of the foaming precursor. During the foaming process, the highly fluid precursor (e.g., sample (a)) is easy to coalesce and generates a solid foam matrix structure. However, low fluidity material is harder to coalesce to generate the solid foam matrix structure. Therefore, the porous structure exists in its matrix. It can be imagined that foam with a porous structure in its matrix will be weak. These results might explain the data in the table above, i.e., why the carbon foam derived from highly fluid precursor is stronger than the one derived from low fluid precursor.

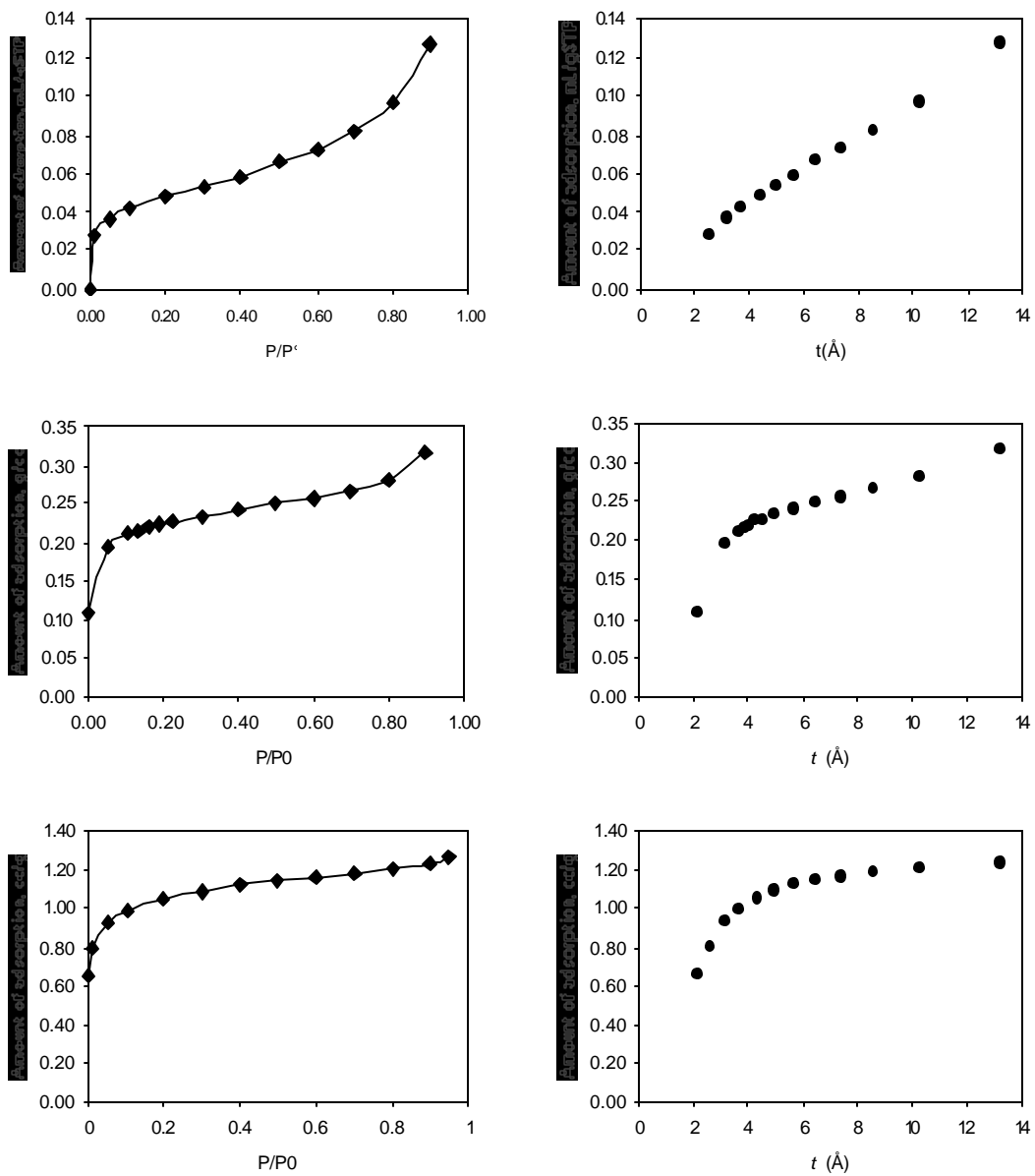


Figure 222. Isotherms and the Corresponding t-plots of the Carbon Foam Derived from Coal with Different Fluidity. Fluidity >10000(a), 1000-10000(b) and <1000(c).

In summary, both raw coal and coal solvent extracts are effective foaming precursors for relatively high strength isotropic foam, which is suitable for structural and energy applications. Pitches, including petroleum pitch, coal tar pitch and coal-derived synthetic pitch, must be treated before foam can be created. Anisotropic pitches can be used to synthesize anisotropic carbon foam. Material properties are controllable by varying the heat pretreatment and anisotropic domain size. The strength of carbon foam is determined by the foam cell structure and the plastic properties of precursor material.

4.6 Isotropic and Mesophase-Based Fibers and Composites

High melting temperature synthetic pitches (Synpitches) can be created using coal derivatives produced from a solvent extraction technique. These pitches form the basis for carbon fibers and composites after additional processing. Solvent extraction is used to separate hydrocarbons from mineral matter as well as other insolubles. Mild hydrogenation can be used to chemically modify resultant material to produce a true pitch.

There are three main techniques which can be used to tailor the softening point of the Synpitch. First, the softening point can be controlled by varying the conditions of hydrogenation, chiefly the temperature, pressure and residence time in a hydrogen overpressure. Second, by selectively distilling light hydrocarbons, the softening point of the remaining pitch can be raised. Third, the Synpitch can be blended with another mutually soluble pitch or hydrocarbon liquid. Through such techniques, spinnable isotropic Synpitches have been created from coal feedstocks. Characteristics of Synpitches include high cross-linking reactivity and high molecular weight, resulting in carbon fibers with excellent mechanical properties. To date, mechanical properties have been achieved which are comparable to the state of the art achievable with conventional coal tar pitch or petroleum pitch.

Although most carbon fiber is currently spun using polyacrylonitrile (PAN) precursors, pitch based carbon fibers continue to find application because of their high modulus, low coefficient of thermal expansion, low electrical resistivity and high thermal conductivity. These fiber properties are influenced by the properties of the precursor pitch.

Synthetic coal derived pitches, or Synpitches, can be produced starting with raw coal by a combination of hydrogenation, separation and careful thermal processing in order to produce a tailored melting point pitch. In contrast to pitches obtained from coking ovens, synthetic coal pitch offers high cross-linking reactivity, high aromatic content, high molecular weight and tailororable properties. A potential cost advantage compared to PAN-derived fibers can be accrued due to the low cost of the feedstock material. Historically, however, processing costs have been consistently higher for pitch-derived fibers. Variability of the feedstock is a major reason for higher processing and quality control costs of pitch fibers. Thus, a more uniform source of feedstock might result in reduced costs. With these objectives in mind, preliminary efforts have been carried out to produce carbon fibers using Synpitch.

In a project sponsored by the Department of Energy through the Consortium for Premium Carbon Products from Coal (CPCPC), Stansberry et al. produced isotropic synthetic pitch which was successfully spun into isotropic carbon fibers.⁹³ Bituminous coal (WVGS 13421) was ground to -60 mesh and vacuum dried at 100 °C overnight. Six hundred grams of ground coal was mixed with 1.8 liters of tetralin, sealed and purged with hydrogen gas and pressurized to 400 psig. Mixing was accomplished using a magnetic stirrer at 1000 rpm. The reactor was heated for one hour at a maximum temperature of about 450 °C for one hour. The reactor was then cooled to ambient

temperature, vented and opened. After washing with solvent, the product was centrifuged at 2000g for one hour to separate solid material (principally mineral matter and undissolved coal) from the liquefied coal. Typical yields ranged from 70 to 80% by mass.

The softening point of the resultant pitch was raised by a combination of thermal processing and vacuum distillation. Fibers were spun by the University of Kentucky Center for Applied Energy Research, using a single hole spinneret. Stabilization occurs via a temperature ramp of 0.05 °C/min to 310 °C. Finally, carbonization was accomplished in a separate furnace with a 20 °C/min ramp to 1100 °C. The result is an isotropic carbon fiber.

The results measured at MER Corporation indicated that strengths as high as 1.3 GPa had been attained on such fibers.^{94,95} If these results were accepted, they would indicate higher strength than had ever been previously achieved with isotropic fibers. This provided the rationale for believing that solvent extraction technology would result in enhanced mechanical properties compared to state-of-the-art methods.

However, after a series of experiments that produced significantly lower strength and modulus values (consistent with state of the art results from other manufacturing processes), the original data was revisited. Retainer samples of the same fibers producing superior results at MER Corporation were split in to two batches. One batch was tested by West Virginia University, and the other batch tested by the University of Kentucky Center for Applied Energy Research (CAER) a world renowned center of excellence for carbon materials and testing. Both institutions tested the retainer samples using ASTM D3379. These results are shown in the table below, and indicate a significantly lower value than originally attained at MER Corporation, but are consistent with the known state of the art for isotropic pitch-derived carbon fibers. Moreover, further review of the results revealed that MER Corporation measured the fiber diameter at 14 microns versus 31.9 and 32.7 by CAER and WVU, respectively. Perhaps the discrepancy in the diameter measurement would help explain the difference in the estimated strength.

In light of the discrepancy, the most conservative approach would be to reject the higher estimates for strength until such time as they are duplicated elsewhere.

Table 44. Tensile Measurements of Synthetic Pitch Fiber.

Property	CAER measurement	WVU measurement
Diameter	31.9 +/- 1.8 microns	32.7 +/- 2.0 microns
Strength	519 +/- 59 MPa	437 +/- 51 MPa
Modulus	38.7 +/- 1.6 GPa	37.9 +/- 5.3 GPa
Strain	1.34 +/- 0.13 %	1.16 +/- 0.16%

An alternate method was also investigated for enhancing the properties of low softening point pitches. In this case the motivation is cost reduction by utilizing lower cost precursors, as well as improving the ease of stabilization processing. For example, Ashland petroleum pitch A-240 can be spun into fiber, but is usually impossible to stabilize owing to its low softening point (240 °F or 116 °C). By combining this low-softening-point pitch with Solvent Extracted Carbon Ore (SECO), it was hoped that the resultant mixture would have a softening point appropriate for fiber spinning, as well as adequate properties after stabilization.

SECO is produced by dissolving ground coal in a solvent such as n-methyl pyrrolidone (NMP). For these experiments, coal from the Lower Bakerstown seam was used. After centrifugation to remove solids (chiefly mineral matter and undissolved carbon), the resultant coal solution is reconstituted and dried.

SECO was combined with A240 pitch to create a solution was 10% SECO by mass. The resultant pitch was spun into fiber and stabilized.

Although stabilization was considered successful, the resultant fibers were brittle and contained significant defects, as shown in the SEM photomicrographs in the next figure. The photomicrographic analysis reveals extensive formation of pores within the body of the fibers, probably due to devolatilization during stabilization and calcining. Mechanical property measurements are listed in the following table.

Table 45. Tensile Measurements of Synthetic Pitch Fiber.

Property	Measured Value
Diameter	35.9 +/- 6.9 microns
Strength	237 +/- 90 MPa
Modulus	33.6 +/- 9.3 GPa

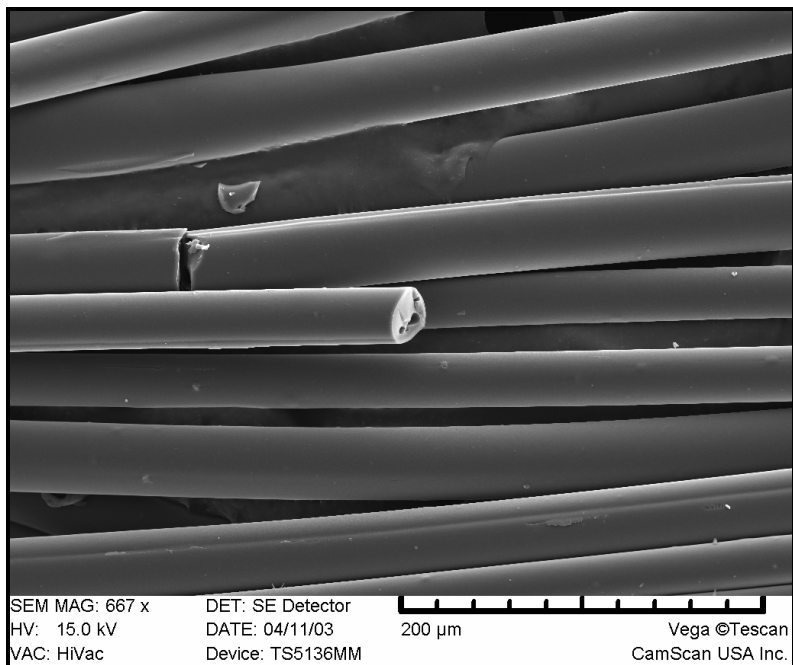


Figure 223. SEM Photomicrograph of Synpitch-Derived Carbon Fibers, Showing Defects and Irregular Surfaces.

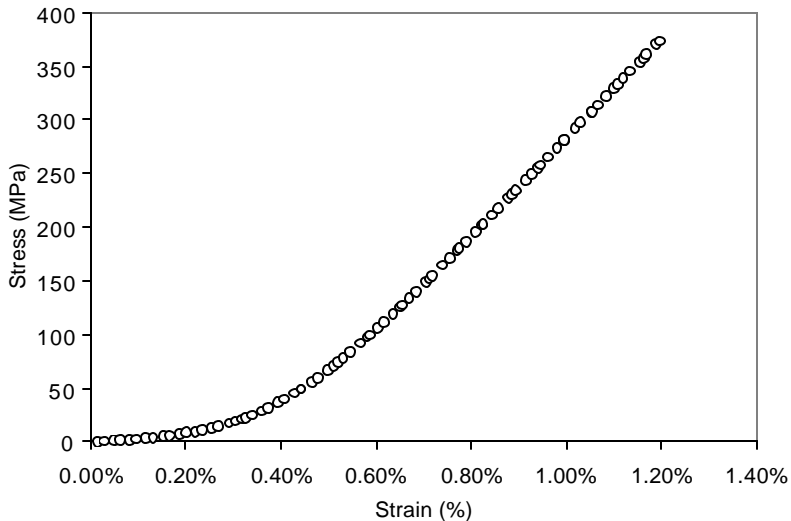


Figure 224. Stress-Strain Plot for A-240/Bakerstown Synpitch Fiber.

In summary, the production of carbon fibers from synthetic coal pitch (Synpitch) as well as from a blend of petroleum pitch augmented with solvent extracted carbon ore (SECO) was demonstrated. Fiber from pure Synpitch demonstrated strength comparable to commercial grade fibers. Future trials will be made using anisotropic pitches now being produced on benchtop scale, and are expected to demonstrate improved strength and especially modulus.

On the other hand, fibers produced from blended pitch exhibited significant nonuniformity, including the presence of pores within the calcined fiber. These defects are potentially correctable, but acceptable fibers have not yet been produced using blended pitch feedstock.

5.0 Economic Considerations

The technology to produce synthetic pitch products, as well as cokes, foams and fibers has been demonstrated. A remaining consideration is to determine whether such processes can be economical when implemented on an industrial scale.

Determination of capital investment and operational costs is a site specific operation and will likely require detailed analysis beyond the scope of this effort. However, the materials cost can be more easily analyzed, at least to first order.

The major feedstocks and products are commodity products whose prices are fairly well established at any one point in time, although due to market volatility the long-term price is not possible to predict with certainty. Approximate prices were determined by consulting industrial experts at companies such as Koppers, GrafTech International, CII Carbon, Air Products and others.

Based on their information, feedstock cost estimates are listed in the table below, along with approximate mass balances based on laboratory and pilot scale testing. The result is that for the baseline protocol, in which coal tar distillate oils are used as the hydrogen donor solvent and recycled, the feedstock costs are listed below.

For a binder pitch product, prices currently hover around \$280 to \$300. It is presumed that a synthetic pitch might be of greater value as a pitch extender, because the low QI's present would allow it to be combined with conventional coal tar pitch with overly high QI's. In other words, the use of synthetic pitch blends would permit substandard material to be brought into manufacturer's specifications.

Energy costs are paid at \$0.05/kW·hr, which is thought to be a pessimistically high estimate.

The tails from the centrifugation (solid/liquid separation) would likely have fuel value or could at least be incorporated in asphalt or some other low value product. However, as the worst plausible case, it is assumed that this material would be disposed of in a landfill, and a disposal cost of \$15/ton is assumed.

Similarly, lost vapors and gases would result in some cost to the producer because of the need to scrub or otherwise treat any potential emissions. This is also assigned a value of -\$15 per ton.

The recycled solvent is not really a product as it is assumed to be immediately reused as a feedstock. Probably consideration should be given to determining whether the recycled solvent might be of greater value as a liquid fuel source. If so, a higher profit margin could be realized.

Table 46. Materials Cost Balance for Synthetic Binder Pitch.

Feedstocks	Mass, US Tons	Specific Energy, kJ/kg	Specific Energy, BTU/ton	Cost per US Ton	Extended Cost, \$	Extended Energy, BTU/ton coal
Recycle Solvent	2.125	45000	19149	\$200	\$425	40691
Catalyst	0.0015	0	0	\$2,000	\$3	0
Solvent (middle distillation cut)	0.375	45000	19149	\$200	\$75	7181
Raw Coal, -50 mesh,dry	1	29375	12500	\$60	\$60	12500
tube trailer hydrogen	0.0075	142000	60426	\$3,991	\$30	453

On-site Hydrogen	0	142000	60426	\$907	\$0	0
Heating Energy Solvent+ H2		600			\$19	600
Heating Energy H-Solvent/Coal Slurry		600			\$19	600
Separations cost undissolved solids		160			\$5	160
Distillation Energy		400			\$11	400
Total Material Feed Costs	3.509		17836	\$184	\$647	62586
Products						
Solid plus residual solvent	0.1	9000	3830	-\$15	-\$2	383
Unrecovered gas+vapors	0.05	42000	17872	-\$15	-\$1	894
Binder Pitch	1.234	36200	15404	\$300	\$370	19009
Recovered solvent	2.125	45000	19149	\$200	\$425	40691
Process Heat						1600
Total	3.509			\$226	\$793	62577
Gross materials value added	1.234				\$146	

On the basis of materials cost, it is possible to be very competitive at today's materials price structures. In other words, the process can be viable if the processing costs are substantially under \$146 per ton of coal. These costs must include not only the operational cost of production, but also the amortized capital investment required.

However, though the prospect of higher profits is attractive to industry, the consumption of additional coal tar distillate oils runs counter to the National Energy Technology Laboratory interest in reducing America's dependence on foreign petroleum and coal tar distillates. In the case of petroleum, the desire for increased petroleum independence is obvious enough. In addition, as explained in Section 2, it is perceived to be in the national interest to reduce dependence on coal tar distillates as well, mainly due to the environmental issues associated with operating the metcoke ovens necessary for the production of coal tar distillate oils. Thus, it is worthwhile considering a scenario in which coal tar distillate oils are not available.

To this end, it would be possible to recycle the pitch product and to re-hydrogenate it so that it can be used as a solvent. In today's economic terms this is unattractive because the pitch is worth \$300 per ton and the solvent is worth only about \$200 per ton. Still, if it were necessary to do so, it is possible to produce a product by this method. Assuming that a production cost of the product of \$200 (versus its selling price of \$300), the table below indicates that the process could be viable, but significantly less attractive than the baseline process.

However, one might also presume that if in the future the coal tar supply were to be eliminated, the market price for binder pitch would be substantially higher than today's price. Moreover, it might be assumed that future synthetic pitch manufacturing processes would maximize its recycling of solvent, in which case improved economy could result.

Table 47. Materials Cost Balance for Synthetic Binder Pitch without Coal Tar or Petroleum Solvents.

	Mass, US Tons	Specific Energy, kJ/kg	Specific Energy, BTU/ton	Cost per US Ton	Extended Cost, \$/ton coal	Extended Energy, BTU/ton coal
Recycle Solvent	2.125	45000	19149	\$200	\$425	40691
Catalyst	0.0015	0	0	\$2,000	\$3	0
Solvent (synthetic pitch)	0.375	45000	19149	\$200	\$113	7181
Raw Coal, -50 mesh,dry	1	29375	12500	\$60	\$60	12500
tube trailer hydrogen	0.0075	142000	60426	\$3,991	\$30	453
On-site Hydrogen	0	142000	60426	\$907	\$0	0
Heating Energy Solvent+ H ₂		600			\$19	
Heating Energy H- Solvent/Coal Slurry		600			\$19	
Separations cost undissolved solids		160			\$5	
Distillation Energy		400			\$11	
Total Material Feed Costs	3.509		17334	\$195	\$684	60826
Products						
Solid plus residual solvent	0.1	9000	3830	-\$15	-\$2	383
Unrecovered gas+vapors	0.05	42000	17872	-\$15	-\$1	894
Binder Pitch	0.859	36000	15319	\$300	\$258	13159
Recovered solvent	2.125	45000	19149	\$200	\$425	40691
Spent energy						1760
Total	3.134			\$217	\$680	56887
Gross materials value added	0.859				-\$4	

Yet another scenario worthy of consideration is that of anode coke production. On the face of it, this would seem to be a difficult task, since the current market price of anode grade coke is about \$100 per ton less than the price of binder pitch. Moreover, since solvent extraction results initially in a low melting point pitch, additional processing would be required in order to produce anode grade coke. Hence it would seem that the production costs of anode grade coke would be higher than the production costs of binder pitch.

However, there are at least two potential mitigating factors that make coke production attractive. First, because the coal-derived feedstocks are highly aromatic, highly anisotropic coke precursors can result. Quinoline insolubles (QI) normally disrupt the formation of anisotropic domains that can lead to the formation of needle coke, which carries a premium of double to triple the price of anode grade coke. This raises the possibility that needle grade coke might be formed.

Second, the production of coke results in the co-production of volatile vapors that are driven off during the coking process. The value of the liquid products has not been

determined and represent a major uncertainty. Typically, however, light volatiles are considerably more valuable than the distillation bottoms that are the focus for production of pitches and cokes. For example, naphthalene is a major component of coal liquids and can be used as a fuel additive, and may be valued at about \$500 per ton. Thus the green coke may range in quality from anode grade to needle grade, and could command a price of about \$180 to \$600. In the table below, \$200 is chosen as a conservative estimate. Similarly, the price of liquid products is estimated to be valued at \$300 per ton, which is also believed to be conservative. Under these conditions, the materials balance is economically favorable.

Table 48. Mass and Cost Balance for Green Coke.

Feedstocks	Mass, US Tons	Specific Energy, kJ/kg	Specific Energy, BTU/ton	Cost per US Ton	Extended Cost, \$/ton coal	Extended Energy, BTU/ton coal
Recycle Solvent	2.125	45000	19149	\$200	\$425	40691
Catalyst	0.0015	0	0	\$2,000	\$3	0
Solvent (middle distillation cut)	0.375	45000	19149	\$200	\$75	7181
Raw Coal, -50 mesh,dry	1	29375	12500	\$60	\$60	12500
tube trailer hydrogen	0.0075	142000	60426	\$3,991	\$30	453
On-site Hydrogen	0	142000	60426	\$907	\$0	0
Heating Energy Solvent+ H2		600			\$19	600
Heating Energy H- Solvent/Coal Slurry		600			\$19	600
Separations cost undissolved solids		160			\$5	160
Distillation Energy		400			\$11	400
Total Material Feed Costs	3.509		17836	\$184	\$647	62586
<hr/>						
Products						
Solid plus residual solvent	0.1	9000	3830	-\$15	-\$2	383
Unrecovered gas+vapors	0.05	42000	17872	-\$15	-\$1	894
Green Coke	0.617	33000	14043	\$200	\$123	8664
Fuel Liquids	0.617	39200	16681	\$300	\$185	10292
Recovered solvent	2.125	45000	19149	\$200	\$425	40691
Process Heat						1600
Total	3.509			\$208	\$731	62524
<hr/>						
Gross materials value added	1.234				\$85	

Thus, the processes for producing pitches and cokes appear to be economically viable. The baseline process for producing binder pitch probably has the least uncertainty and the best potential cost margins. Though a cost model for plant capital investment requirements operation expense has not been developed, the basic unit processes of hydrogenation, solid separation, and distillation are similar to other processes that have been developed for petroleum, coal and other ores. The materials margin of \$146 per ton of coal is sufficiently large that optimism is probably justified.

6.0 References

¹ The Carbon Products Industry Vision for the Future, Industries of the Future, Carbon Products Consortium, WVU-NRCCE, P.O. Box 6064, Morgantown, WV 26506.

² R. H. Wombles, "Experience with Petroleum Enhanced Coal Tar Pitch," 2000 Australasian Smelter Conference, Queenstown, Australia.

³ Zsolt Rumy, "The Future: It's Closer Than You Think" Convention of the Society for the Advancement of Material and Process Engineering — Anaheim, California. June 2, 1998. See also www.jeccomposites.com — "Toray to expand Carbon Fiber Production in France" Jan 20 2003. See also <http://netcomposites.com/news.asp?2507>, "Zoltek Announces \$20 Million Financing to Reduce Debt and Commence Capacity Expansion."

⁴ David Rigby Associates "The World Technical Textiles Industry and its Markets: Prospects to 2005." report prepared for Techtextil Messe Frankfurt GmbH. DRA can be reached at 44-161-236-0303, or by fax at 44-161-236-0310. Email: dra@dratex.co.uk. See also Dick J. Wilkins et al., JTEC Panel on Advanced Manufacturing Technology for Polymer Composite Structures in Japan, April 1994.

⁵ Freedonia Group; "World carbon black demand to reach 8.6 million metric tons in 2006" (News Release), Research Studies 3/27/2003. See also www.unitedcarbon.com.

⁶ Missile Defense Agency Newsletter, "C-Foam Hits the Beach," Article #4302, FALL 2003.

⁷ Cientifica, Nanotubes, March 2004.

⁸ Werner K. Fischer, Felix Keller and Ulrich Mannweiler, "The Changing World of Anode Raw Materials: Can Today's Carbon Technology Cope with it?" ARABAL Conference 1999, Kuwait.

⁹ Schobert, H. Coal: The Energy Source of the Past and Future. American Chemical Society, USA, 1987.

¹⁰ Wiser, W. Preprints Fuel Division ACS Meeting, 20 (2), 122, 1975.

¹¹ Lee, E.S., "Coal Liquefaction" Coal Conversion Technology, editor C.Y. Wen and E.S. Lee, Addison-Wesley Publishing Company, Mass., 1979.

¹² Ergun S., "Coal Classification and Characterization" *Coal Conversion Technology*. Ed. C.Y. Wen and E.S. Lee, Addison-Wesley Publishing Company, Reading, Mass., 1979.

¹³ Vernon, L.W., *Fuel*, 59, 102, 1980.

¹⁴ Wiser, W. H., *Fuel* 47, 475, 1968.

¹⁵ Whitehurst, D.D., Mitchell, T. O., and Farcasiu, M., *Coal Liquefaction: The Chemistry and Technology of Thermal Processes*, Mobil Research and Development Corporation, Central Research Division, Princeton, New Jersey, 1980.

¹⁶ N. Berkowitz, *An Introduction to Coal Technology*. Academic Press Inc., San Diego, 1994.

¹⁷ Neavel, R. C., "Liquefaction of Coal in Hydrogen-Donor and Non-Donor Vehicles", *Fuel*, 55, 237, 1976.

¹⁸ Neavel, R. C., "Liquefaction of Coal in Hydrogen-Donor and Non-Donor Vehicles", *Fuel*, 55, 237, 1976.

¹⁹ Farcasiu, M., Mitchell, T. O., and Whitehurst, D. D., *ACS Div. Fuel Chem. Prepr.* 27(7), 11, 1976.

²⁰ N. Berkowitz, *An Introduction to Coal Technology*. Academic Press Inc., San Diego, 1994.

²¹ N. Berkowitz, *An Introduction to Coal Technology*. Academic Press Inc., San Diego, 1994.

²² Whitehurst, D.D., Mitchell, T. O., and Farcasiu, M., *Coal Liquefaction: The Chemistry and Technology of Thermal Processes*, Mobil Research and Development Corporation, Central Research Division, Princeton, New Jersey, 1980.

²³ Orchin, M. and Storch, H. H., *Ind. Eng. Chem.*, 40, 1385, 1948.

²⁴ R.C. Neavel, *Fuel*, 55,237, 1976.

²⁵ Whitehurst, D.D., Mitchell, T. O., and Farcasiu, M., *Coal Liquefaction: The Chemistry and Technology of Thermal Processes*, Mobil Research and Development Corporation, Central Research Division, Princeton, New Jersey, 1980.

²⁶ Whitehurst, D.D., Mitchell, T. O., and Farcasiu, M., *Coal Liquefaction: The Chemistry and Technology of Thermal Processes*, Mobil Research and Development Corporation, Central Research Division, Princeton, New Jersey, 1980.

²⁷ Mukherjee, D. K., and Chowdry, P. B., *Fuel*, 55, 4, 1976.

²⁸ Whitehurst, D.D., Mitchell, T. O., and Farcasiu, M., Coal Liquefaction: The Chemistry and Technology of Thermal Processes, Mobil Research and Development Corporation, Central Research Division, Princeton, New Jersey, 1980.

²⁹ Whitehurst, D.D., Mitchell, T. O., and Farcasiu, M., Coal Liquefaction: The Chemistry and Technology of Thermal Processes, Mobil Research and Development Corporation, Central Research Division, Princeton, New Jersey, 1980.

³⁰ Whitehurst, D.D., Mitchell, T. O., and Farcasiu, M., Coal Liquefaction: The Chemistry and Technology of Thermal Processes, Mobil Research and Development Corporation, Central Research Division, Princeton, New Jersey, 1980.

³¹ Yen, Y. K., Furlani, D. E., and Weller, S. W., *Ind. Eng. Chem. Prod. Res. Dev.*, 15, 24, 1976.

³² Tomic, J. and Schobert, H.H., *Energy & Fuels*, 10, 709, 1996.

³³ Whitehurst, D.D., Mitchell, T. O., and Farcasiu, M., Coal Liquefaction: The Chemistry and Technology of Thermal Processes, Mobil Research and Development Corporation, Central Research Division, Princeton, New Jersey, 1980.

³⁴ Whitehurst, D.D., Mitchell, T. O., and Farcasiu, M., Coal Liquefaction: The Chemistry and Technology of Thermal Processes, Mobil Research and Development Corporation, Central Research Division, Princeton, New Jersey, 1980.

³⁵ Whitehurst, D.D., Mitchell, T. O., and Farcasiu, M., Coal Liquefaction: The Chemistry and Technology of Thermal Processes, Mobil Research and Development Corporation, Central Research Division, Princeton, New Jersey, 1980.

³⁶ Whitehurst, D.D., Mitchell, T. O., and Farcasiu, M., Coal Liquefaction: The Chemistry and Technology of Thermal Processes, Mobil Research and Development Corporation, Central Research Division, Princeton, New Jersey, 1980.

³⁷ Whitehurst, D.D., Mitchell, T. O., and Farcasiu, M., Coal Liquefaction: The Chemistry and Technology of Thermal Processes, Mobil Research and Development Corporation, Central Research Division, Princeton, New Jersey, 1980.

³⁸ Barr, J. B.; Lewis, I. C. Chemical changes during the mild air oxidation of pitch. *Carbon* (1978), 16(6), 439-44.

³⁹ Zeng, Shu Ming; Maeda, Toyohiro; Tokumitsu, Katsuhisa; Mondori, Juji; Mochida, Isao. Preparation of isotropic pitch precursors for general purpose carbon fibers (GPCF) by air blowing - II. Air blowing of coal tar, hydrogenated coal tar, and petroleum pitches. *Carbon* (1993), 31(3), 413-19.

⁴⁰Fernandez, J. J.; Figueiras, A.; Granda, M.; Bermejo, J.; Menendez, R. Modification of coal-tar pitch by air-blowing - I. Variation of pitch composition and properties. *Carbon* (1995), 33(3), 295-307.

⁴¹Maeda, Toyohiro; Zeng, Shu Ming; Tokumitsu, Katsuhisa; Mondori, Juji; Mochida, Isao. Preparation of isotropic pitch precursors for general purpose carbon fibers (GPCF) by air blowing - I. Preparation of spinnable isotropic pitch precursor from coal tar by air blowing. *Carbon* (1993), 31(3), 407-12.

⁴²Maeda, Toyohiro; Zeng, Shu Ming; Tokumitsu, Katsuhisa; Mondori, Juji; Mochida, Isao. Preparation of isotropic pitch precursors for general purpose carbon fibers (GPCF) by air blowing - I. Preparation of spinnable isotropic pitch precursor from coal tar by air blowing. *Carbon* (1993), 31(3), 407-12.

⁴³Zeng, Shu Ming; Maeda, Toyohiro; Tokumitsu, Katsuhisa; Mondori, Juji; Mochida, Isao. Preparation of isotropic pitch precursors for general purpose carbon fibers (GPCF) by air blowing - II. Air blowing of coal tar, hydrogenated coal tar, and petroleum pitches. *Carbon* (1993), 31(3), 413-19.

⁴⁴Zeng, Shu Ming; Maeda, Toyohiro; Tokumitsu, Katsuhisa; Mondori, Juji; Mochida, Isao. Preparation of isotropic pitch precursors for general purpose carbon fibers (GPCF) by air blowing - II. Air blowing of coal tar, hydrogenated coal tar, and petroleum pitches. *Carbon* (1993), 31(3), 413-19.

⁴⁵Blanco, C.; Santamaria, R.; Bermejo, J.; Menendez, R. A comparative study of air-blown and thermally treated coal-tar pitches. *Carbon* (2000), 38(4), 517-523.

⁴⁶Menendez, R.; Fleurot, O.; Blanco, C.; Santamaria, R.; Bermejo, J.; Edie, D. Chemical and rheological characterization of air-blown coal-tar pitches. *Carbon* (1998), 36(7-8), 973-979.

⁴⁷Yamaguchi, Chiharu; Mondori, Juji; Matsumoto, Akira; Honma, Hidekazu; Kumagai, Haruo; Sanada, Yuzo. Air-blowing reactions of pitch: I. Oxidation of aromatic hydrocarbons. *Carbon* (1995), 33(2), 193-201.

⁴⁸Choi, J. H.; Kumagai, H.; Chiba, T.; Sanada, Y. Carbonization of pitches in air blowing batch reactor. *Carbon* (1995), 33(2), 109-14.

⁴⁹Choi, J. H.; Kumagai, H.; Chiba, T.; Sanada, Y. Carbonization of pitches in air blowing batch reactor. *Carbon* (1995), 33(2), 109-14.

⁵⁰Khandare, Pravin M.. Characterization of Mesophase Pitch Materials from Petroleum and Coal-Derived Precursors: Kinetics and Rheology at Elevated Temperatures. Dissertation. West Virginia University. November 1995.

⁵¹ S. Eser, R. G. Jenkins, and F. J. Derbyshire. *Carbon* (1986), **24**, 77-82

⁵² Yamaguchi, Chiharu; Mondori, Juji; Matsumoto, Akira; Honma, Hidekazu; Kumagai, Haruo; Sanada, Yuzo. *Air-blowing reactions of pitch: I. Oxidation of aromatic hydrocarbons.* *Carbon* (1995), 33(2), 193-201.

⁵³ Fernandez, J. J.; Figueiras, A.; Granda, M.; Bermejo, J.; Menendez, R. Modification of coal-tar pitch by air-blowing - I. Variation of pitch composition and properties. *Carbon* (1995), 33(3), 295-307.

⁵⁴ Maeda, Toyohiro; Zeng, Shu Ming; Tokumitsu, Katsuhisa; Mondori, Juji; Mochida, Isao. Preparation of isotropic pitch precursors for general purpose carbon fibers (GPCF) by air blowing - I. Preparation of spinnable isotropic pitch precursor from coal tar by air blowing. *Carbon* (1993), 31(3), 407-12.

⁵⁵ Menendez, R.; Fleurot, O.; Blanco, C.; Santamaria, R.; Bermejo, J.; Edie, D. Chemical and rheological characterization of air-blown coal-tar pitches. *Carbon* (1998), 36(7-8), 973-979.

⁵⁶ Khandare, Pravin M.. Characterization of Mesophase Pitch Materials from Petroleum and Coal-Derived Precursors: Kinetics and Rheology at Elevated Temperatures. Dissertation. West Virginia University. November 1995.

⁵⁷ Menendez, R.; Fleurot, O.; Blanco, C.; Santamaria, R.; Bermejo, J.; Edie, D. Chemical and rheological characterization of air-blown coal-tar pitches. *Carbon* (1998), 36(7-8), 973-979.

⁵⁸ Menendez, R.; Fleurot, O.; Blanco, C.; Santamaria, R.; Bermejo, J.; Edie, D. Chemical and rheological characterization of air-blown coal-tar pitches. *Carbon* (1998), 36(7-8), 973-979.

⁵⁹ Khandare, Pravin M.. Characterization of Mesophase Pitch Materials from Petroleum and Coal-Derived Precursors: Kinetics and Rheology at Elevated Temperatures. Dissertation. West Virginia University. November 1995.

⁶⁰ Khandare, Pravin M.. Characterization of Mesophase Pitch Materials from Petroleum and Coal-Derived Precursors: Kinetics and Rheology at Elevated Temperatures. Dissertation. West Virginia University. November 1995.

⁶¹ William, M. L., Landel, R. E., and Ferry, J. D., *J. Am. Chem. Soc.*, 77, pg. 3701 (1955).

⁶² Nazem, F. F.; Lewis, I. C. Viscosity and WLF-type behavior of mesophase pitches. *Molecular Crystals and Liquid Crystals.* (1986), 139(3-4), 195-207.

⁶³Nazem, F. F.; Lewis, I. C. Viscosity and WLF-type behavior of mesophase pitches. Molecular Crystals and Liquid Crystals. (1986), 139(3-4), 195-207.

⁶⁴van Krevelen, D. W. ,Graphical-statistical method for the study of structure and reaction processes of coal. Staatmijnen, Limburg, Neth. Fuel (1950), 29 269-84.

⁶⁵Joseph, D. and Oberlin, A. Oxidation of Carbonaceous Matter-I. Elemental Analysis (C,H,O) and IR Spectrometry. Carbon, 21(6), 559-64.

⁶⁶Van Krevelen, D. W. Graphical-statistical method for the study of structure and reaction processes of coal. Staatmijnen, Limburg, Neth. Fuel (1950), 29 269-84.

⁶⁷Joseph, D. and Oberlin, A. Oxidation of Carbonaceous Matter-I. Elemental Analysis (C,H,O) and IR Spectrometry. Carbon, 21(6), 559-64.

⁶⁸ Reliant Electric, Application Solution, Selecting Explosion-Proof Motors And Variable-Frequency Drive Controllers For Hazardous Environmental Applications, Publication D-7736 – September 2000.

⁶⁹Yang, J. A Study on the carbonization of coal-derived pitches. M.S. Thesis, WVU.

⁷⁰ D. Fenton, "Direct Liquefaction of Coal with Coal-Derived Solvents To Produce Precursors from Coal", Thesis, Department of Chemical Engineering, West Virginia University, 2001.

⁷¹ A. Awadalla, D. Cookson and B. Smith, "Coal Hydrogenation: Quality of start-up solvents and partially process-derived recycle solvents", Fuel, 64, 1097, 1985.

⁷²Barr, J. B.; Lewis, I. C. Chemical changes during the mild air oxidation of pitch. Carbon (1978), 16(6), 439-44.

⁷³ Drbohlav and Stevenson Carbon, vol. 33, pp. 693-711 (1995).

⁷⁴ King, Nathan. MS Thesis, West Virginia University, 2004.

⁷⁵ Stiller AH, Stansberry PG, Zondlo JW. Method for making a carbon foam and resultant product. US Patent 5888469, 1999.

⁷⁶ Stiller AH, Plucinski YJ. Method of making a reinforced carbon foam material and related product. US Patent 6183854, 2001.

⁷⁷ Stiller AH, Stansberry PG, Zondlo JW. Method of making carbon foam and resultant product. US Patent, 6346226, 2001.

⁷⁸ Stiller AH, Stansberry PG, Zondlo JW. Method of making a carbon foam material and resultant product. US Patent 6241957, 1999.

⁷⁹ Van Krevelen, DW. Coal. Elsevier Press, New York 1993 .

⁸⁰ Seki H, Kumagai J, Matsuda M, Ito M and Iino M. Fuel 1989; 68: 978-982.

⁸¹ Clemens AH, Matheson, TW Fuel 1995; 74(1): 57-62.

⁸² Clemens AH, Matheson, TW Fuel 1995; 74(1): 57-62.

⁸³ Lewis IC. J Chim Phys. 1984; 81: 751-758.

⁸⁴ Blanco C, Santamaria R, Bermejo J, Menendez R. Carbon 2000; 38: 517-23.

⁸⁵ Gibson LJ and Ashby MF Cellular Solids. Cambridge University Press: New York 1997.

⁸⁶ Wihte JL and Sheaffer PM. Carbon 1982, 27, 697.

⁸⁷ Singer LS. Fuel 1981, 60: 839.

⁸⁸ Jenkins, JC and Jenkins G. Carbon 1986, 24: 93.

⁸⁹ Gregg, SJ, Sing, KSW. Adsorption, Surface area and porosity. 2nd Ed. Academic Press. New York. 1982.

⁹⁰ Rouquerol F, Rouquerol J and Sing K. Adsorption by powders and porous solids. Academic Press. New York. 1999.

⁹¹ Wihte JL and Sheaffer PM. Carbon 1982, 27, 697.

⁹² Singer LS. Fuel 1981, 60: 83.

⁹³ P. G. Stansberry et al., "Production of Fibers and Composites from Coal-Based Precursors," Jan 15, 2000, *Final Report for 1999 Consortium for Premium Carbon Products from Coal, DE-FC26-98FT40350*.

⁹⁴ P. G. Stansberry et al., "Production of Fibers and Composites from Coal-Based Precursors," Jan 15, 2000, *Final Report for 1999 Consortium for Premium Carbon Products from Coal, DE-FC26-98FT40350*.

⁹⁵ J. C. Withers and J. Patel, "Low Cost Carbon Fibers from Coal-Based Precursors," Jan 15, 2000, *Final Report for 1999 Consortium for Premium Carbon Products from Coal, Contract DE-FC26-98FT40350*.